

MODULATION OF TUNING PROPERTIES OF THALAMIC RELAY  
NEURONS BY CORTICOTHALAMIC “FEEDBACK”  
PROJECTIONS IN RATS

By

Lu Li

Dissertation

Submitted to the Faculty of the  
Graduate School of Vanderbilt University  
in partial fulfillment of the requirements

for the degree of

DOCTOR OF PHILOSOPHY

in

PSYCHOLOGY

May, 2006

Nashville, Tennessee

Approved:

Professor Ford F. Ebner

Professor Vivien A. Casagrande

Professor Jon H. Kaas

Professor Anna W. Roe

To my precious fiancée, Pingping Shan,

and

To my beloved family,

my mother, Jinrong Li,

my father, Wenbiao Li,

and my dear sister, Lin Li,

who made all of this possible,

for their exceptionally endless love, encouragement and patience.

## ACKNOWLEDGEMENTS

This work would never have been possible without the freedom and support I was offered by Dr. Ford F. Ebner, my advisor, to pursue my own research interests. I am indebted to Dr. Ford Ebner for his detailed guidance, great patience, endless help and tremendous encouragement throughout my graduate study. As my mentor, it is he who provided me the opportunity to fulfill my dream of exploring the mysterious kingdom of the human brain, and showed me the way to appreciate the beauty of both Science and Life.

Special thanks go to the distinguished faculty members on my committee: Dr. Ford F. Ebner (chair), Dr. Vivien A. Casagrande, Dr. Jon H. Kaas, Dr. Joseph Lappin (Emeritus) and Dr. Anna W. Roe, for their tremendous support, encouragement, patience and insights.

I am grateful to all of our previous and current lab members with whom I have had the pleasure to work, especially Mr. Mark Maguire, Dr. Peter Melzer, Dr. V. Rema and Dr. Heike Sellien. I must express my appreciation to Dr. Michael Armstrong-James for his extensive personal and professional guidance in both scientific research and life.

I'd also like to thank all of the people at Wilson Hall who have made it such a great place. Particular thanks go to Mrs. Pat Burn, for her kindness and warm-hearted nature she impressed me on the first day when I came here.

Finally, I give my deepest thanks to all of the people in my whole family who always love me unconditionally. I can't describe how deep I appreciate the

care, support and encouragement from my parents and my sister, who are with me no matter what happens. And most importantly, I wish to thank my loving and supportive fiancée, Pingping Shan, who provides me with unending inspiration.

## TABLE OF CONTENTS

	<b>Page</b>
DEDICATION .....	ii
ACKNOWLEDGEMENTS .....	iii
LIST OF TABLES .....	ix
LIST OF FIGURES .....	x
 <b>Chapter</b>	
I. INTRODUCTION: CORTICAL MODULATION OF THALAMIC COMPUTATIONAL MAPS.....	1
Brief Introduction to the Rat Vibrissa System.....	6
The Whisker to Barrel Ascending Pathway.....	8
The Whisker Pad.....	8
The Whisker Follicle.....	11
The Trigeminal Ganglion.....	13
Physiological Properties of the Trigeminal Ganglion Neurons.....	14
Trigeminal Brainstem Complex.....	15
Cytoarchitectonic Structure of the Trigeminal Brainstem Complex.....	15
Physiological Properties of Neurons in Trigeminal Brainstem Complex.....	16
Output Projections of the Trigeminal Brainstem Complex.....	18
The Thalamus.....	20
Cytoarchitectonic Structure of VPM Neurons.....	21
Physiological Properties of Thalamic Relay Neurons.....	23
Output Projections of VPM to Barrel Field Cortex.....	26
Output Projections of P <sub>Om</sub> to Barrel Field Cortex.....	27
The Thalamic Reticular Nucleus.....	28
Cytoarchitectonic Structure of RTN.....	29
Physiological Properties of RTN Neurons.....	30
Input and Output Connections of RTN.....	31
The Extrareticular System.....	33
The Barrel Field Cortex.....	34
Physiological Properties of Cortical Neurons.....	35
The Corticothalamic Descending Pathway.....	36
Corticothalamic projections from Layer VI.....	37

Sub-laminar Specificity of Corticothalamic Projections.....	39
Functions of Corticothalamic Projections.....	40
Angular Tuning in Rat's Vibrissa System.....	42
II. CHRONIC SUPPRESSION OF ACTIVITY IN BARREL FIELD CORTEX DOWNREGULATES SENSORY RESPONSES IN CONTRALATERAL BARREL FIELD CORTEX .....	46
Introduction.....	47
Materials and Methods.....	50
Minipump Implantation.....	50
Behavioral Observations.....	53
Electrophysiological Recording.....	54
Muscimol Effective Range Detection <i>in vivo</i> .....	56
Acute.....	56
Chronic.....	56
Histology.....	57
Identification of the Depth of Layer IV.....	58
Data Analysis.....	59
Results.....	60
Behavioral Observations.....	64
Estimating the Area of Muscimol Suppression.....	65
Evoked Response Magnitude in Muscimol BFC Group.....	66
Effects on Spontaneous Activity.....	67
Influence of Muscimol on FSU and RSU.....	70
Laminar Analysis.....	72
Latency Analysis.....	76
Effects of Muscimol on C/S ratio.....	80
Discussion.....	82
Methodological Concerns.....	85
Surgical and Recording Procedures.....	85
Physiological and Pharmacological Effects of Muscimol <i>in vivo</i> .....	86
Physical Connections Underlying the Functional Down-regulation.....	87
III. BALANCING BILATERAL SENSORY ACTIVITY: CALLOSAL PROCESSING MODULATES SENSORY TRANSMISSION IN THE CONTRALATERAL THALAMUS BY ALTERING THE RESPONSE THRESHOLD.....	95
Introduction.....	96

Materials and Methods.....	99
Chamber Implantation.....	100
Electrophysiological Recording.....	102
Receptive Field Mapping.....	103
Threshold Assessment and Baseline Recording.....	104
Muscimol Application.....	106
Data Analysis.....	107
Histology and identification of recording sites.....	109
Results.....	109
Response of Thalamic Relay Neurons to Whisker Stimuli of Various Amplitudes.....	110
Muscimol Application Influences Response Magnitude and Latency of VPM Neurons.....	112
Muscimol Application Alters the Response Curves of VPM Neurons.....	124
Effects of Muscimol Application on POm Neurons.....	128
Discussion.....	135
Methodological Concerns.....	136
Threshold Determination.....	137
Corticothalamic Projections: Anatomy.....	140
Corticothalamic Projections: Function.....	142
Cortical Modulation of Tuning Properties of Thalamic Relay Neurons.....	144

#### IV. BARREL CORTEX ACTIVELY REDEFINES THE ANGULAR TUNING PROPERTIES OF VPM NEURONS.....147

Introduction.....	147
Materials and Methods.....	150
Animal Preparation.....	150
Electrophysiology.....	152
Whisker Stimulation.....	153
Recording in Thalamus.....	154
Receptive Field Mapping.....	155
Threshold Assessment and Angular Tuning Curve Mapping.....	155
Cortical Recording.....	157
Electrical Microstimulation of Layer VI.....	158
Data Analysis.....	159
Cortex.....	160
Parameters to Quantitatively Depict the Angular Tuning Features.....	161
Normalizing and Aligning Tuning Curves of	

Different VPM Units.....	163
Histology.....	164
Results.....	165
Discussion.....	181
V. SUMMARY AND PROSPECT: ROLE OF SPIKE-TIMING-DEPENDENT PLASTICITY IN THE ACTIVE MODULATION OF TUNING PROPERTIES OF THALAMIC RELAY NEURONS BY BARREL FIELD CORTEX IN RATS.....	189
Implications of Response Threshold on Neural Coding Strategies: Information Transmission Fidelity.....	190
Implications of Response Threshold on Rate Coding: Response Saturation.....	191
Implications of Response Threshold on Rate Coding: the Preferential Range.....	192
Implications of Response Threshold on Temporal Coding: Temporal Signature of Responses.....	193
Possible Mechanism for the Active Selection of Incoming Information by Cortex.....	194
REFERENCES .....	197



## LIST OF TABLE

<b>Table</b>	<b>Page</b>
2-1. Data Summary of the Experimental and Control Groups. ....	63

## LIST OF FIGURES

Figure	Page
1-1. Schematic Illustration of Rat's Vibrissa System. ....	7
1-2. Musculature of the Whisker Pad. ....	10
1-3. Delicate Structure of the Whisker Follicle. ....	12
2-1. Experiment design. ....	51
2-2. Histology Showing the Depth of Layer IV Barrels <i>in vivo</i> . ....	61
2-3. Chronic Unilateral Inactivation of SI by Muscimol Significantly Decreased the Evoked Response of Neurons in Contralateral D2 Barrel Column, while the Spontaneous Activity was Unaffected. ....	69
2-4. Chronic Unilateral Inactivation of SI by Muscimol Influenced the FSUs and RSUs in Contralateral D2 Barrel Column Differently. ....	71
2-5. Chronic Unilateral Inactivation of SI by Muscimol Significantly Decreased the Evoked Response of Neurons in both Superficial (Layer II/III) and Granular Layers in Contralateral D2 Barrel Column. But Changes of the Response of Infragranular (Mainly Layer V) Neurons were Insignificant. ....	73
2-6. Influences of Chronic Unilateral Inactivation of SI by Muscimol for 7 Days on the Layer IV FSUs and RSUs in Contralateral D2 Barrel Column. ....	75
2-7. Effect of Muscimol on Response Latency Epochs of Neurons in Contralateral D2 Barrel Column. ....	77
2-8. Effect of Muscimol Application on Response Latency Epochs of Layer IV FSUs and RSUs in the Contralateral D2 Barrel Column. ....	79
2-9. Effect of Muscimol Infusion on the Center/Surround Ratio of Neurons in the Contralateral D2 Barrel Column. ....	81

2-10.	Comparison of Data from Muscimol and Lesioned Animals. ....	84
3-1.	Experiment Design. ....	101
3-2.	Stimulus Intensity-Response Magnitude Curves of Two Selected VPM Neurons. ....	111
3-3.	Averaged PSTHs for a Narrow Range of Stimulus Intensities of Two VPM Neurons Shown in Figure 3-2. ....	113
3-4.	Temporal Changes of Normalized Response Magnitude in 8 VPM neurons after Muscimol was Applied onto the Contralateral BFC. ....	115
3-5.	Temporal Changes of Normalized Response Magnitude after Muscimol was Applied onto the Contralateral BFC in Experimental Group and Control. ....	116
3-6.	Receptive Field Properties of Unit VPM04 Confirmed by Histology. ....	118
3-7.	Response Changes of Unit VPM04 after Muscimol Application. ....	119
3-8.	Spontaneous Discharge and Distributions of the Modal Response Latency of Unit VPM04 before and after Muscimol Application. ....	120
3-9.	Averaged PSTHs of Unit VPM04 Sampled with Various Effective Time of Muscimol Suppression. ....	122
3-10.	Receptive Field Properties of Unit VPM02 Confirmed by Histology. ....	125
3-11.	Response Changes of Unit VPM02 after Muscimol Application. ....	126
3-12.	Spontaneous Discharge and Distributions of the Modal Response Latency of Unit VPM04 before and after Muscimol Application. ....	127
3-13.	Model of the Muscimol-Induced Response Curve Changes. ....	129

3-14.	Contralateral Muscimol Application Has a Greater Effect on POm Neurons than on VPM Neurons. ....	132
3-15.	Changes of Evoked Response and Spontaneous Activity are Greater in POm Units than on VPM Neurons after Muscimol Application. ....	133
4-1.	Experimental Design. ....	151
4-2.	Determination of the Relationship of the Tuning Properties between the VPM Unit Recorded and the Cortical Units Stimulated. ....	167
4-3.	Cortical Stimulation Sharpens the Angular Tuning Curve of Unit VPM12 that is “Both Spatially and Angularly Matched” with Cortex. ....	169
4-4.	Determination of the Relationship of the Tuning Properties between the VPM Unit12 and the Cortical Units Stimulated. ....	171
4-5.	Cortical Stimulation Sharpens the Angular Tuning Curves of “Both Spatially and Angularly Matched” VPM Neurons. ....	173
4-6.	Cortical Stimulation Boardens the Angular Tuning Curves of VPM Neurons that are “Spatially but not Angularly Matched” with Cortex. ....	175
4-7.	Cortical Stimulation Shifts the Angular Tuning Preference of VPM Neurons towards the Direction Cortex Prefers. ....	177
4-8.	Cortical Microstimulation Reduces the Responses of “Spatially Mismatched” VPM Neurons but Has No Apparent Influence on Angular Tuning. ....	179
4-9.	Cortical Microstimulation Has No Consistent Effects on Tuning Ratio Prime (Tr’). ....	180
4-10.	A Model for Cortical Modulation of Tuning Properties of VPM Neurons. ....	185

## CHAPTER I

### INTRODUCTION: CORTICAL MODULATION OF THALAMIC COMPUTATIONAL MAPS

The thalamus, as an informational gateway, conveys visual, auditory, and somatosensory information from periphery to cortex. In return, cortex projects extensively back to thalamus. These corticothalamic (CT) projections, which greatly outnumber the ascending synapses from the brainstem (Guillery, 1969; Liu et al. 1995), are assumed to provide functional “feedback” to the thalamus (Koch, 1987). The “feedback” concept is of special importance since it suggests that cortex is able to actively modulate sensory activity even at subcortical levels. Over the past century, evidence accumulated from numerous studies of different sensory systems in various species has demonstrated that corticofugal projections are involved in changing the transmission mode and/or the balance of center/surround of the receptive field of thalamic relay neurons as well as the firing synchrony during the animal’s sleep/wake cycle (for review, see Guillery and Sherman, 2002; Sherman and Guillery, 1996, 2002; Sillito and Jones, 2002; Steriade and Timofeev, 2003; Suga et al., 2003). Conceptually, in order to adapt to the rapidly-changing environment, the brain has to constantly shift its processing focus to the most salient events (the “hot-spot”) within the continuous information flow. Thus, dynamic mechanisms underlying the “attentive” selection of the most relevant ongoing information need to be clarified. Available literature suggests that top-down processes may facilitate the focus-shifting by cortex

(Alitto and Usrey, 2003; Crick and Koch, 1998; Hillenbrand and van Hemmen, 2002). Hence corticothalamic (CT) feedback projections could constitute a possible pathway for cortex to actively and selectively modulate the representation of the peripheral input near its information source. The anatomical reciprocity of CT projections, together with the findings that CT “feedback” increases the response gain and contrast of thalamic relay cells (Cudeiro and Sillito 1996; Przybylski et al., 2000; Sillito and Jones 1997; Sillito et al. 1994), indicates that CT projections may have precise control over the firing properties of thalamic relay neurons. Unfortunately, fundamental insights of the detailed functions of corticofugal system still remain elusive.

Although the cortical influence on the excitability of thalamic relay neurons was realized a long time ago (Anderson et al., 1972; Diamond et al., 1992b; Kalil and Chase, 1970; Ryugo and Wezinberger, 1976; Tsumoto et al., 1978; Villa et al., 1991; Yuan et al., 1985, 1986), its nature, whether the influence is excitatory or inhibitory, or both, has remained in debate (Anderson et al., 1972; Ryugo and Weinberger, 1976; Mishima, 1992; Diamond et al., 1992b; Villa et al., 1991). Only recently, it was realized that early studies employed a rather coarse method of massive inactivation/removal of cortex, instead of considering how the cortex modulates the responsiveness of thalamic relay neurons might depend on the relationship of the tuning properties between thalamic neurons recorded and cortical neurons manipulated (Suga and Ma, 2003). Currently it is quite accepted that the primary sensory cortex has a regulatory effect on response properties of thalamic relay neurons. Furthermore, other higher-order/associative cortical

areas might also have an indirect influence on thalamic neurons by modulating neurons in primary sensory cortex. For example, in visual systems feedback from Motion area MT onto primary visual cortex (VI) increases the response gain and contrast of neurons in VI (Hupe et al., 1998; Mignard and Malpeli, 1991). In the rat's vibrissa system, several lines of evidence suggest that the firing characteristics of neurons in the primary somatosensory cortex are modulated by neural activity in other cortical areas such as the contralateral homologous primary somatosensory cortex, the secondary somatosensory cortex and the motor cortex (Ahissar and Kleinfeld, 2003; Li et al., 2005; Rema et al., 2003; Krupa et al., 2004). Hence the indirect influence from distant cortical areas on thalamic relay neurons also needs to be examined. However, the knowledge of how the crosstalk between brain areas interacts with corticothalamic modulation is still limited.

Most neuronal cells are tuned to specific stimulus features. Neurons that are specific to different bands of energy (i.e. mechanic, electromagnetic, etc) are further tuned to certain parameters that define the physical properties of a stimulus such as intensity, frequency, orientation and direction. In sensory systems, neuronal cells tuned to different stimuli and/or different parameters of a stimulus are usually organized topographically into "computational maps" within the specific neural structure (Knudsen et al., 1987). These maps are thought to underlie higher order processes leading to perception and cognition. Thus examining changes in tuning properties of thalamic cells could provide the opportunity to investigate how cortex performs higher order functions. On the

other hand, stimulus-tuned neurons can be further categorized into groups that are tuned to “simple” parameters (such as ocular dominance or orientation in vision) or “complex” parameters (such as Doppler shift characteristic frequency, sound-echo interval in hearing) based on their importance to behavior or contribution to perceptual tasks. Thus by looking at how cortex influences the subcortical neurons that are sensitive to “complex” parameters, more subtle mechanisms that are involved in higher-order neuronal information processing may be revealed.

In the rat’s vibrissa (whisker) system, neurons representing whiskers at each brain level are organized into topographic “whisker maps”. These maps correlate well with the anatomically discrete cell aggregates, called “barrelettes” in the brainstem (Ma, 1991), “barreloids” in thalamus (Van der Loos, 1976) and “barrels” in layer IV of the primary somatosensory cortex (SI) (Woolsey and Van der Loos, 1970), each containing a map of the spatial arrangement of whiskers on the face (Figure 1-1). In addition, neurons within the whisker map are also sensitive to many other parameters of whisker deflections such as amplitude and frequency as well as direction, indicating multiple maps of sensory features may co-exist in a single neural structure. The directional preference of neurons in rat vibrissa system has been demonstrated repeatedly. Primary sensory trigeminal neurons are highly tuned to direction (Gibson and Welker, 1983a, b; Lichtenstein et. al, 1990; Zucker and Welker, 1969), and the angular tuning characteristics have been described for neurons in brainstem (Minnery and Simons, 2003; Minnery et. al, 2003; Shipley, 1974), thalamus (Chiaia et al., 1991a, b; Minnery et.



al, 2003; Timofeeva et. al, 2003) and neocortex (Bruno et. al, 2003; Lee and Simons, 2004; Simons and Carvell, 1989). Since direction sensitive neurons provide information about the direction of a stimulus in the receptive field, it is quite reasonable to speculate that neurons sensitive to the direction of whisker deflections would be involved more in higher order information processing stages, compared with the classical receptive field responses based on magnitude alone. Thus, an intriguing question is whether the angular tuning map of VPM neurons is independent of cortical influence.

This thesis is aimed at developing a better understanding of the cortical influence on computational maps at subcortical levels by studying how cortex modulates the tuning properties of thalamic relay neurons using rat's vibrissa system as the model system. In the following section of this Chapter, a brief introduction will be made to the rat's vibrissa system. The well-studied whisker-to-barrel ascending pathway and relatively less well-known, but possibly functionally important corticothalamic descending pathway, will be described. This chapter will also discuss the most recent anatomical and physiological advances in this system, such as the newly discovered extralemniscal pathway and the extrareticular system. Special emphasis will be placed on the angular tuning properties of neurons at each level. Chapter II will discuss the interhemispheric interaction in rat's vibrissa system by demonstrating that the responsiveness of neurons in one barrel field cortex (BFC) to the peripheral inputs could be modulated by the homotopic area in the other hemisphere in an activity-dependent manner. Chapter III will provide novel evidence that thalamic

relay neurons are strongly modulated by activity levels in the contralateral as well as in the ipsilateral SI cortex, with mechanism for the modulation based on shifting the stimulus-response curves (sensitivity) of thalamic neurons, which renders them more or less sensitive to activation by sensory stimuli. Chapter IV will investigate the role of cortical feedback on dynamic adjustments of the thalamic angular tuning map in rats' vibrissa system, by showing that the microstimulation of layer VI of the homologous barrel columns sharpens the angular tuning curves of VPM neurons tuned to the same direction with cortex; but realigns the angular preference of the thalamic neurons tuned to other directions towards the direction that cortex prefers. Stimulating layer VI in the non-homologous barrel columns can suppress responses of VPM neurons, but has no consistent effects on angular tuning. Hence we conclude that cortex actively and continually directs many properties of thalamic VPM neurons, i.e., one way to optimize thalamic relay neurons' ability to reflect the salience of the incoming sensory message. Finally, as concluding remarks, Chapter V will summarize the findings in the preceding chapters and further propose that the active modulation of tuning maps by cortex might be achieved through changing of synaptic efficacy which is related to the spike-timing-dependent-plasticity (STDP).

### **Brief Introduction to the Rat's Vibrissa System**

Unlike human-beings who rely heavily on vision, rats seem to depend more on their whiskers than on visual cues (Vincent, 1912). Rats have roughly 25

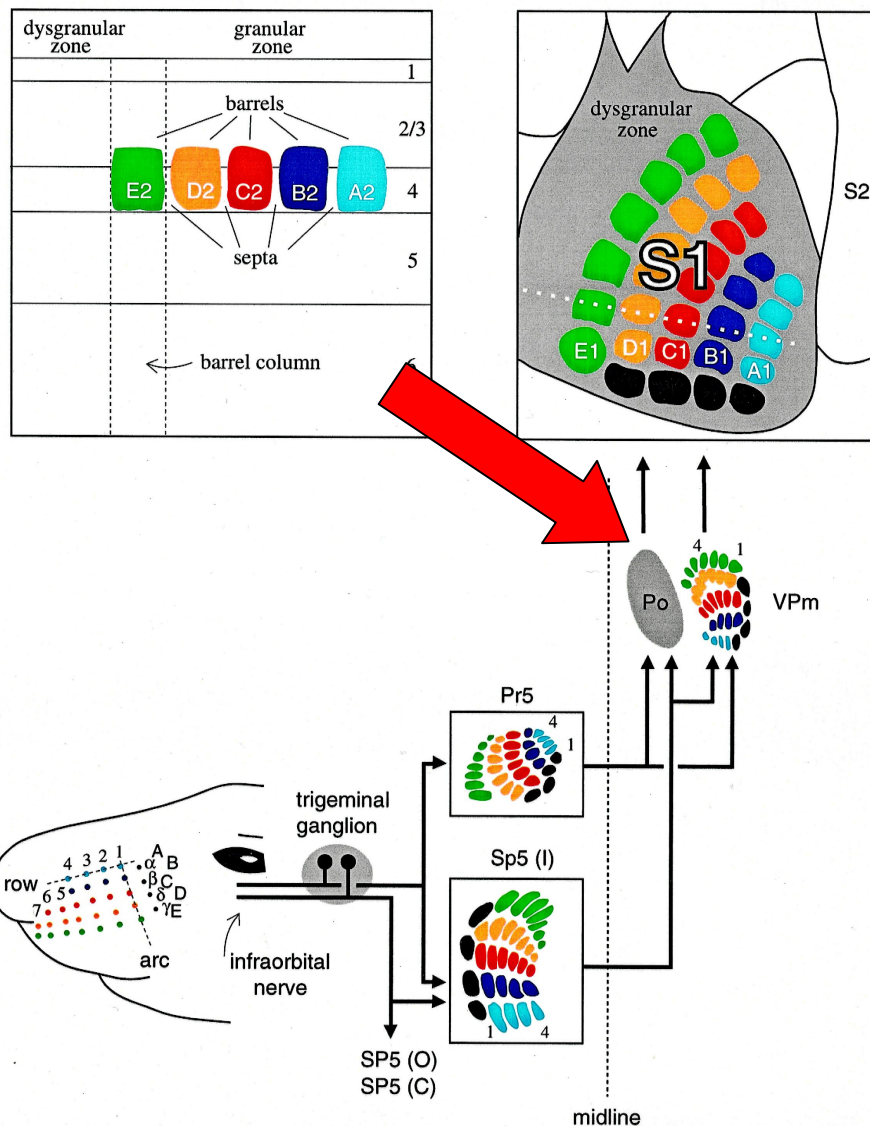


**Figure 1-1. Schematic Illustration of Rat's Vibrissa System.**

Rat has nearly 30 whiskers on each side of its face. These whiskers roughly form a 5X5 array, consisting of A, B, C, D and E rows from dorsal to ventral and 1, 2, 3, 4 and 5 arcs from caudal to rostral with alpha, beta, gamma and delta straddlers between rows. Information sampled by whiskers is conveyed from whisker pad to cortex through clusters of neurons in whisker presentation area at each brain level. These clusters are organized somatotopically, which replicates the spatial arrangement of whiskers at periphery and form a strict one to one relationship between each whisker and each cluster of cells. In addition to the ascending pathway, cortex projects extensively back to thalamus as well. These corticothalamic projections (red arrow) are highly reciprocal and actually outnumber the ascending inputs from brainstem. However, the functional details of the corticothalamic "feedback" system are not clearly understood. (modified from Deschenes et al., 1998)

whiskers on each side of the face, however, this small array of sensors can generate a detailed perception of the outer world, as exemplified by behavioral studies that require rats to perform tasks using only their whiskers (Carvell and Simons, 1990; Guic-Robles et al., 1989; Krupa et al., 2001; Polley et al., 2005). Highly organized somatotopic maps are maintained in the whisker representation areas at each brain level by cell clusters replicating the spatial arrangement of whiskers on the whisker pads, and the encoded important features of whisker movements are inherited and integrated by neurons along the ascending pathway through tremendous convergence and divergence of neural circuitries between and within brain levels (Armstrong-James and Fox, 1987; Chiaia et al., 1991a, b; Gibson and Welker, 1983a, b; Jacquin et al., 1986a, b; Lichtenstein et al., 1990; Simons and Carvell, 1989; Waite, 1973a, b; Welker, 1976; Williams et al., 1994; Zucker and Welker, 1969). Processing of whisker information is greatly facilitated by unique features of the rat vibrissae system, which are briefly introduced in the following text.

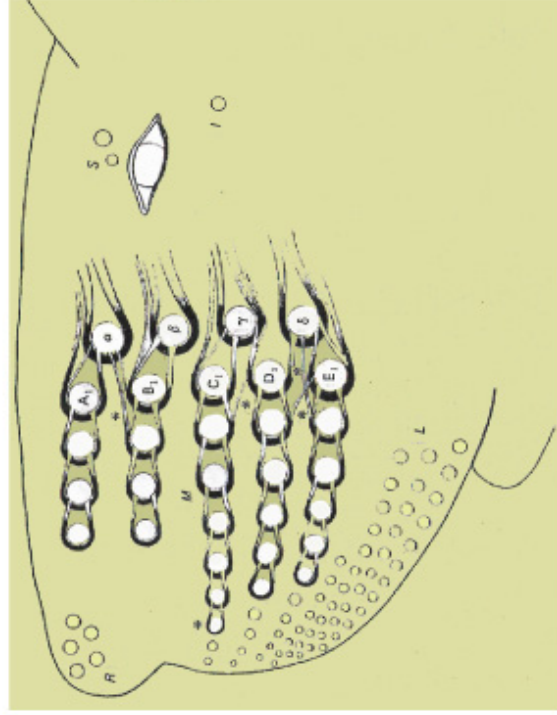
## **The Whisker to Barrel Ascending Pathway**

### ***The Whisker Pad***

Rats' mystacial vibrissae are categorized into two classes by their size: microvibrissae, which are the rostral, short and thin hairs around the nose tip; and macrovibrissae, or mystacial vibrissae (whiskers), referring to the long and thick hairs caudal to microvibrissae (Brecht et al., 1997). Two classes of vibrissae are functionally different (Vincent, 1912; Brecht et al., 1997). It is suggested that

caudal macrovibrissae could contribute more to object localization in space since they are individually controlled in rats and mice; and rostral microvibrissae may be more important to gather detailed information in object recognition due to the fact that they are short and not moved by intrinsic muscles (Brecht et al., 1997). However, evidence from behavioral studies demonstrates that rats are able to successfully perform rather complex perceptual tasks solely with their large whiskers (Carvell and Simons, 1990; Krupa et al., 2001; Polley et al., 2005), indicating that whiskers convey textural as well as spatial information of objects contacted by the whiskers. Whiskers on each side of the rat snout are organized into a 5 x 5 array with five horizontal rows A, B, C, D and E from dorsal to ventral, and 1, 2, 3, 4 and 5 arcs from caudal to rostral, respectively (Fig. 1-1). Freely-behaving rats move their whiskers on both whisker pads back and forth regularly at a frequency of ~8 Hz when exploring the environment (Sachdev et al., 2001; Welker, 1964). The pattern of whisker usage is dependent on the level of vigilance, or alertness of the animal (Fanselow and Nicolelis, 1999; Vincent, 1912; Welker, 1964). Movements of individual whiskers are generated by intrinsic muscles, which are a set of small muscles that have both their origin and insertion in the skin (Dorfl, 1982) (Fig. 1-2). The sensitivity of whisker to displacement can presumably be increased by a cavernous tissue blood sinus surrounding the vibrissa follicle (Dorfl, 1985; Rice et al., 1997), but the exact function of the blood sinus is unknown. Contraction of extrinsic facial muscles moves all vibrissae as a group (Carvell et al., 1991; Dorfl, 1985). These features facilitate the delivery of precise stimuli to the receptors in one follicle and

**a. Intrinsic Muscles**



**b. Extrinsic Muscles**

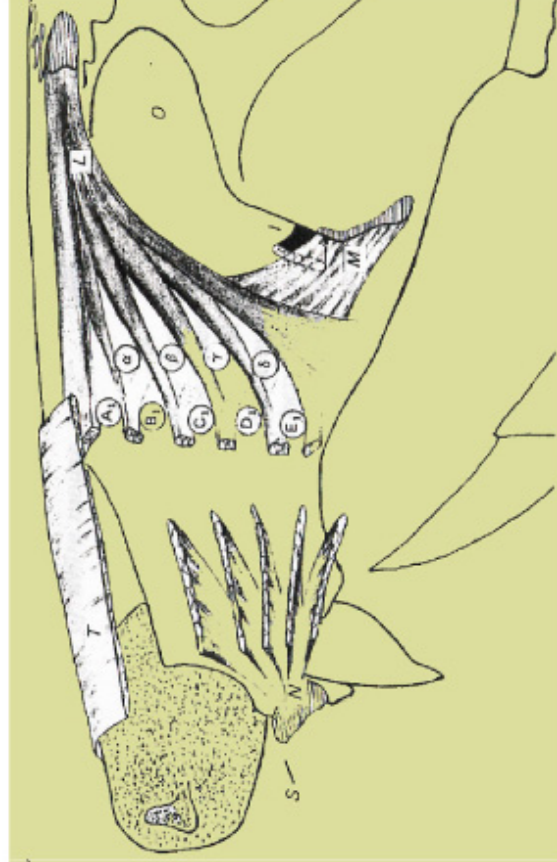


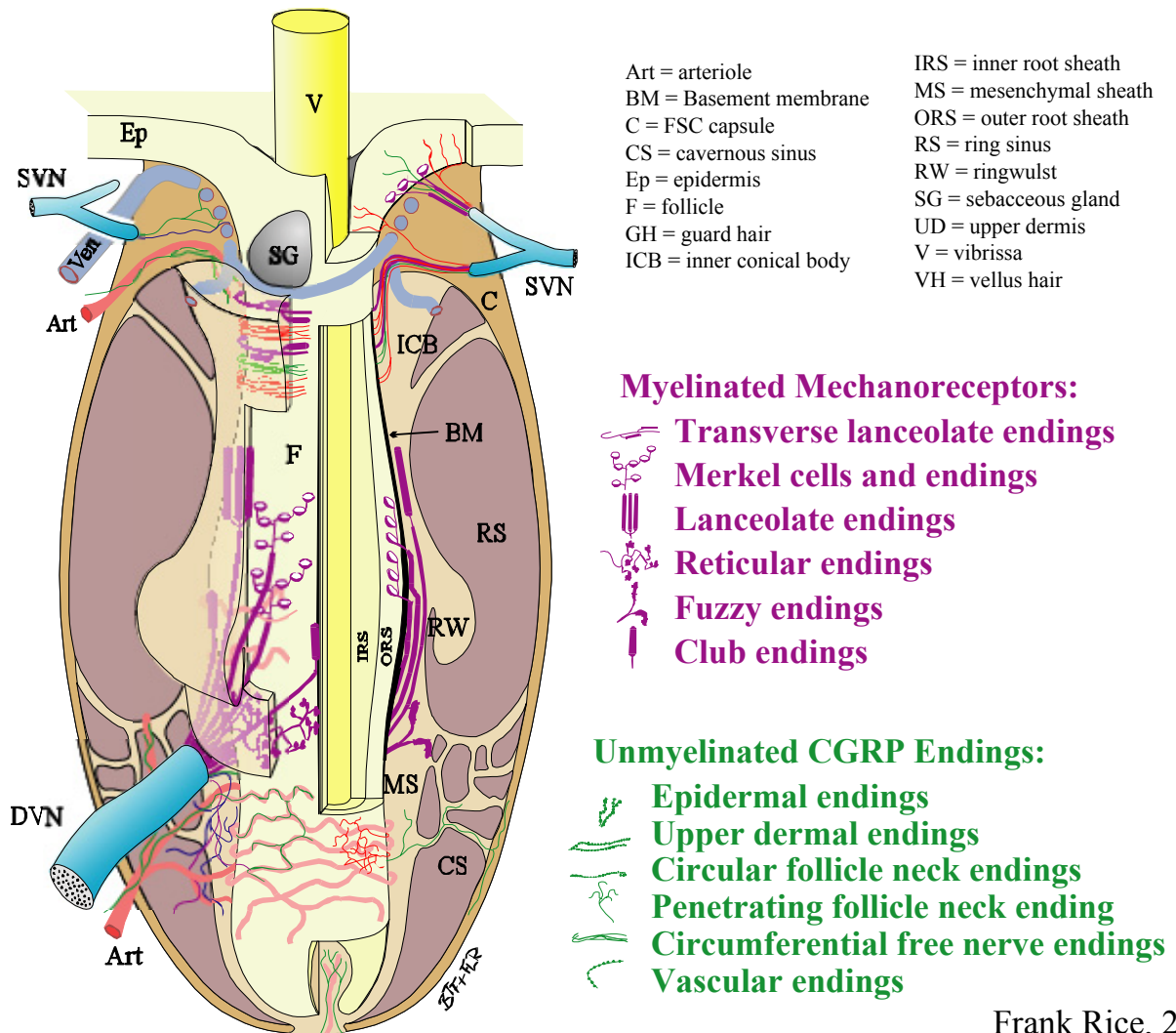
**Figure 1-2. Musculature of the Whisker Pad.**

**a.** Drawing shows the innervation patterns of intrinsic muscles in white mouse. Intrinsic muscles are those without attachment to the bone. Here whisker follicles are presented as big circles. Each of the follicles is surrounded by a sling of intrinsic muscles. Contraction of intrinsic muscles moves whiskers individually. I: infraorbital, L: labial, M: mystacial, R: rhinal, S: supraorbital. Asterisks show rare bundles of muscles. **b.** Drawing illustrates the distribution of extrinsic muscles. Extrinsic muscles are attached to the skull. Follicles of the straddlers and arc 1 are shown as circles. Contraction of extrinsic muscles moves whiskers on the whole whisker pad. I: infraorbital nerve, L: m. levator labia superioris, M: m. maxillolabialis, N: m. nasalis, O: orbit, T: m. transversus nasi, S: septum intermusculare. (From Dorfl, 1982)

reproducibly activate central neurons.

### ***The Whisker Follicle***

In rats' exploratory behavior, whiskers act as mechanical transducers (Halata and Munger, 1980; Hoggan and Hoggan, 1892; Melaragno and Montagna, 1953; Vincent, 1913). As a whisker encounters objects within its trajectory, the contact event is transmitted to its base, presumably in the form of the traveling wave along the whisker, although the details of this procedure is just beginning to be understood (Hartmann et al., 2003; Neimark et al., 2003). Disturbance of whiskers activates low-threshold mechanoreceptors within the whisker follicles. These receptors, including Merkel cell-neurite complexes, Ruffini corpuscles, lanceolate receptors and free nerve endings, arrange themselves around the whisker shaft in vibrissa follicles (Melaragno and Montagna, 1953; Rice et al., 1986, 1997). Merkel cell complexes are the most numerous receptors in follicles. These receptors are highly sensitive to various parameters of a whisker stimulus, such as the amplitude, duration, velocity, acceleration and direction of whisker deflections (Fitzgerald, 1940; Zucker and Welker, 1969). In addition to various tuning properties, receptors within whisker follicles also show different types of adaptation. Merkel cell-neurite complexes and Ruffini corpuscles adapt slowly to sustained whisker deflections; but lanceolate receptors and simple corpuscles are rapidly-adapting (Halata and Munger, 1980). All these features ensure that whisker movements are faithfully



Frank Rice, 2001

**Figure 1-3. Delicate Structure of the Whisker Follicle.**

Schema showing the detailed structure of one typical whisker follicle. Note that the whisker follicle is innervated by several types of mechanoreceptors. These receptors distribute in a predictable arrangement within the whisker follicle. CGRP: Calcitonin gene-related peptide. (Courtesy to Frank L. Rice, see also Ebara et al., 2002)



translated into trains of spikes. Exactly how these receptors encode the amplitude, duration, velocity, acceleration and direction of whisker deflections into spike trains still remains to be worked out. All sinus whisker follicles are the same with the same internal structure (Fig. 1-3). Each follicle is physically separated and functionally independent, innervated by ~200 myelinated and 100 unmyelinated (Waite and Cragg, 1982; Renehan et al., 1988; Rice et al., 1997) axons of trigeminal ganglion cells. These axons arborize to make several contacts with the hair shaft, thus whisker information is relayed to upper levels.

### ***The Trigeminal Ganglion***

Whisker follicles are innervated by distal axons of trigeminal ganglion neurons (Melaragno and Montagna, 1953; Vincent, 1913). Trigeminal ganglion cells are pseudo-unipolar neurons whose cell bodies are located in the trigeminal ganglion with their proximal axons innervating the ipsilateral trigeminal brainstem complex (TBC) (Arvidsson, 1982; Ma and Woolsey, 1984; Vincent, 1913). The trigeminal ganglion is organized topographically with the dorsal whiskers (A row) generally projecting ventral laterally; the rostral vibrissae usually project ventrally and caudal vibrissae dorsally (Zucker and Welker, 1969). Each ganglion cell innervates only one whisker follicle (Rice et al., 1986) and these distal axons enter the follicles as two populations (Hilata and Munger, 1980). One population forms the deep vibrissal nerve, the other forms the superficial vibrissal nerve (Drofl, 1985; Melaragno and Montagna, 1953; Renehan and Munger, 1986; Rice et al., 1986; Waite and Jacquin, 1992). Central processes of trigeminal ganglion

cells bifurcate and enter all nuclei of TBC (Hayashi, 1980; Jacquin et al., 1993). Subtle distinctions exist in the morphology and branching pattern of primary fibers entering different subnuclei in TBC, but physiologically distinct elements (i.e. fast-adapting vs. slowly adapting axons) within each subnucleus are morphologically indistinguishable (Jacquin et al., 1986a, b; Jacquin et al., 1993). Primary fibers innervating the nucleus principalis (PrV) have spatially circumscribed axonal arbors whose major part overlaps well with the CO dense zone of the corresponding whisker in PrV (Jacquin et al., 1993). However, collaterals of the first-order axons entering the SpVi tend to cover the mediolateral extent of the SpVi cells groups (Arvidsson, 1982; Belford and Killackey, 79; Jacquin et al., 1986a, but also see Hayashi, 1982).

### *Physiological Properties of the Trigeminal Ganglion Neurons*

Trigeminal ganglion cells are extraordinarily sensitive to various parameters of whisker movements, including the amplitude, velocity, duration, frequency and direction of deflections (Gibson and Welker, 1983a, b; Lichtenstein et al., 1990; Zucker and Welker, 1969). The response threshold of some first-order neurons is as low as 5-10  $\mu\text{m}$  (Gibson and Welker, 1983a); and other ganglion cells can even follow whisker vibrations as high as 1500 Hz in a phase-lock manner (Gottschaldt and Vahle-Hinz, 1981). Trigeminal ganglion cells adapt to sustained whisker deflections rapidly or slowly, but the proportion of rapidly and slowly adapting units in trigeminal ganglion varies in different reports (Gibson and Welker, 1983b; Jacquin et al., 1993; Lichtenstein et al. 1990; Zucker

and Welker, 1969). The majority of ganglion neurons show low spontaneous activity ( $\leq 1$  Hz), but discharge at a rate significantly higher than the background when certain whisker(s) are deflected (Gibson and Welker, 1983a; Jacquin et al., 1986a; Jacquin et al., 1993; Zucker and Welker, 1969). All physiological studies agreed that trigeminal ganglion neurons strictly respond to the stimulation of only one whisker (Gibson and Welker, 1983a; Lichtenstein et al., 1990; Zucker and Welker, 1969). Responses to more than one whisker have been reported, but there is good reason to attribute such responses to exogenous factors (Lichtenstein et al., 1990). Ganglion cells providing axons to the deep and superficial vibrissal nerve have similar receptive field characteristics in recording (Rice et al., 1986; Waite and Jacquin, 1992).

### ***The Trigeminal Brainstem Complex***

#### *Cytoarchitectonic Structure of the Trigeminal Brainstem Complex*

The whisker-receptant nuclei in the brainstem consist of the principal trigeminal nucleus (PrV) and three subdivisions of the spinal trigeminal nucleus (SpV): oralis (SpVo), interpolaris (SpVi) and caudalis (SpVc) (Arvidsson, 1982; Hayashi, 1980; Henderson and Jacquin, 1995). TBC neurons receiving vibrissa input from the trigeminal ganglion form discrete cell aggregates (in the transverse plane) in each sub-nucleus, except the SpVo (Ma, 1991; Jacquin et al., 1993). There are roughly ~30,000 neurons in PrV, SpVi and SpVc contain around 3,000 and 500 neurons, respectively (Henderson and Jacquin, 1995). Spatial arrangements of cell aggregates mimic the organization of the whisker array in

the periphery (Belford and Killackey, 1979; Hayashi, 1980) hence the entire whisker array is represented somatotopically. These cell clusters, as revealed by staining for mitochondrial enzymes like cytochrome oxidase (CO), or succinic dehydrogenase, were named “barrelettes” (Ma, 1991). Each barrelette in PrV is about 55  $\mu\text{m}$  in diameter and 1.2 mm long (Jacquin et al., 1993; Henderson and Jacquin, 1995) containing 160 - 200 neurons (Timofeeva et al., 2003). Most PrV barrelette neurons have narrow, barrelette-bounded dendritic trees (Jacquin et al., 1993; Veinante and Deschenes, 1999). Neurons in SpVi spread their dendritic arbors into a larger area covering multiple barrelettes and accordingly show responses to many whiskers (Woolston et al, 1982; Jacquin et al., 1986a). Within each nucleus there is a distinction between projection and local circuit neurons (Jacquin et al., 1986b). As we will see in the following text, the PrV and SpVi subnuclei provide the majority of the projections to the thalamus, and they are the main focus of the discussion.

### *Physiological Properties of Neurons in Trigeminal Brainstem Complex*

TBC is the first site of divergence in the pathway. In physiological recording, TBC neurons are usually activated by more than one whisker. The whisker that evokes the highest magnitude responses with shortest latency is called the “principal whisker” (PW) to this neuron (Gibson and Welker, 1983a; Lichtenstein et al., 1990; Simons, 1978). Other whiskers that fire neurons with lower magnitude and relatively longer latency are accordingly named as “adjacent whiskers” (AWs) or “surround whiskers” (SWs) (Armstrong-James and

Fox, 1987; Simons, 1978). The principal whisker plus other whiskers that activate the cell constitute the classical receptive field of a given neuron in the rat vibrissa system. The structure of the TBC RF is more complex in TBC than that of trigeminal ganglion cells. Two physiologically distinct classes of PrV neurons were reported that have parallels in the anatomical data: neurons in PrV that project to the ventroposterior medial nucleus (VPM) in the contralateral thalamus have dendritic trees contained within the single barrelette and, thus show single whisker receptive fields. Large PrV cells usually show expansive dendritic arbors with multi-whisker RFs and these cells innervate the rostral division of posterior nucleus (POm), tectum, pretectum, zona incerta, the medial part of the medial geniculate nucleus and ventral posteromedial nucleus (Jacquin et al., 1988; Shipley, 1974; Veinante and Deschenes, 1999). But the reported proportion of these two neuron classes varies among studies, presumably due to the different anesthetic agent and whisker stimuli employed in individual experiments (Veinante et al., 2000b; Minnery and Simons, 2003; Minnery et al., 2003). PrV neurons respond to sustained whisker deflection tonically or phasically, and tonic neurons typically show a single whisker receptive field, but phasic neurons respond to single or multiple whiskers (Shipley, 1974). The receptive fields of neurons in SpVo, SpVi and SpVc are larger, around 6-8 whiskers. Most SpVi neurons have multiple whisker receptive fields and receptive field size is highly correlated with the size of the dendritic tree area (Jacquin et al., 1989a). Neurons projecting to the thalamus (POm, see following text) have a receptive field of 3-16 whiskers, while neurons projecting to the cerebellum have

receptive fields of 1-20 whiskers (Woolston et al., 1982; Jacquin et al., 1986a; Jacquin et al., 1989a). Local interneurons have single whisker, single tooth, or guard hair receptive fields, while the neurons projecting to cerebellum and thalamus have multiwhisker receptive fields and the receptive field size of local circuit neurons can be modified by cortical lesions (Jacquin and Rhoades, 1990; Jacquin et al., 1989b). SpVc neurons have multiple-whisker receptive fields, including the whisker guard hairs that are located between the large vibrissae (Renehan et al., 1986). ~50 percent of SpVo neurons have multiple whisker receptive fields (Gibson, 1987; Jacquin et al., 1990).

#### *Output Projections of the Trigeminal Brainstem Complex*

At the brainstem level, the TBC projects to the lateral subdivision of the facial nerve nucleus and the hypoglossal nucleus (Aldes and Boone, 1985; Erzurumlu and Killackey, 1979). The TBC also projects to the superior colliculus, cerebellum, medial subdivision of the medial geniculate body (MGBm), zona incerta, anterior pretectal nucleus and inferior olive (Huerta et al., 1983; Peschanski, 1984; Steindler, 1985; Smith, 1973; Yoshida et al., 1992). But the majority of TBC fibers cross the midline and innervate the contralateral thalamus, mainly the VPM, POm and the intralaminar nuclei (Chiaia et al., 1991a; Feldman and Kruger, 1980; Peschanski, 1984; Spacek and Lieberman, 1974; Veinante and Deschenes, 1999; Veinante et al., 2000b; Williams et al., 1994). At least two types of projecting neurons were identified within PrV. Most PrV neurons (70~90%) have small cell bodies with dendritic trees constrained within single

barrellets and innervate the “core regions” of VPM (the medial dorsal part of VPM, VPMdm) (Saporta and Kruger, 1977; Veinante and Deschenes, 1999) through the medial lemniscus. The remainder of the PrV neurons (10~30%) are larger in soma size and their dendritic trees cover a broader area. These neurons mainly project to POm and the tectum (Veinante and Deschenes, 1999, see preceding text). PrV also send collaterals to the superior colliculus, MGm, zona incerta, anterior pretectal nucleus and inferior olive (Huerta et al., 1983; Peschanski, 1984; Smith, 1973; Yoshida et al., 1992). Axons of the spinal trigeminal subnuclei are generally sparser but distribute relatively more widely than those of PrV. They mainly innervate POm and/or VPM through the “paralemniscal” pathway (Erzurumlu et al., 1980; Veinante et al., 2000b). SpVi projects to both VPM and POm (Veinante et al., 2000b). Two classes of neurons can also be identified in SpVi (Jacquin et al., 1986a; Jacquin et al., 1989; Veinante et al., 2000b). Neurons in SpVi with thick axons (conducting faster) go to POm while those having thin axons with slow conducting speed innervate the “tail region” of VPM (the ventral lateral part of VPM, VPMvl) (Williams et al., 1994; Pierret et al., 2000; Veinante et al., 2000b). The distribution of trigeminal terminals in VPM creates a complementary pattern, with PrV fibers terminating in the barreloids and SpVi fibers terminating in the zones surrounding the barreloids and the ventral lateral “tail” area (VPMvl). Projections from SpVc also terminate in the VPM tail region, in a way similar to the thin axons of SpVi. SpVo sends only a few axons to POm (Veinante et al., 2000b).

## ***The Thalamus***

As mentioned, VPM, POm and the intralaminar nuclei are the major thalamic targets of TBC (Chiaia et al., 1991a; Diamond, 1995; Feldman and Kruger, 1980; Spacek and Lieberman, 1974; Veinante and Deschenes, 1999; Veinante et al., 2000b; Williams et al., 1994). In VPM, the vibrissae representation area is organized into discrete finger-like structures, as revealed by CO staining (Van der Loos, 1976; Woolsey et al., 1979). These cell aggregates, called “barreloids” (Van der Loos, 1976), receive driving inputs from whiskers at periphery in a strict one-to-one manner (Land and Simons, 1985; Sugitani et al., 1990; Waite, 1973a). In adult rats, the whisker map in VPM is distorted, with the ventral rows of whiskers (e.g., E row) projecting to the rostral part of VPM, dorsal rows to the caudal part; caudal arcs (e.g., arc 1 and straddlers) to the dorsolateral portion and rostral whiskers to the ventromedial area of VPM (Haidarliu and Ahissar, 2001; Sugitani et al., 1990; Waite, 1973a). After three-dimension reconstruction from histological sections, barreloids are oblong cylinder-like structures, with a length of 500~900  $\mu\text{m}$  and the size of the barreloids is positively correlated with the length of whiskers on the whisker pad (Haidarliu and Ahissar, 2001; Timofeeva et al., 2003). Each barreloid consists of a dorsomedial part, which is usually the darker staining area after CO and called the “core region”, with a lightly stained “tail region” extending ventrolaterally (Saporta and Kruger, 1977). POm is more homogeneous than VPM. No barreloid-like structures are found in POm. However, there is evidence that POm is organized topographically (Diamond et al., 1992a).



### *Cytoarchitectonic Structure of VPM*

Each barreloid contains around 200 neurons that convey vibrissa information (Land et al., 1995; Varga et al., 2002). Unlike the sensory-specific thalamus for other modalities, VPM in rats is devoid of inhibitory interneurons (Barbaresi et al., 1986; Harris, 1986; Ohara and Havton, 1994). VPM relay neurons are stellate cells, with most of their dendritic arbors constrained within the home barreloids (Chiaia et al., 1991b). However, the distal dendrites of VPM neurons always extend into the adjacent barreloids (Lavallee et al., 2004; Varga et al., 2002). Dendritic trees of VPM cells are not symmetrical but take an ellipsoidal or bitufted shape (Chiaia et al., 1991b). Although some dendrites of VPM cells extend as far as 180  $\mu\text{m}$  away from the soma, most synaptic contacts occur within the radius of 60-70  $\mu\text{m}$  (Chiaia et al., 1991b; Liu et al., 1995). The dendritic trees of barreloid neurons usually generate four to nine primary branches. These features remain consistent among VPM neurons but the orientation of the dendritic arbors varies (Chiaia et al., 1991b). One VPM cell receives roughly 5,500 - 9,000 synapses on average (Guillery et al., 1969; Liu et al., 1995), including the glutamatergic synapses from TBC axons, GABAergic cells in the thalamic reticular nuclei (RTN), glutamatergic from layer VI of BFC, the cholinergic from the parabrachial region of the brainstem (PBR) (Castro-Alamangos, 2004; Liu et al., 1995). Synapses by lemniscal afferents are the largest and locate on the soma and proximal dendrites (de Biasi et al., 1994; Liu et al., 1995; Williams et al., 1994). They are classified as 'RL' type (standing for round vesicle and large profile) using electron microscopy due to their spherical

vesicles and multiple, asymmetric synaptic contacts. RL type synapses are more frequent on the proximal dendrites and soma, decrease rapidly along the dendritic shaft. The signatures of lemniscal synapses are their complex ultrastructure called “glomeruli” (Spacek and Lieberman, 1974). A glomerulus is about 5  $\mu\text{m}$  in diameter, in which the presynaptic terminals of trigeminal axons embrace the excrescences or protrusions of the postsynaptic dendrites of VPM neurons (Spacek and Lieberman, 1974). On average a glomerulus contains ~10 excrescences with a total of 44 synaptic contacts and the whole structure is ensheathed by glial cell (Spacek and Lieberman, 1974). Intracellular studies indicate that in average individual barreloid neurons receive synaptic inputs from one to three medial lemniscal fibers (Castro-Alamancos, 2002; Deschenes et al., 2003). But these unique structural features, together with their somatal and proximal location, lead to a very powerful and reliable drive to VPM neurons. Similar synaptic structures of ascending input have also been found in the lateral geniculate nuclei (LGN) of cats and monkeys and called “triads” (Sherman and Guillery, 2002). The GABAergic synapses of RTN cells are relatively small, exhibit flattened or pleomorphic vesicles and symmetric contacts. Thus, these are called ‘F’ (short for flattened vesicle) terminals. Like the other terminals so far described, these are strictly presynaptic. RL and F type synapses are predominant on the proximal dendrite and soma (~50% each) (Liu et al., 1995), but the density of F type synapses remains at a considerable level even on the distal dendrite arbors (Liu et al., 1995). The terminals from cortical layer VI and PBR are relatively small. They have spherical vesicles and form asymmetric

contacts (usually one per terminal) and never postsynaptic. They are known as 'RS' type (for round vesicle and small profile) and synapse the distal dendrites of thalamic neurons (Bourassa et al., 1995; Erisir et al., 1997; Jones and Powell, 1969; Li et al., 2003; Zhang and Deschenes, 1997). The small terminals formed by layer VI corticothalamic fibers have a small postsynaptic density that is consistent with the presence of a single release site. In rats' VPL, synapses from cortex are predominant in number: only 15% synapses on one VPL neuron are from brainstem while around 50% are RS type, which mostly are from cortex (Liu et al., 1995). Unfortunately, the corresponding data of VPM is actually absent. However, similar results have also been reported in cat and monkey visual system (Sherman and Guillery, 2002; Sillito and Jones, 2002).

### *Physiological Properties of Thalamic Relay Neurons*

Both *in vivo* and *in vitro* recording demonstrates that thalamic relay neurons generally fire in two modes: tonic and bursting (for review, see Sherman and Guillery, 1996, 2002). Transition from tonic to bursting firing requires inactivation of the voltage-dependent, low-threshold  $\text{Ca}^{2+}$  current  $I_T$  (for review, see Sherman, 2001a; Sherman and Guillery, 2002). Interestingly, this procedure seems to be regulated by neuromodulators which control the arousal level of the animal (Castro-Alamancos, 2004; Steriade et al., 1986). Thus, the spatial and temporal response properties of thalamic relay neurons greatly depend on the recording conditions. As discussed above, under anesthesia neurons in the dorsomedial part of VPM respond only to 1 or 2 whiskers (Chiaia et al., 1991b;

Ito, 1988; Sugitani et al., 1990; Waite, 1973a). The RF size of neurons in the VPM “core” region varies as a function of the anesthesia depth (Friedberg et al., 1999; Minnery et al., 2003; Nicolelis et al., 1995). As the anesthesia becomes lighter, neurons in VPMdm respond to whiskers other than PWs which evoke weaker responses with longer latency. VPM neurons receive input from PrV, SpVi, barrel cortex and thalamic reticular nucleus, thus the receptive field of VPMdm cells is strongly influenced by these brain areas/nuclei. The receptive field size is gated by the thalamic reticular nucleus and involves GABA-mediated inhibition (Lee et al., 1994). Ipsilateral BFC can also alter the center-surround organization of VPMdm neurons through the CT feedback projections (Temereanca and Simons, 2004). Lesioning the contralateral SpVi shrinks the RF size of neurons in VPMdm as well (Timofeeva et al., 2003; Friedberg et al., 2004). As for the temporal response properties, VPMdm neurons can follow repetitive whisker stimuli at low frequency. At higher frequency (>10Hz), responses will be greatly suppressed by inhibitory feedback from RTN (Castro-Alamangos, 2004). However, as the arousal level of the animal increases, the membrane properties of relay and RTN neurons are greatly altered so that higher frequency information is relayed to cortex more efficiently due to the disinhibition from RTN (Castro-Alamancos, 2004). So far little is known about the physiological properties of neurons in VPM “tail” region. VPMvl cells have a receptive field much larger than VPMdm neurons and may fire in synchrony with whisker touch (Timofeeva et al., 2003; Yu et al., 2006). Recent study suggests that VPMvl neurons might be specialized for encoding the whisker contact with objects (the

“touch” signal) (Yu et al., 2006). The distinct properties of VPMvl neurons lead to a postulate of the extralemniscal pathway (Yu et al., 2006). Studies also indicate the existence of whisker map in POm (Diamond et al., 1992b; Alloway et al., 2003). The topography of whisker map in POm is roughly a mirror image to that in VPM (Diamond et al., 1992a, b). Compared with VPM cells, receptive fields of POm neurons are larger, usually 6-8 whiskers. In anesthetized preparations, single POm neurons show a weaker response to single whisker deflections, and in contrast to the classic strong preference to single whisker in VPM, POm neurons are lack of whisker preference (Diamond et al., 1992b; Ahissar, 1998). On the contrary, POm cells are best driven by simultaneous disturbance of several whiskers such as a brush stroke across the whisker pad. And many POm neurons show responses to multimodal cutaneous and even deep receptor stimuli (Sachdev et al., 2001). The blur image of RF and wild tuning properties of POm neurons make them difficult to study, and since the drive that POm receives from cortical layer V is more powerful than the ascending inputs from brainstem, POm neurons are highly modulated by the cortical feedback (Diamond et al., 1992b; for review, see Sherman and Guillery, 2002). These features distinguish POm from VPM in the functional role in brain circuitries. VPM seems to be more like a relay station while POm is suggested to play a role in the information exchange between cortical areas through the cortico-thalamo-cortical loop (Sherman and Guillery, 1996, 2002). Hence VPM and POm are accordingly named as “first order” and “higher order” relay nuclei respectively (Guillery, 1995). In response to repetitive whisker stimulations, POm neurons adapt much faster

than VPM neurons (Ahissar et al., 2000). As for the intralaminar thalamic nuclei, they are innervated by sensory and motor cortices and subcortical regions, such as superior colliculus, and project to the medial and deep layers of sensory and motor areas in cortex (Grunberg and Krauthamer, 1990; for review, see Groenewegen and Berendse, 1994). Recent studies (Crabtree and Isaac, 2002) indicate that the connections between intralaminar thalamic nuclei and RTN may provide a possible pathway for the intra-modality and cross-modality inhibition in dorsal thalamus. The response properties of cells between barreloids have not been described.

#### *Output Projections of VPM to Barrel Field Cortex*

VPM, POm and intralaminar nuclei all relay vibrissae information to the ipsilateral cortex, but the areal and laminar distribution of their axonal arbors is quite different. Efferents of VPM neurons in the “core” region of barreloids terminate in the corresponding layer IV “barrel” through the thalamic radiation and establish a precise one-to-one relationship between the VPM barreloids and cortical layer IV barrels (Wise and Jones 1978; Jenson and Killacky 1987; Korelek et al., 1988; Lu and Lin, 1993). RTN and the upper section of layer VI of BFC are also innervated by collaterals of the ascending projections from VPM. Distribution of VPM projections in cortex is laminar-specific. Only layer IV and VI of BFC are innervated by VPM efferents. Although axons of VPM neurons bifurcate within barrels and some branches tend to extend into the deep layer III, this observation can be well attributed to the irregularity of the layer III/IV

boundary. Within layer IV, barreloid neurons innervate the corresponding “barrels” exclusively (Chmielowska et al., 1989; Jensen and Killackey, 1987; Lu and Lin, 1993). Studies employing single axon tracing techniques failed to support the multi-barrel projection of VPM neurons (Jensen and Killackey, 1987), but few of the axons extend horizontally into the septal region surrounding the layer IV barrels. Early studies reported a broader projection of VPM (Land et al., 1995), however, now it is believed that the extra-barrel labeling was resulted from tracer uptake by damaged fibers de passage (Jensen and Killackey, 1987). As for the neurons in the “tail” region of barreloids, they do not directly project to barrels in BFC. Nevertheless, they project sparsely to septal regions surrounding barrels and more heavily to the secondary somatosensory area (Pierret et al., 2000).

#### *Output Projections of POm to Barrel Field Cortex*

In general, POm projections to cortex are more diffusive, compared with VPM. POm projects to almost all sensorymotor area of the somatosensory cortex, including the primary somatosensory, second somatosensory (SII), perirhinal, insular and motor cortices (Dechenes et al., 1998). Ascending axons from POm to cortex also send collaterals to RTN, but these axons are sparser and less specific than those from VPM. In cortex, the major laminae that POm projections terminate are layer Va and layer I, although certain extent of variations do exist across areas. In rat’s BFC, the spatial distribution of POm projections is more complex due to the heterogeneity of the cortex (barrels vs. septa). The POm

axons mainly terminate in the septal column, which includes the septal region surrounding the barrel, and the regions directly above and below the septum. POm projections innervate the whole septal column and distribute nearly evenly from layer I to layer Va (Koralek et al., 1988; Lu and Lin, 1993). In the barrel column, POm projections show a laminar preference and mainly concentrate in layer I and layer Va. Hence in BFC, VPM projections are largely segregated from those of POm. Along the horizontal axis, VPM terminates in barrel, but POm innervates septum, vertically VPM projects to layer IV and VI while POm sends axons to layer I and Va. This complementary organization of VPM and POm projections in rat's BFC hence may indicate that in the ascending pathway, VPM inputs could functionally compete with inputs from other sources, such as POm and collosal inputs. Furthermore, since many layer Va neurons project to other cortical areas, as a higher-order relay nucleus, POm could be part of the cortico-thalamo-cortical circuitry in the cortex (for review, see Sherman and Guillery, 2002).

### **The Thalamic Reticular Nucleus**

Within the centralward projection, VPM and POm both send collaterals to innervate the thalamic reticular nucleus (Jones, 1975; Deschenes et al., 1998). The discovery of RTN can be dated back to the 19th century, but the detailed connections and functional importance of RTN were understood only much later. RTN is located in a key position between thalamus and cortex. Since VPM is devoid of inhibitory interneurons, inhibitory RTN neurons act as the main functional filter in the thalamocortical circuitry. Several lines of evidence



demonstrate that RTN could modulate the information transfer between thalamus and cortex (for review, see Crabtree, 1999; Guillery and Harting, 2003; Lee et al., 1994; McCormick, 1992; Pinault, 2004; Sherman and Guillery, 1996, 2002; Steriade et al., 1986).

### *Cytoarchitectonic Structure of RTN*

RTN consists of a thin rind of neurons that surround the dorsal and lateral parts of the thalamus (Scheibel and Scheibel, 1966; Houser et al., 1980). Separate regions in RTN are innervated by auditory, visual, somatosensory, gustatory and other sensory systems, respectively, and accordingly RTN is divided into several sectors, which interconnect with thalamic relay nuclei and cortical area in the corresponding sensory modality (for review, see Crabtree, 1999; Guillery and Harting, 2003; Pinault, 2004). RTN neurons are all GABAergic (Houser et al., 1980; Oertel et al., 1983; Barbaresi et al., 1986; De Biasi et al., 1986) with F type synapse on soma and proximal dendrites of VPM neurons (Liu et al., 1995). In the somatosensory sector, fusiform reticular neurons usually generate two or more dendritic branches extending over relatively long distances (Liu and Jones, 1999). These dendrites tend to be parallel to the plane of RTN. The thalamocortical and corticothalamic axons traverse orthogonally and synapse the processes of RTN neurons (Scheibel and Scheibel, 1966; Ohara and Lieberman, 1985; Spreafico et al., 1991; Ohara and Havton, 1996). In the rat's vibrissa system, RTN neurons mainly receive input from cortical layer VI (Bourassa et al. 1995), thalamic relay nuclei (Harris, 1987) and neighboring RTN

neurons (Landisman et al. 2002; Shu and McCormick, 2002). Synapses formed by collaterals of thalamic relay neurons are large, asymmetrical and glutamatergic, locating on proximal dendrites (Liu and Jones, 1999). Corticothalamic terminals are the most numerous, they have small profiles and distribute along the proximal and distal dendrites (Liu and Jones, 1999). Axon collaterals of RTN neurons also make GABAergic contact with each other, but these synapse are relatively sparse, and never dendrodendritic (Liu and Jones, 1999; Shu and McCormick, 2002). Interestingly, RTN neurons in rats are also closely coupled with gap junctions (Fuentelba et al., 2004; Landisman et al. 2002). The existence of electrical synapses in RTN are confirmed recently in other sensory modalities (for reviews, see Cruikshank et al., 2005), but the detailed function of the electrical coupling between RTN neurons is just starting to be understood.

### *Physiological Properties of RTN Neurons*

Similar to VPM neurons, RTN neurons show two firing modes: tonic and burst firing (for review, see Guillery et al., 1998; Pinault, 2004). Shifting between two firing modes is also mediated by  $I_T$ . In slow-wave sleep, RTN neurons fires in burst mode, which has the effect of disengaging relay neurons from peripheral inputs by strong inhibition. In contrast, in awake animals, RTN works in a tonic firing mode, which is thought to facilitate VPM to relay phasic sensory information to higher-order functions (for review, see Steriade and Timofeev, 2003; Steriade et al., 1993). In function, RTN interacts closely with thalamic relay nuclei, but the

response properties of RTN neurons differ substantially from those of relay neurons. On large scale, RTN and VPM neurons fire in a complementary pattern. RTN neurons in the somatosensory sector respond robustly to whisker stimulation (Hartings et al., 2000, 2003). The response magnitude of RTN neurons is surprisingly higher under certain recording conditions than that of VPM neurons (lightly narcotized rats, see Hartings et al., 2000), which is probably due to the fact that more bursting occurs in narcotized preparations. In lightly narcotized preparations, RTN neurons show almost the same angular tuning as VPM neurons (Hartings et al., 2000). However, In urethane anesthetized rats, most RTN neurons demonstrate a receptive field of single vibrissa (Shosaku, 1985; Sumitomo and Iwama, 1987) without obvious directional preference (Sumitomo and Iwama, 1987). The apparent difference can be attributed to recording conditions, since animal status heavily affects the physiological properties of RTN cells (Steriade and Timofeev, 2003; Steriade et al., 1993).

#### *Input and Output Connections of RTN*

RTN within the somatosensory sector in rats receives input from the thalamic relay nuclei (VPM and POm), cortical layer VI of the BFC, neighboring RTN cells within the same sector and modulatory afferents from several sources (for review, see McCormick, 1992). RTN projects to those thalamic nuclei that innervate RTN, but does not directly project to cortex (Scheibel & Scheibel, 1966; Jones, 1975; for review, see Crabtree, 1999; Guillery and Harting, 2003; Pinault,

2004). Synaptic connections between thalamic relay cells and RTN neurons are strong and reliable (Gentet and Ulrich, 2004). Anatomical and electrophysiological evidence shows that the projection from RTN back to VPM could be highly reciprocal (Lam and Sherman, 2005; for review, see Crabtree, 1999; Guillery and Harting, 2003; Pinault, 2004). Axons of RTN neurons ramify in the corresponding barreloid, but localized within a limited zone (Pinault et al., 1998b). Non-reciprocal connections are also evident in RTN (Pinault et al., 1998a). These synapses are on the distal part of VPM neurons, which probably accounts for the inter-barreloid inhibition observed in VPM (Desilets-Roy et al., 2002; Lavallee and Deschenes, 2004). RTN projects to VPM and POm, those neurons that project to VPM organize somatotopically (Pinault et al., 1995). This map is perpendicular to the plane of RTN. However, no somatotopic map was found within reticular cells projecting to POm (Pinault et al., 1995). Furthermore, many RTN neurons project to VPM and POm simultaneously, which constitutes one substrate for intrathalamic interactions (Crabtree et al., 1998). In vitro studies demonstrated that RTN mediated mutual inhibition between the first-order (VPM) and higher-order (POm) relay nuclei through a disynaptic pathway (Crabtree et al., 1998; Crabtree, 1999). On the other hand, it is also evident that POm neurons receive their driving excitatory inputs from the cortex (Diamond et al., 1992b) and strong inhibitory inputs from the extrareticular system (see below), thus more studies are still needed to elucidate the intrathalamic inhibition between VPM and POm mediated by RTN.

### *The Extrareticular System*

Recent data indicate that RTN is not the only source providing inhibitory inputs to thalamic relay nuclei, especially the “high-order” relay nuclei. A group of nuclei outside of RTN innervate POm with prominent GABAergic projections (Bokor et al., 2005; Lavalley et al., 2005). This group of nuclei is hence termed as extrareticular inhibitory system (Bokor et al., 2005), which consists of the anterior pretectal nucleus (APT), substantia nigra pars reticulata (SNR), medial globus pallidus (MGP), zona incerta (ZI) and ventral lateral geniculate nucleus (vLGN). The extrareticular system is substantially distinct from RTN in many aspects. Briefly, extrareticular axons form big terminals with multiple releasing sites on the proximal part of dendritic arbors of POm cells, which is quite distinct from the synapses formed by reticular terminals. Furthermore, Extrareticular nuclei receive glutamatergic inputs from the periphery and cortical layer V and project to higher order thalamic nuclei and brainstem motor centers. Whereas RTN receives inputs from the first-order thalamic relay and cortical layer VI and its output innervates all thalamic nuclei. Hence the extrareticular synapses exhibit synaptic effectiveness, release probability, kinetics and short term plasticity quite different from reticular synapses (Bokor et al., 2005). All these features of the extrareticular system are consistent with the fact that POm is a higher order thalamic relay nucleus and cortex is its driving input.

## **The Barrel Field Cortex**

The vibrissae representation, which is formally known as the posteromedial barrel sub-field (PMBSF), occupies relatively a large portion in the primary somatosensory cortex (Chapin and Lin, 1990). PMBSF is laminated and also heterogeneous in the horizontal plane. After CO staining, the layer IV of PMBSF consists of darkly stained, cell dense “barrel” units and lightly stained, cell sparse interbarrel “septa” (Woolsey and Van der Loos, 1970; Welker and Woolsey, 1974). Whiskers are represented somatotopically by barrels with one barrel corresponding to one whisker so that the PMBSF is always called the “barrel field cortex”. Thalamic efferents from VPM innervate both the excitatory spiny stellate neuron and the aspiny inhibitory interneurons. Extraordinary convergence/divergence takes place within the excitatory/inhibitory local circuits between barrel neurons and other cells around. About 50% neurons within barrels are GABAergic interneurons with smooth dendrites. They distribute in other layers as well but the percentage is lower (10~20%). The distinctions in morphology between relay neurons and inhibitory interneurons are parallel to the difference in electrophysiology, since BFC neurons can be categorized by their spike duration into “fast-spiking unit” (FSU) and “regular-spiking unit” (RSU) (Mountcastle et al., 1969; Simons and Carvell, 1989). Most GABAergic inhibitory neurons are FSUs and relay neurons are usually RSUs (McCormick et al., 1985). As we will discuss below, FSUs and RSUs differ in many aspects such as the RF size, responsiveness, spontaneous discharge and adapting features. Neurons within one layer IV barrel project heavily to layer II/III directly above the barrel

and the septal areas project above septum (Kim and Ebner, 1999; Feldmeyer et al. 1999; Petersen and Sakmann, 2000). Axons of barrel neurons make powerful monosynaptic connections on layer II/III cells, propagating information efficiently from layer IV to layer II/III (Lubke et al. 2000; Feldman, 2000). Some axons enter the adjacent barrels, but a few of them extend further than two barrels (Brecht and Sakmann, 2002; Kim and Ebner, 1999; Peterson and Sackmann, 2000). Septal cells project along the septal regions and to some extent into surrounding barrels. Projections of septal neurons are less dense than those of barrel neurons, but tend to innervate a larger area (Kim and Ebner, 1999). Septal neurons also project to layer II/III above the septal region, they also innervate the secondary somatosensory cortex (SII) and primary motor cortex (Kim and Ebner, 1999). As for the supragranular layers (mainly Layer II/III), their targets include the surrounding layer II/III, layer V, MI, SII, dysgranular cortex, and the contralateral SI (Koralek et al., 1990; Hayama and Ogawa, 1997; Kim and Ebner, 1999). The detailed structure and function of callosal projections in rat's vibrissa system will be discussed thoroughly in Chapter II.

### *Physiological Properties of Cortical Neurons*

The receptive field properties of neurons in BFC are quite different from those in VPM. About ninety percents of the cortical neurons respond to more than one whisker in both awake and anesthetized animals. Receptive field properties are layer-specific. In layer IV barrels are the major recipient of thalamic relay in the lemniscal pathway. RF has a structure of excitatory center and excitatory

surround: neurons respond vigorously to deflections of the corresponding principal whisker with short response latency, while they also show a milder response to several surround whiskers with longer latency (Simons, 1978; Ito, 1985; Armstrong-James and Fox, 1987). As for the genesis of the RF surround, recently it has been shown that the surround of RF are generated by intracortical projections in barrel neurons (Fox et al., 2003). Within layer IV, corresponding with the anatomical heterogeneity, neurons in septal regions show quite different responses to whisker stimulations from barrel neurons. Septal neurons don't have a preference to certain whisker, they usually respond to 2 or 3 whiskers equally and the RF size is broader (Armstrong-James and Fox, 1987; Brecht and Sakmann, 2002). Septal neurons receive thalamic inputs from POm and it has been indicated that the multiwhisker RFs are at least resulted from the more widespread thalamocortical projections (Fox et al., 2003). Supragranular (mainly layer II/III) neurons in one barrel columns are strongly innervated by layer IV barrel (Brecht and Sakmann, 2002; Feldman, 2000; Kim and Ebner, 1999), and they fire ~3 ms after barrel cells discharge (Armstrong-James et al., 1992). In addition, layer II/III integrates information from multiple sites such as the neighboring barrel columns, contraetral BFC and other cortical areas like SII. Consequently, the RF size of layer II/III neurons is broader and response magnitude is lower (Ito, 1985; Armstrong-James and Fox, 1987). Neurons in infragranular layers (layer V and VI) are responsive to more than one whisker. Layer V neurons are lack of whisker specificity and respond to ~25 whiskers. And on average, layer VI neurons respond to 14 whiskers (Sachdev et al., 2001).



## **The Corticothalamic Descending Pathway**

As in other mammals, corticothalamic projections in rats mainly originate from pyramidal cells in layer V and VI (Hoogland et al, 1987; Land et al., 1995; see Deschenes et al., 1998 for review). Corticofugal projections from cortical layer V and VI are distinguished by their targets, collaterals to RTN, terminal morphology, synaptic ultrastructure and axon branching patterns. CT projections from layer V in all sensory modalities innervate the “high-order” relay nuclei (for review, see Guillery and Sherman, 2002; Sherman and Guillery, 2002). In rat’s vibrissa system, layer V projections are actually collaterals of corticobulbar or corticospinal fibers, which always form small clusters of large terminals in POM (Bourassa et al., 1995; Hoogland et al., 1987; Land et al., 1995). Layer V collaterals innervate the intralaminar and associative thalamic nuclei, extrareticular nuclei but not RTN. In general, available data indicate that layer V projections only innervate thalamic nuclei in the paralemniscal pathway but do not interact directly with VPM neurons. Thus only projections from layer VI are of direct relevance in current study and from now on, the term “corticothalamic projections” in the following text refers only to those from layer VI of BFC. Bilateral projections from cortex to thalamus do exist in rats. However, most of these reported projections originate outside BFC and terminate in nuclei of the anterior group, medial dorsal and submedial nuclei but not VPM (Leonard, 1969; Beckstead, 1979; Kaitz and Robertson, 1981; Reep and Winans, 1982; Oda,

1997). Thus, these bilateral projections may play only a limited role in the plasticity of sensory relay nuclei (VPM) after cortical manipulations in BFC.

#### *Corticothalamic Projections from Layer VI*

As introduced in the preceding text, synapses formed by cortical layer VI are “RS” type, which are relatively small compared with those by ascending brainstem axons and terminate on the distal dendrites. In cat’s visual system, approximately only 6~7% of synapses on LGN neurons are from the retinal ganglion cells, while ~40% are formed by CT axons (Sillito and Jones, 2002). The relative number of CT terminals in rat VPM is unknown. However, reconstruction of electron microscopy data demonstrates that cortical influence is predominant in rat VPL. The data reveal that only ~15% of synapses in rat’s VPL are “RL” type, which are formed by brainstem ascending axons, while ~50% are “RS” type (Liu et al., 1995). The fine-grained knowledge of the interconnections between layer VI, VPM and RTN is still incomplete. Within BFC, CT feedback projections to the barreloids are areal and laminar specific. CT projections to VPM originate mainly from the upper section of layer VI (layer VIa) within the barrel columns and the non-barrel “septal” columns (Chmielowska et al., 1989; Killackey and Sherman, 2003, see also Deschenes et al., 1998). After injection of retrograde tracer into the dorsomedial “core region” of the barreloids in VPM, labeled cells formed a continuous band in layer VIa of BFC (Killackey and Sherman, 2003). Sparse labeled neurons were also found in the lower section of layer VI (layer VIb) as well (Killackey and Sherman, 2003; Deschenes et al.,

1998). The deeper section of layer VI (layer VIb) of both the barrel and septal columns projects to P<sub>Om</sub>, but only the layer VIa of the septal columns innervates P<sub>Om</sub>. When the retrograde tracer was injected into P<sub>Om</sub>, labeled cortical neurons were found mainly in layer Vb and VIb of both the barrel and septal columns, but only layer VIa of septal columns was labeled (Killackey and Sherman, 2003; Veinante et al., 2000a). Only sparse anatomical data are available about the CT projections from the dysgranular zone in the rat's SI.

#### *Sub-laminar Specificity of Corticothalamic Projections*

In brief, ipsilateral CT projections are highly ordered, and neurons in different sublayers (layer VIa v.s. layer VIb) display different axon branching patterns in the thalamus. Layer VIa only projects to the sensory specific nuclei (VPM) but layer VIb generally innervates the associative and/or intralaminar thalamic nuclei. Axons from the upper section of layer VI obey a strict one-to-one relationship between barrels and barreloids while Layer VIb cells extend their collaterals to cover a much larger area in VPM and further invade into P<sub>Om</sub> (Bourassa et al, 1995). The fine topography of CT projections from layer VI of BFC to VPM has been recently examined and discussed in detail (Deschenes et al., 1998) by injecting anterograde tracer BDA into different depth of layer VI of BFC. When the injection was well localized within the layer VIa of one barrel column, marked axons are only present in a small region within VPM. The terminal field is rod-like and probably within one single barreloid. But when the injection site moves to the deeper section of layer VI, feedback axons tend to

cover multiple barreloids in VPM and, in addition, extend into POm. Similar sub-laminar specific distribution of CT projections has been reported in the auditory and visual system recently (Ojima, 1994; Usrey and Fitzpatrick, 1996). It is clear that cells in upper and lower sections of layer VI innervate thalamic relay nuclei differently, and identifying the functional implications of these differences in anatomy would be important future studies.

### *Functions of Corticothalamic Projections*

In the visual system, Kalil and Chase found both the spontaneous activity and light-evoked responses of most cat LGN neurons decreased after a reversible cooling of the primary visual cortex (Kalil and Chase, 1970). This result suggested that the excitability of LGN and pulvinar neurons was under the influence of the primary visual cortex. This was supported by a complementary study by Tsumoto and Creutzfeldt showing that iontophoretized glutamate into a certain region of cat primary visual cortex excited ipsilateral LGN neurons whose receptive field overlapped with those cortical neurons under iontophoresis (Tsumoto and Creutzfeldt, 1978). Sillito et al. (1994) further demonstrated that corticofugal projections influenced LGN neuron's receptive fields by facilitating the synchronization of thalamic neurons showing the same receptive field features to those cortical cells. Suga and colleagues reported a shift of tuning curve of MGN neurons in the bat's auditory system after an acute and reversible cortical inactivation: MGN neurons tuned to a certain frequency responded less to its characteristic frequency after the auditory cortical area representing the same

frequency was silenced by lidocaine while nearby MGN neurons tuned to an “adjacent” frequency responded more (Yan and Suga, 1994). Similar findings were also reported in subcortical levels other than thalamus, such as inferior colliculus (Yan and Suga, 1998).

Early studies in rat’s vibrissa system reported that “of 20 units studied both before and after SI suppression with topically applied lidocaine, 14 (70%) showed a similar reduced response to repetitive stimuli with no consistent changes in spontaneous activity, somatic stimulus threshold, response latency, or size of receptive field” (Yuan et al., 1985). Together with their work in awake rats, they concluded that corticothalamic neurons were the primary facilitatory source of thalamic neurons from observation that 19 of 29 VB units reduced their responses to repetitive electrical test stimuli applied to the medial lemniscus, 6 of 16 VB units showed comparable reduction of their response to electrical somatic stimulation (Yuan et al., 1986). Furthermore, Diamond et al. (1992b) suggested the lemniscal and paralemniscal pathway in rat somatosensory system may be differentially under the influence of corticothalamic projections since responsiveness of POm neurons decreased dramatically after magnesium sulfate suppression of ipsilateral barrel field cortex (BFC) under conditions where VPM neurons continued to fire (Diamond et al., 1992b). Other studies indicate VPM is affected by cortical feedback, since the spatiotemporal receptive field structure of VPM units changed immediately after reversible inactivation of SI cortex (Krupa et al., 1999). Changes of receptive field properties in thalamic neurons were confirmed in the Macac monkey’s somatosensory system. Acute or

chronic APV application to area 3b resulted in an enlargement of the receptive field of ventroposterior neurons (Ergenzinger et al., 1998). A recent report showed that microstimulation of layer VI neurons of one barrel column can increase the response magnitude of matched barreloid neurons to the principal whisker stimulation, while reduce the responsiveness of mismatched barreloids (Temereanca and Simons, 2004). Thus they showed that the cortical feedback exerts a facilitory influence of VPM neurons, can secondly sharpen the response, probably by some mechanisms similar to “egocentric selection”, a word coined by Suga to describe the selectivity of corticofugal influences in the auditory system. Hence results from both somatosensory and auditory systems converge onto a single conclusion. Sillito et al. showed that corticofugal projections influenced LGN neurons in such a way of facilitating the synchronization of thalamic neurons with same receptive field features to those cortical cells (Sillito et al., 1994). In Chapter III, the specific functions of CT projections in rat’s vibrissa system will be discussed in detail.

### **Angular Tuning in Rat’s Vibrissa System**

Neurons along the ascending pathway in rats’ vibrissa system, from the receptors in whisker follicles to cells in the neocortex, are sensitive to parameters that define a whisker stimulus, such as the amplitude, duration, velocity, acceleration, direction and so on. A newly published behavioral study demonstrated that rats can discriminate object orientations with their whiskers under a one-trial learning paradigm (Polley et al., 2005). The directional

preference to whisker movements of neurons in the vibrissa system has been reported by different labs. Trigeminal ganglion cells clearly exhibit directional selectivity to deflections of the principal whisker (Zucker and Welker, 1969; Gibson and Welker, 1983a, b; Lichtenstein et al., 1990). The direction at which the highest magnitude of responses was evoked was termed as the “preferred direction”. When tested with the controlled ramp-and-hold sustained whisker deflections, trigeminal ganglion neurons demonstrate a directional consistency (Lichtenstein et al. 1990) which means that the preferred angle is independent of the initial direction of whisker movements. For instance, a neuron may respond robustly to both the onset and offset of sustained whisker displacement at a certain angle (Minnery and Simons, 2003; Lichtenstein et al. 1990). Under pentobarbital anesthesia, the majority (>80%) of the slowly-adapting ganglion cells respond with significantly higher magnitude (more spikes) to 1~2 directions than to other directions (Lichtenstein et al., 1990). Rapidly-adapting units show both on and off-response to sustained whisker deflections and are less angularly tuned than slowly-adapting cells (Lichtenstein et. al, 1990). Data also indicate that trigeminal ganglion cells are more tuned to upward movements of vibrissae since the preference to the ventro-dorsal direction is more frequently observed (Lichtenstein et. al, 1990). A few studies have characterized the angular tuning properties of the trigeminothalamic neurons. PrV neurons show highly direction-tuned response to their principal whisker stimulations, slightly but significantly less tuned than trigeminal ganglion cells (Minnery and Simons, 2003; Minnery et. al, 2003; Shipley, 1974; Veinante and Deschenes, 1999). In Fentanyl sedated

rats, response magnitude to the preferred direction is roughly twice as much as the average magnitude to all directions (Minnery and Simons, 2003). Unfortunately, so far not data indicates the existence of a topographic angular tuning map in TBC. PrV neurons also respond to 1~2 adjacent whiskers (AWs), although with a much weaker response magnitude. It was suggested that PrV neurons were also sensitive to the direction of AW stimulations, but are generally less tuned than to PWs. Comparison of the tuning curve of the same PrV neurons to AWs with that of corresponding PWs failed to reveal significant correlations in directional tuning. Thus AW and PW inputs onto individual PrV cells are not necessarily matched for preferred direction (Minnery and Simons, 2003). The quantitative data for angular preference of SpV neurons has not been reported. The angular tuning properties of single VPM neurons are similar to those of PrV neurons (Minnery et al., 2003; Simons and Carvell, 1989; Timereanca and Simons, 2003; Timofeeva et al., 2003). However, by combining double labeling with electrophysiology, Timofeeva et al. (2003) revealed that barreloidal neurons with the same preferred direction were clustered together and organized into an angular tuning map in each barreloid (Timofeeva et al., 2003). The clustering is statistically significant along the dorsal-ventral dimension of barreloids in such a way that neurons tuned to forward and upward whisker movements are located mainly in the dorsal barreloid, and cells in the central and ventral sectors of barreloids are more tuned to backward and downward deflections (Timofeeva et al., 2003). The angular tuning properties of POm neurons and cells between barreloids are still largely unknown. Neurons in barrel



columns are also sensitive to the directionality of whisker movements (Simons and Carvell, 1989). Within one single barrel column, usually layer IV barrel neurons show stronger angular tuning than neurons in any other layers and the regular-spiking units are more angularly tuned than those fast-spiking units (Kida et al., 2005; Simons and Carvell, 1989; Lee and Simons, 2004). No angular tuning map was found consistently within and between barrel columns, although cortical neurons within the same “minicolumn” along the vertical axis of the cortex share a similar angular tuning curve (Bruno et. al, 2003). RSUs also respond robustly to most of the surround whiskers (Armstrong-James and Fox, 1987; Simons and Carvell, 1989). A newly conducted study demonstrated that neurons in barrel columns showed highly correlated angular tuning curves to both the principal whisker and the immediate adjacent whiskers (Kida et al., 2005). As for the angular tuning properties of septal neurons (here “septal neurons” referring to those above, within and below the layer IV septum) still remain unclear. Although the directional preference of VPM neurons is generated by the inheritance and integration of brainstem ascending inputs, cortical feedback could modulate the angular tuning of thalamic relay neurons pretty much. The cortical modulation of the angular tuning properties of VPM neurons will be discussed in Chapter IV.

## CHAPTER II

### **CHRONIC SUPPRESSION OF ACTIVITY IN BARREL FIELD CORTEX DOWNREGULATES SENSORY RESPONSES IN CONTRALATERAL BARREL FIELD CORTEX**

The study described in this chapter was published in 2005 (Li L, Rema V, Ebner FF. *J Neurophysiol.* 2005 94(5):3342-56).

Numerous lines of evidence indicate that neural information is exchanged between the cerebral hemispheres via the corpus callosum. Unilateral ablation lesions of barrel field cortex (BFC) in adult rats induce strong suppression of background and evoked activity in the contralateral barrel cortex and significantly delay the onset of experience-dependent plasticity (Rema and Ebner, 2003). The present experiments were designed to clarify the basis for these interhemispheric effects. One possibility is that degenerative events, triggered by the lesion, degrade contralateral cortical function. Another hypothesis, alone or in combination with degeneration, is that the absence of interhemispheric activity after the lesion suppresses contralateral responsiveness. The latter hypothesis was tested by placing an Alzet minipump subcutaneously and connecting it via a delivery tube to a cannula implanted over BFC. The minipump released muscimol, a GABA<sub>A</sub> receptor agonist at a rate of 1  $\mu$ l/hr, onto one barrel field cortex for 7 days. Then, with pump still in place, single cells were recorded in the contralateral BFC under urethane anesthesia. The data show a ~50% reduction

in principal whisker responses (D2) compared to controls, with similar reductions in responses to the D1 and D3 surround whiskers. Despite these reductions, spontaneous firing is unaffected. Fast spiking units (FSUs) are more sensitive to muscimol application than regular spiking units (RSUs), in both the response magnitude and the center/surround ratio (C/S ratio). Effects of muscimol are also layer specific. Layer II/III and layer IV neurons decrease their responses significantly, unlike layer V neurons that fail to show significant deficits. The results indicate that reduced activity in one hemisphere alters cortical excitability in the other hemisphere in a complex manner. Surprisingly, a prominent response decrement occurs in the short latency (3-10 ms) component of principal whisker responses, suggesting that suppression may spread to neurons dominated by thalamocortical inputs after interhemispheric connections are inactivated. Bilateral neurological impairments have been described after unilateral stroke lesions in the clinical literature.

## **Introduction**

The integration of sensory information between the cerebral hemispheres is important for many perceptual tasks that require bilateral coordination. The function of the left and right somatic sensory cortex is closely linked through the corpus callosum (Ebner and Myers, 1962; Glickstein and Sperry, 1960; Krupa et al., 2001; Schnitzler et al., 1995). The integration of sensory information through the corpus callosum is still unexplained at a cellular level, but several recent papers have begun to explore cellular interhemispheric dynamics in the somatic

sensory system (Calford and Tweedale, 1990; Harris and Diamond, 2000; Shuler, et al., 2001; Swadlow, 1988, 1989; Wiest, et al., 2005). However, the extent to which real time activity changes in one cortical area are reflected in that of its contralateral counterpart is still an open question.

The subcortical pathways from the whiskers on the right and left side of the face are kept quite separate from periphery to cortex (Chiaia et. al, 1991; Peschanski, 1984) leading to a functional lateralization in cortex. However, while barrel neurons respond best to stimulations of the contralateral whiskers, they are also influenced by the whiskers on the ipsilateral side of the face as well. Stimulating ipsilateral whiskers evokes both local field potential (LFP) (Pidoux and Verley, 1979) and spikes in single layer V neurons in BFC (Shuler et al., 2001). Responses of cortical neurons to the ipsilateral whiskers are mediated via callosal connections, since blocking activity in one hemisphere eliminates all responses in the hemisphere ipsilateral to the whiskers stimulated (Pidoux and Verley, 1979; Shuler et al., 2001). Behavioral studies (Harris and Diamond, 2000) have shown that tactile learning occurring in one BFC leads to significant transfer to the homologous barrel on the other side. Indeed, rats exhibit the capability of integrating bilateral whisker information to determine whether movable walls on the left and right side of the face are close to the head, far from the head, or asymmetrically different distances from the head using only their whiskers (Krupa et al., 2001; Shuler et al., 2002). And this capability of making a correct comparison with whiskers is a function of the corpus callosum (Shuler et. al, 2002). These results indicate that 1) integration of whisker information from both

sides of the face occurs continuously during a rat's normal behavior and 2) cortex is the dominant location where this integration occurs.

Bilateral reorganization in cortex occurs after temporary and reversible inactivation of the periphery (Calford and Tweedale, 1990; Shin et. al, 1997). However, since peripheral sensory deafferentation induces immediate unmasking of new receptive fields at multiple levels along the sensory system (thalamus: Garraghty, 1991; Nicolelis et al., 1993; spinal cord: Pettit and Schwark, 1993), and these subcortical changes could also play a fundamental role in cortical plasticity. Studies with manipulations at the cortical level are needed to further specify the role of neocortex in bilateral interactions. One chronic study in our lab reported that a subpial aspiration lesion of one BFC significantly degraded both the background and evoked activity in the contralateral BFC (Rema and Ebner, 2003). However, a cortical lesion produces several types of change, including reactive events such as axon degeneration, decrease in growth factors and neurotransmitter release from lesioned area as well as elimination of ongoing interhemispheric activity arising from the lesioned area. All of these events are possible modulators of firing characteristics of neurons on the contralateral side. In the present study, we tested the hypothesis that some or all of the interhemispheric effects of a cortical lesion are due to the decrease or elimination of interhemispheric activity. To test this idea, we silenced one cortex for 7 days with minipumped muscimol and measured the spontaneous and evoked activity levels of neurons in the contralateral D2 barrel column. The results show a significant reduction in principal whisker responses (D2) compared to controls,

with similar reductions in responses to the D1 and D3 surround whiskers. The results suggest that severe reductions in activity between the two hemispheres by itself may be a major contributor to the bilateral clinical deficits seen after unilateral cortical lesions.

## **Materials and Methods**

Adult male Long-Evans rats (250 gm to 350 gm, 2 to 3 months old, n = 24) were used in this study. All procedures were approved by the Institutional Animal Use Committee and followed guidelines set by the National Institutes of Health and the Society for Neuroscience. Figure 2-1 shows the design of the experiments. In each experimental case, one barrel field was silenced for 7-days using continuous muscimol infusion before responses were recorded in the other BFC to stimulation of its contralateral whiskers. Controls were carried out with saline minipumped onto BFC for the same period of time and with muscimol released onto visual cortex for the same 7 day period before recording cortical responses (Fig. 2-1).

### **Minipump Implantation**

Muscimol solution was prepared by dissolving muscimol (Sigma) in sterile saline (10 mM concentration) just prior to the experiment. Osmotic minipumps (Alzet, model 2001) were attached to right angle cannulae (Plastics One, Inc) with tip shortened to 0.5-1 mm before surgery so they would not extend past the

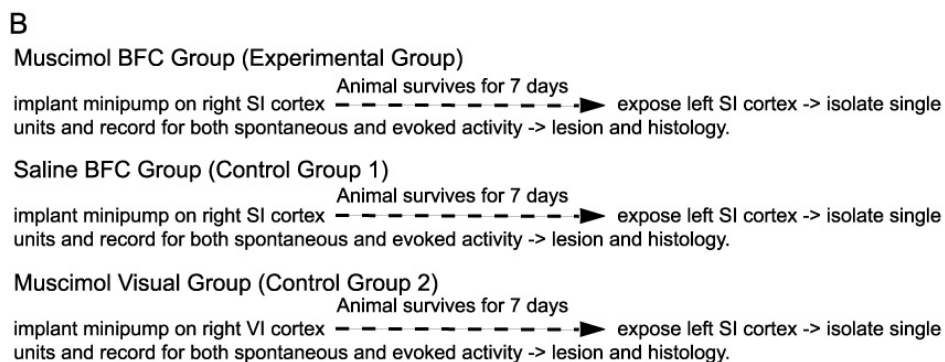
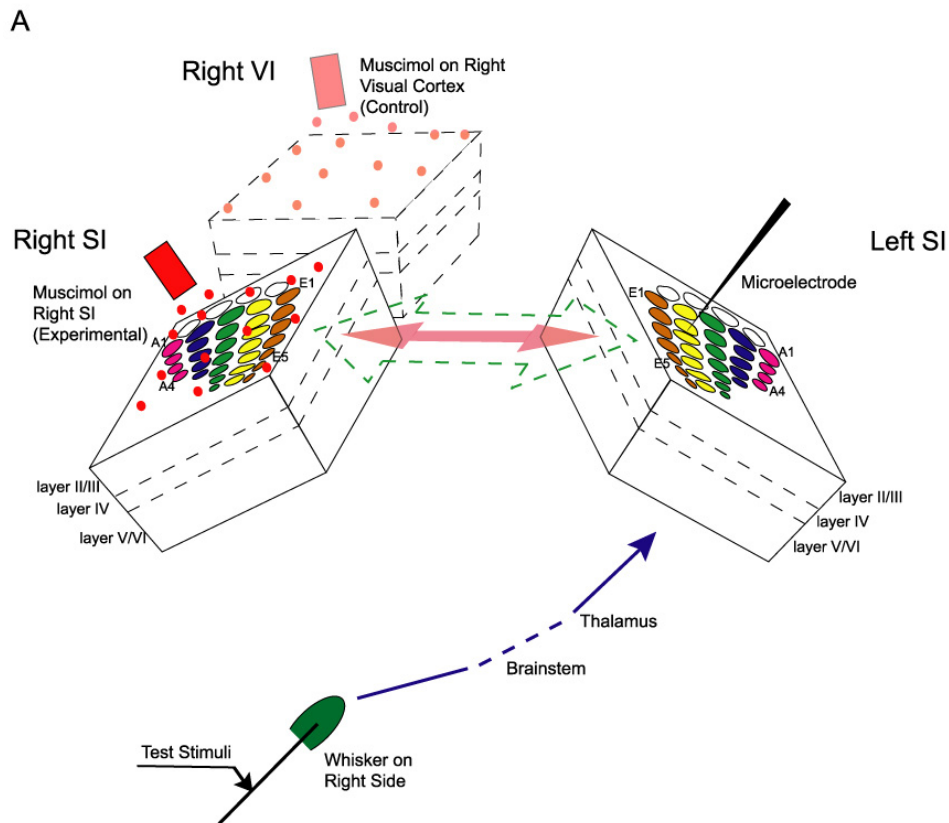


**Figure 2-1. Experiment design.**

**a.** Schematic diagram showing the location of minipump implantation over right SI (which delivers either muscimol or saline solution), the implantation on left visual cortex as control, and the recording site in the D2 barrel column of the contralateral (right) BFC. When the right SI was inactivated by muscimol for 7 days, the facilitatory influence of transhemispheric projections (dashed green arrow) would decrease. When this happens, the neurons in the left BFC could change their responsiveness to peripheral whisker stimulation. **b.** Recording Procedure in Experimental and Control Groups.

thickness of the skull, and then polished by fine sand paper and sterilized. The whole assembly (Minipump chamber, connection tubing and cannula) were completely filled with muscimol solution, then immersed in sterile saline several hours prior to the implant procedure. The 2001 minipump model delivered the muscimol solution at the rate of 1  $\mu$ l/hour and had a capacity of 200  $\mu$ l, which was more than enough capacity to provide the 168  $\mu$ l muscimol needed for the 7 day pumping period. Rats were anesthetized with Nembutal (50 mg/kg, i.p.) then transferred to the stereotaxic headholder (Narashige). Supplements (10% of initial dose) were given as needed. Body core temperature was maintained at 37<sup>o</sup>C by a heating pad, feedback controlled by a rectal thermometer (Harvard Labs). After a midline cut and soft tissue retraction, a small hole was carefully drilled on the right skull with a fine dental burr at the location of 2 mm posterior and 6 mm lateral to Bregma. The bone dust was frequently cleaned with saline during drilling. When the bone was thinned to a transparent layer, a fine forceps and 32 gauge syringe needle were used to strip off the bone film, expose the dura and make only 1 or 2 openings in the dura to facilitate the penetration of the pumped solution. Care was taken to avoid any injury to blood vessels in the dura, and gel foam was applied to quench any oozing. After the surface of the parietal and temporal bone was dried as completely as possible, a thin layer of super glue was applied onto the dried bone surface while leaving the area around the bone opening uncontaminated. The minipump was embedded subcutaneously between the shoulder blades by blunt dissection of the connective tissues and the pump with tube attached was inserted into the subcutaneous cavity. The



cannula was then held in position just touching the dura with a micromanipulator, and the cannula and a short segment of the tube were securely cemented to the skull with dental cement. The skin edges were then sutured and antibiotic (Neuropracin) was applied to the incision. The rat was removed from the stereotax to recover from anesthesia. All animals were allowed to survive for 7 days from day of implantation surgery.

Two control groups were prepared: one with sterile saline minipumped onto the right BFC for 7 days (n = 5) and another by applying muscimol to the surface of visual cortex (P 6.0, L 2.0mm from Bregma, n = 4) in the same way to determine the effect of visually applied muscimol on neurons in the contralateral BFC.

### **Behavioral Observations**

The animals were returned to their home cages after full recovery from anesthesia. The animals were observed every day for whisker movements, gait, response to whiskers and skin touch when the animal was fully awake. Under each experimental and control condition the animals were tested behaviorally in two ways. First we stimulated the ipsi- and contralateral whiskers and skin with a hand-held probe to determine whether the rat reacted to the tactile stimulus (i.e., orientate head towards stimulated side, withdraw foot, etc). We also checked the limb posture reflex. When the body of a normal rat is supported and the forelimb is placed in an unusual position, the animal will quickly return the limb to its anatomical position. However, if the forelimb area in SI is silenced or removed

these reflexes are reduced or abolished. Since the cannula is placed at the medial edge of the BFC in SI cortex it is equally close to the forelimb representation, and the existence of the limb posture reflex can be used as a general indicator of muscimol release. Reflexes were tested on both forelimbs and both hindlimbs. The muscimol effect on cellular function was determined precisely by electrophysiology (see below).

### **Electrophysiological Recording**

One week after the minipump implantation, the rat was anesthetized with urethane (1.5 g/kg, 30% aqueous solution, i.p.) and mounted in a stereotaxic apparatus (Narashige). With the muscimol cannula still in place and pumping, the skin was opened, and a craniotomy opening made from 4 to 7 mm lateral to the midline and from 0 to 5 mm posterior to Bregma to expose the left (untreated) BFC. Body temperature was maintained at 37<sup>o</sup>C. Supplementary injections (10% of the initial dose) were given as needed to maintain the anesthesia at stage III-3 (Friedberg et al., 1999; Guedel, 1920). Both the spontaneous activity and evoked activity of single units were recorded using carbon-fiber microelectrodes with impedance from 0.2 to 1 M $\Omega$  (typically around 0.5 M $\Omega$ ) at 1 KHz (Armstrong-James and Millar, 1979; Armstrong-James et al., 1980). Single neurons were discriminated by their waveforms using a time-amplitude window discriminator (Bak Instruments). Spikes generated by each single unit were digitized in 1 ms bins by a CED 1401 Plus processor (Cambridge Electronic Design) controlled by a PC (Dell), pre-processed and displayed on-line using the Spike 2 software

(Cambridge Electronic Design) driven by in-house scripts and stored on the PC for further off-line analysis. All whiskers on the right face were trimmed to 10 mm. A piezoelectric stimulator was used to give standardized 3 ms duration, 300  $\mu\text{m}$  ramp and hold forward deflections to one whisker at a time. The duration of every neuronal spike was measured by displaying it on a storage oscilloscope. Microelectrodes were advanced perpendicular to the cortex surface by a precision mechanical microdrive (Kopf Instruments). Contact of the electrode tip with the pia was identified both visually through an operation microscope and by noise reduction heard on the audiomonitor. Each unit was marked by its subpial depth read off of the microdrive control unit. All penetrations reported here were confirmed to be in the D2 barrel column. They were initially located by coordinates, then by short (7~10 ms) latency layer IV cell responses to the principal whisker (Armstrong-James and Fox, 1987; Armstrong-James et al., 1992, 1994). Electrodes were advanced in 70  $\mu\text{m}$  intervals before searching for another cell to avoid repeated sampling from the same unit. Penetrations were continued down to layer VI. At each recording site, single units were isolated, tested and recorded. For every unit, several measurements were made: spontaneous activity, responses to stimulation of the D2 (principal) whisker and responses to two immediately adjacent D-row surround whiskers (D1 and D3). Spike duration was measured, and neurons were separated into fast spiking (<750  $\mu\text{s}$ ) and regular spiking units (>750  $\mu\text{s}$ ). For each neuron studied, one block of 50 trials at 1 stimulus per second was presented to the D1, D2 and D3 whisker in sequence. Spontaneous firing was recorded for 200 sec after whisker

stimulation, with the piezoelectric stimulator still close to the whisker but not moving.

### **Muscimol Effective Range Detection *in vivo***

**Acute** We tested the effectiveness and reversibility of muscimol suppression acutely in one rat. After the left BFC was exposed as described above, a small (6 mm diameter) home-made plastic chamber was cemented watertight to the skull with dental cement. One 32 gauge syringe needle was used to make a small opening in the dura. A carbon-fiber electrode was advanced through the opening until the D2 barrel column was located. The chamber was filled with warm saline. Responses of D2 barrel column neurons were measured to stimulations of the principal and surround whiskers. Then saline within the chamber was removed and replaced by 10mM muscimol. Spontaneous discharge and evoked response to whisker stimulations of the same neuron(s) were recorded. The period of muscimol effectiveness was estimated by measuring the response levels of neurons over time. Then the cortical surface was washed repeatedly with warm saline with the electrode still in place and test stimuli were delivered every 10 minutes to determine the duration of muscimol suppression.

**Chronic** To assay the effective distance of muscimol suppression *in vivo*, 2 rats were implanted with muscimol minipumps identical to the BFC group. On the 8<sup>th</sup> post-implantation day, the rat was anesthetized with urethane (1.5 g/kg, i.p.), and the skull bone within a 3 mm radius anterior and medial to the cannula was removed with the pump still working. The same recording procedure was

carried out as described above. The brain area surrounding the cannula tip was examined using concentric movements of the electrode to see if neurons at various distances and depths from the cannula tip would respond to the whisker stimulation: first, by using a hand-held probe stimulus, and then the piezostimulator. Both spontaneous firing and evoked responses were recorded. The coordinate and depth of active neurons were charted for spontaneous firing or responses to whisker stimulation. The evoked response magnitudes were analyzed off-line.

## **Histology**

At the termination of recording in one penetration, cortical recording sites were marked in vivo by passing a DC current (electrode tip positive) of 2  $\mu$ A for 10 seconds. This current produced a spherical microlesion, which was clearly visible in histological sections stained for cytochrome oxidase (CO) staining. On completion of recording, animals were given a lethal dose of urethane and perfused transcardially with PBS followed by phosphate-buffered 4% paraformaldehyde. Brains were postfixed overnight, saturated in 10%, 20% and 30% sucrose, and the cortex was flattened, sectioned tangentially, and stained for CO activity (Wong-Riley and Welt, 1980) to localize barrels and microlesion sites. A penetration was considered to be within the D2 barrel column if the recording sites were localized within, above or below the horizontal boundaries of the D2 barrel as defined by the appropriate patch of high CO activity in layer IV. Only penetrations located within D2 barrel territories were included in the results.

### **Identification of the Depth of Layer IV**

The location of layer IV was identified in 3 separate cases by comparing the location of lesions made at micrometer measured depths (450 and 800  $\mu\text{m}$  respectively) with that of the “barrels” revealed by CO staining. The rat was prepared as described above. The carbon-fiber microelectrode was oriented perpendicular to the surface of the barrel field cortex ( $\sim 40\text{-}45$  degrees lateral for the D row barrels), then advanced slowly ( $>10$  s between 20  $\mu\text{m}$  steps) into the cortex. Contact of the electrode tip with the surface of the cortex, which is the zero point, was carefully identified by two persons independently and by the transient amplifier noise created by the pulsing of the surface vessels. Whiskers were deflected by a hand-held probe as the electrode advanced into the cortex to ensure the electrode was in the barrel column and PSTHs were built as needed (see Materials and Methods for detailed description). Once the electrode was confirmed within the barrel column, the electrode was advanced into layer V ( $\sim 1000$   $\mu\text{m}$  underneath cortical surface, from the read-out of the microdrive, same below) and held in place for  $\sim 5$  mins to compensate the possible compression of the tissue during the penetration. Then the electrode was retracted at the same rate to 800  $\mu\text{m}$ . And the recording site was marked by passing a DC current (electrode tip positive) of 2  $\mu\text{A}$  for 5 seconds. Another electrolytic lesion was made at 450  $\mu\text{m}$  using the same method. The loss of local spike activity always signaled a successful lesion. The depth data from the read-out of the microdrive was calibrated as we withdrew the electrode out of the cortex after lesion making. Then the electrode was moved  $\sim 300$   $\mu\text{m}$  lateral to aim

at another barrel column. And an additional pair of lesions was made at 450 and 800  $\mu\text{m}$  with the same procedure. After the lesions were made the rat was overdosed with urethane and perfused transcardially. The brain was postfixed overnight, saturated in sucrose and blocked in the stereotaxic apparatus at the same angle as the electrode. Coronal sections were made parallel to the electrode penetration for CO reaction.

### **Data Analysis**

In this study, units sampled were grouped by their depth read from the microdrive and corroborated by histology. Neurons collected from depths of  $\sim 450\text{-}800\ \mu\text{m}$  *in vivo* were usually found within a CO dense patch corresponding to the D2 barrel. Neurons above 450  $\mu\text{m}$  were categorized as supragranular (layer II-III) cells. Neurons collected below 800  $\mu\text{m}$  were considered to be in the infragranular layers, mainly layer V. The criteria used here are consistent with previous reports from several labs (Armstrong-James and Fox, 1987; Brecht and Sakman, 2002).

Responses evoked by whisker stimulation were assessed by averaging poststimulus time histograms (PSTHs). PSTHs were constructed using 1 ms bins, the bin 0-1 was registered as the first bin after stimulus. Response magnitude was constructed by counting the action potentials occurring within 100 ms after the stimulus onset. The correction for spontaneous activity was applied by subtracting the averaged number of spontaneous events per 1 ms bin occurring 100 ms before each stimulus. Both the onset response latency (1<sup>st</sup> bin in a

latency histogram) and the modal response latency (bin with the greatest number of spikes) were calculated. Poststimulus responses were further grouped into several intervals, namely, 3-10 ms, 10-20 ms, 20-50 ms and 50-100 ms for PSTH "epoch" analysis. For a first approximation, the first 10 ms are dominated by thalamic (VPM) inputs, 10-20 ms by adjacent barrel columns, 20-50 ms by other cortical areas (Armstrong-James and Fox, 1987; Armstrong-James et al. 1991). Spikes within 3 ms poststimulus were rejected as being too early to be evoked responses to whisker stimulation. For each unit, the center/surround response ratio was also calculated. The center/surround ratio (C/S ratio) was defined as:

$$\text{C/S ratio} = \text{response to D2 whisker} / [(\text{response to D1} + \text{response to D3 whisker}) / 2].$$

Thus the ratio indicates changes of the selectivity (contrast) of neurons in D2 barrel column. The 200 sec spontaneous firing was analyzed separately. Student's t-test was performed on the data to estimate significant effects.

## **Results**

The first result of these studies was to determine the depth of layer IV in the barrel field cortex of adult Long Evans rats. Lesions were localized after CO staining and photographed to demonstrate the relationship between the micrometer readings and the histological borders of layer IV. The histological results from one animal are illustrated in Figure 2-2, which is representative of all



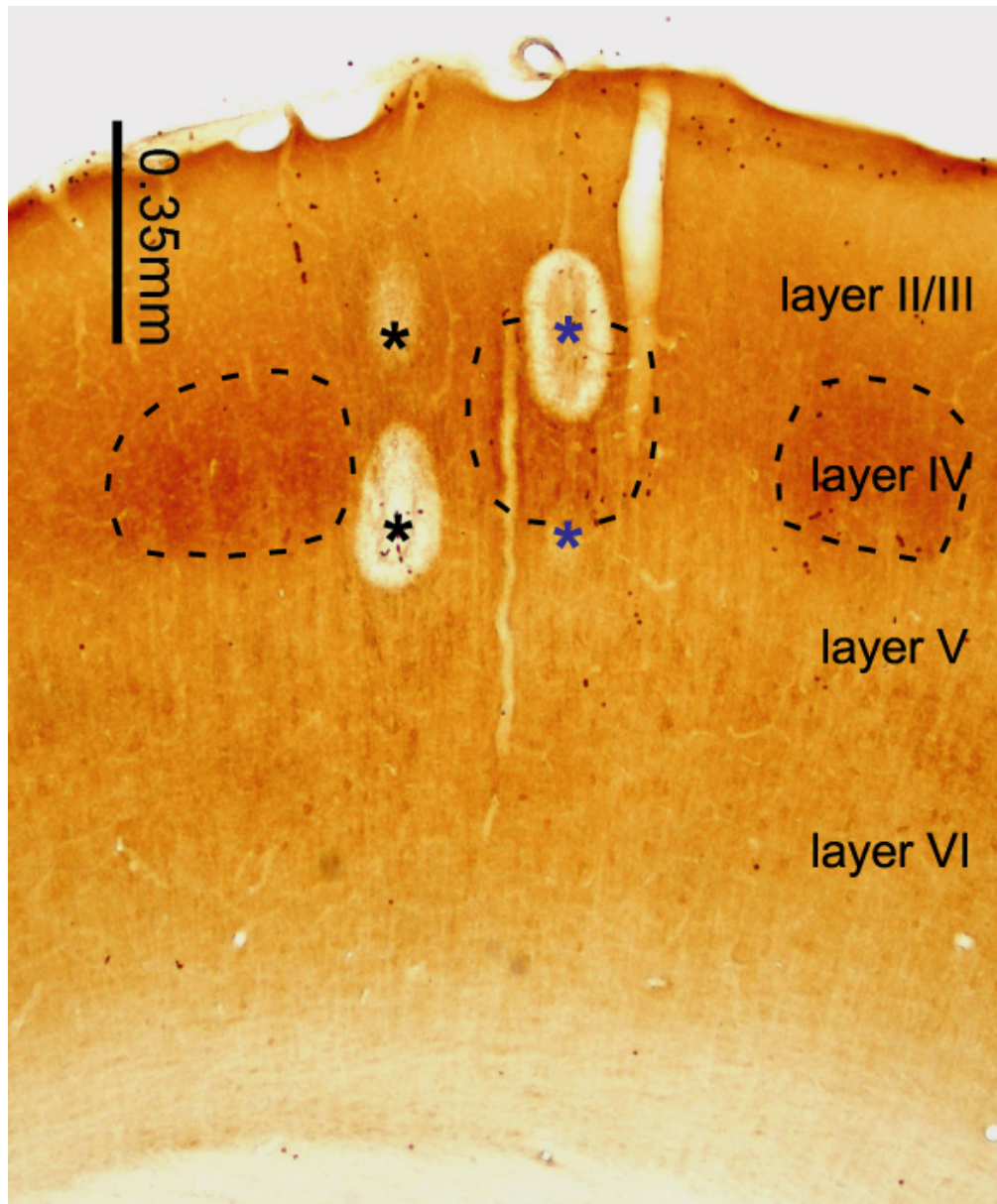


**Figure 2-2. Histology Showing the Depth of Layer IV Barrels *in vivo*.**

Image was taken from one coronal section of animal #03 showing the location of the lesions after CO staining. Two penetrations were made in this animal with two lesions in each penetration at 450  $\mu\text{m}$  and 800  $\mu\text{m}$  (indicated from the read-out of the microdrive) respectively as described in the Materials and Method section. Centers of the lesions were determined by reconstructing the lesions from several adjacent sections and marked by stars. Black stars mark penetration 1 which was localized by physiology as in the septum close to D1. Blue stars mark penetration 2 in D2 barrel. Layer IV barrels were roughly delimited by dashed line. Scale bar: 350  $\mu\text{m}$ . (Contrast was adjusted in Photoshop). Note that the lesions are located near the upper and lower border of layer IV.

of the cases studied. Figure 2-2 shows that the centers of lesions at 450  $\mu\text{m}$  and 800  $\mu\text{m}$ , made *in vivo*, are co-extensive with the top and bottom boundary of CO dense barrels that define layer IV in this cortex. This was also supported by the direct measurement from the section. Using section measurements, the layer III/IV boundary is approximately 370  $\mu\text{m}$  from the surface and the thickness of layer IV is roughly 300  $\mu\text{m}$ . After correction for the shrinkage of the tissue in histological procedure, the predicted depth of layer IV *in vivo* should be  $\sim 480$   $\mu\text{m}$  and the thickness of layer IV should be  $\sim 400$   $\mu\text{m}$ . The histological data are close enough to our micrometer readings of layer IV to make reasonable estimates of layer position from the micrometer lesions alone. We realized that a  $\pm 30$   $\mu\text{m}$  or less error existed between the depth read-out of the microdrive and the real depth of the lesion sites when we made the lesion in the cortex. However, this error could only constitute a minor error in the depth classification. We repeated our experiment in 3 rats, results from 6 penetrations in different barrel columns in different animals were highly consistent. Our data clearly demonstrate that our classification of layer IV is reliable in current experiment paradigm. In the animals used for recording, the brains must be cut tangentially to the cortical surface to accurately identify the barrel and septal position of each penetration, and in these cases the histological estimate of depth is more difficult to reconstruct than in coronal sections.

Histology confirmed 122 neurons were within the D2 barrel column of the left SI in 9 rats after 7-days of muscimol inactivation of the right BFC. Thirteen units were in supragranular layer II/III of the D2 barrel column, 92 were in Layer

IV and 17 were in infragranular layers (mostly layer V). Within the total population of cells, the waveform duration of 111 units was measured, and 27 units were categorized as fast spiking units, 84 were regular spiking units and the remaining 11 units could not be classified for various reasons. Seventy neurons were identified within the D2 barrel column in 5 animals with sterile saline pumped onto the right BFC for 7 days. Twenty units were localized in superficial layer II/III, 42 units were in layer IV, and 8 units were in layer V. The waveform duration of these 70 neurons was known in most cases. Twenty units were fast spiking units, 49 units were regular spiking units and only 1 unit was unclassified. 44 neurons were also identified within the D2 barrel column in 4 control animals with muscimol solution pumped onto the right visual cortex for 7 days. These units were also analyzed here. See table 2-1 for details.

Table 2-1. Data Summary of the Experimental and Control Groups. All units were grouped by the subpial depth and spike duration, see text for details.

	<i>Muscimol SI</i>	<i>Saline SI</i>	<i>Muscimol Visual</i>
# of animal	9	5	4
# of units	122	70	44
Supragranular	13	20	
Layer IV	92	42	
Infragranular	17	8	
FSU	27	20	
RSU	84	49	

## **Behavioral Observations**

Observations of animal behavior began within 24 hours after minipump implantation surgery. Each animal was tested for forelimb placing and posture reflex every day at random times. Nine rats with muscimol minipumped onto BFC all showed a clearcut absence of forelimb posture reflex during the 7 day recovery period. The earliest onset of hyporeflexia was the next day after surgery. On the other hand, they responded quite well to the posture, pinch and placing with the forelimb ipsilateral to the muscimol and with both hindlimbs. These 9 rats also failed to orientate or move their heads when the whiskers contralateral to the implantation side were stimulated by hand-held probe, while in contrast they did turn their head when whiskers ipsilateral to the implantation side were stimulated. Behavioral observations were consistent across the 9 animals. These animals didn't show any apparent dyskinesia. Behavioral asymmetry has been reported after unilateral vibrissae removal (Steiner et al., 1986). In our experiment, rats also tended to maintain contact with the wall of the cage most of the time although they behaved normally in walking or forelimb usage in their cages. Thus from the behavior we conclude that the release of muscimol onto cortex significantly suppressed neuronal activity in cortex, and that chronic muscimol application by minipump covered a brain area larger than the BFC in SI. However, the effect of pumped muscimol was restricted to the extent that it didn't appear to spread to visual cortex. The same behavioral tests showed no deficits in either the saline pumped or the VI muscimol infused rats (no visual tests were carried out).

## **Estimating the Area of Muscimol Suppression**

It has been shown that suppression of neuronal activity in cortex by muscimol is reversible using an experimental paradigm similar to that of the current study (Reiter and Stryker, 1988). Our recording in BFC with muscimol acutely applied confirmed that suppression of cortical activity by 1  $\mu$ l of 10 mM muscimol solution per hour is completely reversible in rat BFC. At 20 min after muscimol application, layer IV neurons in the D2 barrel reduced their spontaneous activity and evoked responses to whisker test stimuli by >50%. However, it is still important to define the size of the area that was blocked by muscimol 7 days after implanting the minipump, and results from chronic muscimol application *in vivo* with electrophysiology in 2 rats were very consistent. The effective range of muscimol is near circular in shape with a point release site, which centered around the tip of the cannula. Neuronal activity, both the spontaneous firing and evoked activity to whisker stimulation, was completely suppressed in any radius within 1.5 mm away from the tip of the cannula. No action potentials, (occasionally injury discharges), were recorded from the pial surface to the white matter within this zone. When the whiskers were deflected with moderately intense manual stimulation, axonal background noise could be heard on the audiomonitor. The deep layer cells around the 1.5 mm distance showed some activity, but still far below normal. The brain area that was from 1.5 mm to 2.5 mm away from the cannula tip was partially suppressed by muscimol. Neurons in this region exhibited response decrements, but they had more spontaneous activity and more responses to test stimuli compared with the

fully blocked region. Neurons would often fire in clusters at low frequency (<1/3sec) especially infragranular neurons when whiskers were stimulated. These results are consistent with previous studies which reported blockade of muscimol was still detectable 2 mm anterior to the cannula after 2 days of 10 mM muscimol application (Reiter and Stryker, 1988). During this type of recording, muscimol was still being pumped onto the brain surface, but we also applied warm saline to the cortical surface when it appeared dry. This dilution may shrink the size of the area delineated by our recording. We conclude that 10 mM muscimol from the minipump can diffuse horizontally over a large enough area to suppress much of the BFC and some of the forelimb area if applied near the medial border of the BFC.

### **Evoked Response Magnitude in Muscimol BFC Group**

The responses evoked in neurons from layer II to layer V of D2 barrel column in left BFC to test stimuli applied to the principal whisker D2 and surround whiskers D1 and D3 were reduced significantly after 7 days of muscimol application to the right BFC. Applying muscimol to the right visual cortex for 7 days had no effect on the evoked response of neurons in the left BFC. Figure 2-3a plots the average number of action potentials generated per 50 stimuli by the neurons from layer II to layer V from three groups in response to D1, D2 and D3 whisker stimulations. The effect of muscimol diffusion can be measured by data from the visual cortex group because we chose to implant minipumps over the visual cortex at a location that would ensure the distance from the cannula tip

(either over right SI or right visual cortex) to the area studied (left BFC) is the same between muscimol BFC group and muscimol visual group. Our data indicates 7 days of muscimol application to right visual cortex didn't alter the response magnitude of neurons in D2 barrel column of left BFC to principal whisker D2 stimulation (42.9spikes/50stimuli v.s. 43.8spikes/50stimuli, muscimol VI v.s. Saline,  $p < 0.43$ , one-tail test, same below unless specified). Responses to surround whiskers D1 and D3 were decrease, but not statistically significantly (D1: 19.3spikes/50stimuli v.s. 24.9spikes/50stimuli, muscimol VI v.s. Saline,  $p < 0.07$ ; D3: 16.9spikes/50stimuli v.s. 21.4spikes/50stimuli, muscimol VI v.s. Saline,  $p < 0.08$ ). Hence neurons in the left BFC were not significantly suppressed by diffused muscimol. However, applying muscimol to the right SI for 7 days significantly degraded the responsiveness of D2 barrel column neurons in the left BFC, to both the principal whisker and the surround whiskers. When compared with the saline group, muscimol decreased responses to the principal whisker D2 by 42% (23.1spikes/50 stimuli vs. 43.8spikes/50 stimuli, muscimol BFC vs. saline,  $p < 8.7 \times 10^{-10}$ ). Similarly, responses to surround whiskers D1 and D3 decreased by 47% (13.2 vs. 24.9,  $p < 4.4 \times 10^{-6}$ ) and 55% (9.6 vs. 21.4,  $p < 3.3 \times 10^{-8}$ ). Responses in muscimol BFC group are also significantly smaller than those from the visual group. Compared with the visual group data, responses to the principal whisker D2 reduced 46% in BFC group (23.1spikes/50 stimuli vs. 42.9spikes/50stimuli, muscimol BFC vs. muscimol visual,  $p < 1.7 \times 10^{-10}$ ). Response to D1 and D3 whiskers also decreased 31% and 43% respectively (D1: 13.2 vs. 19.3,  $p < 0.005$ ;

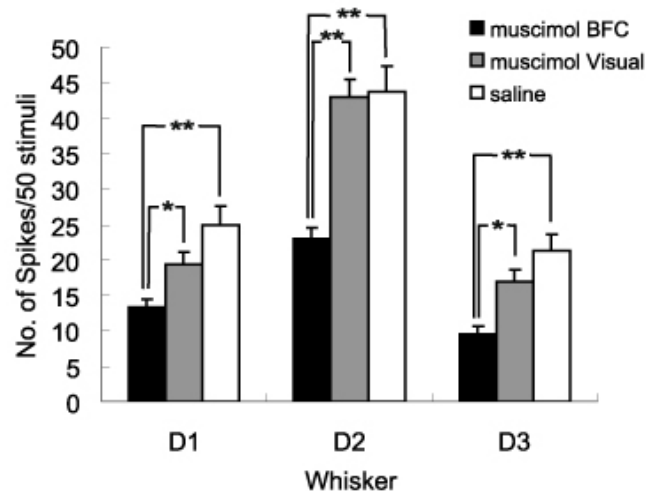
D3: 9.6 vs. 16.9,  $p < 3 \times 10^{-4}$ ). Figure 2-3a shows the comparison of evoked responses of neurons from these 3 groups.

### **Effects on Spontaneous Activity**

Spontaneous activity was assessed in 117 neurons out of 122 units from 9 muscimol BFC rats, 65 of 70 units from 5 saline animals and 42 of 44 units from 4 muscimol VI rats. After 7 days of pumping sterile saline onto the right BFC, the average spontaneous activity level of 65 neurons from layer II to layer V of the D2 barrel column in the contralateral BFC was 0.95 spikes/second. This number is not significantly different from the spontaneous firing rate in adult Long Evans rats under urethane anesthesia, which is typically around 1 spike/second (Armstrong-James and Fox, 1987). Therefore we concluded that the implantation and surgery didn't alter the excitability of BFC neurons and the saline group served as a good control for this parameter. After 7 days of muscimol application to right visual cortex the spontaneous firing of neurons didn't change from layer II to layer V in D2 barrel column of left BFC. The average spontaneous firing rate of 42 neurons from muscimol visual group is 1 spike/second, which is statistically insignificant when compared with saline group (1 spike/s v.s. 0.95 spike/s,  $p < 0.69$ , two-tail t test). Unlike the evoked response, applying muscimol to the right BFC for 7 days slightly decreases the spontaneous activity level of neurons in the D2 barrel column of the left BFC to 0.75 spikes/s (averaged from 117 units), which is not statistically significant (muscimol BFC v.s. saline,  $p < 0.10$ , one-tail t test; muscimol BFC v.s. muscimol VI,  $p < 0.06$ , one-tail t test). Figure 2-3b compares



### a Evoked Response



### b Spontaneous Activity

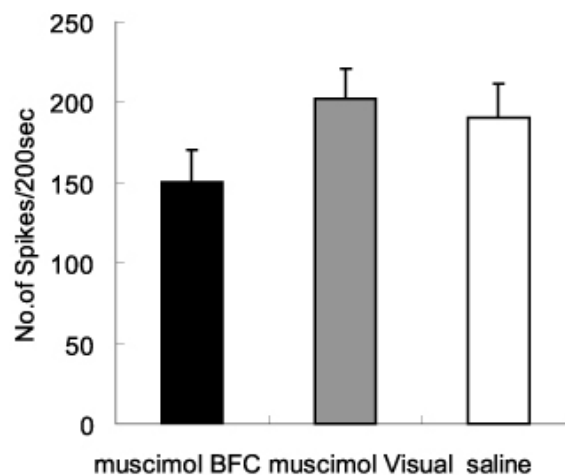


**Figure 2-3. Chronic Unilateral Inactivation of SI by Muscimol Significantly Decreased the Evoked Response of Neurons in Contralateral D2 Barrel Column, while the Spontaneous Activity was Unaffected.**

**a.** Histograms representing mean response magnitudes for 122 neurons from 9 muscimol BFC group (black bars) animals, 44 neurons from 4 muscimol VC animals (grey bars) and 70 neurons from 5 saline control animals (white bars). For each neuron, 50 stimuli were applied to each of the three D-row whiskers. Error bars represent SEM. (\*,  $p < 0.05$ ; \*\*,  $p < 0.01$ . See Results for details.)

**b.** Bar graph showing the number of spikes per 200 seconds of D2 barrel column neurons from 9 muscimol BFC animals, 4 muscimol VC animals and 5 saline control animals. No difference of the spontaneous discharge level was found between muscimol VC group and saline group. 7 days of muscimol application on contralateral SI slightly decreased the spontaneous discharge, however, statistical test failed to prove the significance.

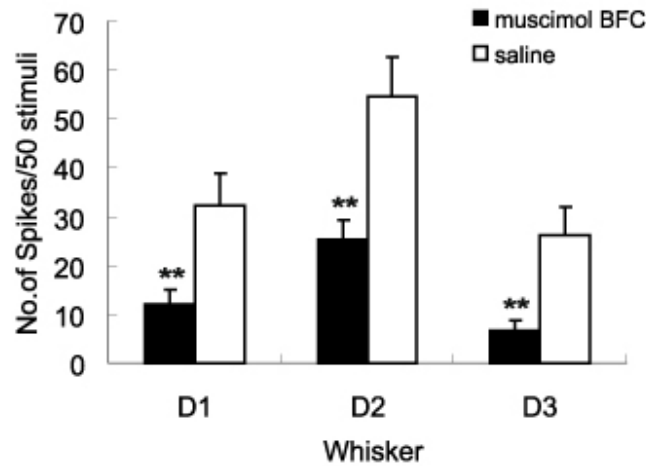
the mean value ( $\pm$ SEM) for spontaneous activity when all units in each of 3 groups are pooled together.

### **Influence of Muscimol on FSU and RSU**

BFC neurons can be categorized by their spike duration into FSU and RSU cells (Mountcastle et al., 1969; Simons and Carvell, 1989). Since FSUs are mostly GABAergic inhibitory neurons (McCormick et al., 1985), it is of particular interest to see if inactivating one BFC with muscimol for 7 days changes the excitatory-inhibitory balance in the contralateral homotopic area. 20 FSUs and 49 RSUs were identified in the saline group. Most of the FSUs were in layer III and IV while RSUs were evenly distributed from layer II to layer V. Generally the FSUs were more responsive than RSUs, in that they generated more spikes on average to test stimuli. The frequency of encountering FSU's in the muscimol suppressed cortex is reduced compared to controls. Of the population of cells that were found, contralateral BFC suppression affected FSUs and RSUs quite differently. After muscimol application, responses of contralateral FSUs were significantly reduced to all three whiskers. On average, responses of FSUs to the D2 principal whisker stimulations are only 47% of the control value ( $p < 0.0005$ ). The FSU reductions are 38% ( $p < 0.002$ ) and 26% ( $p < 0.0004$ ), respectively, to surround D1 and D3 whisker stimulations.

RSUs are more resistant to muscimol application, with responses to the principal whisker stimulation being more reduced than responses to surround whiskers. After 7 days of muscimol application, the response of RSUs to the D2

### a Fast Spiking Units (FSUs)



### b Regular Spiking Units (RSUs)

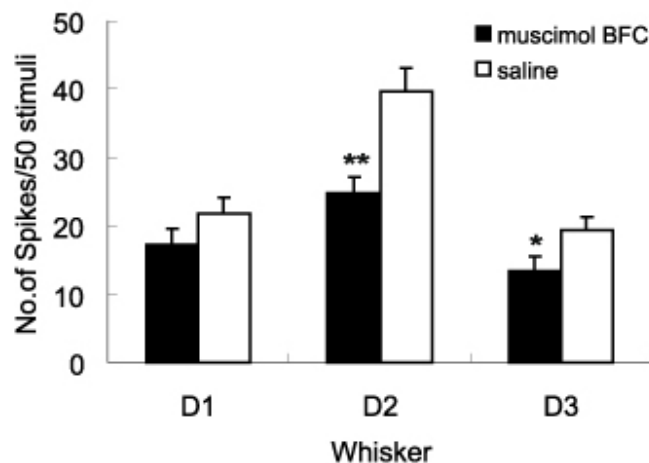


### Figure 2-4. Chronic Unilateral Inactivation of SI by Muscimol Influenced the FSUs and RSUs in Contralateral D2 Barrel Column Differently.

**a.** Histogram comparing the average response for 27 FSUs from 9 muscimol BFC group animals and 20 FSUs from 5 saline control animals. FSUs (whose spike duration < 0.75 ms) typically are more spontaneously active and responsive to whisker stimulations. Muscimol application significantly reduced the mean response magnitude of FSUs to stimulations of both principal whisker D2 and row surround whiskers D1 and D3.

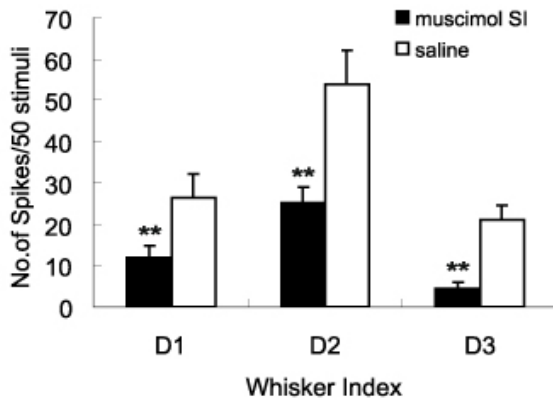
**b.** Histogram represents the average response for 84 RSUs from 9 muscimol BFC group animals and 49 RSUs from 5 saline control animals. RSUs also decreased responses, but the response reduction was only significant in response to the principal whisker stimulations.

whisker stimulations decreased significantly (63% of the control value,  $p < 0.0003$ ) while changes of response to D1 and D3 whiskers stimulations were less prominent. Figure 2-4 shows the effects of muscimol on FSUs and RSUs. RSUs still generated average responses that were 80% ( $p < 0.12$ ) and 70% ( $p < 0.03$ ) of the control value to surround whiskers D1 and D3, respectively. Figure 2-4 shows the details.

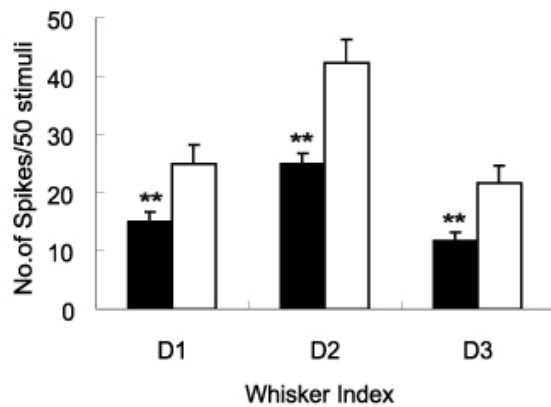
### **Laminar Analysis**

In order to see whether inactivation by muscimol depressed neurons in contralateral BFC in a layer specific manner, units were grouped by their subpial depth after histological correction. Muscimol application considerably reduced the frequency of isolating supragranular neurons in each electrode penetration. The percentage of neurons recorded in superficial layers in muscimol animals is 11% (13/122), but in control (saline) animals sampled in the same way the supragranular subset constitutes 29% (20/70) of the sample. Supragranular neurons in muscimol animals typically produce small spike amplitudes, and while they show robust spontaneous activity, they are less responsive to whisker stimulation. Figure 2-5 compares the average response of neurons in the same laminar category between different animal groups. Data indicate that reduction of responsiveness mainly affects neurons in the layers II/III and IV of the D2 barrel column. The infragranular neurons also decrease their average response magnitude, but the decrease does not achieve significant levels. The lack of significance in infragranular neurons could be due to the limited size of the

**a** Supragranular layers



**b** Layer IV



**c** Infragranular layers

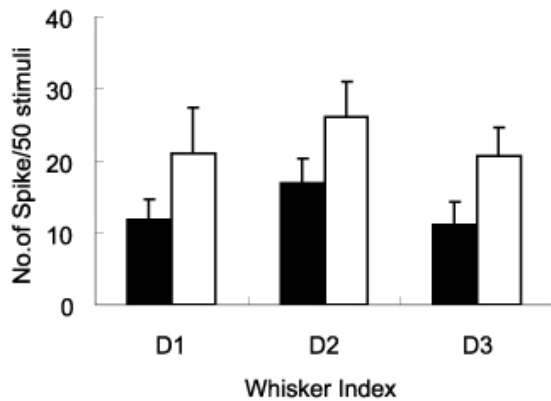


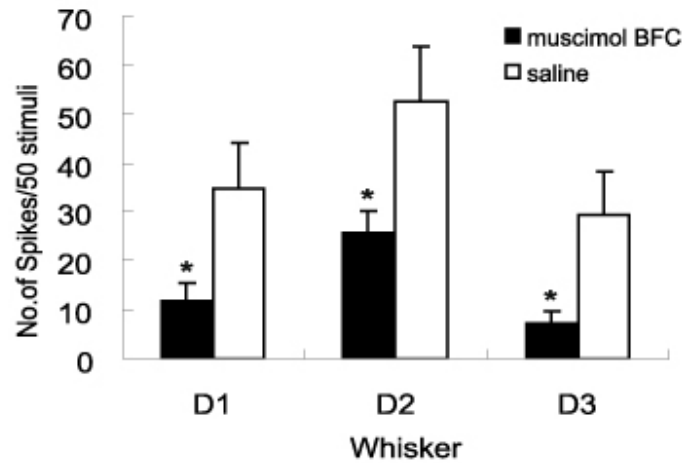
**Figure 2-5. Chronic Unilateral Inactivation of SI by Muscimol Significantly Decreased the Evoked Response of Neurons in both Superficial (Layer II/III) and Granular Layers in Contralateral D2 Barrel Column. But Changes of the Response of Infragranular (Mainly Layer V) Neurons were Insignificant.**

**a.** Histogram showing the average response for 13 supragranular neurons from 9 muscimol BFC animals and 20 neurons in superficial layers from 5 saline control animals.  
**b.** Histogram comparing the average response for 92 granular neurons from 9 muscimol BFC animals and 42 layer IV neurons from 5 saline control animals.  
**c.** However, the average response for 17 infragranular neurons from 9 muscimol BFC animals is not different from the response magnitude of 8 infragranular neurons from 5 saline control animals.

sample. Responses to surround whiskers D1 and D3 were affected as well as principal whisker D2. In brief, layer II/III neurons in the D2 barrel column in muscimol animals only gave an average response at 45% to D1 (12 spikes/50 stimuli vs. 26.5 spikes/50stimuli,  $p<0.03$ ), 47% to D2 (25.2 vs. 53.9,  $p<0.006$ ) and 23% to D3 (5 vs. 21.1,  $p<0.0005$ ) of the control value respectively. Layer IV neurons ( $n = 92$ ) in muscimol BFC group were also compared with 42 granular layer neurons from saline animals. Their relative response magnitude is 68% (15.1 spikes/50 stimuli v.s. 24.9 spikes/50 stimuli,  $p<0.03$ ) to D1, 62% (24.8 v.s. 42.3,  $p<0.0002$ ) to D2 and 61% (11.7 v.s. 21.6,  $p<0.01$ ) to D3 stimulations, compared to controls respectively. We also recorded 17 infragranular neurons (mostly layer V neurons) in muscimol animals and 8 neurons from saline rats. Although these neurons exhibited response decrease, statistical test failed to prove significance: 67% (11.8 v.s. 21,  $p<0.12$ ) to D1, 72% (16.9 v.s. 26.1,  $p<0.11$ ) to D2 and 58% (11.4 v.s. 20.6,  $p<0.05$ ) to D3.

Barrel neurons in layer IV were examined separately since it was not expected that these neurons would show a response decrement after muscimol application. Eleven layer IV FSUs and 31 RSUs were identified from 42 barrel cells in saline control, and 22 FSUs and 61 RSUs were localized within layer IV in muscimol BFC rats. Figure 2-6a compares the average response to peripheral whisker stimulation in 22 layer IV FSUs (BFC muscimol group) and 11 barrel FSUs in saline controls. Responses of FSUs in the barrel to both the principal whisker and surround whiskers were heavily suppressed. The response reduction was 50% ( $p<0.02$ ) to D2, 65% ( $p<0.02$ ) and 76% ( $p<0.02$ ) to D1 and

**a Layer IV FSU**



**b Layer IV RSU**

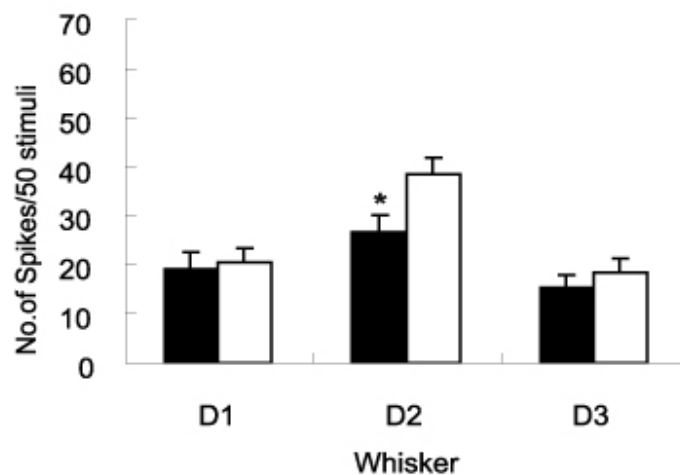


**Figure 2-6. Influences of Chronic Unilateral Inactivation of SI by Muscimol for 7 Days on the Layer IV FSUs and RSUs in Contralateral D2 Barrel Column.**

**a.** Bar graph comparing the average response for 22 FSUs in layer IV from muscimol BFC group and 11 FSUs from saline control. Muscimol application significantly reduced the mean response magnitude of FSUs to stimulations of both principal whisker D2 and row surround whiskers D1 and D3.

**b.** Bar graph represents the average response for 61 RSUs from muscimol BFC group and 31 RSUs from saline control group. Only the response to the principal whisker D2 reduced significantly.

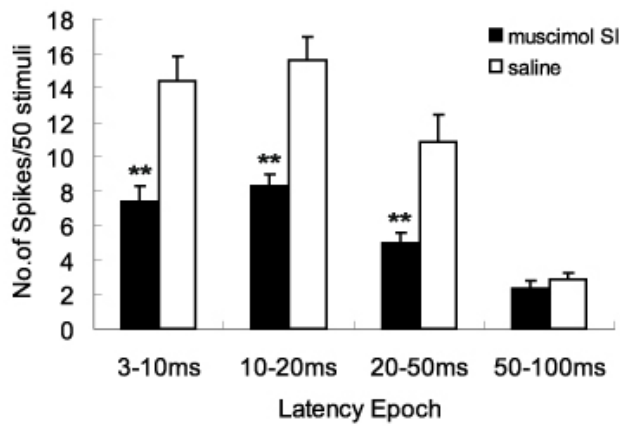
D3 respectively. However, as shown in Figure 2-6b, layer IV RSUs decreased their response to the principal D2 whisker only ( $p < 0.01$ ) after muscimol application, while the responses to the surround whiskers D1 and D3 remained unchanged ( $p < 0.75$ ,  $p < 0.37$ , two-tail t test).

### **Latency Analysis**

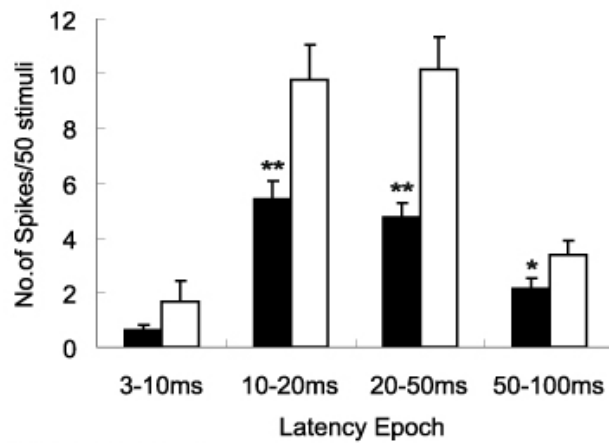
Responses of a barrel neuron to whisker stimulation consist of the temporal interactions of excitation/inhibition from different circuits. Thus investigating the temporal structure of the response offers an opportunity to differentiate the role of various brain areas in cortical function. Latency epochs are dominated by different inputs to barrel column neurons. It is of interest to see how inactivation of BFC influences the temporal structure of BFC neuron responses on the contralateral side. Figure 2-7 compares the mean values of 4 latency epochs from cells in all layers. Effects of muscimol on latency epochs substantially differ between principal whisker D2 and row surround whiskers D1 and D3. Response decrease was observed in the longer (10-100 ms) latency components in response to D1 and D3 whisker stimulation where the short latency component is normally small. Response to the principal whisker D2 decreased prominently in both the robust short latency (3-10 ms) and the more variable long latency (10-50 ms) components. On average, spike number to D2 stimuli in 3-10 ms component decreased 49% ( $p < 9.6 \times 10^{-6}$ ), 10-20 ms epoch



**a Response to D2**



**b Response to D1**



**c Response to D3**

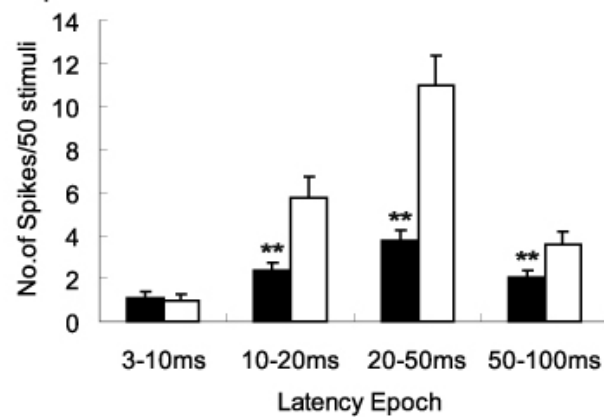


**Figure 2-7. Effect of Muscimol on Response Latency Epochs of Neurons in Contralateral D2 Barrel Column.**

**a.** Comparison of the average response magnitude within 4 latency epochs to principal whisker D2 stimuli. Muscimol application reduced both the short (3-10 ms) and longer (10-50 ms) latency components.

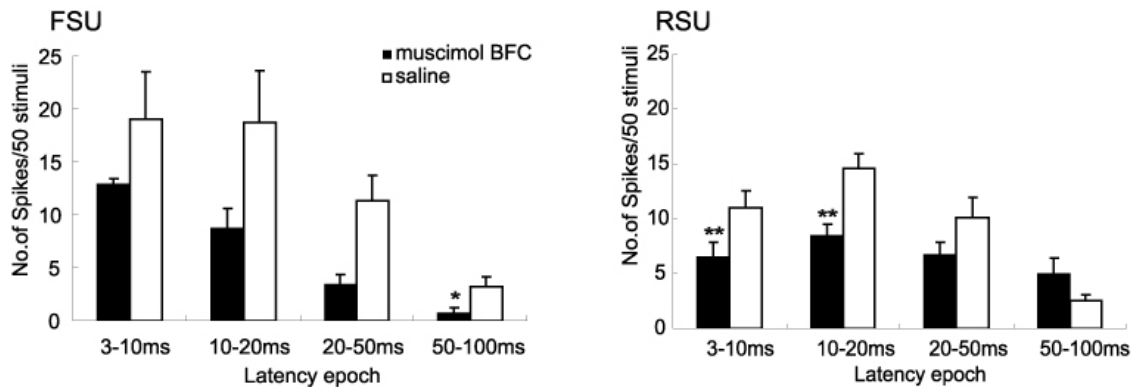
**b** and **c** Comparison of the average response in 4 latency epochs to surround whisker D1 and D3 stimulations respectively. Muscimol application only decreased the long (10-100 ms) latency components in surround whiskers.

component reduced about 47% ( $p < 1.3 \times 10^{-7}$ ), 20-50 ms reduced 54% ( $p < 3.4 \times 10^{-5}$ ), but responses in the small 50-100 ms component remained unchanged ( $p < 0.22$ ). The response to the surround whisker D1, the spike number within 3-10 ms decreased by 62% ( $p < 0.05$ ), by 45% ( $p < 0.0004$ ) in 10-20 ms epoch, by 54% ( $p < 1.8 \times 10^{-6}$ ) in 20-50 ms and by 36% ( $p < 0.03$ ) in 50-100 ms respectively. Similarly, response to D3 decreased by 59% ( $p < 3.8 \times 10^{-5}$ ) in 10-20 ms epoch, 66% ( $p < 1.2 \times 10^{-8}$ ) in 20-50 ms, 43% ( $p < 0.008$ ) in 50-100 ms while 3-10 ms component was unchanged ( $p < 0.41$ ). Latency epochs of FSUs and RSUs within layer IV were also analyzed and the results were shown in Figure 2-8.

Comparison of the data between 22 layer IV FSUs in muscimol BFC group and 11 FSUs from the saline control in response to the principal whisker D2 found that only the neural response within 50-100 ms in barrel FSUs was significantly suppressed by muscimol application ( $p < 0.03$ ). Responses in other latency epochs, although also lower than controls, failed to reach significance (3-10 ms:  $p < 0.08$ ; 10-20 ms:  $p < 0.06$ ; 20-50 ms:  $p < 0.06$ ). This can be largely attributed to the small sample size and the huge variance we have for the layer IV FSUs.

However, the influences of muscimol infusion were more prominent on the latency epochs of layer IV RSUs. After comparing 64 barrel RSUs in muscimol animals with 31 layer IV RSUs in control, significant response reduction was found in 3-10 ms ( $p < 0.02$ ) and 10-20 ms ( $p < 0.0003$ ) latency epochs, while the responses within 20-50 ms and 50-100 ms were less unaffected ( $p < 0.05$ ,  $p < 0.07$  respectively). On the other hand, responses of these layer IV FSUs to the surround whiskers D1 and D3 shifted significantly in temporal structure, while no

**a Response of Layer IV cells to the principal whisker D2**



**b Response of Layer IV cells to the surround whisker D1**

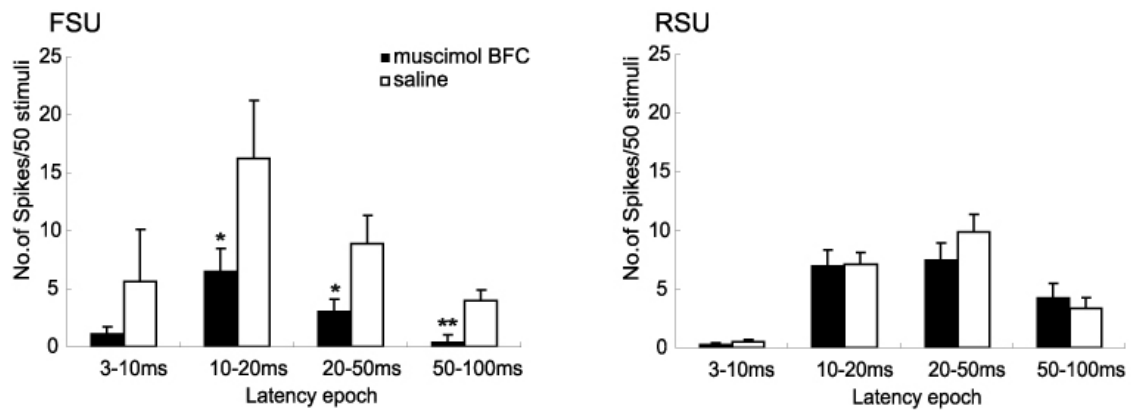


**Figure 2-8. Effect of Muscimol Application on Response Latency Epochs of Layer IV FSUs and RSUs in the Contralateral D2 Barrel Column.**

**a.** Comparison of latency epochs of layer IV neurons in response to D2 whisker stimuli between muscimol BFC and saline group. Left panel: bar graph comparing the latency epochs of 22 layer IV FSUs from muscimol BFC group with that of 11 barrel FSUs from saline control group. Right panel: bar graph comparing the latency epochs of 61 layer IV RSUs from muscimol BFC group with that of 31 barrel RSUs from saline control group.

**b.** Comparison of latency epochs of layer IV neurons in response to D1 whisker stimuli between muscimol BFC and saline group. Left panel: bar graph comparing the latency epochs of 22 layer IV FSUs from muscimol BFC group with that of 11 barrel FSUs from saline control group. Right panel: bar graph comparing the latency epochs of 61 layer IV RSUs from muscimol BFC group with that of 31 barrel RSUs from saline control group.

change of latency epochs was found in barrel RSUs after muscimol application. Figure 2-8b shows the influences of muscimol infusion on the latency epochs of layer IV FSUs and RSUs in response to D1 whisker stimuli. Responses within 10-100 ms were affected (3-10 ms:  $p < 0.18$ , 10-20 ms:  $p < 0.05$ , 20-50 ms:  $p < 0.02$ , 50-100 ms:  $p < 0.0007$ ). But all the 4 latency epochs of layer IV RSUs in response to D1 and D3 stimulations failed to show significant changes (D3 data not shown).

### **Effects of Muscimol on C/S Ratio**

When all units were pooled together, the data lead to the conclusion that muscimol didn't have an effect on the C/S ratio. The mean value of the C/S ratio of 120 units from layer II to layer V in 9 muscimol BFC rats is 4.20, which is not significantly different ( $p < 0.13$ , two-tail t test, same below unless specified) from the number of 3.03 from 70 units in 5 saline control animals. In saline control rats, the average C/S ratio of FSUs in all layers ( $n = 20$ ), which is 3.39, is not different from that of RSUs ( $n = 49$ ) ( $p < 0.62$ ), which is 2.92. Muscimol treatment didn't alter the center/surround contrast between FSUs and RSUs. The average C/S ratio for FSU in all layers ( $n = 27$ ) is 4.73 in muscimol BFC rats. When compared with the mean value of 4.25 from RSUs ( $n = 82$ ), statistical test failed to prove the significance ( $p < 0.70$ ). Furthermore, neither FSU nor RSU showed a significant change in C/S ratio after muscimol (FSU:  $p < 0.31$ , muscimol BFC vs. saline control; RSU:  $p < 0.19$ ), although the numbers did tend to increase after muscimol application. However, when layer IV units were examined separately, it was found that muscimol application did have a significant influence on the C/S ratio

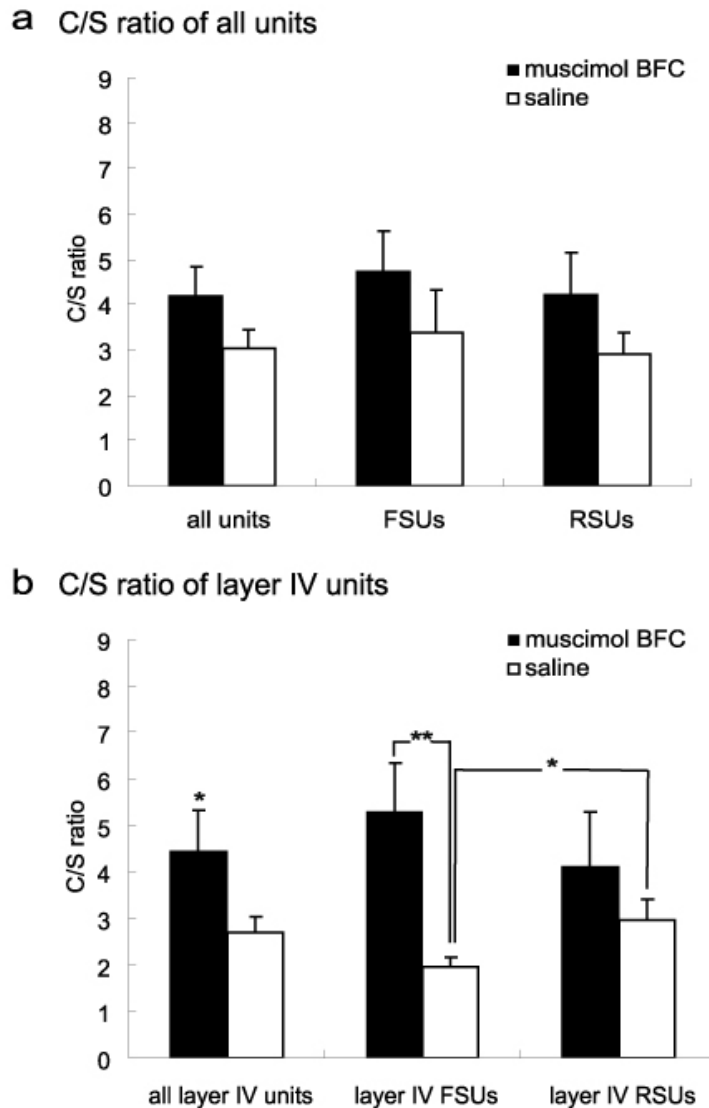


**Figure 2-9. Effect of Muscimol Infusion on the Center/Surround Ratio of Neurons in the Contralateral D2 Barrel Column.**

**a.** Bar graph comparing the center/surround (C/S) ratio of units from all layers between muscimol BFC group (n = 120) and saline control (n = 70) (left); when all units were categorized into FSUs (n = 27 in muscimol BFC group, n = 20 in saline control) (middle) and RSUs (n = 82 in muscimol group and n = 49 in saline) (right). No difference was detected.

**b.** Bar graph comparing the C/S ratio of all layer IV units between muscimol BFC group (n = 81) and saline control (n = 42) (left); when all layer IV units were categorized into FSUs (n = 22 in muscimol BFC group, n = 11 in saline control) (middle) and RSUs (n = 59 in muscimol group and n = 31 in saline) (right).

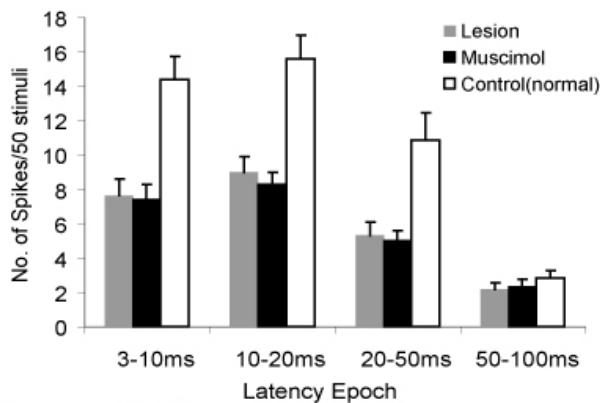
of barrel neurons. For 42 layer IV neurons in normal rats, the average C/S ratio is 2.70. Muscimol significantly increased the value to 4.59 ( $p < 0.03$ , one-tail t test) when the data from 83 barrel neurons in muscimol BFC group were analyzed. The increase was mainly due to changes in FSUs. The C/S ratio of FSU significantly increased from 1.95 ( $n = 11$ ) to 5.29 ( $n = 22$ ) after muscimol treatment ( $p < 0.003$ , one-tail t test). But RSUs didn't change their ratio: the mean value of 4.33 from 61 layer IV RSUs after muscimol application didn't differ from the 2.96 ratio in 31 barrel RSUs in control ( $p < 0.27$ ). Muscimol also seemed to alter the selectivity profile between FSUs and RSUs. In saline control animals, layer IV RSUs were more selective than layer IV FSUs (C/S ratio 2.96 vs. 1.95,  $p < 0.02$ , one-tail t test). However, in muscimol animals, the difference between RSUs and FSUs disappeared (4.33 vs. 5.29,  $p < 0.54$ ). Figure 2-9 shows the details.

## Discussion

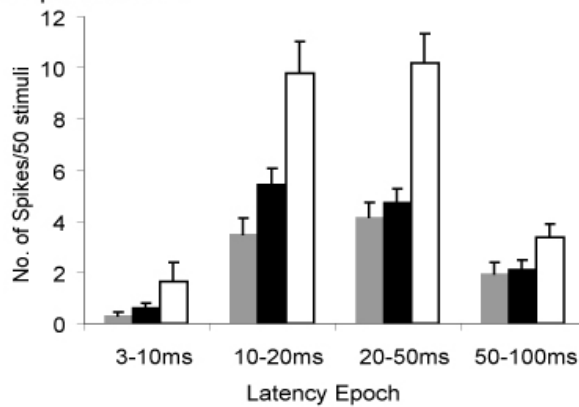
This study documents a significant decrement of evoked responses in rat SI cortical neurons to peripheral whisker stimulation, especially in the supragranular layers, after 7 days of activity suppression in the contralateral BFC. These data support the hypothesis that the cerebral hemispheres maintain an active bilateral balance of sensory processing activity. The crosstalk between the two hemispheres is achieved by modulating the responsiveness of neurons to sensory inputs at a single unit level independent of the general level of background excitability. The present results provide insights into the way that

callosal activity modulates cells in primary sensory cortex. Since the responses of BFC neurons after 7 days of muscimol treatment are reduced by roughly the same magnitude as in animals with BFC lesions, we conclude that most the neural response decrement 8 days after BFC neurons is induced by the effect on callosal activity. Comparison of muscimol and lesion data revealed a high degree of consistency in the evoked response profile (Fig. 2-10). After brain lesions, the response magnitude of neurons to test stimuli in the contralateral D2 barrel column was equally severely depressed in rats (Rema and Ebner, 2003), which is in agreement with the present results. However, lesions of one BFC also decreased the background activity of neurons in contralateral BFC by nearly 80%, which was not true after reversible pharmacological silencing. We conclude that lesions produce a more global deficit than simple silencing as produced in the present study. Taken together, both the previous and current studies speak to the specific cellular changes that underlie interhemispheric 'diaschisis-like' effects in sensory cortex and supports the hypothesis that primary sensory cortex in each cerebral hemisphere actively interacts in such a way that changes in activity on one side are registered continuously by neurons in connected areas. An unexpected finding was that the short latency component of the evoked response that is usually associated with thalamocortical inputs were affected in both lesion and muscimol studies. We speculate that the contralateral VPM thalamic nuclei may be indirectly affected by the chronic unilateral cortical suppression by muscimol, and we are currently testing this possibility.

**a** Response to D2



**b** Response to D1



**c** Response to D3

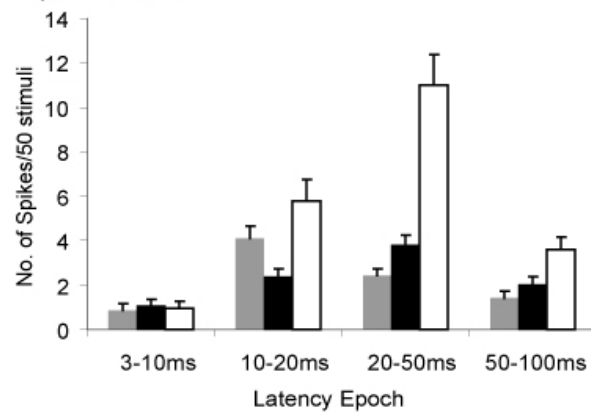


**Figure 2-10. Comparison of Data from Muscimol and Lesioned Animals.**

**a.** Comparison of the average response magnitude within 4 latency epochs to principal whisker D2 stimuli between animals 7 days after ablation lesion of contralateral BFC (yellow bars, n = 77, Rema and Ebner 2003), 7 days after inactivation of contralateral BFC by muscimol (black bars, n = 122) and 7 days after saline infusion onto contralateral BFC (white bars, n = 70). Data from muscimol animals and lesioned animals demonstrate highly consistency.

**b** and **c** Comparison of the average response in 4 latency epochs to surround whisker D1 and D3 stimulations respectively between lesion group (yellow bars), muscimol group (black bars) and the control (white bars). Muscimol application only decreased the long (10-100 ms) latency components in surround whiskers. (Courtesy to Rema and Ebner, 2003)



## **Methodological Concerns**

### ***Surgical and Recording Procedure***

The present study was designed to distinguish between impairments induced by reduced callosal activity resulting from cortical lesions that trigger degenerative events as well as activity decrements. Whether the cortex was effectively silenced without cell death emerges as a crucial issue. In the present studies certain precautions were taken to prevent damage to cortex. Special care was taken during stabilizing and cementing to ensure the muscimol was delivered onto the surface of cortex without any direct damage. Furthermore, the brain was examined by histology after recording. Data from one rat with muscimol on SI was excluded after histology showed a small zone of cell loss directly under the cannula that must have occurred during implantation. We feel confident that direct brain damage had been minimized and the role of activity in interhemispheric interaction could be isolated. Spontaneous firing rate remained stable and equivalent between the experimental and control animals. Thus we concluded that changes in responsiveness in BFC after contralateral BFC inactivation is not due to “exogenous” factors such as changes in our recording conditions.

We concluded that muscimol application decreased the occurrence of recordable neurons using our set of selection criteria, especially in the superficial layers. Neurons responsive to whisker stimulation in muscimol animals typically tend to have rather smaller amplitude spikes as displayed individually compared with units isolated in normal rats, although we have not quantified this difference.

Neurons with large waveforms tend to be spontaneously active, but less drivable. Although we realize that the ratio of the more responsive but less discriminable units to the higher amplitude but less responsive neurons should be similar between experimental and control animals, this difference is also difficult to quantify. These changes may become important when comparing how neurons were selected in data from different studies.

### ***Physiological and Pharmacological Effects of Muscimol in vivo***

Muscimol is a powerful and selective GABA<sub>A</sub> receptor agonist (DeFeudis, 1980a, 1980b; Krogsgaard-Larsen et al., 1979; Naik et al., 1976). Since GABA is the principal inhibitory neurotransmitter in all layers of cerebral cortex, pharmacological activation of GABA<sub>A</sub> receptors successfully suppresses activity in almost all neurons (Hendrickson et al., 1981; Hess and Murata, 1974). The inhibitory action of GABA is generally associated with a direct postsynaptic effect (Newberry and Nicoll, 1985). Muscimol had been widely used to reversibly inactivate a circumscribed neuronal population, but it is still necessary to characterize its physiological and pharmacological effects in each application. First, we needed to establish whether the pharmacological effect of muscimol introduced any bias to our observations; and second, whether the muscimol solution at the concentration used (10 mM) effectively suppress neuronal activity over the target area.

The acute muscimol experiments demonstrated that 10mM muscimol solution, applied directly to the surface of barrel area, produces a reversible

suppression of cortical activity. The suppression developed over time and by 20 min post-muscimol-application, spontaneous firing and responses of layer IV neurons in D2 barrel column to peripheral stimuli were reduced by >50%. Although there is little question that muscimol suppresses neural activity in cortex, it is also the case in the acute experiments that muscimol could enter cortex along the electrode tract and alter the onset time. We mapped the effect area of muscimol *in vivo* by electrophysiology, and the results are highly consistent with what had been reported using muscimol solution with the same concentration (Edeline et al., 2002; Reiter and Stryker, 1988). Our data show that 10 mM muscimol can diffuse horizontally over a large area to affect the majority of BFC. An autoradiographical study (Martin, 1991) in rat spinal cord showed that when 5 mM (1 mg/ml) muscimol was injected into the spinal cord, a sphere of suppression with radius of 1.5~1.7 mm was formed. Given the concentration of muscimol solution (5 mM) is one half of ours (10 mM), and assuming that muscimol diffuses with similar speed in the brain and spinal cord, it is reasonable to conclude that the 10 mM muscimol solution we applied to the surface of cortex could suppress a large enough area to affect the majority of the BFC.

### **Physical Connections Underlying the Functional Down-regulation**

Early studies reported an unmasking and expansion of receptive fields of homologous areas in neocortex after a peripheral denervation on the ipsilateral side (Carlford and Tweedale, 1990; Clarey et al., 1996). The extensive homotopic/nonhomotopic commissural projections presumably serve as the

underlying circuit for the interhemispherically transferable plasticity (Krubitzer et al., 1998). In rats, the anatomy of commissural connections correlates well with our finding that suppressing one BFC with muscimol for 7 days significantly downregulates the evoked responses of neurons in the contralateral BFC in most layers (infragranular neuron changes failed to show significance). Extensive connections exist between SI in the two hemispheres of rats, as well as other mammals including cats, raccoons, grey squirrels and monkeys (Gould and Kaas, 1981; Jones and Wise, 1977; Jones et al., 1975; Kroalek et al., 1988; Koralek et al., 1990; Krubitzer et al., 1986; Olavarria and van Sluyters, 1995; Olavarria et al., 1984; Wise and Jones, 1976; for review, see Innocenti, 1986). Commissural projections were reported to be mostly reciprocal between homotopic and nonhomotopic SI areas in rats and the density of these connections varies as a function of the body part representation examined (Akers and Killackey, 1978; Koralek et al., 1990). It was once believed that commissural cells and terminals mainly distributed in the agranular zone medial to the BFC with a columnar structure, while the callosal projections in BFC were absent (Akers and Killackey, 1978; Wise and Jones, 1976). However, more recent studies using axonal transport tracing techniques have revised this picture, so the vibrissae area in SI is not devoid of direct callosal projections. By injecting HRP into one BFC, callosal cell bodies and terminations were visualized in both supragranular and infragranular layers of BFC on the other side (Olavarria et al., 1984). Those projections also terminated within the 'septa' region in layer IV and preferred whisker rows to arcs, while only sparse terminals were observed in layer IV

barrels (Olavarria et al., 1984). Similar results have also been reported in the upper and lower jaw representation areas of the granular zone in rat SI (Hayama and Ogawa, 1997). These authors also reported moderately dense labeled callosal cell bodies and terminals in the septa of the posteromedial barrel subfield (whisker input cortex) after injections in the contralateral barrel area, compared with sparse to absent labeling inside of the layer IV barrels *per se* (Hayama and Ogawa, 1997). Anatomical studies provide a substrate for physiological observations of interhemispheric interactions. Bilateral receptive fields have been described in several components of the somatosensory system in rats (Armstrong-James and George, 1988; Shuler et al., 2001) and non-human primates (see Iwamura, 2000; Iwamura et al., 2001 for review). Although it is possible that the ipsilateral body part close to the midline is represented in cortex via subcortical structures (Armstrong-James and George, 1988), distal body parts such as digits (Iwamura et al., 1994) and vibrissae (Shuler et al., 2001) are bilateralized through the corpus callosum. On the other hand, plasticity induced in one hemisphere transfers to another hemisphere after either peripheral deafferentation (Calford and Tweedale, 1990; Clarey et al., 1996; Shin et al., 1997) or a central lesion (Reinecke et al., 2003; Rema and Ebner, 2003) in mammals, and these interhemispheric changes are also mediated by the corpus callosum. Previous studies showed that the exchange of sensory information between two cerebral hemispheres is dependent upon the intactness of the contralateral cortex and corpus callosum either by evoked field potential (Pidoux and Verley, 1979), single unit recording (Shuler et al., 2001) or behavior tasks

(Krupa et al., 2002; Shuler et al., 2002). These studies unequivocally demonstrated that functional interlink between two BFCs are mediated via callosal connections in an activity dependent way. More details were revealed by examining the laminar distribution of callosal projections in BFC. Callosal axons originate almost entirely from pyramidal neurons in layer II/III and layer V/VI in rat (Hayama and Ogawa, 1997; Wise, 1975; Wise and Jones, 1976). They terminate with excitatory asymmetric synapses on spines of the apical or basal dendrites of pyramidal neurons in the superficial layers of the target regions of the contralateral cortex (Cipolloni and Peters, 1983; Wise and Jones, 1976; but see Vaughan, 1983 for the callosal terminals in infragranular layers). Thus it is expected to see that BFC neurons in the superficial layers would be affected most after the contralateral BFC was silenced. This is indeed what we found in the present experiments. Both the current study and our previous lesion study (Rema and Ebner, 2003) converge at this point. This result further indicates an integrative role of supragranular layers in the barrel cortex: it is the place where the integration of the thalamic and callosal information collides. Since layer IV barrels are more or less devoid of direct callosal inputs, it is rather surprising to find a significant decrease of responses in layer IV barrels. Two possible explanations may account for the layer IV effects. One is that changes in nearby septa and layers above and/or below layer IV barrels after inactivation of contralateral BFC alter the response properties of barrel neurons. It has been reported that whisker pairing plasticity was first observed in supra and infragranular layers before they occur in layer IV (Diamond et al., 1994). Similarly,

since neurons in septa and superficial layers receive more callosal inputs relative to barrel neurons, layer IV neurons may be influenced indirectly. The difficulty with this explanation is that available evidence suggests that callosal inputs are segregated from thalamic inputs in the primary sensory areas in mammals (Gould and Kaas, 1981; Jones and Wise, 1977; Jones et al., 1975; Kroalek et al., 1988; Koralek et al., 1990; Krubitzer et al., 1986; Olavarria and van Sluyters, 1995; Olavarria et al., 1984; Wise and Jones, 1976), but little is known about the details of the recipients of callosal projections in septa, in the sense of cell types (e.g., FSU vs. RSU). Thus no consistent theory emerges to explain the response decrease observed in layer IV neurons. Another explanation is that changes in the layer IV barrels are due to plasticity in dorsal thalamus. Callosal fibers also terminate in infragranular layers (see above) and stimulating the corpus callosum activates only two classes of cells: suspected inhibitory neurons (SINs) and corticothalamic neurons in layer VI (Swadlow, 1988, 1989). Since corticothalamic projections are the driving input to P<sub>Om</sub> neurons and an important modulator to VPM neurons (Diamond et al., 1992a, b; Krupa et al., 1999; Sherman and Guillery, 1996), it is possible that response decrease in layer IV is actually a reflection of the indirect effects of chronic silencing of contralateral BFC on thalamic relay neurons. We found that muscimol suppression had profound effects on several latency components of a response. When neurons from different layers were averaged, the longer latency components (>10ms) exhibited significant decreases after both principal and surround whisker stimulation (Fig. 6). These latency components are thought to be responses generated by

ipsilateral intracortical and interhemispheric connections. However, even layer IV neurons are influenced by muscimol application (Figure 2-5, 2-7). Since barrel neurons are driven predominantly by VPM, it is unexpected to find decrements in response to sensory stimuli in layer IV neurons. More surprisingly, the shortest latency component (3-10ms) decreased significantly. Responses of BFC neurons generated within 10 ms after stimulus onset are strongly driven by direct connections from VPM (Armstrong-James et al. 1993). These findings also indicate that thalamus may be affected indirectly by muscimol suppression as well. Traditionally thalamic sensory relay nuclei were viewed as an autonomous relay conveying information to cortex with little modification. The classical view can hardly explain the current results. As a matter of fact, cortex projects extensively back to thalamus, which can have an impact on thalamic cell responses (Diamond, et al., 1992b; Li and Ebner, 2003).

The ascending lemniscal thalamocortical projections ending in layer IV determine the center of the classic receptive field of barrel neurons, while the surround of receptive field is thought to be largely generated via the intracortical connections between layers/barrel columns (Armstrong-James and Fox, 1987; Armstrong-James et al., 1991; Simons and Carvell, 1989). Hence the center/surround ratio of barrel neurons indicates the interactions of neural circuits which cortex employs in whisker information processing. As discussed above, the thalamocortical and callosal projections form a complementary and layer-specific pattern in BFC, suggesting that in adult rat BFC the thalamic inputs may have complex interactions with the function of callosal inputs. Thus by examining



the center/surround ratio of barrel neurons before and after removal of the callosal projections we can detect changes in the balance of center and surround circuits. Our data show that FSUs are more sensitive to the removal of commissural inputs than RSUs. Callosal projections seem to converge more on FSUs since stimulating the corpus callosum activated SInS but not RSUs (Swadlow, 1988, 1989), thus removal of excitatory callosal inputs to SInS can degrade their response, but the predicted outcome would be disinhibition. Commissural fibers also contact pyramidal neurons in layer II/III of the contralateral cortex (Cipolloni and Peters, 1983; Wise and Jones, 1976), the excitatory nature of commissural fibers and their spatial segregation indicates that in normal rats, the interhemispheric inputs reach a general equilibrium with the thalamic inputs so that the responsiveness of neurons in SI is maintained. Hence after chronic inactivation of one BFC, a mixed effect should be observed. When interhemispheric plasticity was acutely induced in cortex, suppression was recorded following an initial increase of responsiveness of neurons in contralateral homotopic area (Clarey et al., 1996; Reinecke et al., 2003). Removal of callosal inputs has a complex impact on the neural circuits on the contralateral side. First disinhibition occurs when some FSUs lose their excitatory input from the corpus callosum, however, since pyramidal neurons in superficial layers as well as in septa receive commissural influences, effects on RSUs diminish the disinhibition from FSUs and the responses to both principal and surround whiskers decrease significantly after chronic inactivation of the contralateral BFC. Thus the effect reported would be strongly biased by the

duration of the silencing. It is important to emphasize that the decrease in FSU responses also can be influenced by changes in the level of thalamocortical inputs. The muscimol application chronically inactivated one BFC, thus neurons in infragranular layers on the contralateral side changed their responses. Corticothalamic projections to both VPM and POm could affect transmission through the lemniscal and/or paralemniscal pathways back to the BFC. Since infragranular neurons are generally less responsive to whisker stimuli, paradigms other than comparing spike numbers to whisker stimuli may be more sensitive to these changes.

## CHAPTER III

### **BALANCING BILATERAL SENSORY ACTIVITY: CALLOSAL PROCESSING MODULATES SENSORY TRANSMISSION IN THE CONTRALATERAL THALAMUS BY ALTERING THE RESPONSE THRESHOLD**

The study described in this chapter was published in 2006 (Li L, Ebner FF. Exp Brain Res. 2006 Jan 21:1-19 [Epub ahead of print])

Rats tactually explore a nearly spherical space field around their heads with their whiskers. The information sampled by the two sets of whiskers is integrated bilaterally at the cortical level in an activity dependent manner via the corpus callosum. We have recently shown that sensory activity in one barrel field cortex (BFC) modulates the processing of incoming sensory information to the other BFC. Whether interhemispheric integration is dynamically linked with corticothalamic modulation of incoming sensory activity is an important hypothesis to test, since subcortical relay neurons are directly modulated by cortical neurons through top-down processes. In the present study, we compared the direct sensory responses of single thalamic relay neurons before and after inactivating the BFC contralateral to the thalamic cell under urethane anesthesia. The data show that silencing one BFC reduces response magnitude in contralateral thalamic relay neurons, significantly and reversibly, in response to test stimuli applied to the principal whisker at 2 times response threshold (2T) for each unit. Neurons in the ventral posterior medial (VPM) nucleus and the medial

division of the posterior nucleus (POm) react in a similar manner, although POm neurons are more profoundly depressed by inactivation of the contralateral BFC than VPM neurons. The results support the novel idea that the subcortical relay of sensory information to one hemisphere is strongly modulated by activity levels in the contralateral as well as in the ipsilateral SI cortex. The mechanism of the modulation appears to be based on shifting the stimulus-response curves of thalamic neurons, thereby rendering them more or less sensitive to sensory stimuli. We conclude that global sensory processing is created by combining activity in each S1 cortex and continually balancing the flow of information to cortex by adjusting the responsivity of ascending sensory pathways.

## **Introduction**

Rats use their whiskers to explore the space around their heads in a manner analogous to humans using their hands to negotiate space in the dark. Sensory information from the roughly 25 whiskers on each side of a rat's face is projected to the contralateral cortex through pathways that are thought to dynamically update the representation of objects in space, mainly within the detection distance of the moving whiskers. The pathway from sensory receptors in the whisker follicles to contralateral cortex consists of "barrelettes", clusters of neurons in the ipsilateral brainstem trigeminal complex (Ma, 1991), which project to "barreloids" in the contralateral thalamus (Van der Loos, 1976), and "barrels" in the primary somatosensory (SI) cortical layer IV; with one barrel for each whisker (Woolsey and Van der Loos, 1970). The lemniscal component of the whisker to

barrel ascending pathway in rats is highly lateralized subcortically (Peschanski, 1984; Chiaia et. al, 1991). Accordingly, objects on the left side of a rat's face are represented by neurons in the right barrel cortex, and vice versa.

Previous studies have shown that barrel neurons respond most strongly to stimulation of the contralateral whiskers, but evidence also supports that cortical neurons are influenced by inputs from the whiskers on the ipsilateral side of the face (Harris and Diamond, 2000; Pidoux and Verley, 1979; Shuler et al., 2001; Weist, et al., 2005). The responses of cortical cells to ipsilateral whiskers are generated by interhemispheric connections through the corpus callosum, since blocking activity in one hemisphere eliminates bilateral responses in the other hemisphere (Pidoux and Verley, 1979; Shuler et al., 2001). The behavioral relevance of integrating information from the two sides of the face has been demonstrated by learning problems that require the animal to compare whether movable walls on the left and right side are close to or far from the head using only their whiskers (Krupa et al., 2001; Shuler et al., 2002).

Bilateral integration requires cortex to control the levels/types of sensory information coming in from both sides of the face. To detect disturbances in left and right side input activity, cortex in each hemisphere would need to compare activity levels in the sensory pathways bringing sensory information into both sides of the system, even at subcortical levels. Anatomically, projections from BFC back to thalamus greatly outnumber the ascending projections from brainstem to thalamic relay neurons (Guillery, 1969; Liu et al, 1995), which correlates with the functional evidence that the thalamic "relay" cells are strongly

modulated by cortical feedback (Diamond et al., 1992b; Nicolelis et al., 1995). Corticothalamic projections from layer VI in one barrel column of BFC have a general facilitatory effect on the relay cells in the corresponding barreloid (Temereanca and Simons, 2004). Moreover, functional reorganization, in the form of a shift in the spatiotemporal structure of the receptive fields (RFs) in VPM (Krupa et al., 1999), had been reported after BFC neuronal activity was reversibly blocked. Recent studies have demonstrated a direct facilitatory effect of sensory cortex on thalamic “relay” nuclei via corticothalamic “feedback” projections (for review, see Sherman and Guillery, 2002; Suga et al., 2003). Meanwhile, several lines of evidence have emerged showing that activity levels in one hemisphere can regulate sensory response levels in the other hemisphere. Thus, the interhemispheric integration may interact with corticothalamic regulation. For example, decreases in neuronal activity in one barrel cortex, caused by either a lesion (Rema and Ebner, 2003) or by chronic suppression of activity (Li, et al., 2005), produces a remarkable decrease, even in the early 3-10 ms response component, which is an early response component often assigned to activation of cortical neurons by thalamic inputs (Armstrong-James and Fox, 1987; Armstrong-James et al. 1991). These findings, taken together, led us to test the hypothesis that cortex in one hemisphere can indirectly modulate the responsiveness of relay neurons in the contralateral thalamus.

In present study, response curves of thalamic relay neurons were measured by systematically varying the amplitude of test stimuli under urethane anesthesia. Responses of the same thalamic relay neurons to whisker stimuli

were compared before and after inactivating the contralateral BFC using stimulus intensities of two times the response threshold. Under these conditions (under urethane anesthesia, tested at 2T), the responsiveness of VPM and POm neurons to test stimuli at 2T applied to their principal whiskers is significantly depressed after inactivating the contralateral BFC with muscimol in the absence of any CNS damage. Our data also indicate that response curves of thalamic relay neurons are greatly shifted toward the right after the neural activity in the contralateral BFC was suppressed with muscimol. Thus, silencing cortex can down-regulate responses to sensory inputs in the thalamus bilaterally. Our findings suggest that cortex in one hemisphere can indirectly modulate the responsiveness of relay neurons in the contralateral thalamus by acting through direct excitability changes in the contralateral cortex. The cortical modulation on thalamic neurons could be mediated by adjusting the response threshold/response curves of thalamic relay neurons.

## **Materials and Methods**

Sixteen male Long-Evans rats (250 ~ 350g or 2 to 3 months old) were used for these experiments. Changes of spontaneous activity (SA) and evoked responses (ER) to repetitive whisker stimulation before and after inactivation of contralateral BFC by muscimol were systematically investigated in 8 animals (1 neuron per animal). The influence of contralateral cortical inactivation on POm was studied in 4 other rats. Controls consisted of VPM neurons that were monitored before and after muscimol was applied ONLY onto the contralateral

visual cortex surface using the same paradigm as in our experimental group (n = 4 rats). The experiment design is illustrated in Figure 3-1. All procedures were approved by the Vanderbilt University Institutional Animal Use Committee and followed guidelines by National Institutes of Health and Society of Neuroscience.

### **Chamber Implantation**

Detailed description of the surgery, electrophysiology and histology has been published elsewhere (Li et al., 2005; Rema and Ebner, 2003) and will only be briefly repeated here. For recording single cell responses, urethane anesthetized rats (1.5 g/kg, 30% aqueous solution, i.p.) were placed in a stereotaxic headholder (Narashige). Body temperature was maintained at 37°C by rectal thermometer feedback to an electronically controlled heating pad. In twelve experimental group animals, a craniotomy was performed to make a circular opening in the right skull with a fine dental burr. The opening was centered at 2 mm posterior and 6 mm lateral to Bregma with ~4 mm in diameter, which provided access to most of the BFC. The edge of a 32 gauge syringe needle was used to make a small opening in the dura to facilitate the penetration of muscimol when it was applied. Care was taken to avoid any injury to dural or cortical blood vessels, and gel foam was applied in case of bleeding. After the surface of the bone surrounding the opening was carefully dried, super glue was applied onto the bone surface around the opening. A small plastic chamber was put above the opening then cemented watertight to the skull with dental cement. The exposed cortical surface within the chamber was kept from drying with warm saline.



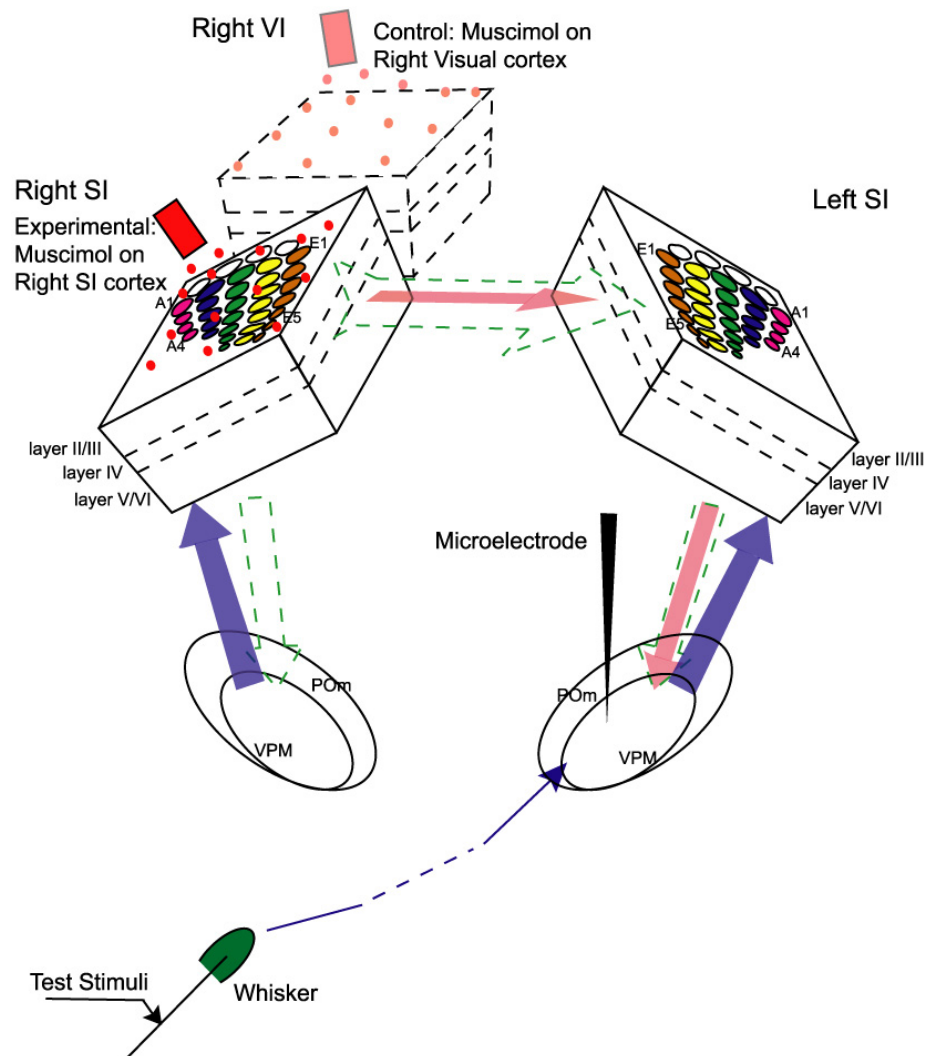


**Figure 3-1. Experiment Design.**

Illustration of the experimental design and working hypothesis. BFC neurons on both sides are interlinked in an activity dependent manner in normal rats. When the right SI is inactivated, influence from the blocked BFC would decrease significantly (horizontal red arrow). We postulate that this could down-regulate the influence of the corticothalamic projections (red arrow) from un-manipulated BFC (left). Hence the neurons in the left VPM could reduce their responsiveness to peripheral whisker stimulation.

Another rectangular opening was made in the left skull to gain access to the contralateral thalamus. This opening exposed the cortical surface 2-5 mm posterior and 2-4 mm lateral to Bregma. Small openings were made in the dura before the microelectrode was advanced vertically into the brain. The bone debris was carefully removed with saline during drilling.

In the visual control group rats, a circular opening was made on the right skull to expose the right visual cortex instead of the right SI cortex. The center of the opening was located at 6 mm posterior and 2 mm lateral to Bregma. Similar to the experimental group, a small opening was made in the dura with a 32 gauge syringe needle and the chamber was cemented over the opening. The rectangular opening was made at the same location as in the experimental group.

### **Electrophysiological Recording**

Extracellular single unit recording was conducted with carbon-fiber microelectrodes (Armstrong-James and Millar, 1979; Armstrong-James et al., 1980). The microelectrode was advanced vertically into the thalamus by a stepping motor microdrive (Kopf instruments). Contact of the electrode tip with the pial surface was identified visually using an operation microscope and by reduction in noise when the electrode touched the brain surface. The location of VPM or POm was estimated by X-Y coordinates linked to the depth below the surface of cortex (Brown and Waite, 1974; Haidarliu and Ahissar, 2001; Ito, 1988; Land et al., 1995; Sugitani et al., 1990; Waite, 1973a, b;). As the electrode was advanced into the dorsal thalamus, whiskers were deflected by a hand-held probe

to identify responsive neurons. Single unit isolation was carried out on-line with a time-amplitude window discriminator (Bak Instruments). Spikes were digitized with the CED 1401 Plus processor and displayed on-line using Spike 2 software (Cambridge Electronic Design). Peri-stimulus time histograms (PSTHs) were built on-line to visualize the response characteristics of each isolated unit with a bin width of 1 ms. The unit candidate had to be clearly distinguished by its waveform from other units. To ensure the quality of the single unit isolation, the unit with the largest waveform was typically selected at each penetration depth. Neuronal activity of both evoked response and spontaneous activity was recorded for more than 1 hour before muscimol application as an indicator of satisfactory stability of a given unit. Spike duration of all VB units isolated was recorded in a notebook for later reference. Data was stored on a PC (Dell) for further off-line analysis. Data collected before muscimol application established the baseline for each cell. During baseline recording, supplements of anesthetic (10% of initial dose) were given as needed to maintain the anesthesia level at stage III-3 (Friedberg et al., 1999). At this anesthetic depth, VPM units display low spontaneous firing (Waite, 1973b) and respond to 1 Hz whisker stimulation without inducing bursts (Diamond et. al, 1992a; Friedberg et. al, 1999; Sherman and Guillery, 1996).

### ***Receptive Field Mapping***

When the microelectrode was thought to be in VPM and a single unit with a good response to manual whisker deflections was isolated, all whiskers on the right side of the face were trimmed to a length of 10 mm. Under urethane

anesthesia stage III-3, neurons in dorsal VPM exhibited small RF size (1-2 whiskers) with low spontaneous firing (Diamond et al., 1992a; Friedberg et al., 1999; Waite, 1973b; but see Rhoades et al., 1987; Timofeeva et al., 2003 for multiwhisker RF VPM neurons). Only units within C or D row whiskers as their principal whisker were selected to go through the silencing and recovery procedure since these barreloids localized in the middle of VPM which facilitated our selection of VPM units. The RFs of VB neurons were initially mapped with a hand-held probe. Once the principal whisker was identified, a home-made bimorph piezoelectric stimulator was used to refine the RF with 50 ramp-and-hold forward deflections of each whisker at the rate of 1 stimulus per second. The ramp and hold stimulus was 300  $\mu\text{m}$  in amplitude and 3 ms in duration. After the threshold (see below) was measured, the RF of this unit would be re-mapped at 2 times threshold (2T) stimulus intensity level.

### ***Threshold Assessment and Baseline Recording***

The piezoelectric wafer was driven by a digital stimulator (DS8000, WPI Inc.) to deliver standardized magnitudes between 0 and 1.6 mm to one whisker at a time. The stimulator was calibrated under a high-speed digital camera (Canon) (500 frames per second) so that we can translate the voltage applied to the piezoelectric wafer into the distance in  $\mu\text{ms}$  that the whisker was displaced. VPM neurons responded to whisker stimuli with higher firing probability and shorter modal latency than P<sub>Om</sub> cells (Diamond et al., 1992a). If one isolated unit didn't generate a robust response with a prominent response peak and modal response

latency at ~5 ms to the test stimuli, it was bypassed and the electrode was advanced until another unit was located. If the isolated unit produced “good” responses, the threshold of the principal whisker stimulation was determined. Here threshold was defined as the lowest amplitude of whisker deflections (i.e., lowest voltage applied to the piezo stimulator) that produced a statistically significant response (operationally, at least three spikes in one of the poststimulus bins in the PSTH, see the Method section of Armstrong-James and Fox, 1987 for mathematical implications) to principal whisker stimulation. The threshold was determined by varying the amplitude of whisker deflections in a linear-interpolation manner. For instance, if a 200  $\mu\text{m}$  deflection evoked a robust response, the next test stimuli would be at 100  $\mu\text{m}$ ; if the 100  $\mu\text{m}$  deflections generated no response, the next stimulation would be at 150  $\mu\text{m}$ ; and so on. When two successive test stimuli were close in amplitude ( $<50 \mu\text{m}$ ), the amplitude of test stimuli be increased with step of 10  $\mu\text{m}$  to get an accuracy of  $\pm 10 \mu\text{m}$ . The responsiveness of this unit was thereafter periodically measured with the stimulus intensity of 2 times threshold (2T). At each assessment time, a recording session consisted of 3 or 4 evoked response (ER) blocks with 1 spontaneous activity (SA) recording session randomly inserted. Each ER block documented the 3-100 ms post-stimulus time neuronal activity generated from 50 stimuli delivered at 1 per second (bin width, 1 ms). The SA block recorded 200 sec of spontaneous firing when the stimulator was still in contact with the whisker without activating the stimulator.

## **Muscimol Application**

Muscimol solution was prepared prior to each experiment by dissolving muscimol (Sigma) in sterile saline (10 mM in concentration). When the isolated unit showed stable responses, i.e., each ER block gave a similar number of spikes over a period of time longer than 1 hour, warm saline within the cemented chamber was removed and the surface of exposed dura was cleaned. A small piece of gelfoam saturated with the 10 mM muscimol solution was placed in the chamber to seamlessly cover the exposed dura. Responsiveness of the same isolated unit was tested periodically from the onset of muscimol application. The post-muscimol recording usually lasted about 1 hour during which drops of muscimol solution was added to the gelfoam by a 20  $\mu$ l syringe to keep it moist. We also re-tested the threshold in some units after muscimol application. We continued to monitor the anesthesia depth after muscimol application as described in previous studies (Friedberg et al., 1999), and supplements (10% of the original does) were given when necessary to maintain the anesthesia at stage III-3. In most of the cases, no signs of drastic changes of anesthesia depth (i.e., corneal/hindlimb pinch reflex, voluntary whisker movements etc.) were noticed in the 1-hour post muscimol application recording. Only ER blocks collected when the isolated unit was in tonic firing mode were included in the data analysis. ER blocks when the unit responded in the bursting firing mode were excluded, based on the interspike interval of post-stimulus spikes.

Several criteria were used to select units: they had to 1) be clearly distinguished by their waveform from other units, 2) maintain their initial response

to stimulation for at least 1hr, 3) have a stable modal response latency, 4) show a single whisker that produced the best response, 5) respond well at 2T stimulus levels, and 6) be confirmed histologically to be in the VPM or POm thalamic nucleus. We chose to study the response characteristics of each unit carefully and thoroughly before we applied muscimol and required each unit to meet “rigorous” criteria. Although these requirements greatly reduced our sample size, it enhanced the quality of our recording due to the fact that only stable neurons reliably detected effects of blocking contralateral BFC.

### **Data Analysis**

A PSTH was generated for each ER block with bin size of 1 ms in off-line data processing. Spikes collected prior to 3 ms post-stimulus were rejected as being too early to be responses evoked by whisker stimulation. Spontaneous activity was corrected by subtracting the average number of spikes in the 50 pre-stimulus time bins from each post-stimulus time bin. Spikes within 3-100 ms post-stimulus time were summed for 50 stimuli to calculate the response magnitude (spikes/50 stimuli) and divided by 50 to get spikes/stimulus. Response magnitude was averaged from ER blocks at the same stimulus intensity and the same recording time point to calculate the baseline response. Then the average response magnitude was plotted against the stimulus intensity to construct the intensity-response curve for each unit. For data sampled at 2T, the average response magnitude at different time points before muscimol application was compared to identify unstable units. Latency histograms (LHs) were constructed

from histograms that include only the first spike after each stimulus to assess onset latency and modal response latency. Data acquired after muscimol application were processed in the same manner. In-house spike 2 scripts were used to calculate the background levels using 200 sec of spontaneous activity.

Both the response magnitude and latency were compared before and after muscimol application to analyze the effect of silencing the contralateral BFC. For each unit, the average response magnitude at 2T was plotted against poststimulus time. Data from ER blocks at 2T in baseline recording were further pooled together and compared with data assessed at each recording time point after muscimol application. Student's t test was performed to identify significant differences between groups. Frequency distributions of the modal response latency were generated and compared between pre- and post-muscimol recording to determine whether there was any latency shift after muscimol. The intensity-response curves from the same unit were compared between baseline and post-muscimol application when possible.

To amalgamate several cases of each type for comparison, data from different VPM neurons were normalized. For each VPM unit, the normalization procedure took the averaged neuronal response at 2T in pre-muscimol recording as 100%, and data at every recording time point after muscimol application (3 to 4 recording blocks) were normalized by this value. Then the normalized values from different animals were grouped by recording time points, averaged and plotted against the time. This normalization procedure emphasized response *changes* within each VPM unit over time and between different VPM units at



each time point so that data from different animals could be compared. Student's t-test was performed on the data to determine significance levels.

### **Histology and Identification of Recording Sites**

On completion of recording, recording sites were marked by passing a DC current (electrode tip positive) of 2  $\mu$ A for 10 seconds. After making a lesion, the rat was overdosed with urethane and perfused transcardially with PBS followed by 4% paraformaldehyde in buffer. Brains were saturated in 10%, 20% and 30% sucrose, blocked and sectioned coronally, and stained for cytochrome oxidase activity (Wong-Riley and Welt, 1980) to localize thalamic lesion sites (Rema and Ebner, 2003).

## **Results**

Histology confirmed the location of 8 VPM (muscimol on contralateral BFC), 4 VPM (muscimol on contralateral visual cortex) and 4 POm (muscimol on contralateral BFC) units in 16 animals. Response characteristics of these units before muscimol application were similar to those reported for these nuclei in previous studies (Armstrong-James and Callahan, 1991; Diamond et al., 1992a; Simons and Carvell, 1989; Waite, 1973b). Under our experiment design, only one neuron could be studied per animal due to the possibility that muscimol could produce long term changes that could bias the results. There was no reliable way to control for possible contaminating effects of the muscimol application procedure. This factor, together with our unit-selecting criteria,

resulted in the small sample size. However, as shown in the following text, each unit responded stably to test stimuli for the duration of the observations. More importantly, our experiment design also led to a highly consistency of response changes among units we recorded after muscimol application, which supported the validity of the experiment design.

### **Response of Thalamic Relay Neurons to Whisker Stimuli of Various Amplitudes**

The data confirmed that VPM neurons are very sensitive to whisker deflections. The lowest response threshold measured was produced by a ~20  $\mu\text{m}$  deflection. For the 12 VPM neurons the threshold ranged from ~50  $\mu\text{m}$  to 150  $\mu\text{m}$ , with a mode of ~100  $\mu\text{m}$ . When the stimulus was stronger (for example, >300  $\mu\text{m}$ ), VPM neurons fire ~50 spikes/50 stimuli or 1 spike/stimulus at a short modal latency (~5 ms). It was important for these experiments that the cells be in the tonic firing mode, in which the VPM neurons are rapidly inhibited by feedback from the thalamic reticular nucleus (RTN) after activation by whisker stimulation (for review, see Castro-Alamancos, 2004). As the stimulus intensity decreased, VPM neurons tended to fire fewer spikes with longer response modal latency. At threshold, VPM neurons generated roughly 20 spikes/50 stimuli, and these spikes occurred with temporal dispersion in a PSTH. Increasing the stimulus by only 10  $\mu\text{m}$  can identify the threshold because the cell transitions from a few scattered spikes/50 stimuli to a significant response to stimulation (Fig. 3-2, 3-3). That is, the VPM neurons transition from nearly unresponsive to many post-

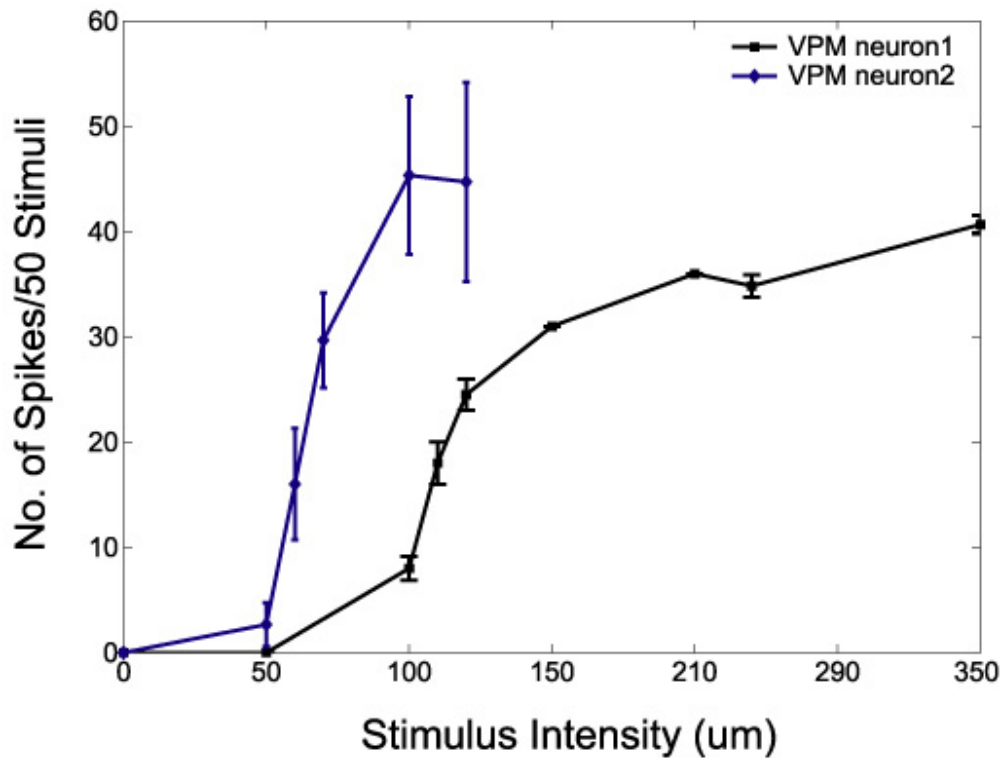


**Figure 3-2. Stimulus Intensity-Response Magnitude Curves of Two Selected VPM Neurons.**

Response curves of VPM neuron 1 (Black) and VPM neuron 2 (Blue) before muscimol application. Data were collected using standard whisker stimuli of various amplitudes (see Materials and Methods for details) at the rate of 1 stimulus per second. Response magnitude (spike count/50 stimuli) was plotted against the extent of whisker deflections (in  $\mu\text{m}$ ). The threshold of these 2 VPM neurons is 110  $\mu\text{m}$  and 60  $\mu\text{m}$  under our criteria (see Methods). Error bar: SEM.

stimulus spikes aggregated in a narrow post-stimulus time window. Generally speaking, at 2T, VPM neurons fired below asymptote, producing ~40 spikes/50 stimuli. Although the threshold varied from one VPM neuron to another, their stimulus intensity-response magnitude curves shared several common features. Figure 3-2 shows the intensity/response curves of 2 VPM neurons. All response curves were roughly sigmoid in shape and the slope around threshold was steep. The steep slope near threshold indicates dramatic changes of the responsiveness may occur during this “sensitive” epoch. Figure 3-3 shows the average PSTHs generated by different stimulus intensities in these 2 VPM neurons, respectively. For example, in VPM neuron 1, when the stimulus was just below threshold (100  $\mu\text{m}$  in this case), only a few spikes were generated per 50 stimuli and they were scattered in the PSTH; at threshold (110  $\mu\text{m}$ ) the VPM neuron did give a response peak, while at 10  $\mu\text{m}$  above threshold the spike number was substantially larger and at 2 times of the threshold, the response was very robust. Increasing stimulus intensity also shortened the response modal latency in all VPM neurons we recorded, as exemplified in Figure 3-3. These response characteristics were very consistent across all VPM neurons included in the present results.

### **Muscimol Application Influences Response Magnitude and Latency of VPM Neurons**

Muscimol on the contralateral BFC didn't alter the RF size, or affect the spontaneous firing of VPM units. Further, VPM responses were not changed

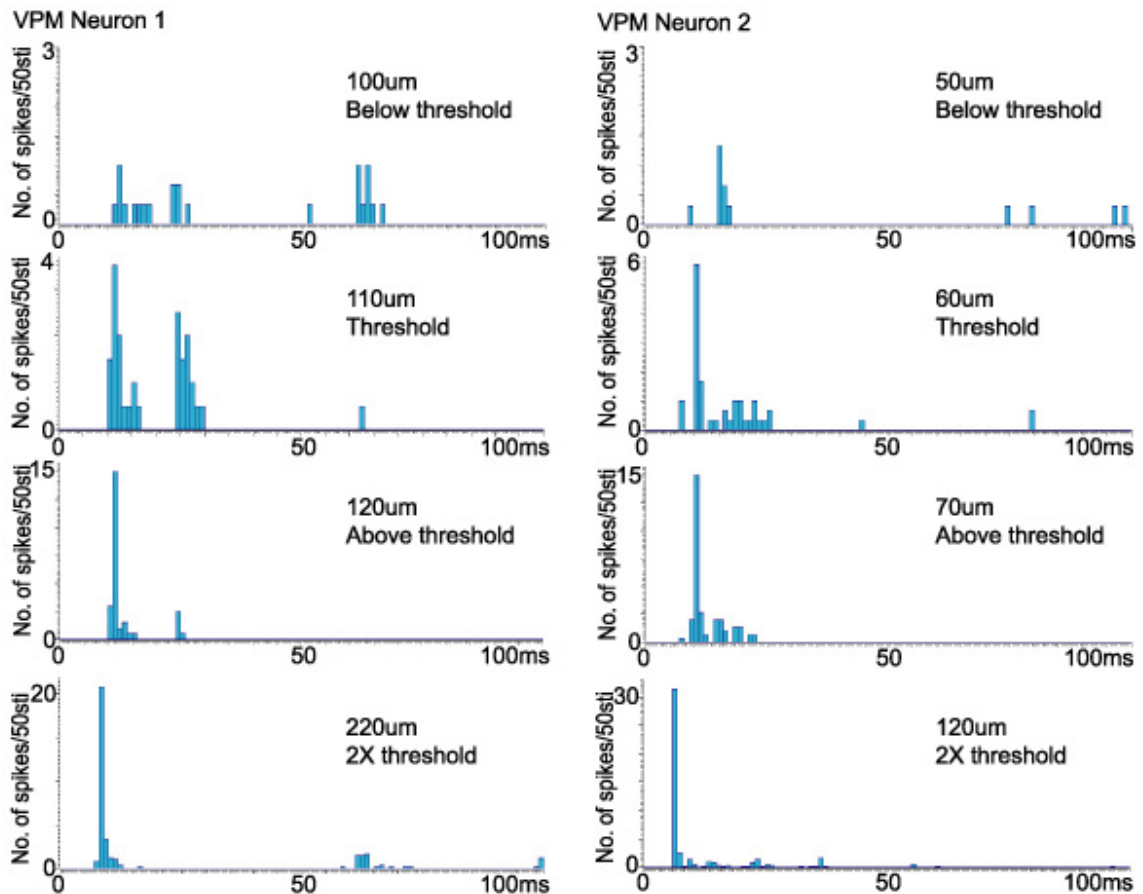


**Figure 3-3. Averaged PSTHs for a Narrow Range of Stimulus Intensities of Two VPM Neurons Shown in Figure 3-2.**

Left column: data from VPM neuron 1. from top to bottom: PSTH to 100  $\mu\text{m}$  stimulus ( $8 \pm 1$  spikes/50 stimuli, mean  $\pm$  SEM averaged from 150 trials); PSTH to 110  $\mu\text{m}$  stimuli ( $18 \pm 2$  spikes/50 stimuli, averaged from 100 trials); PSTH to 120  $\mu\text{m}$  stimuli ( $24.5 \pm 1.5$  spikes/50 stimuli, averaged from 100 trials); PSTH to 220  $\mu\text{m}$  stimuli ( $33 \pm 1$  spikes/50 stimuli, averaged from 300 trials).

Right column: data from VPM neuron 2 from top to bottom: PSTH to 50  $\mu\text{m}$  stimuli ( $2.7 \pm 2$  spikes/50 stimuli, averaged from 150 trials); PSTH to 60  $\mu\text{m}$  stimuli ( $16 \pm 5$  spikes/50 stimuli, averaged from 150 trials); PSTH to 70  $\mu\text{m}$  stimuli ( $30 \pm 4.5$  spikes/50 stimuli, averaged from 150 trials); PSTH to 120  $\mu\text{m}$  stimuli ( $45 \pm 9$  spikes/50 stimuli, averaged from 350 trials). Note that the latency systematically became shorter and shorter as the amplitude of whisker deflections increased. (Y-axis: spike count/50 stimuli; X axis: 1ms bins. Note change in Y axis scale)

when muscimol was applied to the visual (VI) cortex in control animals (Fig. 3-5). However, within 30 minutes after muscimol was applied to the contralateral BFC, each thalamic neuron showed a significant decrease in whisker-evoked response magnitude, as well as a shift of the response modal latency to principal whisker stimulation (Fig. 3-4, 3-5). As shown in Figure 3-4, the influence of muscimol depended upon its application time. The time course of muscimol did vary slightly among VPM units, especially during the “initial phase”. Shortly after muscimol was applied onto the contralateral BFC, the responsiveness of VPM neurons remained unchanged, even increased in some units (Fig. 3-4). However, after reaching a “turning point”, the response magnitude of the VPM neurons began to drop. Response reduction developed a similar temporal course in all eight VPM units. When normalized data from 8 individual cases were averaged, the first significant change of VPM neuron responsiveness appeared at ~20 minutes after muscimol application (Fig. 3-5). VPM neurons responded in the first 15 minutes at 102% ( $p < 0.36$ , t-test) of the pre-muscimol magnitude level, but the response decreased to 92% ( $p < 0.004$ ) at ~20 minutes then further reduced to 77% ( $p < 6.4 \times 10^{-16}$ ), 69% ( $p < 6.5 \times 10^{-20}$ ), 65% ( $p < 1.2 \times 10^{-25}$ ) and 59% ( $p < 2.5 \times 10^{-17}$ ) at 30, 40, 50 and 60 minutes after muscimol was applied, respectively. Another interesting observation is that VPM neurons elongate their modal response latency after muscimol. VPM neurons responded to whisker stimuli at 2T faithfully with very short modal response latency (~5-7 ms). However, at a certain time after muscimol was applied, VPM neurons began to respond to the same 2T test stimulus with longer modal response latency and reduced response magnitude.

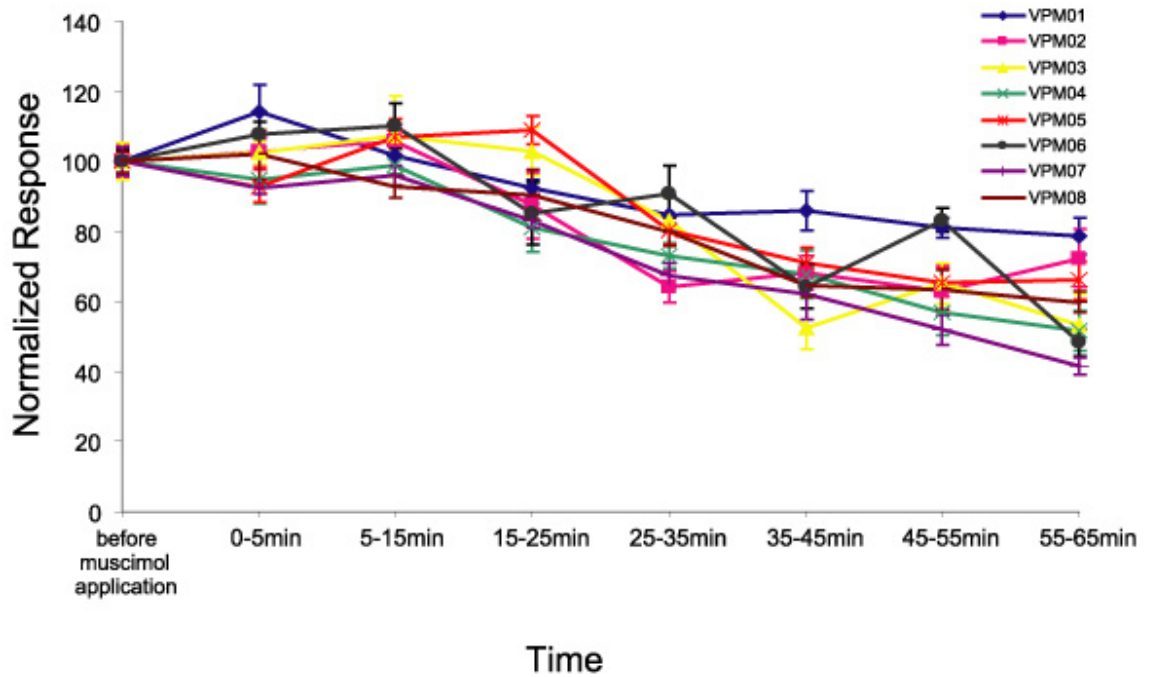


**Figure 3-4. Temporal Changes of Normalized Response Magnitude in 8 VPM neurons after Muscimol was Applied onto the Contralateral BFC.** Time-course of normalized response magnitude in 8 VPM neurons after muscimol application. Normalized response magnitude (taking the average control response level of each unit before muscimol as 100) was plotted against the post-muscimol time. Colors identify data from 8 different individual VPM neurons (1 per animal).

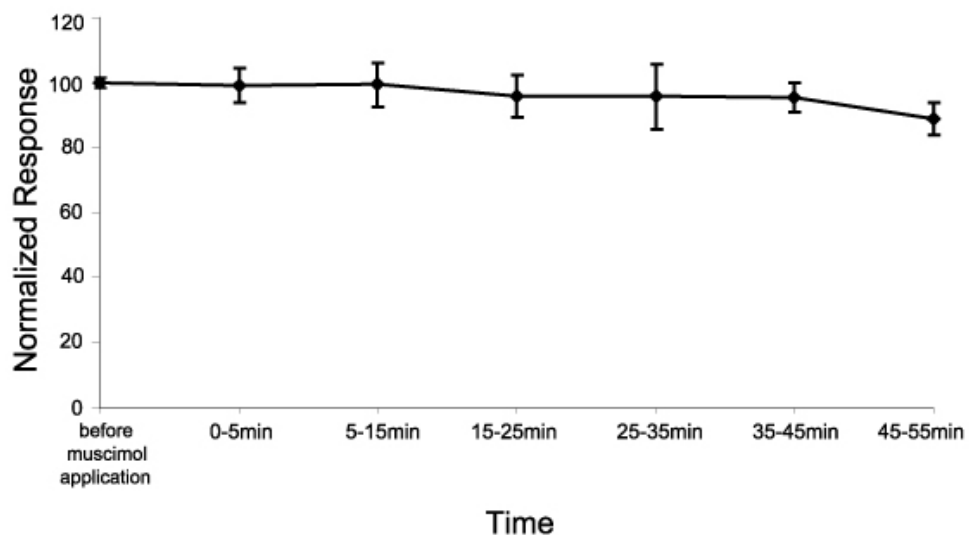
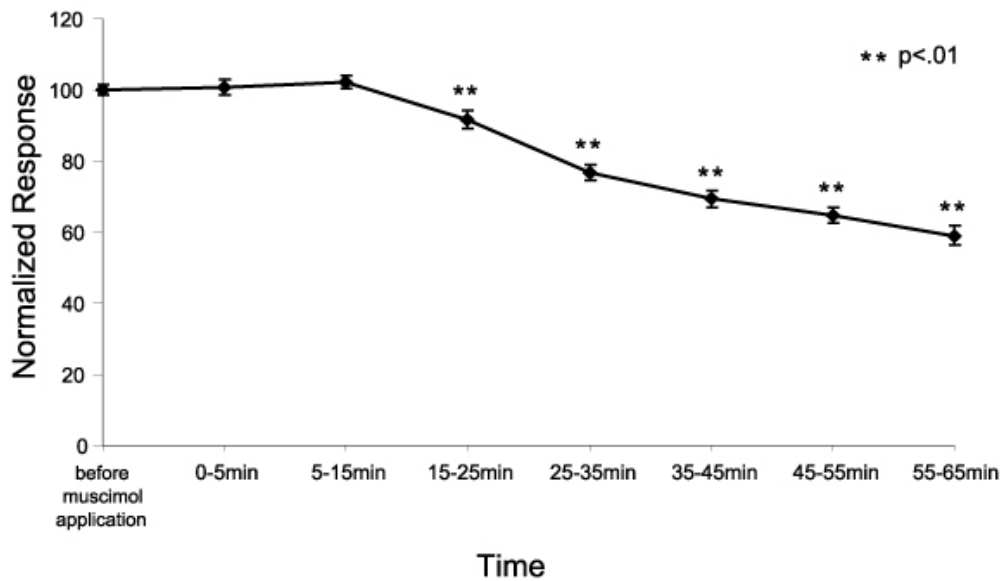


**Figure 3-5. Temporal Changes of Normalized Response Magnitude after Muscimol was Applied onto the Contralateral BFC in Experimental Group and Control.**

Top: Grand average response levels for the 8 VPM neurons after normalization. Data from different animals were averaged over time. Inactivating the contralateral BFC had an overall suppressive influence on VPM neurons. Asterisks show that significant decreases first occur in the 15-25 minute time window.

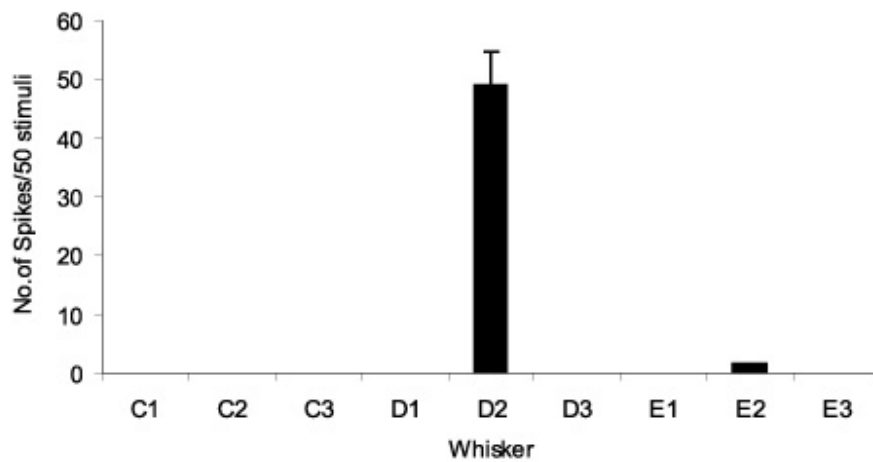
Bottom: Response levels in control animals (muscimol on contralateral visual cortex). No decrease in response magnitude was detected in controls. Normalized data from 4 control animals were also plotted against the time. No significant decrease in response magnitude was found after muscimol application.



Details are highlighted by analyzing data from two of the 8 VPM neurons (case VPM04 and VPM02). Before muscimol application, neuron VPM04 was marked by small receptive field size (1 whisker, Fig. 3-6), short modal response latency (5ms) and robust and stable response to its principal whisker D2 (Fig. 3-7). However, unit VPM04 gradually but steadily changed its response to principal whisker stimulations after muscimol was applied: response magnitude was decreased and response temporal structure shifted. This response modification is clearly seen when PSTHs before and during muscimol application were averaged and compared individually for each case (Fig. 3-7). Figure 3-7 shows that muscimol had no effect in the first 20 minutes: 21 minutes after muscimol was applied unit VPM04 generated an average of 40 spikes to 50 principal whisker stimulations, which is 81% ( $p < 0.06$ ) of its normal value. This percentage was reduced to 73% ( $p < 4 \times 10^{-4}$ ) at 29, 68% ( $p < 0.02$ ) at 38, 57% ( $p < 0.004$ ) at 47, and 52% ( $p < 7 \times 10^{-4}$ ) at 56 minutes, respectively.

Inactivation of contralateral BFC by muscimol also changed the temporal structure of this unit's response to the peripheral stimulus. The change can be demonstrated by comparing two averaged PSTHs before and during muscimol application (Fig 3-7). Before muscimol application, modal response latency of unit VPM04 was 5 ms (13 of 13 recording blocks, Fig. 3-8), and after muscimol was applied, only 77% (20 of 26 blocks) gave a modal latency still at 5ms, while the modal response latency shifted to 8 ms in 23% (6 of 26) of recording blocks (Fig. 3-8). This new 8 ms modal latency first appeared at 21 minutes after

### Receptive Field before Muscimol Application



### Histology (CO staining)

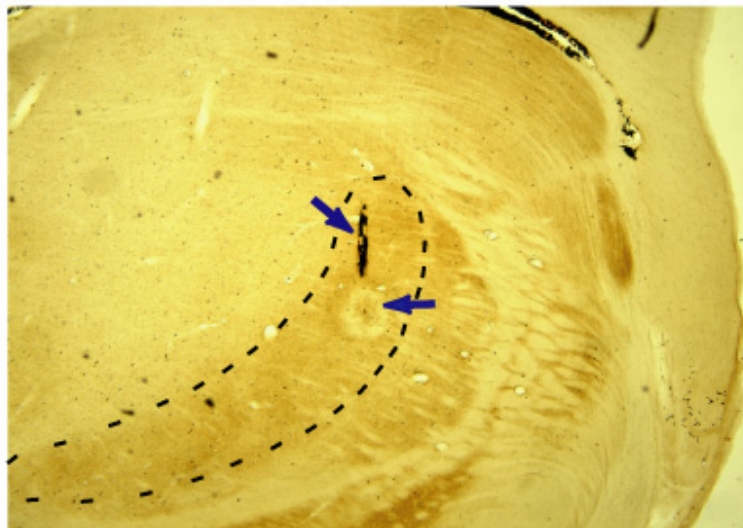


### Figure 3-6. Receptive Field Properties of Unit VPM04 Confirmed by Histology.

Top: RF of unit VPM04 before muscimol application mapped at 2T. The response magnitude (spike count/50 stimuli) was plotted for each whisker we tested. Note that unit VPM04 has single whisker RF, as did almost all of the VPM neurons studied.

Bottom: Histology. The location of electrolytic lesion for VPM04 is shown in one coronal section after CO staining. The left blue arrow points to the electrode tract and the right blue arrow points to the electrolytic lesion. The VPMdm border was indicated by the dashed line. (Contrast was adjusted in Photoshop 6.0).

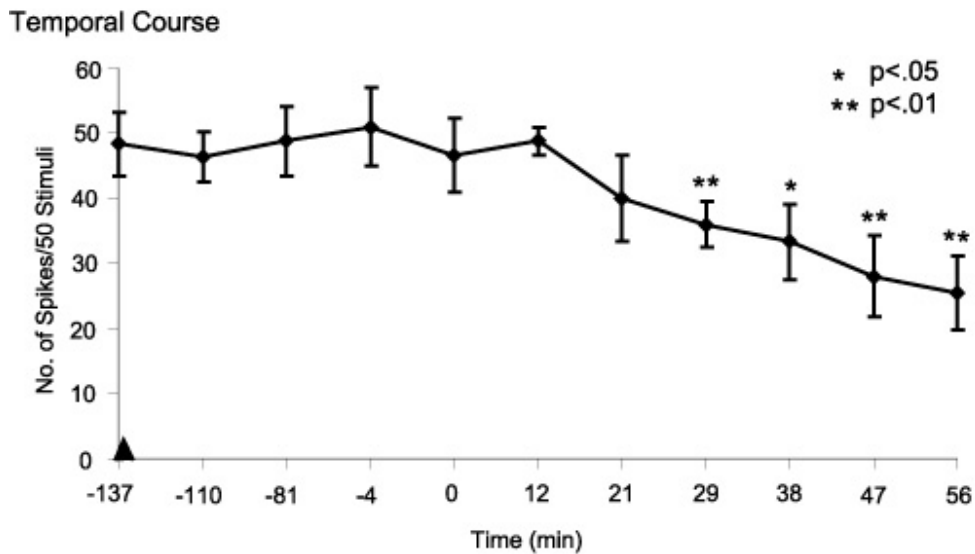
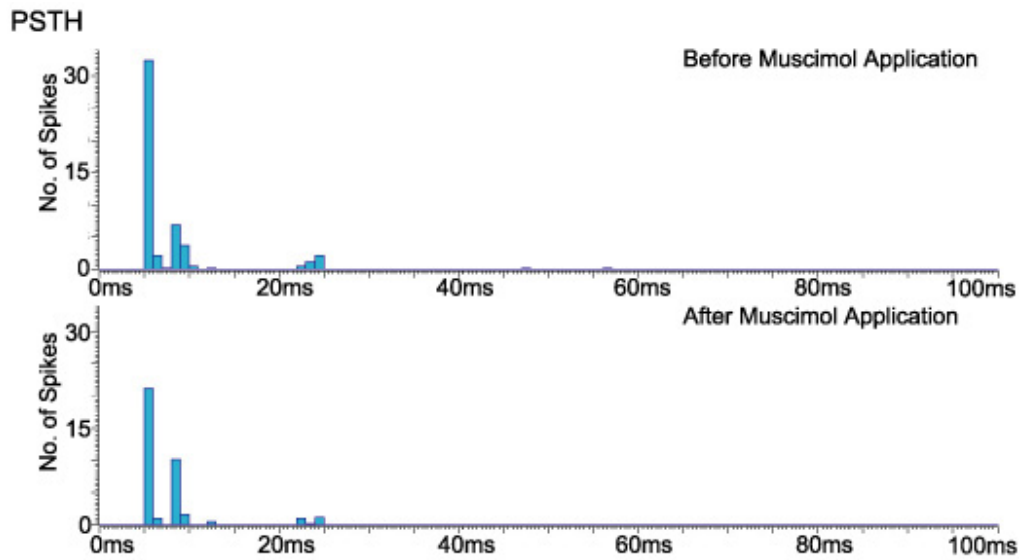
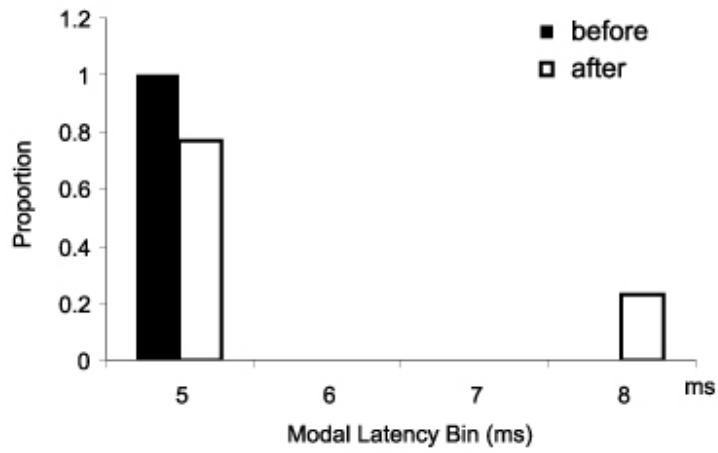


**Figure 3-7. Response Changes of Unit VPM04 after Muscimol Application.** Top: Comparison of averaged PSTHs before and after muscimol application. Top panel: PSTH before muscimol application averaged from 650 trials during the 137 minutes period of baseline recording. Bottom panel: PSTH averaged from 1300 trials after muscimol was applied. Note that overall changes occurred in both response magnitude and latency. Bottom: Time-course before and after muscimol application. Response magnitude (not normalized) of unit VPM04 to stimulation of its principal whisker D2 was plotted against the time. The black triangle on the X-axis shows the last time of supplementary anesthetic injection.

Proportional Distribution of Modal Latency



Spontaneous Activity

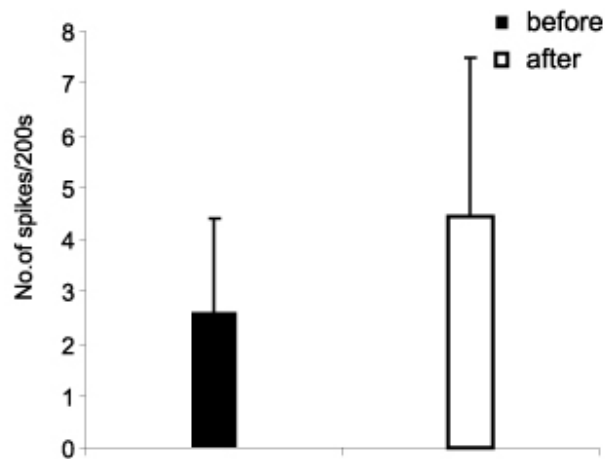


**Figure 3-8. Spontaneous Discharge and Distributions of the Modal Response Latency of Unit VPM04 before and after Muscimol Application.** Top: Modal response latency shifted after muscimol application. Note the appearance of new modal latency at 8ms after muscimol was applied. Bottom: The spontaneous activity did not change significantly after muscimol application.

muscimol was applied, which is the time when the significant response reduction occurred.

The time-dependent influences of muscimol on the magnitude and temporal structure of responses in unit VPM04 were demonstrated in Figure 3-9 by comparing the averaged PSTHs at different time points based on responses generated at 2T stimulus strength. Unit VPM04 originally responded to test stimuli with two peaks at 5 ms and 8ms, respectively (Fig. 3-9a). We continued to test it repetitively for > 2 hours. The cell responded to test stimuli with almost identical PSTH's each time, for > 2-hours (Fig. 3-9b, c). Thus we classified unit VPM04 as a reliable unit in a stable animal preparation. However, the response peak at 5 ms lowered significantly after the contralateral BFC was inactivated for 29 minutes, while the peak at 8 ms increased first then decreased (Fig. 3-9d, e and f). Hence muscimol application greatly changed the shape of the PSTHs of the same VPM neuron. No change in spontaneous firing rate was recorded before or after muscimol application.

Data from unit VPM02 is shown in Figure 3-10. This unit represents another type of VPM neuron, presumably located in the tail region of VPM (Pierret et al., 2000) since it had a much larger RF size than VPM04, but was still anatomically located within VPM (Fig. 3-10). Muscimol also produced a response magnitude decrease and a modal latency shift (Fig. 3-11). The time course of muscimol effects of was very consistent in all VPM neurons. In unit VPM02, the first detectable response decrease occurred 30 minutes after muscimol was applied: the cell responded on average at 31 spikes to 50 D1

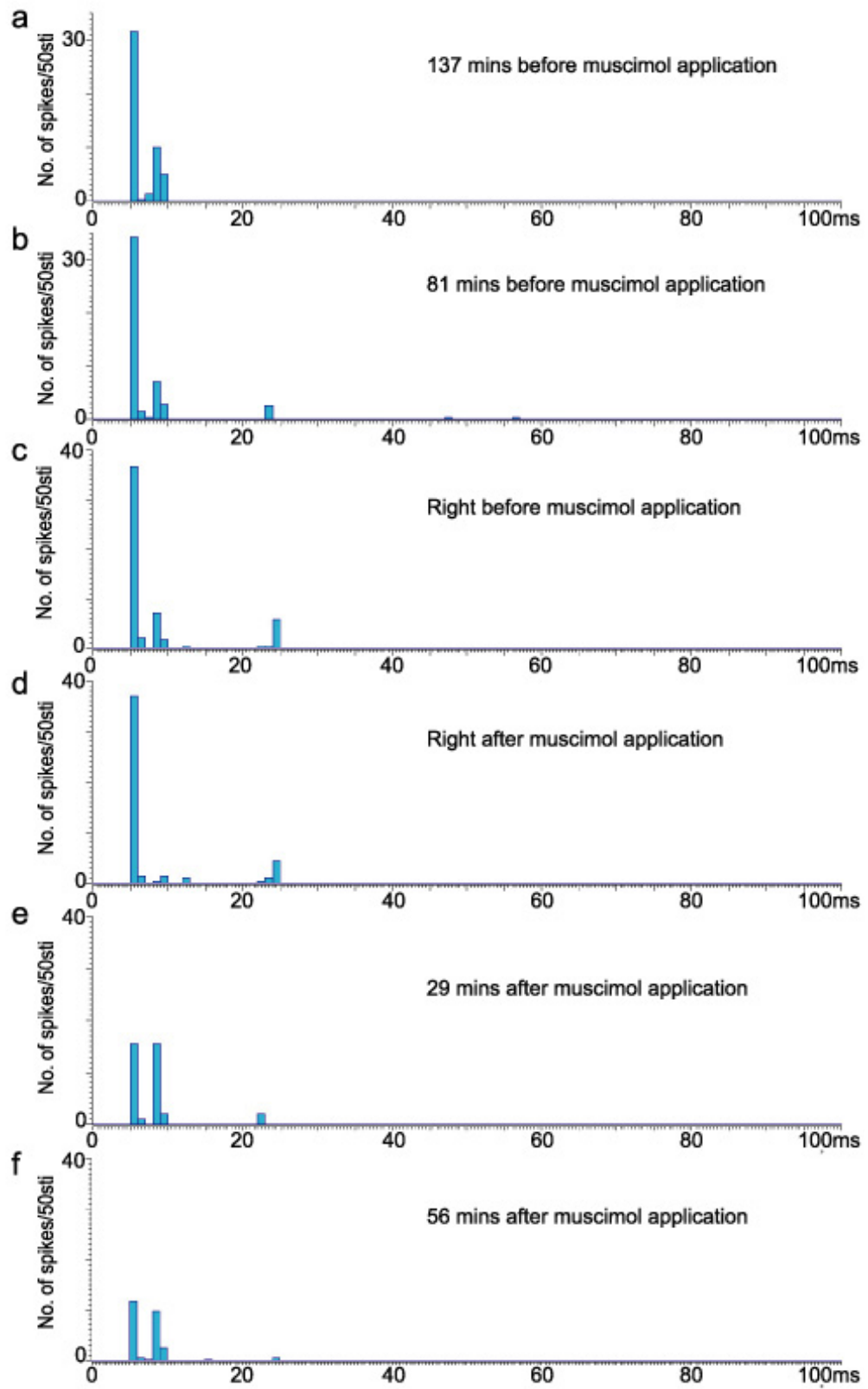


**Figure 3-9. Averaged PSTHs of Unit VPM04 Sampled with Various Effective Time of Muscimol Suppression.**

- a.** Averaged PSTH of neuron VPM04 from 150 trials collected 137 minutes before muscimol application. Response magnitude is  $48.3 \pm 2.8$  spikes/50 stimuli (Mean $\pm$ SEM, sampled at 2T stimulus intensity level, same for all panels).
- b.** Averaged PSTH from 200 trials at 81 minutes before muscimol application. Response magnitude is  $48.8 \pm 2.7$  spikes/50 stimuli.
- c.** Averaged PSTH from 150 trials at 4 minutes before muscimol application. Response magnitude is  $51.0 \pm 3.5$  spikes/50 stimuli. Note that the shape of the PSTHs before muscimol application is almost identical.
- d.** Averaged PSTH from 150 trials immediately after muscimol application (time 0). Response magnitude is  $46.7 \pm 3.3$  spikes/50 stimuli.
- e.** Averaged PSTH from 200 trials at 29 minutes after muscimol application. Response magnitude is  $36.0 \pm 1.8$  spikes/50 stimuli.
- f.** Averaged PSTH from 200 trials at 56 minutes after muscimol application. Response magnitude is reduced by roughly 50% ( $25.5 \pm 2.8$  spikes/50 stimuli). Note that muscimol effect gradually reduced the response magnitude and shifted the response latency.

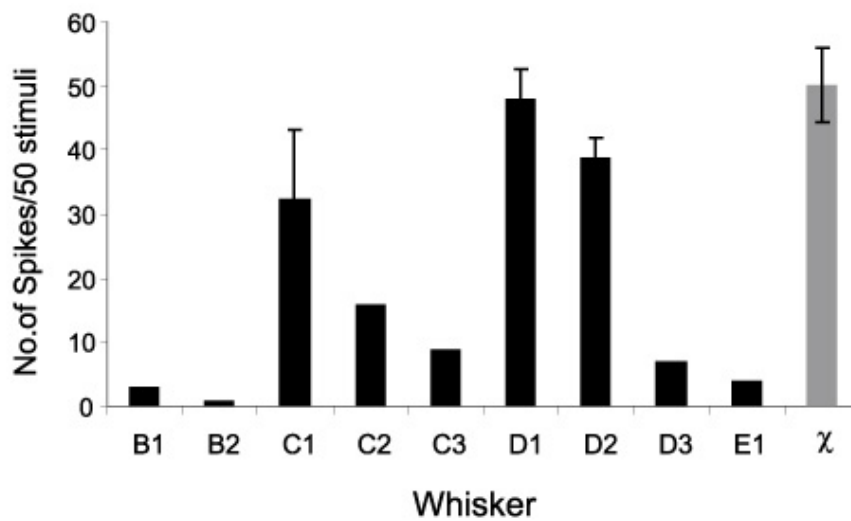
stimuli, which is only 64% ( $p < 0.002$ ) of its pre-muscimol value (Fig. 3-11). Responses at 21 minutes post-muscimol time were also decreased but not significantly ( $p < 0.30$ ), which may be due to the variance commonly observed at this time point. The responses reduced further to 68% ( $p < 0.003$ ) at 40 minutes, 63% ( $p < 0.008$ ) at 50, 72% ( $p < 0.03$ ) at 60, 57% ( $p < 0.008$ ) at 180 and 84% ( $p < 0.08$ ) at 200 minutes respectively (Fig. 3-11). Here, the modal response latency remained unchanged (Fig. 3-12). Modal latency was changed in only 10% of the recording blocks after muscimol application: however, the appearance of long latency is potentially important since long modal latency in lemniscal pathway cells may constitute a response modification. Seven out of 8 VPM units showed latency shifts similar to unit VPM02 and VPM04.

### **Muscimol Application Alters the Response Curves of VPM Neurons**

Normal VPM neurons in normal cortex on both sides showed increased response magnitude when the stimulus intensity increased above subthreshold, accompanied by shorter modal response latencies. The stimulus intensity-response magnitude curve in Figure 3-2 indicates how VPM neurons respond to stimuli of different intensity, but neglects latency changes. We conclude that the response characteristics of one VPM neuron can be completely defined only when the information from the response magnitude is linked with the response latency. The data support the idea that response decreases, together with the elongation of the modal response latency after muscimol application, actually alters the threshold of VPM neurons, or to be more precise alters the response



### Receptive Field before Muscimol Application



### Histology (CO staining)

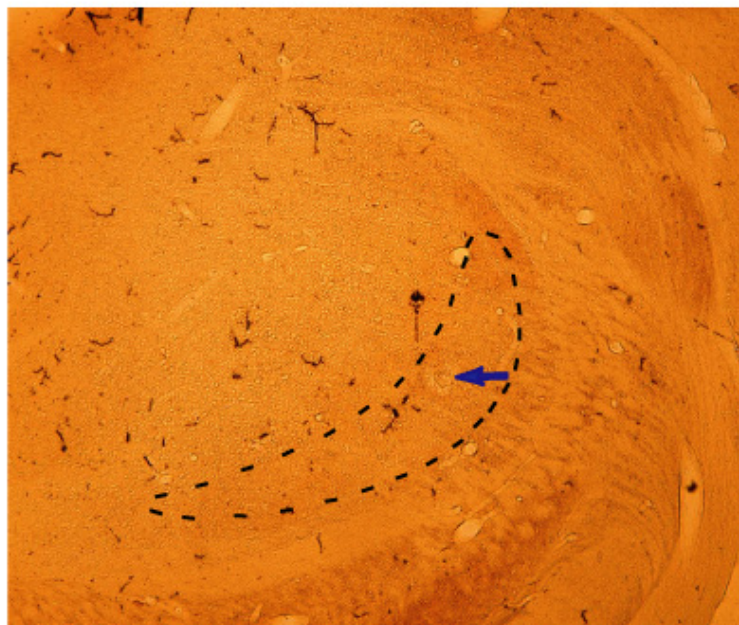
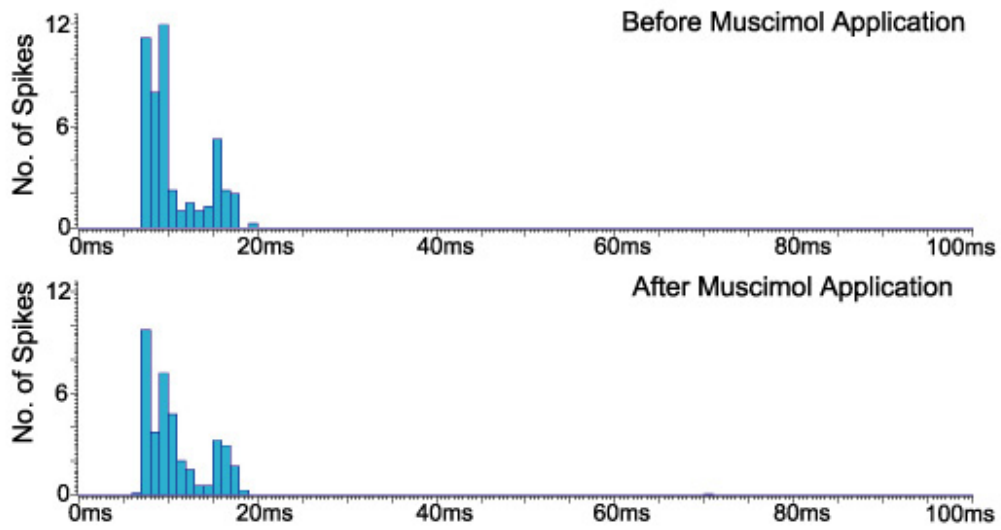


### Figure 3-10. Receptive Field Properties of Unit VPM02 Confirmed by Histology.

Top: Receptive field of unit VPM02 before muscimol application mapped at 2T. The response magnitude (spike count/50 stimuli) was plotted for each whisker tested. Note that unit VPM02 has a multi-whisker RF.

Bottom: Histology. The location of electrolytic lesion for VPM02 was visualized in one of the coronal sections after CO staining. The blue arrow pointed to the electrolytic lesion. The VPM border is indicated by the dashed line.

## PSTH



## Temporal Course

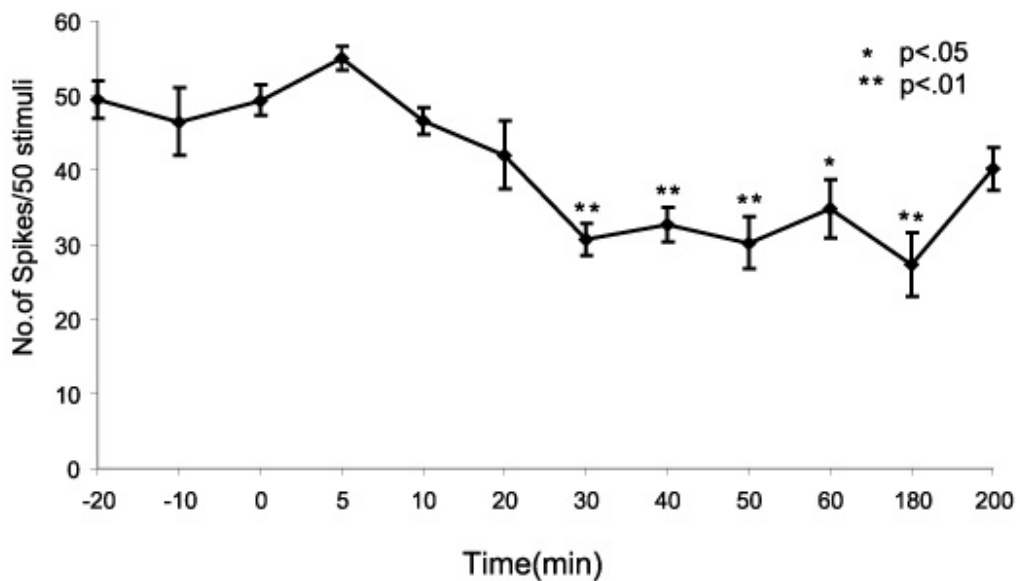
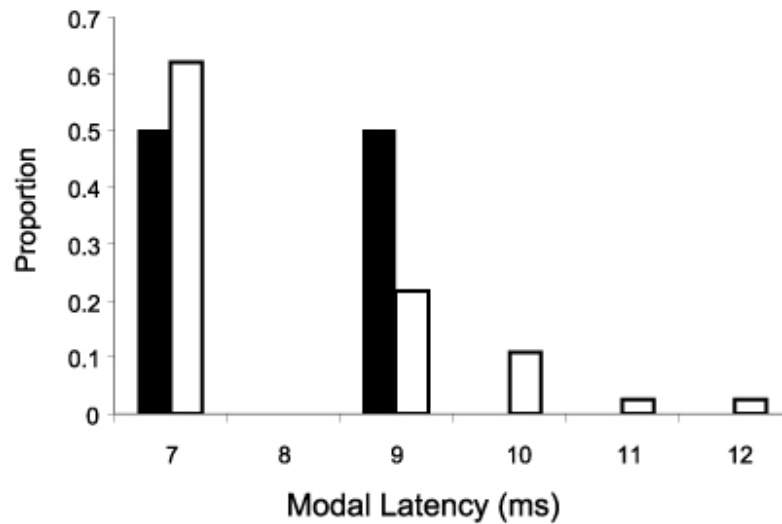


**Figure 3-11. Response Changes of Unit VPM02 after Muscimol Application.** Top: Comparison of averaged PSTHs before and after muscimol application. Top panel: PSTH before muscimol application averaged from 200 trials during the 20 minutes period of baseline recording. Bottom panel: PSTH averaged from 1850 trials after muscimol was applied. Bottom: Time-course of muscimol application. Response magnitude (unnormalized) of unit VPM02 to its principal whisker D1 stimulations was plotted against the time. No supplements were given since the rat didn't show any apparent sign of changes in anesthesia depth after muscimol was applied.

### Proportional Distribution of Modal Latency



### Spontaneous Activity

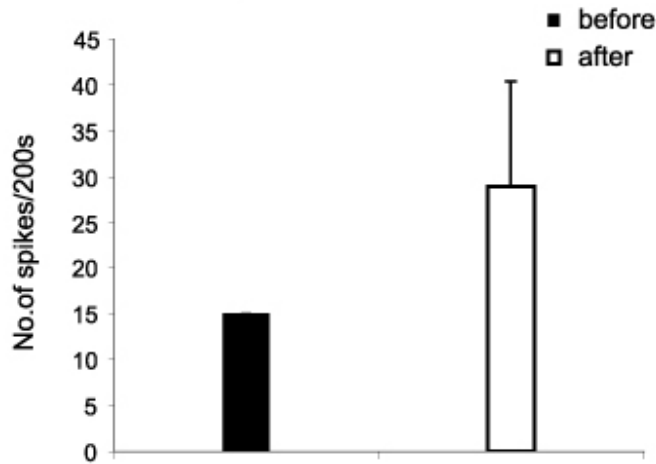


**Figure 3-12. Spontaneous Discharge and Distributions of the Modal Response Latency of Unit VPM04 before and after muscimol application.**

Top: Modal response latency in unit VPM02 showed a different pattern of latency shift after muscimol application. Note the appearance of new modal latencies >10 ms after muscimol application. These longer latency epochs were only present in this unit.

Bottom: The spontaneous activity had no significant change after muscimol application.

curve of the VPM neurons. We re-measured the response curves in 4 of 8 units after muscimol was applied, the intensity-response curves of these 4 units before and after inactivating the contralateral BFC were shown in Figure 3-13. In general, suppressing the contralateral BFC with muscimol produced consistently shifted response curves in all 4 neurons. For example, in unit VPM07, the threshold is 150  $\mu\text{m}$  (blue solid line) before muscimol application. After inactivating the contralateral BFC, the threshold increases to 280  $\mu\text{m}$  (blue dashed line). Muscimol also alters the slope of the response curve, and thus many fewer spikes could be generated at 2T after muscimol application.

### **Effects of Muscimol Application on POm Neurons**

Four units, whose response properties matched our unit-selection criteria for VPM neurons, were histologically located in the posterior nucleus (POm). POm neurons are also responsive to sensory inputs (Ahissar et al., 2000; Diamond et al., 1992a), but interact with barrel cortex differently than VPM neurons (Diamond et al., 1992b). Data from these 4 neurons were also included here. In general, POm units decreased their response more quickly, and dropped their response magnitude more dramatically than the VPM neurons after contralateral muscimol application.

Changes in response of POm unit POM01 (Fig. 3-14) was tested by stimulating the principal A4 whisker. Muscimol application almost eliminated responses to the A4 whisker within 15 min (Fig. 3-15). Decrease of response magnitude and shift in response temporal structure is reflected in the shape

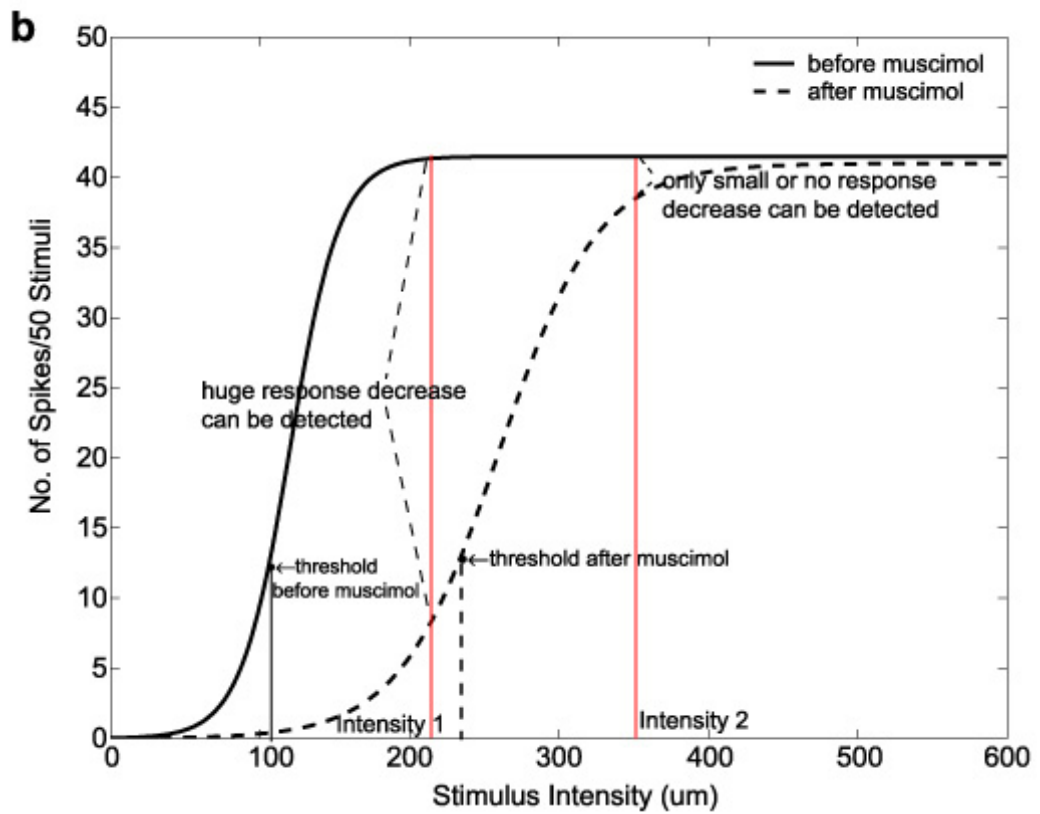
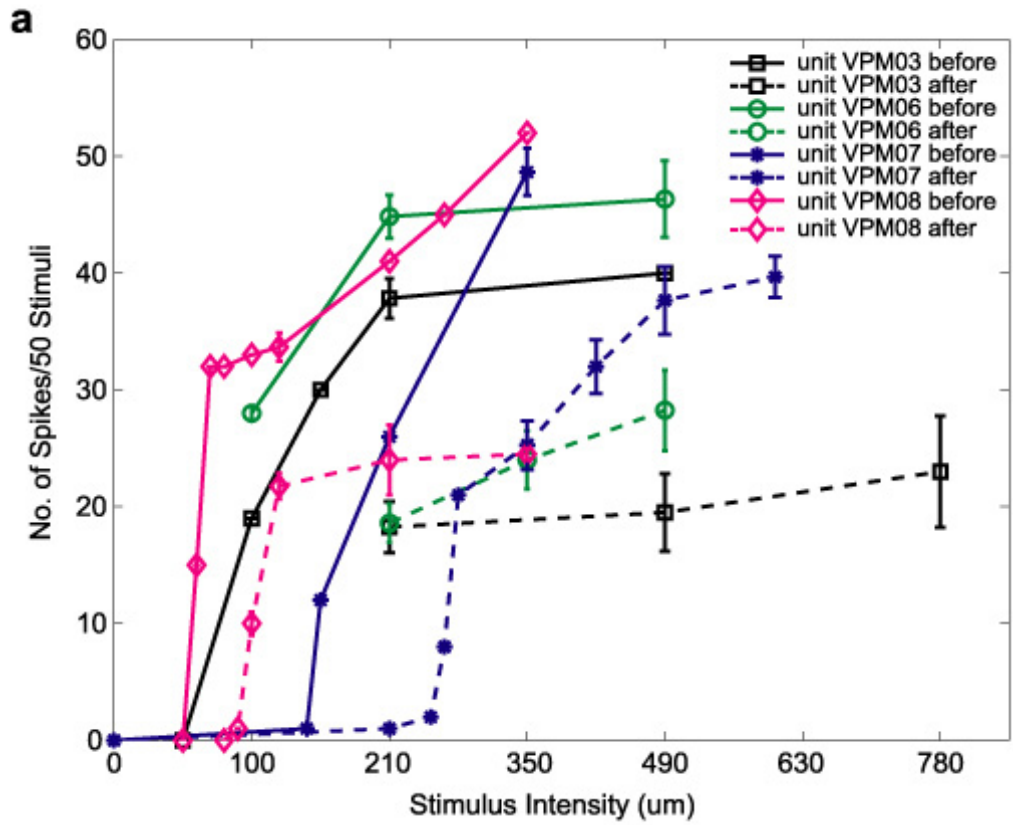


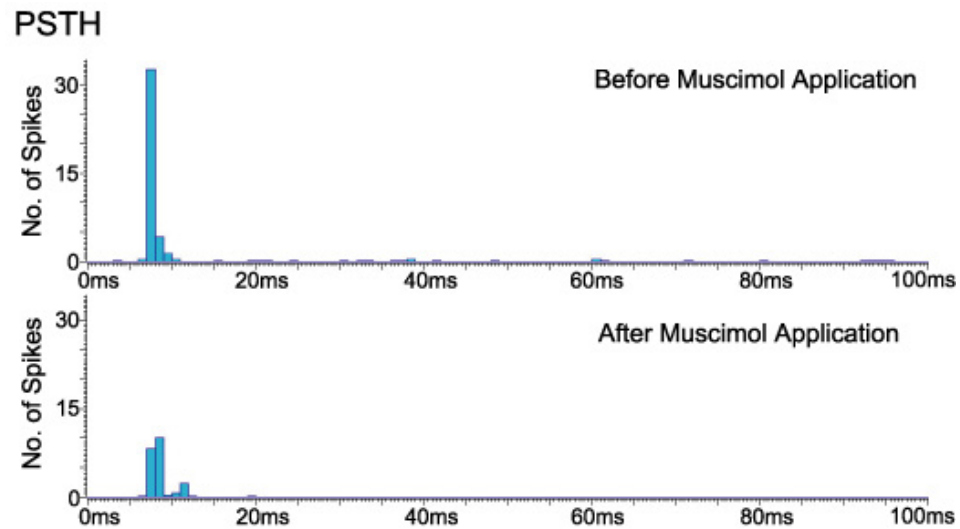
**Figure 3-13. Model of the Muscimol-Induced Response Curve Changes.**

**a.** Response curves shifted in VPM neurons ( $n = 4$ ) after muscimol application. Response magnitude (spike count/50 stimuli) was plotted against the amplitude of whisker deflections (in  $\mu\text{m}$ ). Data from the same VPM unit are rendered in the same color. The response curves of the same VPM neuron is shown before muscimol application (solid lines) and 60 mins after muscimol application (dashed lines). Note that muscimol application systematically shifted the response curves of all 4 VPM neurons we tested. Error bar: SEM

**b.** An hypothesis for how cortex could regulate the responsiveness of VPM neurons by shifting their response curves. Solid and broken lines represent the response curves of the same virtual VPM neuron when the cortex is intact (solid line) or inactivated (dashed line). We propose that the influence of cortical feedback is exerted through increasing or decreasing the sensitivity of the VPM neurons to ascending sensory inputs. This hypothesis highlights the idea that stimulus intensity level is a crucial variable when testing sensory neuron responses. For example, when stimuli are applied in the rising phase of the response curve (e.g. intensity 1 in the figure), response changes could be detected easily with the whisker stimulation paradigm. On the other hand, when test stimuli are applied at saturating levels of intensity (e.g. intensity 2 in the figure), the VPM neuron would be predicted to show small or no changes in the response magnitude (arbitrary scales were used for x and y axes). The present results would not be reproducible with stimuli of 0.5 mm or higher intensity.

changes of the PSTHs. Fifteen minutes after muscimol was applied, this unit changed from 42 spikes/50 stimuli to 7 spikes per 50 whisker stimuli, which is only 14% ( $p < 9 \times 10^{-4}$ ) of its normal value. The response was maintained near 16% ( $p < 6 \times 10^{-4}$ ) at 20 minutes when muscimol was removed. These effects were reversible, in that 15 min after wash-off (second black triangle along the x-axis), the response began to recover. Two hours after muscimol wash-off, the response returned to its pre-muscimol level (Fig. 3-15). The decrease of response magnitude in P<sub>Om</sub> units was accompanied by a shift in modal latency. At 2T stimulus strength, P<sub>Om</sub> neurons in 4 out of 5 trial blocks (80%) showed modal latencies of 7 ms, and 1 of 5 (20%) responded at 8 ms before muscimol application. After muscimol was applied, only 30% of trial blocks (7 of 23) retained a modal latency at 7 ms, while 70% (16 of 23) shifted to 8 ms (Fig. 3-15). Muscimol application altered spontaneous activity in some P<sub>Om</sub> cells (Fig. 3-15), but not others.

Other changes, such as unmasking of new units, were qualitatively noted. Units that were unresponsive before muscimol application began to respond to whisker stimulation after muscimol was applied. Appearance of new units in some recording sessions was highly correlated with contralateral cortical inactivation. Unmasking of a new unit was clearly observed by the appearance of a novel waveform on the reference oscilloscope, but couldn't be quantitatively measured using our experiment design.



**Histology (CO staining)**

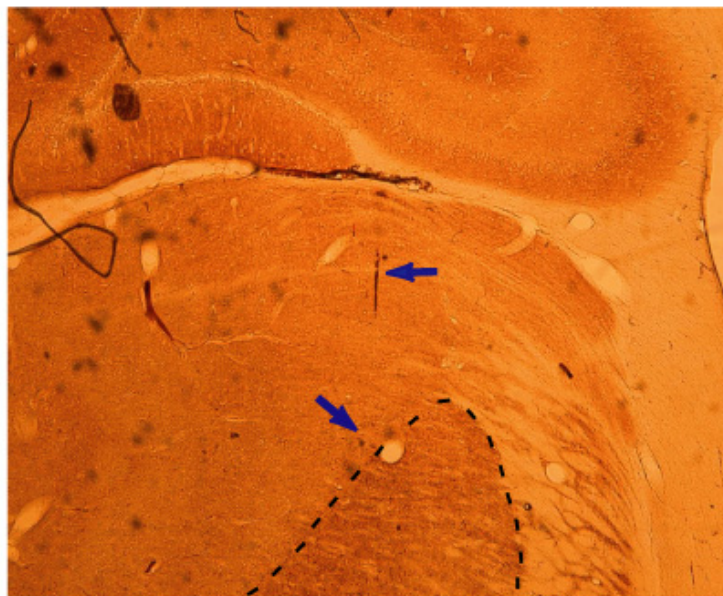


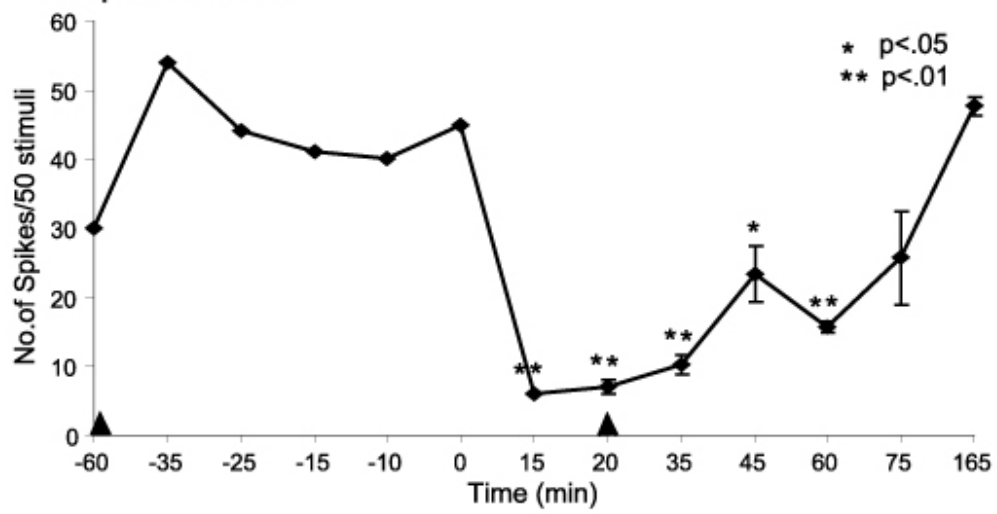
**Figure 3-14. Contralateral Muscimol Application Has a Greater Effect on POM Neurons than on VPM Neurons.**

Top: Comparison of averaged PSTHs before and after muscimol application. Top panel: PSTH before muscimol application averaged from 250 trials during the 60 minute period of baseline recording. The bottom panel was averaged from 1000 trials after muscimol was applied.

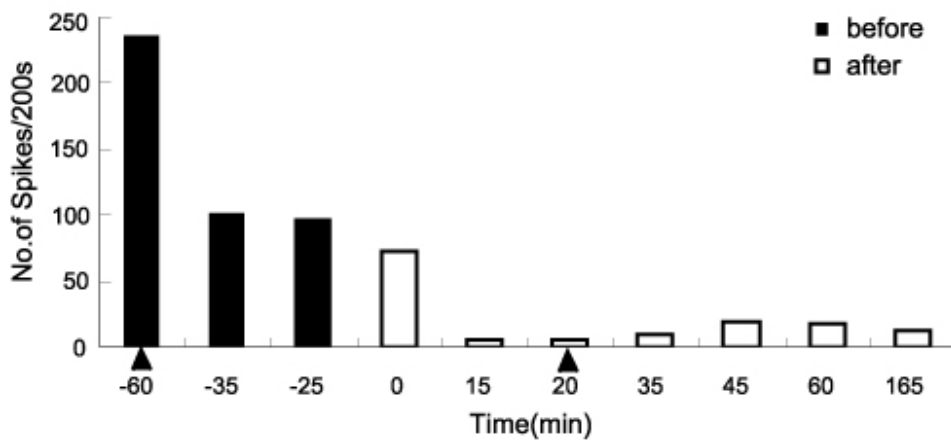
Bottom: Histological localization of the recording site lesion places the tip of the electrode in POM. The left pointing arrow indicates the electrode tract and the right pointing arrow shows the lesion location in the CO stained section. The dashed line shows the boundary of the VPM nucleus.



**a Temporal Course**



**b Spontaneous Activity**



**c Proportional Distribution of Modal Latency**

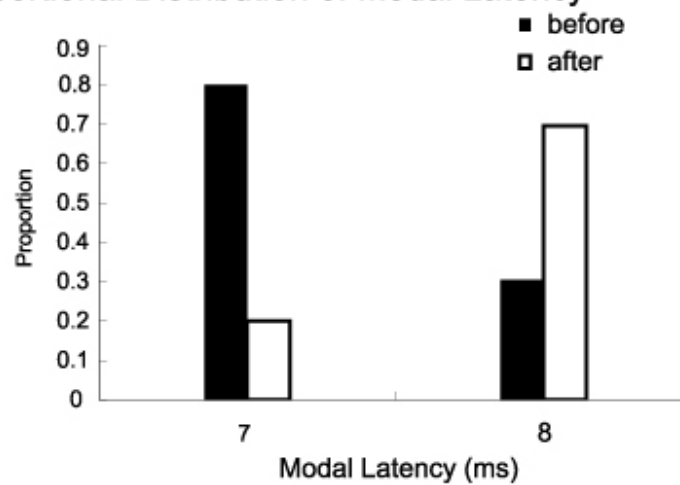


**Figure 3-15. Changes of Evoked Response and Spontaneous Activity are Greater in POm Units than on VPM Neurons after Muscimol Application.**

**a.** Temporal course of the response magnitude change to “best whisker” (A4) stimulation before and after muscimol application. Receptive field was only mapped by a hand-held probe but not quantitatively. Time of anesthetic supplements is indicated by the left black triangle on the X-axis. The black triangle on the right indicates the wash-off time of muscimol by warm saline.

**b.** Change of spontaneous activity during the entire recording period. In contrast to VPM cells, there is a decrease in spontaneous activity of POm cells after the supplementary anesthetic injection that persists through the muscimol application period.

**c.** Modal latency before and after muscimol application. Response latency showed a clear shift to longer modal latency (8ms) after muscimol.

## Discussion

The present results document two new findings: first, cortex indirectly influences thalamic relay neurons on the contralateral side, and second, cortex regulates thalamic relay neurons' responses by altering their response threshold/curve. Many previous reports have shown that responsiveness of thalamic relay neurons can be modulated by cortex (for review, see Castro-Alamancos, 2004; Sherman and Guillery, 1996, 2002; Sillito and Jones, 2002). The current study provides evidence that thalamic relay neurons can be influenced from both hemispheres. The present data offers an explanation for the observation that after muscimol is applied to the BFC there are response decrements in the 3-10 ms component of responses of contralateral BFC neurons. The shortest latency (3-10 ms) responses in cortical neurons are usually ascribed to inputs from thalamic relay cells (Armstrong-James and Fox, 1987; Armstrong-James et al. 1991). The functionally bilateral cortical activity could be the physical substrate for the rat to successfully perform perceptual tasks which require the bilateral integration of information sampled by the full array of whiskers (Krupa et al., 2001; Shuler et al., 2002). Our data indicate that one new way for cortex to regulate the response properties of thalamic relay neurons is to alter their response threshold/sensitivity curve. They suggest that cortex monitors thalamic activity very closely and the cortical regulation of thalamic relay neurons may not solely achieved through lateral inhibition. Previous work suggests that the metabotropic receptors play a role in such control (Castro-Alamancos, 2004), however, more studies are needed to clarify

the individual molecular/cellular mechanisms for the threshold-shifting seen in VPM neurons.

### **Methodological Concerns**

The most interesting finding in the present study is that VPM neurons change their responsiveness after silencing contralateral cortex. Muscimol has been widely used to reversibly block neural activity within a circumscribed region. Effects of muscimol have been proven to be well-circumscribed and reversible when applied acutely, or chronically in auditory, somatic sensory and visual cortex of bats, cats and rats (Fox et al., 2003; Li et al., 2005; Krupa et. al, 1999; Reiter and Stryker, 1988; Zhang and Suga, 1997). We mapped the effective area of muscimol suppression *in vivo* by electrophysiology, and the results are highly consistent with what had been reported using similar muscimol concentration in previous studies (Edeline et al., 2002; Li et al., 2005; Reiter and Stryker, 1988; Wallace et al., 2001). The results of our acute muscimol suppression experiment showed that cortical activity was significantly suppressed (>50%) by 10 mM muscimol solution within 20 minutes after application, as judged by reduced spontaneous activity and smaller evoked responses to whisker stimuli in layer IV neurons in the D2 barrel. Recovery from muscimol suppression occurred within 1 hour after removal, consistent with previous studies using a similar experimental paradigm (Reiter and Stryker, 1988). Although there is little question that muscimol suppresses neural activity in cortex, it is also the case in the acute

experiment that muscimol could enter cortex along the electrode tract and alter the onset time of suppression by muscimol.

Thalamic relay neurons fire in two modes: tonic and burst (Lo et al., 1991; for review see Sherman, 1996, 2001b). Tonic firing mode is thought to be more involved in information processing while bursting firing is suggested as a “wake-up call” stimulus to cortex (Sherman, 2001a; for review see Sherman and Guillery, 2002). It has been reported that inactivation of cortex shifts the firing mode of ipsilateral cat LGN neurons (Sillito and Jones, 2002). In the present study all VPM neurons were operationally kept in the tonic firing mode by maintaining a steady depth of anesthesia. This also eliminated the confounding influences of recording condition changes. During our recording, no signs, such as voluntary whisker movement, response to squeezing the foot or increase of spontaneous firing, were detected. And the fact that VPM and POm cells showed a different time course under the same experimental conditions diminished the possibility that the changes were induced by direct suppression of diffused muscimol. We also found that VPM neurons tended to fire more in bursts (or spindles) after long term muscimol application when stimulus intensities were well above 2T, which is consistent with what has been reported in cats’ LGN (Sillito and Jones, 2002).

### **Threshold Determination**

Neurons along the whisker-barrel pathway are sensitive to different stimulus parameters, such as amplitude, frequency, direction, velocity and

acceleration (Armstrong-James and Fox, 1987; Gibson and Welker, 1983a, b; Ito, 1985, 1988; Lee and Simons, 2004; Lichtenstein and Simons, 1990; Minnery and Simons, 2003; Temereanca and Simons, 2003; Waite, 1973b; Wilent and Contreras, 2004). Stimulus threshold has been investigated mostly by long duration ramp-and-hold stimuli (Ito, 1988; Lee and Simons, 2004; Minnery and Simons, 2003; Temereanca and Simons, 2003). Stimulus amplitude interacts with velocity (Ito, 1988; Waite, 1973b; Wilent and Contreras, 2004), and layer IV neurons are more sensitive to changes in stimulus amplitude than they are to velocity (Ito and Kato, 2002), suggesting that VPM neurons could be sensitive to stimulus amplitude, too. Furthermore, since we want to determine whether latency is shifted after inactivation of cortex, we chose to use a stimulus with short duration (3 ms) pulse with a very brief rise time. Here we operationally defined response threshold as the lowest stimulus intensity that would cause the cell to generate action potentials at a criterion level above background. Practically small increases of around 10  $\mu\text{m}$  in stimulus intensity can reproducibly move the VPM neuron from subthreshold to threshold response levels (Fig. 3-2, 3-3). Our data indicate that this definition is very useful for comparing responses between cells in different animals. In this study VPM neurons showed quite a wide range of response thresholds, which could be due in part to differences in the driving power from the brainstem trigeminal complex. It is also important to emphasize that the VPM neurons were tested only by forward whisker deflections. In fact, VPM neurons show clear angular preferences (Simons and Carvell, 1989) and are organized topographically into an angular tuning map in

VPM (Timofeeva et al., 2003). Thus, the variety of response thresholds can be partially due to the fact that not all VPM neurons analyzed in our experiments were tuned to forward whisker movements. However, since we didn't map the angular tuning properties of each VPM neuron systematically, it remains unknown how the angular tuning preference interacts with muscimol suppression. Each cell was tested at 2T- intensity level, and from the response curves constructed in normal VPM neurons, it is clear that 2T is near a midpoint in the response range of VPM neurons. The response curves also emphasize that "supramaximal" stimuli similar to those usually applied in our previous studies and typically in studies from other laboratories, produce responses at saturation levels. Thus 2T stimulus intensity has relevance to natural stimuli encountered by a rat. Our results support the idea that studies on cortical excitability should select stimulus parameters relevant to the experimental goal, since subtle thalamic and cortical response levels could depend on the stimulus configuration used to test the system. If the test stimuli were too high or too low the target neuron could be saturated or under-driven by the whisker stimulation as a result of excitability levels changing during the experiment. Therefore caution is required when directly comparing the current results with others due to this significant feature of the experimental design. For example, VPM neurons have been shown to maintain their response latency to stimuli at different frequencies, which has been used as a cardinal characteristic of the nucleus (Ahissar et al., 2000). However, in those experiments VPM neurons were tested with ~2 mm whisker displacement produced by air-puff. This stimulus would be considered as

very “supramaximal” under current experimental conditions. Thus, the differences in latency modulation identified in different studies can be attributed in part to the stimulus characteristics. Several studies have shown a decrease in response latency with increases of stimulus intensity in thalamus (Ito, 1988) and cortex (Ito, 1985; Wilent and Contreras, 2004).

### **Corticothalamic Projections: Anatomy**

All nuclei in the dorsal thalamus receive massive feedback projections from cortex. It has been reported that corticothalamic projections greatly outnumber the ascending sensory projections in the lateral geniculate nucleus (Guillery, 1969; Liu et al, 1995). A better understanding of the structure of thalamo-cortico-thalamic circuitries is necessary to understand their functions in the working brain. As in other mammals, corticothalamic projections in rats mainly originate from pyramidal cells in layer V and VI (Hoogland et al, 1987; Land et al., 1995; for review, see Deschenes et al, 1998). These two groups of projections are distinguished by 1) their targets, 2) collaterals to RTN, 3) synapse morphology and 4) axon branching patterns. The recipients of layer VI and V corticothalamic projections are accordingly named as “first order” and “higher order” relay nuclei respectively (Guillery, 1995). Layer V projections are actually collaterals of corticobulbar or corticospinal fibers (Bourassa et al., 1995; Hoogland et al., 1987; Land et al., 1995). They always form small clusters of terminals, with larger terminal size in POm, and they don't innervate the thalamic reticular nucleus (RTN). On the other hand, projections from layer VI do send



numerous collaterals to RTN (for review, see Deschenes et al., 1998). Layer V and VI projections accordingly differ substantially in function (for review, see Guillery and Sherman, 2002; Sherman and Guillery, 2002). The fine topography of CT projections from layer VI of BFC to VPM has been recently examined and discussed in detail (Deschenes et al., 1998). In brief, ipsilateral CT projections are highly ordered, and neurons in different sublayers (superficial section v.s. deeper sections of layer VI) display different axon branching patterns in the thalamus. Axons from the upper section of layer VI obey a strict one-to-one relationship between barrels and barreloids while deeper cells tend to extend their collaterals to cover a much larger area in VPM and further invade into POM (Bourassa et al, 1995). Bilateral projections from cortex to thalamus do exist in rats. However, most of these reported projections don't originate from BFC and none terminate in VPM: the labeled fibers end in nuclei of the anterior group, medial dorsal and submedial nuclei (Leonard, 1969; Beckstead, 1979; Kaitz and Robertson, 1981; Reep and Winans, 1982; Oda, 1997). Thus, these bilateral projections may play only a limited role in the plasticity of sensory relay nuclei (VPM) after cortical manipulations in BFC. CT terminals form synapses on the distal part of the dendritic tree of VPM neurons, these synapses are glutamate-gated which indicates the excitatory and regulatory nature of corticothalamic projections, while the fine-grained knowledge of the interconnections between layer VI, VPM and RTN is still incomplete. It is clear that cells in upper and lower sections of layer VI innervate thalamic relay nuclei differently, and identifying the functional implications of these differences in anatomy would be important future

studies. We conclude that ipsilateral layer VI corticothalamic projections are the most likely substrate for the contralateral corticothalamic influences, and indeed Swadlow has reported an inhibitory effect of callosal stimulation on layer VI neurons in somatic sensory cortex of the rabbit (Swadlow, 1989).

### **Corticothalamic Projections: Function**

Previous studies of different sensory systems and from various species have demonstrated that corticofugal projections are involved in the transmission mode change and/or the balance of center/surround components of the receptive field of thalamic relay neurons and in sleep/wake cycles (see Guillery and Sherman, 2002; Sherman and Guillery, 1996, 2002; Sillito and Jones, 2002; Steriade and Timofeev, 2003; Suga et al., 2003 for review). Available literature indicates a facilitatory role of CT fibers on thalamic neurons. Early studies in visual system show that the primary visual cortex influences the general excitability of thalamic relay neurons (Kalil and Chase, 1970, Tsumoto et al., 1978). In bat's auditory system MGB neurons shift their frequency tuning depending on the correspondence of the best frequency between cortical layer VI neurons stimulated and MGB neurons recorded (Yan and Suga, 1996; Zhang et al., 1997; Yan and Suga, 1998; see Suga and Ma, 2003; Suga et al., 2003 for review). It has also been reported that in monkey's somatosensory system, inactivation of ipsilateral area 3b either acutely or chronically with D-APV enlarges the RF size of thalamic neurons (Ergenzinger et al., 1998). Despite the numerous effects demonstrated, the detailed functions of CT projections still

remain unclear. In rats, typically inactivating SI with lidocaine decreased the response of the majority of recorded VB neurons under anesthesia (Yuan et al., 1985) as well as in awake rats (Yuan et al., 1986). These results fit well with the synaptic arrangements of CT projections. CT projections influence lemniscal and paralemniscal neurons in rat somatosensory system differentially since responsiveness of P<sub>Om</sub> neurons decreased more after magnesium sulfate suppression of ipsilateral barrel field cortex (BFC) under conditions where VPM neurons continued to fire (Diamond et al., 1992b). Other studies indicate VPM is affected by cortical feedback, for reversible inactivation of SI cortex immediately changed the spatiotemporal structure of receptive field in subtle ways (Krupa et al., 1999), and the effects can be non-linear (Ghazanfar et. al, 2001). Since these studies employed a method of global inactivation or removal of sensory cortex, instead of considering the possible dependence of observed thalamic response changes on the relationship of the tuning properties between thalamic neurons recorded and cortical neurons manipulated (Suga and Ma, 2003), the complexity of results reported may be simplified when the topography of cortex and VPM is considered. Temereanca and Simons (2004) recently reported that micro-stimulation of layer VI neurons in one barrel column increases the response magnitude of neurons in the corresponding barreloid to principal whisker stimulation, and at the same time reduces the responsiveness of cells in mismatched barreloids. These results demonstrate that matched cortical feedback exerts a topographic facilitatory influence on VPM neurons, and secondly, can sharpen the response probably through mechanisms similar to

Suga's "egocentric selection". The latter is a term arising from studies of auditory thalamus, and refers to a modulation in the best frequency of a subcortical neuron by its recent history of intense cortical input activity (Yan and Suga, 1996; Zhang et al., 1997). The current concept in the somatosensory system is consistent with a similar cortical influence on sensory transmission through subcortical structures.

### **Cortical Modulation of Tuning Properties of Thalamic Relay Neurons**

Various hypotheses had been proposed to explain thalamic and cortical interactions mostly based on lateral inhibition (Alitto and Usrey, 2003; Krupa et al., 1999; Rauschecker, 1998). We noticed that while lateral inhibition could account for the response magnitude change, it did not appear to explain the latency shift seen in the current study. Pharmacological activation of layer VI of barrel column with bicuculline selectively enhances the response of ipsilateral "matched" (homologous) barreloid neurons but suppresses those neurons in "non-matched" barreloids (Temereanca and Simons, 2004). Their results convincingly demonstrate an important type of cortical modulation of "spatial tuning" (the RF characteristics) of VPM neurons, however, the underlying mechanisms still remain unclear. Our observations of the response curve shift after inactivation of cortex can be one of the possible ways that cortex regulates neurons at subcortical levels. Here we propose another way that cortex may regulate the responsiveness of VPM neurons, namely, by affecting their activation threshold (Fig. 3-13). That is, the facilitatory role of increased cortical

feedback is enacted through its influence on the response curves of VPM neurons (Fig. 3-13). By modulating the threshold, VPM neurons can gate/filter certain information (Prezybyszewski et al., 2004), and/or enhance/weaken the contrast between different stimuli (see Sillito and Jones, 2002 for review). Threshold changes could also influence plasticity of VPM neurons after the cortical manipulations through latency as well as magnitude modulation. It is clear that in most cases corticothalamic modulation depends heavily on the topography of corticothalamic projections and on interactions between cortex, reticular nucleus and thalamus, and the contribution of each of these parameters still need to be sorted out.

The response curves of VPM neurons could be viewed as the “stimulus intensity tuning curves”. From this point of view, cortex unquestionably influences the “intensity tuning” of VPM neurons in addition to the “spatial tuning” reported by Temereanca and Simons (2004). Since neurons in the whisker to barrel pathway are tuned to several parameters such as the whisker specificity, amplitude (described in the present study), frequency and direction of whisker movements (angular tuning), many other tuning properties may be under cortical influence as well. Sillito et al. (1994) showed that corticofugal projections influenced LGN neurons by facilitating the synchronization of thalamic neurons with similar receptive field features as those of their cortical input cells. Experiments are ongoing to determine whether VPM cells lose their synchrony, or change their intrinsic pattern of synchronization, after the cortex on either side is silenced. These results are designed to address the unmasking effect: the

appearance of newly responsive neurons that respond to whisker test stimulation only after contralateral muscimol application. This unmasking, together with the latency shift effect, may reveal additional features of the complicated influence of cortical feedback on transmission through the thalamus.

## CHAPTER IV

### **BARREL CORTEX ACTIVELY REDEFINES THE ANGULAR TUNING PROPERTIES OF VPM NEURONS**

The massive feedback projections from the neocortex to thalamus have important but subtle, effects on sensory information transmission. We investigated the role of cortical feedback on whisker angular tuning (AT) in rat ventral posterior medial (VPM) nucleus by comparing AT properties of single VPM neurons before and after intense activation of layer VI in ipsilateral barrel columns. Microstimulation of layer VI in “matched” (homologous) barrel columns sharpens the AT curves of VPM neurons that are tuned to the same direction as the stimulation site in cortex, and rotates the angular preference of VPM neurons initially tuned to different directions towards the direction that cortical neurons prefer. Stimulation in mismatched barrel columns suppresses responses without consistent effects on AT. We conclude that cortex actively regulates two feature maps in the thalamus simultaneously, which predicts that the tuning properties of VPM cells are continually optimized for detecting the most salient incoming message.

#### **Introduction**

One fundamental question in neuroscience is how the brain adapts to a rapidly changing world. From many pioneering studies, it is well established that sensory information is represented in an orderly manner in the brain, and these

neural representations are continually modified by sensory experience, injury and deprivation. In sensory systems, neuronal cells tuned to different stimuli and/or different parameters of a stimulus are topographically organized into specific neural structures, called “computational maps” (Knudsen et al., 1987). These maps are thought to underlie higher order processes leading to perception and cognition. Conceptually, since the brain deals with continuous information flow, it has to constantly shift the processing focus to the most salient events in the environment (the “hot-spot”), which should receive the most careful scrutiny. Thus, local and dynamic mechanisms operating on a time-scale measured in seconds and minutes are required for adaptive processing. Unfortunately, how the maps at different brain levels are dynamically refined and updated in real-time is largely unknown.

Available literature suggests that top-down processes may facilitate selective attention (Alitto and Usrey, 2003; Crick and Koch, 1998; Hillenbrand and van Hemmen, 2002). For example, feedback from area MT increases the response gain and contrast of neurons in the primary visual cortex (VI) (Hupe et al., 1998). The primary sensory cortex in addition plays a regulatory role on response properties of subcortical neurons, as recently demonstrated by studies in auditory, somatosensory and visual systems in bats, cats, rats and monkeys (Sherman and Guillery, 2002; Sillito and Jones, 2002; Suga and Ma, 2003; Suga et al., 2003). Hence corticothalamic (CT) feedback projections could constitute a possible pathway for cortex to actively and selectively modulate the representation of the peripheral input near its information source. Within the



feedback from layer VI, layer VIa projections are anatomically precise while those from layer VIb cells are more diffuse (Deschenes et al., 1998), but how CT feedback helps neocortex to attentively select the relevant epochs in the continuous information stream still remains elusive.

In the rat's vibrissa (whisker) system, neurons representing whiskers at each brain level are organized into topographic "whisker maps". These maps correlate well with the anatomically discrete cell aggregates, called "barrelettes" in the brainstem (Ma, 1991), "barreloids" in thalamus (Van der Loos, 1976) and "barrels" in layer IV of the primary somatosensory cortex (SI) (Woolsey and Van der Loos, 1970), each replicating the spatial arrangement of whiskers on the face (Figure 1-1). In addition, neurons within the whisker map are also sensitive to many other parameters of whisker movements such as amplitude and frequency as well as direction, indicating multiple maps of sensory features could co-exist in a single neural structure. Direction selectivity, or angular tuning, to whisker movements has been repeatedly investigated in the rat's vibrissae system (Bruno et al., 2003; Lee and Simons, 2004; Lichtenstein et al., 1990; Minnery and Simons, 2003; Minnery et al., 2003; Simons and Carvell, 1989; Timofeeva et al., 2003), and angular tuning maps have been identified within the whisker map in thalamus (Timofeeva et al., 2003) and cortex (Andermann and Moore, unpublished). Cortical modulation of thalamic whisker response has shown that increasing layer VI feedback from one barrel column enhances the responses of VPM neurons with the same principal whisker (Temereanca and Simons, 2004). Cortical influences on other properties of thalamic neurons, such as directional

tuning, have not been demonstrated. Direction sensitive neurons encode fundamental information about whisker stimulations, and the information may contribute to certain higher order processing stages. Thus examining effects of cortical feedback on directional tuning of thalamic cells could provide an opportunity to reveal the dynamic mechanism(s) in which cortex performs sensitivity enhancement in real time, which is thought to be related to attention. By exploring how cortex influences the subcortical neurons sensitive to multiple parameters, more subtle details of the cooperation between co-localized yet functionally linked maps can be clarified.

## **Materials and Methods**

### **Animal Preparation**

Animal preparation, electrophysiology and histology have been described in detail previously (Li and Ebner, 2006; Li et al., 2005) and will only be briefly summarized here.

Experiments were carried out in twenty-four male Long-Evans rats (250 ~ 350 gm) in compliance with the federal and institutional guidelines for animal use. Figure 4-1 illustrates the experiment procedure. Rats were anesthetized with urethane (1.5g/kg, 30% aqueous solution, i.p.). The head was then mounted in a stereotaxic apparatus (Narashige). Body temperature was maintained at  $37 \pm 2^{\circ}\text{C}$  with a heating pad feedback-controlled by a rectal thermometer (Harvard Labs). A rectangular craniotomy was made in the left skull to expose the brain area 2-4 mm posterior and 2-4 mm lateral to Bregma, to provide access to the left

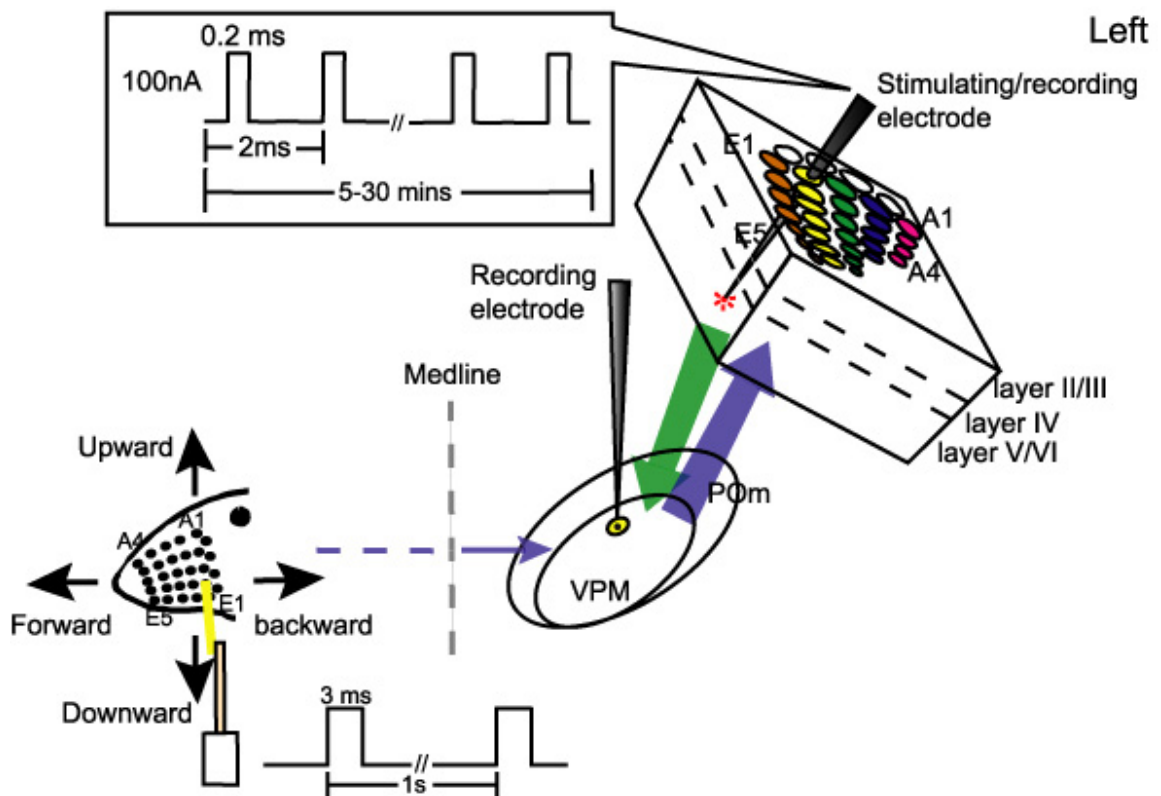


**Figure 4-1. Experimental Design.**

In rat's vibrissa system, neurons within the whisker-to-barrel lemniscal pathway show preference to certain whiskers (PW), at the same time, these neurons also have a directional preference to whisker deflections and a topographical angular tuning map can be identified in thalamus and cortex. For example, VPM cells in D1 barrelette, D1 barreloid and D1 barrel (yellow) will respond best to stimulations of the D1 whisker (yellow). The co-existence of an angular tuning map and a spatial whisker map in thalamus and cortex makes this an ideal model system. The first step was to map the angular tuning curves of single VPM neurons at 2T. Then another electrode (stimulating/recording electrode) was advanced into layer VI of an ipsilateral barrel column. The angular tuning curves of the same VPM neurons were mapped and then re-mapped after cortical feedback neurons were stimulated.

thalamus. Another circular opening was made over the left primary somatosensory cortex (SI), which was centered at 2 mm posterior and 6 mm lateral to Bregma with a diameter of ~4mm. Small slits were made in the dura to facilitate electrode penetration. The bone debris was carefully cleaned with saline during drilling. Warm saline was applied to the brain surface to prevent the cortex from drying.

### **Electrophysiology**

Extracellular single unit recording was conducted in both thalamus and cortex with carbon-fiber microelectrodes (Armstrong-James and Millar, 1979; Armstrong-James et al., 1980). One carbon-fiber microelectrode (the recording electrode) was advanced vertically into the left thalamus through the rectangular opening by a mechanical stepping motor microdrive (Kopf instruments) with an accuracy of ~1  $\mu\text{m}$  per step. Orientation of the recording electrode was calibrated using a plumb line prior to the initial penetration. Another carbon-fiber microelectrode (the stimulating/recording electrode) was advanced into the left barrel field cortex (BFC) by another mechanical stepping motor drive (Kopf Instruments). For cortical recording the electrode holder and the microdrive were carefully orientated before each cortical penetration (usually 40~45 degree laterally deviated from the sagittal plane and 10~12 degree anteriorly deviated from the coronal plane, depending on the barrel column being studied) to ensure the electrode went orthogonal to the brain surface. Contact of the electrode tip with the pial surface was identified visually under an operation microscope and by

contact noise when the electrode touched the brain surface. Single units were isolated on-line by waveforms with a time-amplitude window discriminator (Bak Instruments). For each unit isolated, spikes were recorded with a CED 1401 Plus processor (Cambridge Electronic Design) controlled by a PC (Dell). Peri-stimulus time histograms (PSTHs) were generated online with bin width of 1ms by in-house Spike 2 scripts (Cambridge Electronic Design) to visualize the response properties. At the same time, analog signals from the thalamus and cortex were digitized at 20 kHz and stored on a PC (Dell). Offline sorting methods were later employed to confirm the quality of single unit recording in thalamus and cortex. Depth of anesthesia was monitored by various signs (burst firing in thalamus/cortex, breath/heart beat rate, voluntary whisker/body movements and corneal/hindlimb-pinch reflex) and supplements of anesthetic (10% of initial dose) were given as needed to maintain the anesthesia level at stage III-3 (Friedberg et al., 1999). To ensure the reliability of data recorded, all experiments were forced to terminate no later than 14 hours after the induction of anesthesia.

### **Whisker Stimulation**

Individual whiskers on the right side of the snout were stimulated by a customized piezoelectric bimorph ceramic wafer mounted on a rotatable shaft, which enabled us to deflect each whisker from its neutral position in any single direction. The piezoelectric advice was driven by brief (3 ms) square-wave pulses delivered from a computer-controlled digital stimulator (WPI DS8000). We calibrated our piezoelectric stimulator by constructing the empirical function

between the voltage applied to the piezoelectric stimulator and the actual amount of movement it produced under a high-speed digital camera (Redlake). One block of trials consisted of fifty whisker stimulations delivered ~10 mm away from the base of the whisker at 1 Hz (1 stimulus per second) with the amplitude specified by the experiment protocol. Whisker stimuli used in thalamus and cortex were generally similar, but significant distinctions also existed. In the following text, detailed experimental procedures were elaborated for recording in thalamus and cortex, respectively.

### **Recording in Thalamus**

As the electrode was advanced into the dorsal thalamus, whiskers were stimulated by a hand-held probe. When robust firing was evoked, all whiskers on the right side of the face were trimmed to 10mm. VPM neurons were first estimated by the X-Y coordinates and the depth read-out of the microdrive (Haidarliu and Ahissar, 2001; Land et al., 1995; Sugitani et al., 1990) then refined by response characteristics to piezoelectric whisker deflections. At urethane anesthesia stage III-3, most VPM neurons exhibit small receptive field size (1-2 whiskers) (Diamond et al., 1992a; Rhoades et al., 1987; Timofeeva et al., 2003; Waite, 1973), a tonic response mode to 1 Hz whisker stimulation (Sherman and Guillery, 1996), high firing probability, short modal latency and low spontaneous firing (Li and Ebner, 2006). If one isolated unit couldn't generate a robust response with a modal response latency of ~5 ms to the test stimuli, this unit was discarded and the electrode was moved to a new place until another unit was

identified and tested. The unit candidate was required to be clearly distinguishable by its waveform from other units around, and usually the neuron with the highest waveform amplitude was selected at each penetration depth. Neuronal activity of both evoked response and spontaneous activity was recorded for more than 1 hour to ensure satisfactory stability of every unit before proceeding.

### ***Receptive Field Mapping***

The RF of VPM neurons was first mapped manually with a hand-held probe to determine the principal whisker (PW) then quantified by fifty deflections (300  $\mu$ m forward movements) to the PW and the immediately adjacent whisker (AWs) respectively. PW always evoked the largest number of spikes with the shortest modal latency. The RF was re-mapped at 2 times of threshold (2T) stimulus intensity level in the “preferred direction” (see the following text).

### ***Threshold Assessment and Angular Tuning Curve Mapping***

The customized piezoelectric stimulator was used to map the angular tuning curves of VPM neurons by deflecting the PW in forward (caudal to rostral), upward (ventral to dorsal), backward (rostral to caudal) and downward (dorsal to ventral) 4 directions pseudo-randomly at the amplitude specified by our protocols. Previous studies of angular tuning in rats vibrissa system typically mapped the angular tuning curves with 45 degree increments (in 8 directions), but our data suggested that mapping the angular tuning curves with four behaviorally important directions sufficiently summarized the angular tuning characteristics of

VPM neurons with satisfactory resolution, at the same time improving efficiency. In one round of mapping, 50 stimuli were applied to the PW in each of 4 directions pseudo-randomly. The first round of mapping was done with 300  $\mu\text{m}$  deflections to determine the “preferred direction” (PD), which is the direction that VPM neurons responded with the highest magnitude and shortest latency. Accordingly, the other three directions were termed as the “non-preferred directions” (NPDs). Repeated rounds were carried out when necessary for consistency check. As reported in previous studies (Bruno et al., 2003; Minnery et al., 2003; Simons and Carvell, 1989; Timofeeva et al., 2003), VPM neurons clearly display directional selectivity under urethane anesthesia, indicating a differential sensitivity (response threshold) to whisker movements in different directions. When the response magnitude (number of spikes) was plotted against the amplitude of whisker stimulation, angularly well-tuned VPM neurons showed different response threshold to each direction and the threshold to PD is usually the lowest. The response threshold of VPM cells for PW stimulation in the PD was determined. In the current study, the response threshold was defined as the lowest amplitude of PW deflection in the PD (i.e., lowest voltage applied to the piezoelectric stimulator) that statistically produced a response significantly different from the background (operationally, at least three spikes in one of the poststimulus bins in the PSTH) (Armstrong-James and Fox, 1987). In the current study, the threshold was determined by varying the voltage applied to the piezo stimulator in a linear-interpolation manner (Li and Ebner, 2006). For example, if one VPM neuron responded to 200  $\mu\text{m}$  deflections robustly, it would be tested by



100  $\mu\text{m}$  deflections next; if the 100  $\mu\text{m}$  whisker movements failed to fire the neuron, 150  $\mu\text{m}$  would be tested; otherwise 50  $\mu\text{m}$  would be used, and so on. When two successive amplitudes were close ( $<50 \mu\text{m}$ ), voltage would be increased volt by volt to get an accuracy of  $\pm 10 \mu\text{m}$ . We occasionally measured the threshold of NPDs in some VPM neurons that we analyzed. Once the threshold to PD was determined, the angular tuning curve would be mapped again at 2 times of threshold (2T) intensity level over a period of time ( $>1$  hour). Data acquired were checked for consistency and used as the baseline. Spontaneous activity (SA) was recorded for 50 sec when the stimulator was positioned at the neutral position of the whisker without invoking movement.

### **Cortical Recording**

One major aim of the current study was to examine how specifically the BFC modulates the angular tuning properties of thalamic relay neurons. Recently it has been shown that the relationship of tuning curves between thalamic neurons recorded and cortical neurons manipulated plays a key role in interpreting the function of cortical feedback (Suga and Ma, 2003; Temereanca and Simons, 2004). Thus it is necessary to map the angular tuning properties of layer VI neurons to be stimulated. As demonstrated in Figure 4-2, after the properties of the VPM unit isolated were thoroughly documented, the cortical stimulating/recording electrode was positioned in the corresponding barrel column (the barrel column homologous to the VPM neuron), or one of the immediate adjacent barrel columns. Penetration was continued until the tip of the stimulating

electrode reached upper layer VI (1500  $\mu\text{m}$  underneath the cortical surface) (Temereanca and Simons, 2004). Single cortical units along the penetration were isolated as described in preceding text with spacing of  $\sim 100 \mu\text{m}$ , which was calculated by the subpial depth read out of the microcric, to avoid repeat sampling. Multi-unit activity (MUA) was also digitized at 20 kHz and stored on hard disk for offline analysis. RFs of layer IV barrel cells were mapped for location check. Angular tuning curves of cortical units along the penetration were mapped with the same piezoelectric stimulator in a way similar to VPM units. Fifty  $300 \mu\text{m}$  deflections were presented to the ***PW of the cortical unit*** in upward, backward, downward and forward 4 direction pseudo-randomly without measuring the response threshold. Spontaneous discharge and spike duration of each cortical unit was also documented. The angular tuning curve of layer VI neurons was mapped when possible.

### **Electrical Microstimulation of Layer VI**

Corticothalamic (CT) projections from the upper section of layer VI terminate exclusively within the corresponding barreloid while the projections from lower section of layer VI tend to extend their collaterals to cover a larger area in VPM and further invade into POm (Deschenes et al., 1998). The higher precision of upper layer VI projections was a selection factor for investigating the cortical feedback on the angular tuning of thalamic relay neurons. The cortical stimulation paradigm was modified from previous studies in bat auditory system (Yan and Suga, 1998; Zhang and Suga, 2000) to activate layer VI neurons around the tip of

the stimulating electrode. Trains of small currents (100 nA for 0.2 ms with 2 ms interval) was injected through the stimulating electrode (tip positive) at the depth of 1500  $\mu\text{m}$  for 5, 10, 15, 20, 25 or 30 mins, depending on the experiment protocol. Multiple units around the tip of the stimulating electrode were recorded after stimulation and compared with that before stimulation. The angular tuning curve of the same VPM unit was remapped at 2T over the time from the end of cortical stimulation to see if any changes/recovery would take place following the stimulation procedure.

### **Data Analysis**

PSTHs (bin size: 1 ms) were generated from neural activity occurring within 3-100 ms post-stimulus time for 50 stimuli in each recording block after correction for spontaneous discharge (Li and Ebner, 2006). Spikes prior to 3 ms post-stimulus were rejected as being too early to be evoked responses. Angular tuning curves of thalamic and cortical units were built for each mapping epoch by plotting the spike counts against the corresponding direction in a polar map. For each VPM unit, angular tuning curves mapped at 2T during baseline recording were averaged at each sampling time to check for the temporal consistency of angular preference. Units without continued fidelity in angular tuning were excluded from further analysis. The average response magnitude to the PD was also plotted against the stimulus intensity to construct a response curve. Latency histograms (LHs) were built to assess the onset and modal response latency. Data from the same VPM unit sampled after cortical stimulation was processed in

the same manner. The shape of angular tuning curves, response magnitude and latency were compared before and after cortical stimulation.

### **Cortex**

Angular tuning curves of cortical neurons (mostly in layer II/III, IV and V) in the same penetration were also plotted in a similar manner. Cortical neurons were classified into fast spiking units ( $<750 \mu\text{s}$ ) (FSUs) and regular spiking units ( $>750 \mu\text{s}$ ) (RSUs) by their spike duration. Angular tuning curves were plotted mainly for RSUs, since RSUs show relatively better tuning than FSUs (Lee and Simons, 2004), but data from FSUs were also included. Under anesthesia layer VI neurons are largely unresponsive to whisker stimulation. However, the present study requires the identification of the angular preference of layer VI neurons that we stimulated, since the exact cortical influences on thalamic relay neurons heavily depend on the correspondence of tuning properties between thalamic neurons recorded and cortical neurons manipulated (Suga and Ma, 2003; Temereanca and Simons, 2004). To reconcile the apparent conflict, the following criteria were set up to determine the angular preference of layer VI neurons:

First we attempted to map the angular tuning curves of layer VI neurons near the tip of the stimulating electrode directly by searching for responsive units. In 30% of the cases (8 animals) we managed to build the angular tuning curves of layer VI neurons at  $1500\mu\text{m}$ . If the angular tuning curves could not be determined in layer VI, the angular tuning properties of cortical neurons above layer VI along the penetration were examined. Once cortical neurons that were

sampled at the last 3 (or more) successive depths showed similar angular preference (i.e., tuned to the same direction), the penetration was categorized as within one of the barrel subdivisions (Andermann and Moore, unpublished), or angular “minicolumns” (Bruno et al., 2003; Mountcastle, 2003) that has specified angular tuning properties. Thus the angular preference of those unresponsive layer VI neurons to be stimulated was determined indirectly by the preferred directions of the cortical neurons in the same sub-barrel structure. 50% of our population (12 animals) was determined in this way. In the remaining cases (20%, 4 animals) where the two methods above both failed, the PD of layer VI neurons was estimated by the angular preference of neurons sampled immediately above layer VI (usually at 1200  $\mu\text{m}$ ).

***Parameters to Quantitatively Depict the Angular Tuning Features:***

Most VPM neurons in the (“core region” or VPMdm) of the barreloids are directionally tuned under urethane anesthesia (Timofeeva et al., 2003). In order to quantitatively characterize the angular preference of VPM neurons, a Tuning Ratio (Tr) was calculated. Here the tuning ratio is defined as:

$$\text{Tr} = \frac{\text{response of one VPM neuron to PD}}{\text{average response to all 4 directions tested.}} \quad \text{----- (1)}$$

By definition, Tr has a value range from 1 “poorly tuned” to 4 “highly tuned”. Hence Tr acts as an index of the directional selectivity of VPM neurons,

which enables direct comparison of the angular tuning properties within and between VPM neurons before and after cortical stimulation. It should be noticed that the form of  $Tr$  calculated here is very similar, to what has been used by other researchers (Minnery and Simons, 2003; Minnery et al., 2003). For every VPM neuron,  $Tr$  was computed for each mapping session to capture the temporal evolution of the angular specificity of every VPM neuron.

To further quantify the influence of cortical stimulation on angular tuning of VPM neurons, we introduced the Tuning Ratio Prime (short for  $Tr'$ ).  $Tr'$  is defined as:

$Tr'$  = response of one VPM neuron to the preferred direction of **cortical neurons stimulated**/average response of **the same VPM neuron** to all 4 directions tested. ----- (2)

For example, suppose VPM unit  $A$  responds best to direction  $a$  while the cortical layer VI neurons to be stimulated preferred direction  $b$  ( $a$  and  $b$  can be the same or different), then:

$Tr = A$ 's response to  $a$ /average of  $A$ 's response to all 4 directions;

$Tr' = A$ 's response to  $b$ /average of  $A$ 's response to all 4 directions.

By its definition,  $Tr'$  has a value range from 0 to 4. For each VPM neuron,  $Tr$  and  $Tr'$  usually have different values (since VPM neurons and cortical neurons were tested in the same 4 directions, there is a 25% chance that VPM and

cortical neurons were tuned to the same direction, which means  $Tr$  and  $Tr'$  have the same value).  $Tr$  is actually an indicator of the selectivity of cortical influence on the angular preference of thalamic relay neurons. The direction of  $Tr$ 's change reflects whether the shifts of angular tuning curves of VPM neurons after cortical stimulation correlates with the angular preference of layer VI neurons stimulated or not.  $Tr'$  was also compared before and after cortical stimulation. T test (one-tail) was performed to detect the significance. The 50 sec spontaneous recording was analyzed separately using in-house spike 2 scripts.

***Normalizing and Aligning Tuning Curves of Different VPM Units:***

angular tuning curves were normalized for each VPM neuron by taking the average response magnitude to PD in baseline recording period as 100. Thus for every unit, the normalized tuning curve was compared for similarity or difference between pre- and post-stimulation phases. Tuning curves from various units were further aligned to their preferred directions in a clock wise manner. For example, suppose VPM unit A was tuned to upward movement and VPM unit B was tuned to forward movement, and their values were normalized. To do the alignment, the angular curve of each unit before cortical stimulation was rotated in a clockwise direction so that their preferred directions overlapped with each other. Hence the upward direction in tuning curve of unit A was overlapped with the forward direction of unit B, the backward direction of unit A was then overlapped with the upward direction of unit B, and so on. Then data at each "direction" point were averaged to generate a new tuning curve. Post-stimulation

data were processed in the same way. To visualize the “redirecting” effect of cortex on VPM neurons, tuning curves of each unit were aligned to the direction cortex preferred and compared before and after cortical stimulation.

## **Histology**

On completion of recording, the thalamic recording site was marked by passing a DC current (electrode tip positive) of 2  $\mu$ A for 10 seconds. The location of layer VI stimulation was also marked by a lesion at 1500  $\mu$ m and the cortical stimulating electrode was retracted back to 600  $\mu$ m to mark layer IV. The rat was overdosed with urethane and perfused transcardially with PBS followed by 4% paraformaldehyde in buffer. The brain were postfixed overnight and saturated in 10%, 20% and 30% sucrose. The cortex on the recording side was flattened, sectioned tangentially, and stained for cytochrome oxidase (CO) activity (Wong-Riley and Welt, 1980) to localize barrels and microlesion sites. The cortical penetration was considered to be within the same barrel column if both lesions were localized within or below the horizontal boundaries of one barrel as defined by the appropriate patch of high CO activity in layer IV. Otherwise the stimulating electrode was thought to be under the septal region in layer VI. The remaining part of the brain was blocked, sectioned coronally and stained for CO activity. The current produced a roughly 50  $\mu$ m spherical lesion that was clearly visible as shown in the figures in CO stained sections.



## Results

In the present study, we compared the directional preference of single VPM neurons before and after focally and reversibly increasing CT feedback by electrical stimulation of neurons in the upper section of layer VI (layer VIa) in the homologous barrel column, or one of the immediately adjacent barrel columns in barrel field cortex (BFC). Stimulation consisted of current pulses (100 nA, 0.2 ms in duration with 2 ms inter-stimulus interval) (Yan and Suga, 1998; Zhang and Suga, 2000) through the stimulating/recording electrode at 1500  $\mu\text{m}$  (Temereanca and Simons, 2004) underneath the cortical surface for 5-30 mins. The angular tuning curves of single VPM neurons were mapped at low intensity (2X threshold, or 2T, see Experimental Procedures) by deflecting the principal whisker (PW) in a forward (caudal to rostral), upward (ventral to dorsal), backward (rostral to caudal) or downward (dorsal to ventral) directions in a pseudo-random order. The angular preference of layer VI feedback neurons that we stimulated was determined using either direct or indirect measures (see Experimental Procedures). We recorded twenty-four pairs of VPM+layerVI neurons. Since the cortical influence on thalamic relay neurons is dependent on the relationship of tuning properties between thalamic neurons and cortical neurons manipulated (Suga and Ma, 2003; Temereanca and Simons, 2004), we established the correspondence within each interacting pair by carefully examining both the RF and angular tuning properties of each locus. From the location of the recording sites in thalamus and the stimulating sites in cortex, eighteen VPM neurons were classified as “spatially matched” with cortex,

meaning that the stimulating electrode was in the matched (homologous) barrel column, and six neurons were “spatially mismatched”, which means that the stimulating electrode was in one of the mismatched (non-homologous), or adjacent barrel columns. By comparing the angular preferences of VPM neurons we recorded and the layer VI neurons we stimulated, three VPM neurons further were found to be both “spatially and angularly matched” with cortex, meaning that they were in the corresponding barreloids and tuned to the same direction as the layer VI neurons we stimulated (Fig. 4-2). Fifteen VPM cells were “spatially matched but angularly mismatched”, meaning that they were in the corresponding barreloids but tuned to different directions. All six spatially mismatched VPM neurons turned out to be angularly mismatched with cortex. Response properties of the twenty-four VPM units, such as the RF size, response magnitude/latency, response threshold and angular tuning features, were characterized by repeated recording for more than 1 hour before cortical stimulation to ensure the response stability of each unit. The response characteristics of VPM units during baseline recording were consistent with those reported in previous studies (Armstrong-James and Callahan, 1991; Diamond et al., 1992a; Li and Ebner, 2006; Waite, 1973). The recording sites were confirmed by histological reconstruction.

Our cortical stimulus parameters were derived from studies of the bat’s auditory system, where similar electrical microstimulation on cortical neurons was well-localized, time-dependent and reversible (Yan and Suga, 1998; Zhang and

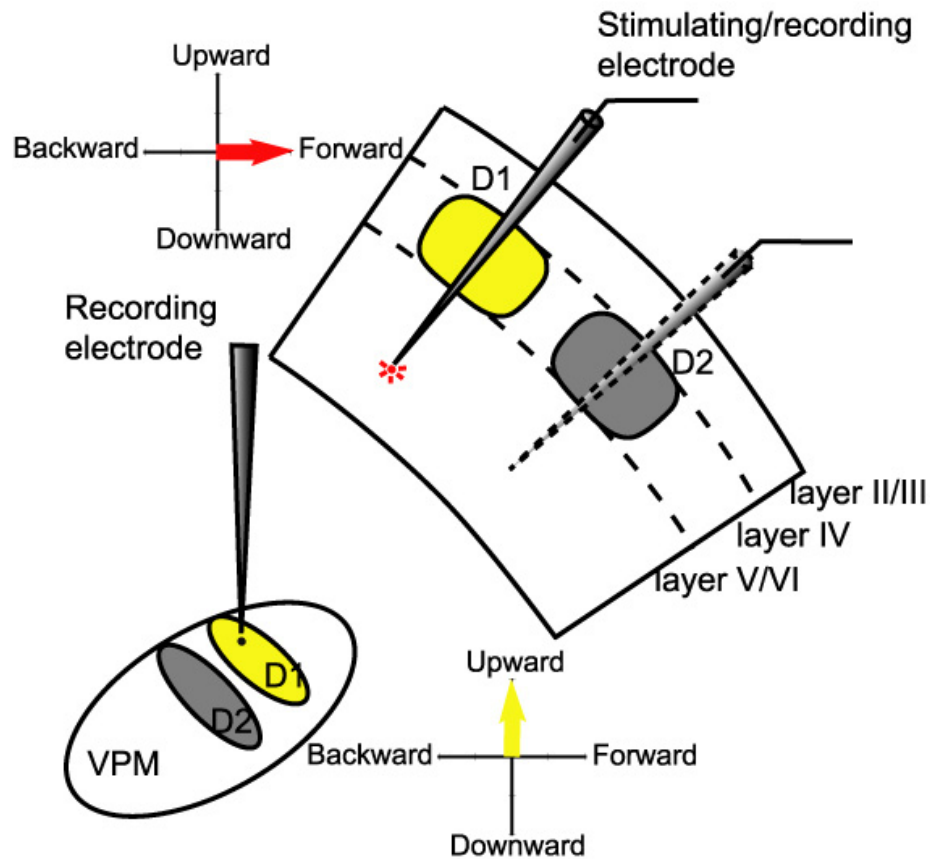


**Figure 4-2. Determination of the Relationship of Tuning Properties between the VPM Unit Recorded and the Cortical Units Stimulated.**

In order to determine the specificity of cortical modulation of the angular tuning properties of VPM neurons, first the location of the recording site was checked with the stimulating site in cortical layer VI. Based on whether or not the stimulating electrode was in the homologous barrel column, VPM neurons were classified as “spatially matched” or “spatially mismatched” with the cortex. Then the angular tuning properties of the VPM neurons were further examined for the relationship with the cortical stimulating site. Thus VPM neurons could be classified as “angularly matched” and “angularly mismatched” with the directional preference of a cortical neuron. Hence, VPM neurons could be categorized into up to four groups by the relationship of the spatial and angular tuning properties of VPM neurons with those of cortical neurons. We describe results from each of the four combinations of neuronal responses.

Suga, 2000). Initial studies indicated that electrical stimulation elevated the spontaneous activity of layer VI neurons. After 10-30 mins of stimulation, layer VI neurons showed increased spontaneous “bursting” discharge (data not shown). Spontaneous firing rate was not significantly altered in VPM neurons after cortical stimulation. However, sensory evoked responses of VPM neurons were reversibly affected after layer VI stimulation. The changes of evoked response varied as a function of the period of cortical microstimulation, as illustrated by data from unit VPM12 in Figure 4-3. In the baseline recording, unit VPM12 responded robustly to stimulation of its principal whisker D5 with a short modal response latency (8ms). Unit VPM12 had a one-whisker RF (only D5), and was sharply tuned to upward stimuli of the principal whisker (Fig. 4-3b, blue line in the right panel) at a low response threshold (80  $\mu\text{m}$ ) (Fig. 4-3a). After mapping the angular tuning curve of VPM12 at 2T (160  $\mu\text{m}$  whisker deflection), the stimulating electrode was advanced into layer VI of the ipsilateral D5 barrel column. The angular tuning curve of unit VPM12 was remapped at 2T after layer VI stimulation of the ipsilateral D5 barrel column for 5, 10 and 15 mins, each followed by a 30 min recovery time. The data show that stimulating cortex for 5 mins slightly increased VPM12’s response to its preferred direction by 17%. Ten mins of stimulation elevated the response of this neuron robustly by 61%. A 50% response increase was also observed after 15 mins stimulation (Fig. 4-3b). Hence at the single unit level, cortical feedback has a facilitatory influence on VPM neurons, which is consistent with studies using multi-unit recording (Temereanca and Simons, 2004). However, to our surprise, individual cells

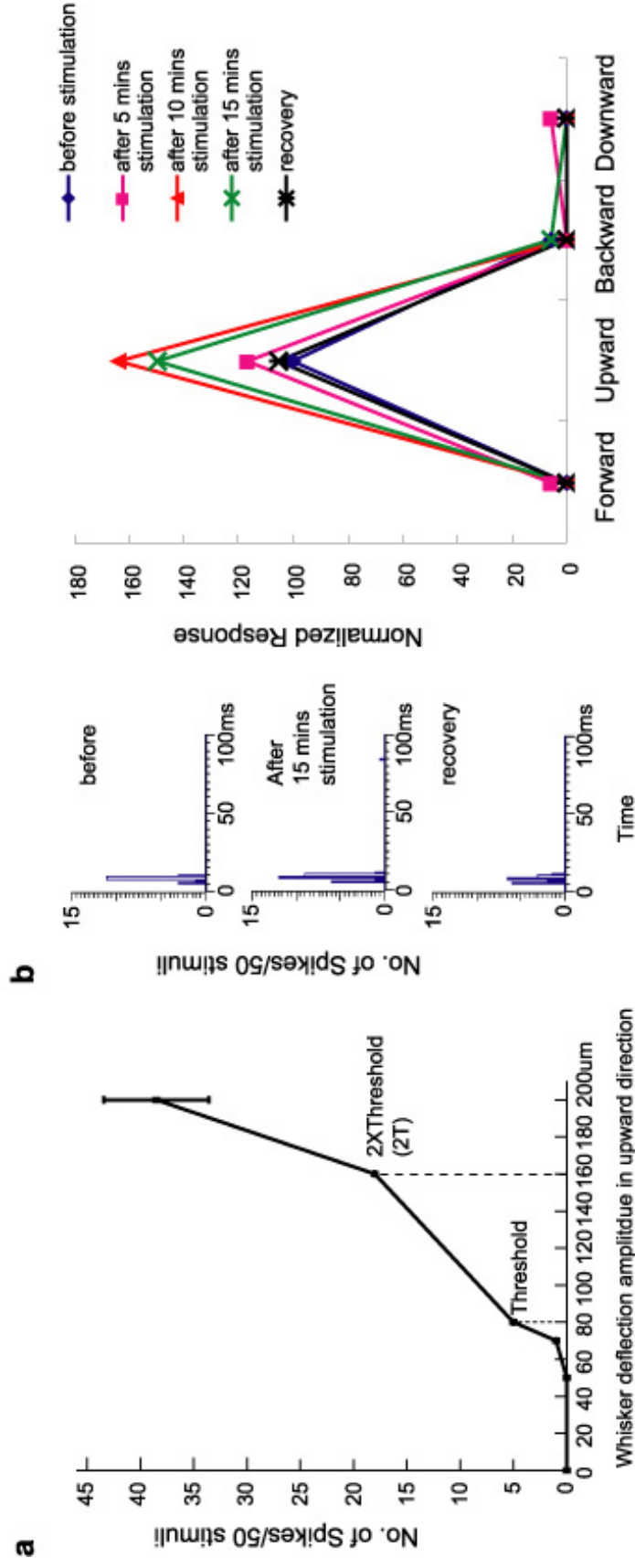


**Figure 4-3. Cortical Stimulation Sharpens the Angular Tuning Curve of Unit VPM12 that is “Both Spatially and Angularly Matched” with Cortex.**

**a.** Plot of stimulus intensity (x axis) against response magnitude (y axis) for unit VPM12 to its preferred direction. The principal whisker is D5. VPM12 responded best to the upward direction of D5 movements with a threshold response at 80 μm. At 2T (160 μm), VPM12 is a typical relay neuron with short response latency (8 ms).

**b.** Left panel: PSTHs of unit VPM12 to its preferred direction before and after cortical stimulation. All data were sampled at 2T (160 μm) to each direction. Top: original response before cortical stimulation. Middle: enhanced response after stimulating layer VI of ipsilateral D5 barrel column for 15 mins. Bottom: recovered response at 30 minutes after the 15 minute stimulation period. Data were averaged from 50 trials.

Right panel: normalized angular tuning curves of unit VPM12. Data were sampled before cortical stimulation (blue line), and after stimulating cortex for 5 mins (pink line), 10 mins (red line) or 15 mins (green line). Cortical stimulation enhanced the response magnitude of unit VPM12 selectively, thus sharpening the tuning curve. The facilitatory effects of cortical stimulation were completely reversible (black line).

showed response enhancement only to the preferred direction. Responses to all other directions increased only slightly, but not significantly. Thus cortical activity selectively enhanced the responsiveness of VPM neurons. The facilitation by cortex was reversible since the response magnitude returned to the pre-stimulation level after a 30 min recovery period (Fig. 4-3b).

Repeated analysis of the angular tuning properties of cortical neurons in animal VPM12 revealed that it was both “spatially and angularly matched” with the cortical site. As shown in Figure 4-4, all 5 cortical neurons sampled in animal VPM12 as the stimulating electrode approached layer VI of the D5 barrel column preferred upward movements of the D5 whisker. These five cortical neurons, most of them were regular spiking units (RSUs), were sampled at the depth of 540, 610, 720, 930 and 1200  $\mu\text{m}$  respectively. We conclude that the stimulating electrode was within one sub-barrel domain, or a directional “minicolumn” (Bruno et al., 2003; Mountcastle, 2003), tuned to upward whisker deflections. Therefore in this case the layer VI neurons stimulated were tuned to the same direction as unit VPM12. After layer VI was stimulated, unit VPM12 greatly increased its response magnitude, as well as its tuning ratio [Tr] (see Experimental Procedures), to test stimuli applied in an upward direction. These results were consistent in the 3 VPM neurons that were both “spatially and angularly matched” with the layer VI neurons stimulated. The data were summarized in Figure 4-5. On average, stimulating cortex for 30 minutes increased the response magnitude (unnormalized) of VPM neurons to the preferred directions by 30%: from 30 spikes/50 stimuli to 39 spikes/50 stimuli ( $p < 0.01$ ), but the average responses to 3

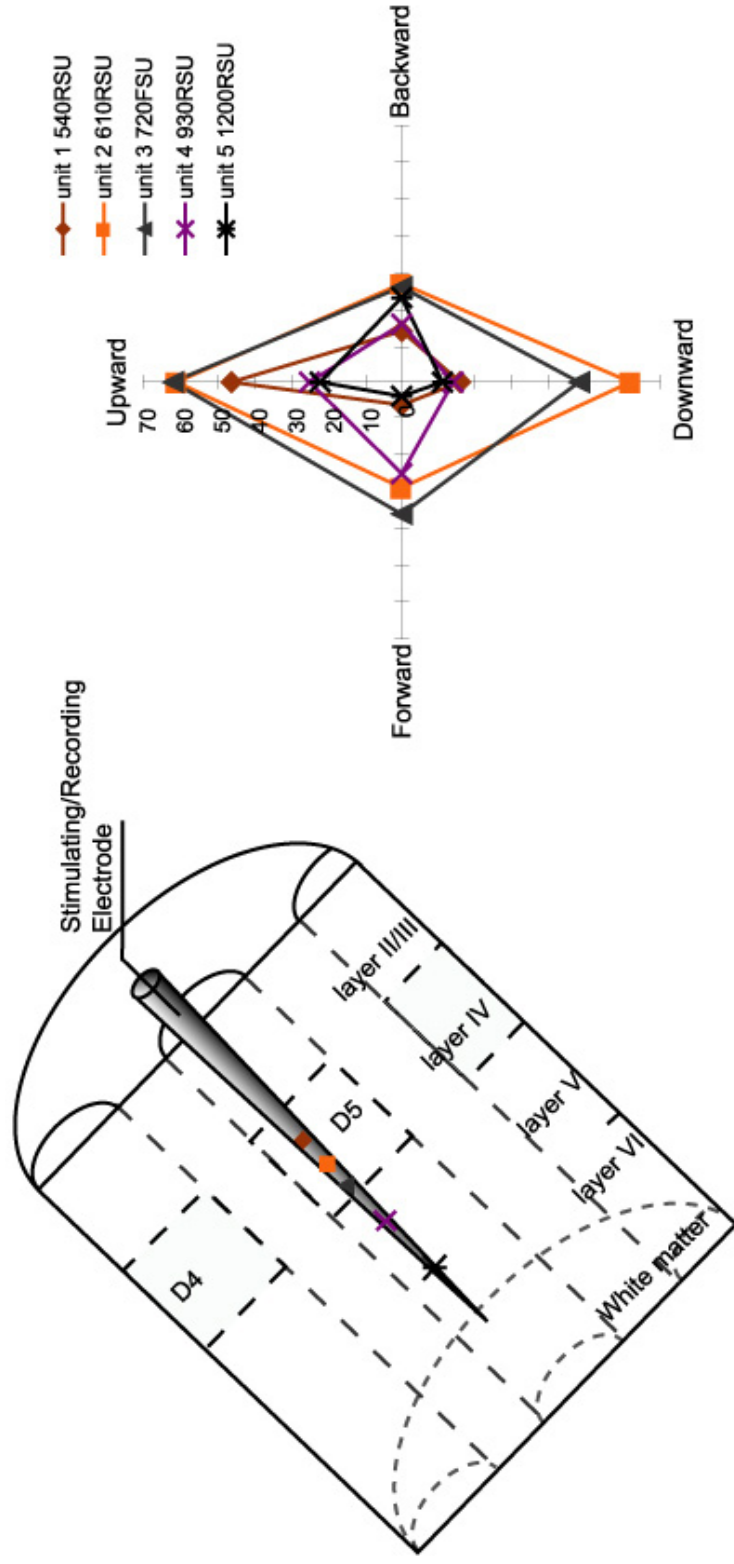


**Figure 4-4. Determination of the Relationship of the Tuning Properties between the VPM Unit12 and the Cortical Units Stimulated.**

Left panel: Schematic drawing to show how the angular preference of unresponsive layer VI neurons was estimated by the tuning features of cortical neurons sampled along the electrode penetration. Symbols are corresponding with those in the right panel.

Right panel: Angular tuning curves of 5 cortical neurons we recorded in animal VPM12 as the recording/stimulating electrode approached layer VI of the ipsilateral D5 barrel column. D5 whisker was deflected with 300  $\mu\text{m}$ , 3ms stimuli (1 per second, 50 in total) 10 mm away from the face. The number of spikes/50 stimuli was plotted against each direction tested. The depth of each unit is indicated. All five cortical neurons preferred the upward direction of whisker movements, thus we concluded that the stimulating electrode was in one “minicolumn” tuned to the upward direction. Thus, unit VPM12 was both “spatially and angularly matched” with cortex. Note that symbols in the right panel correspond with those in the left panel which indicate the depth of each cortical neuron.

“non-preferred” directions was not changed ( $p < 0.45$ ). When normalized data were compared, cortical stimulation increased responses of 3 VPM units to the preferred directions by 22% (100 vs. 122,  $p < 0.0005$ ) (Fig. 4-5b). Furthermore, VPM units became more tuned to their preferred direction (which was also the direction cortex preferred) after cortical stimulation, as reflected in the significant increase in the value of Tr from 2.07 to 2.75 ( $p < 0.03$ ) (Fig. 4-5a). The sharpening effect is clear when the normalized tuning curves from 3 units were aligned by their preferred directions in a clockwise manner (Fig. 4-5b). Thus stimulating layer VI neurons in the homologous barrel column sharpens the angular tuning curves of VPM cells that are angularly matched with cortex. These data indicate that the BFC is capable of modulating the angular tuning preference, and at the same time the response magnitude of the same VPM unit.

For VPM neurons that were in the homologous barreloids, but tuned to different preferred directions of whisker movements from layer VI neurons, stimulating cortical feedback neurons broadened the tuning curves of the VPM neurons. In VPM neurons that were spatially but not angularly matched with cortex, responses to the preferred direction decreased from 36 spikes/50 stimuli to 31 spikes/50 stimuli after cortical stimulation, which is not significant ( $p < 0.06$ ). Interestingly, the average response to the other 3 non-preferred directions was increased significantly from 21 spikes/50 stimuli to 25 spikes/50 stimuli ( $p < 0.03$ ) (Fig. 4-6b). These changes were confirmed after normalization of the data, and comparing pre- and post-stimulation time. Thus, stimulating homologous layer VI neurons had no significant effect on the responses of VPM neurons to their



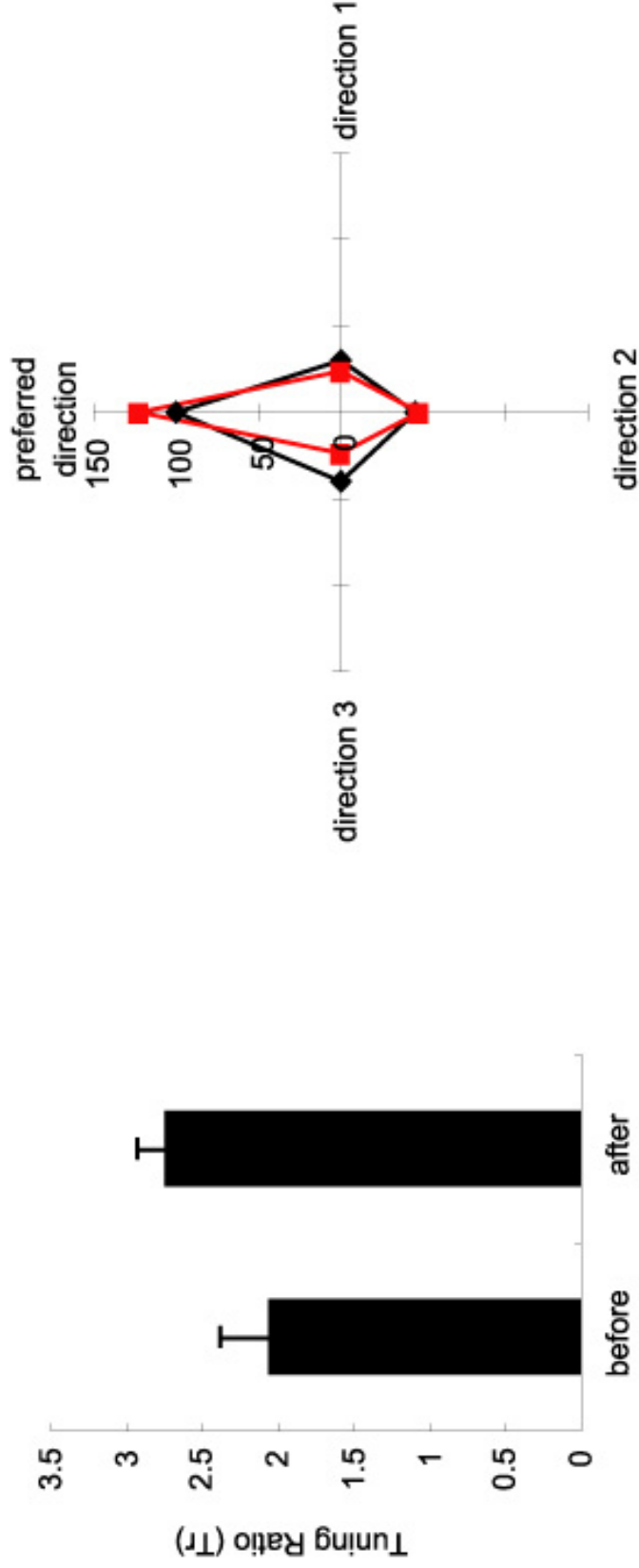


**Figure 4-5. Cortical Stimulation Sharpens the Angular Tuning Curves of “Both Spatially and Angularly Matched” VPM Neurons.**

Left: Comparison of Tuning Ratio (Tr) value of 3 VPM units that were “spatially and angularly matched” with cortex before and after cortical stimulation. The value of Tr increased significantly from 2.07 to 2.75 after cortical stimulation ( $p < 0.03$ ) (\*:  $p < 0.05$ , \*\*:  $p < 0.01$ , Error bar: SEM)

Right: Normalized tuning curves of 3 “spatially and angularly matched” VPM neurons before and after cortical stimulation. Tuning curves were aligned by their preferred directions thus changes in magnitude and tuning features were both visualized. Note that cortical stimulation enhanced the response to the preferred direction resulting in a sharpening effect in the tuning curve.

preferred directions (100 vs. 96,  $p < 0.6$ ), but the averaged response to 3 non-preferred directions were increased significantly from 60 to 75 ( $p < 0.001$ ) (Fig. 4-6c). This increase, as described below, was produced in large part by the augmentation of response level to the direction which the stimulated layer VI neurons were tuned. These changes resulted in a significant reduction of Tr value from 1.62 to 1.23 ( $p < 0.002$ ) after stimulating cortex (Fig. 4-6a). The normalized tuning curves of the VPM neurons were aligned by the preferred directions of these VPM neurons to show the broadening effects of the cortex. In general, cortex weakened the tuning specificity of spatially but not angularly matched VPM neurons (Fig. 4-6c).

Although cortex seems to influence the angular tuning features quite differently in angularly matched or mismatched homologous VPM neurons, in fact the role of cortex remains consistent. That is, cortex always enhanced the responses to the direction that cortex preferred no matter which direction the VPM neuron originally preferred. We compared the responses of the spatially matched VPM neurons to the direction which cortex preferred before and after cortical stimulation. The response magnitude increased significantly from 17 spikes/50 stimuli to 28 spikes/50 stimuli ( $p < 0.0001$ ) (Fig. 4-7b). Augmentation of the response to the direction which cortex preferred were also found in normalized data (56 vs. 93,  $p < 7.2 \times 10^{-5}$ ) (Fig. 4-7c). Accordingly, the tuning ratio calculated by the direction which cortex preferred (denoted as Tuning Ratio Prime [Tr'], see Experimental Procedures for details), almost doubled from 1.09 to 1.85 ( $p < 0.0001$ ) after cortical stimulation (Fig. 4-7a), indicating that VPM

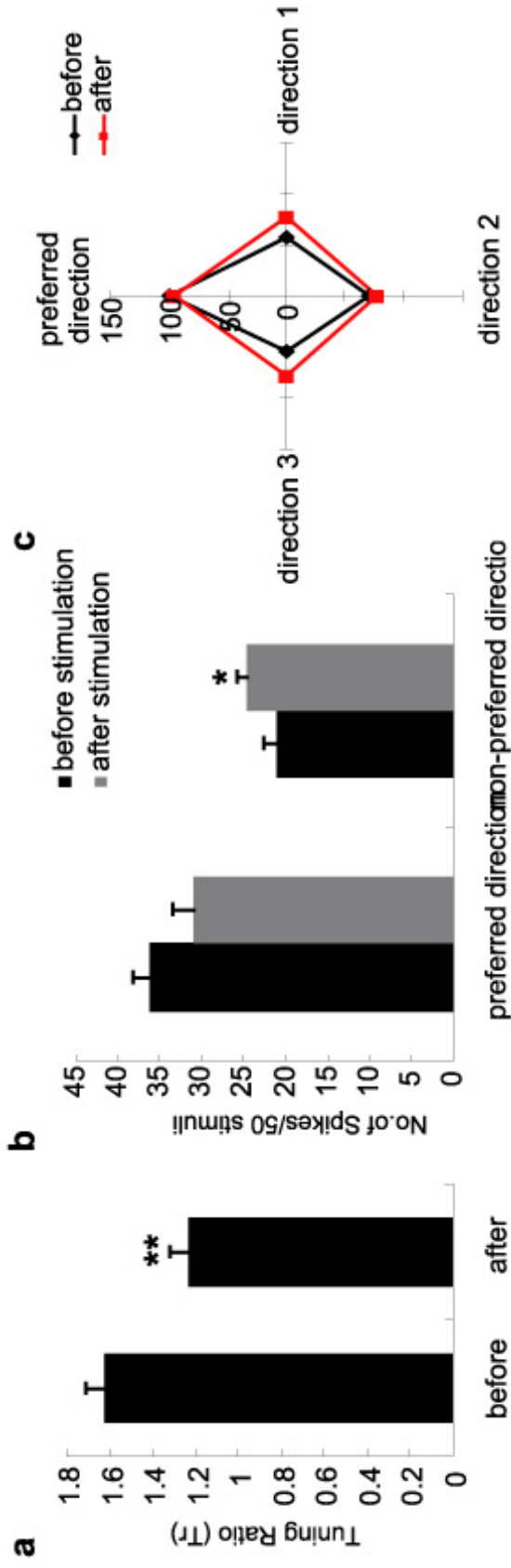


**Figure 4-6. Cortical Stimulation Boardens the Angular Tuning Curves of VPM Neurons that are “Spatially but not Angularly Matched” with Cortex.**

- Comparison of Tuning Ratio (Tr) value of 12 VPM neurons that were “spatially but not angularly matched” with cortex before and after cortical stimulation. Cortical stimulation significantly decreased Tr value from 1.62 to 1.23 ( $p < 0.002$ ). (\*:  $p < 0.05$ , \*\*:  $p < 0.01$ , Error bar: SEM)
- Comparison of the response magnitude of 12 VPM neurons that were “spatially but not angularly matched” with cortex before and after cortical stimulation. Data shown were prior to normalization. Stimulating cortex decreased the response magnitude slightly but not significantly toward the direction that VPM neurons originally preferred (36 vs. 31 spikes/50 stimuli,  $p < 0.06$ ). However, average response magnitude to the non-preferred directions increased significantly (21 vs. 25 spikes/50 stimuli,  $p < 0.03$ ). As shown in Fig. 4-7c, this increase was mainly due to the response augmentation to the direction that cortex preferred.
- Normalized tuning curves of 12 “spatially but not angularly matched” VPM neurons aligned by the direction that VPM neurons were originally tuned. Note the broadening effect of cortical stimulation.

neurons developed a new preferred direction, which is the preferred direction of cortical neurons stimulated. The normalized tuning curves after alignment were displayed in Figure 4-7c. The results further suggest that cortical stimulation actually redirects the angular preference of VPM neurons towards the direction that cortical neurons are tuned, no matter which direction the VPM neurons originally preferred. Thus, cortex could actively shift the angular tuning preference of the thalamic relay neurons towards the direction “preferred” by cortex.

Evidence is emerging that each barrel column in BFC may have a full set of angular tuning domains (Bruno et al., 2003; Andermann and Moore, unpublished), raising the question of how two sub-barrel structures, which are tuned to the same direction of whisker movement but located in different barrel columns, are functionally integrated with each other. We investigated this issue by comparing the angular tuning preference of VPM neurons before and after stimulating layer VI of an immediately adjacent barrel column. When the stimulating electrode was in an immediately adjacent barrel column, activating layer VI confirmed that the responses of VPM neurons to their principal whisker test stimuli were clearly suppressed. After applying the stimulation procedure, VPM neurons decreased their responses to the preferred direction significantly from 38 spikes/50 stimuli to 21 spikes/50 stimuli ( $p < 0.004$ ). The responses to 3 non-preferred directions were slightly reduced from 15 spikes/50 stimuli to 12 spikes/50 stimuli, but not significantly ( $p < 0.19$ ) (Fig. 4-8b). Thus, stimulating layer VI of a non-homologous barrel column produced a purely suppressive effect on

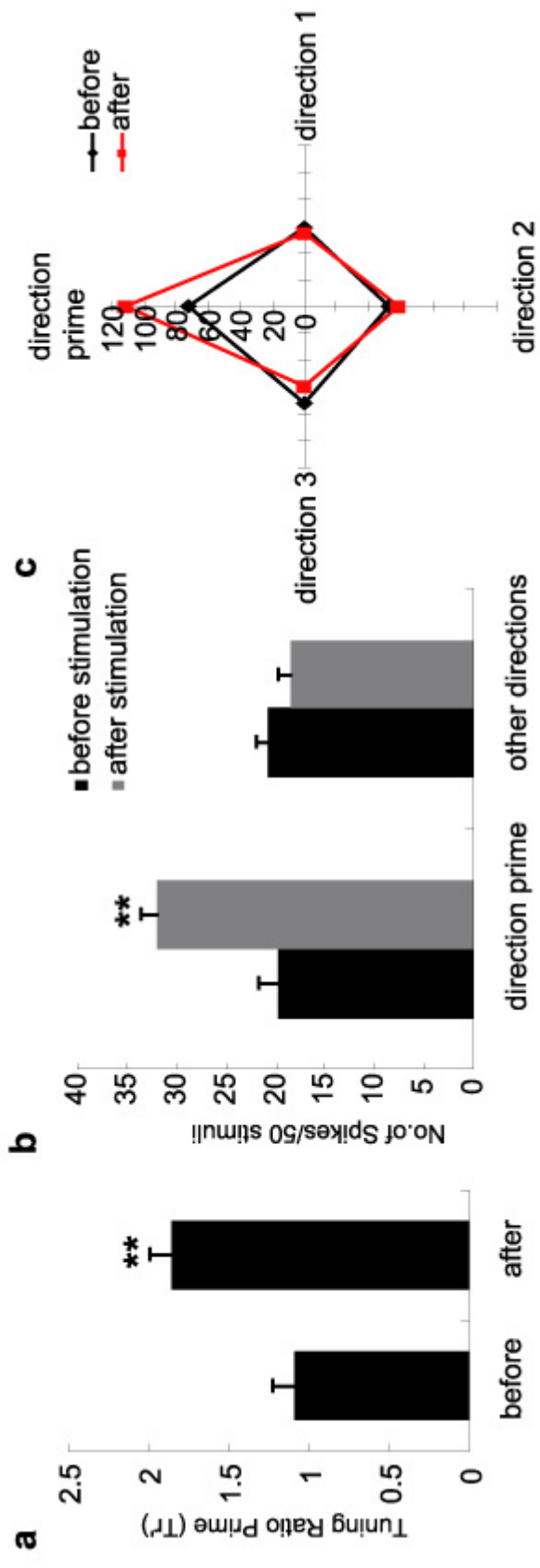


**Figure 4-7. Cortical Stimulation Shifts the Angular Tuning Preference of VPM Neurons towards the Direction Cortex Prefers.**

- a. Comparison of Tuning Ratio prime ( $Tr$ ) of 12 VPM neurons before and after cortical stimulation. Cortical stimulation significantly increased  $Tr$  value from 1.09 to 1.85 ( $p < 0.0001$ ).
- b. Comparison of the response magnitude of 12 VPM neurons before and after cortical stimulation. Data were plotted without normalization. Stimulating cortex significantly increased the response magnitude to the direction that cortex preferred (17 vs. 28 spikes/50 stimuli,  $p < 0.0001$ ). However, average response magnitude to other directions remained unchanged (19 vs. 19 spikes/50 stimuli,  $p < 0.11$ ).
- c. Normalized tuning curves of 12 VPM neurons aligned by the direction prime (the direction cortex preferred). Note the “re-directing” effect by cortical stimulation.

VPM neurons, with a significant decrease of the average response to the 4 directions tested (22 spikes/50 stimuli vs. 14 spikes/50 stimuli,  $p < 0.03$ , data not shown). The tuning specificity of VPM neurons appeared less influenced by non-homologous cortical inputs. The value of  $Tr$  showed some decrease from 1.96 to 1.62 after stimulation, but didn't reach significance ( $p < 0.24$ ) (Fig. 4-8a). The suppressive effect of stimulating the non-homologous barrel column on VPM neurons was clear after the tuning curves of 6 VPM neurons were aligned by their own preferred directions (Fig. 4-8c). Although all 6 units were angularly mismatched with cortex, cortical stimulation didn't shift the angular tuning curves of VPM units. We also calculated the  $Tr'$  for these neurons,  $Tr'$  did increase from 0.83 to 1.64 after stimulation, but the increase is not significant ( $p < 0.09$ ) (Fig. 4-9a). After cortical stimulation, the response of VPM neurons to the direction that cortex preferred were less influenced (21 vs. 19 spikes/50 stimuli,  $p < 0.41$ ), while the responses to other 3 directions were reduced significantly (26 vs. 14 spikes/50 stimuli,  $p < 0.01$ ) (Fig. 4-9b). However, cortex appeared unable to redirect the tuning curves of non-homologous VPM neurons (Fig. 4-9c). In general, enhancing the feedback from the immediate adjacent barrel columns only produced a pure suppression on VPM neuronal response. No consistent, significant differences could be identified in the response changes of these 6 VPM units.

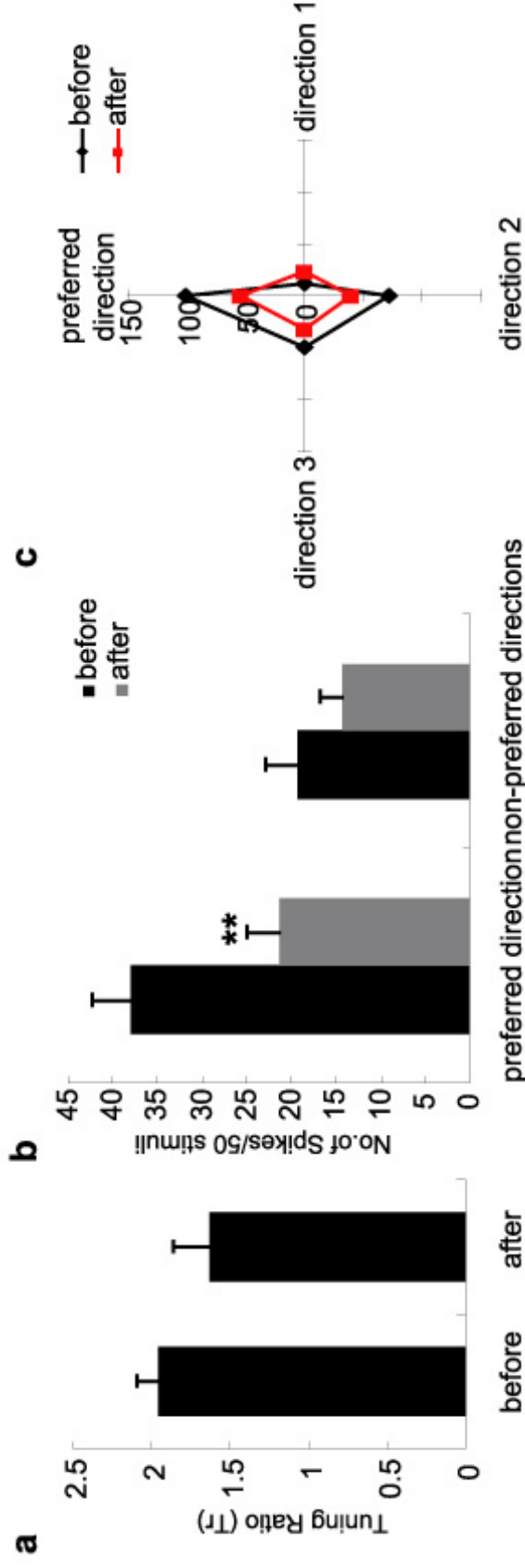


**Figure 4-8. Cortical Microstimulation Reduces the Responses of “Spatially Mismatched” VPM Neurons but Has No Apparent Influence on Angular Tuning.**

- Comparison of Tuning Ratio (Tr) value of 6 VPM neurons that were “spatially mismatched” with cortex before and after cortical stimulation. Cortical stimulation slightly decreased Tr value from 1.96 to 1.62, but not significantly ( $p < 0.12$ ).
- Comparison of the response magnitude of 6 VPM neurons that were “spatially mismatched” with cortex before and after cortical stimulation. Stimulating cortex significantly decreased the response magnitude to the direction that VPM neurons originally preferred (38 vs. 19 spikes/50 stimuli,  $p < 0.004$ ). However, average response magnitude to the non-preferred directions failed to show a significant change (19 vs. 14 spikes/50 stimuli,  $p < 0.12$ ).
- Normalized tuning curves of 6 “spatially mismatched” VPM neurons aligned by their preferred directions. Note the suppressing effect on response magnitude.

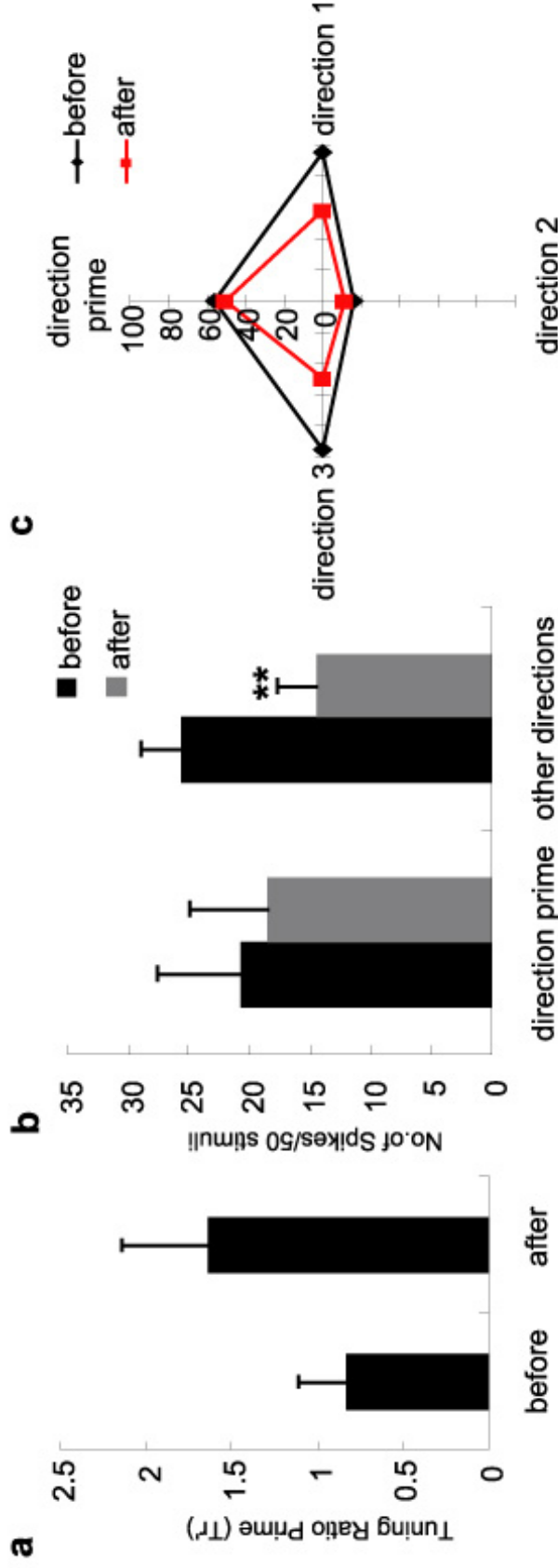


**Figure 4-9. Cortical Microstimulation Has No Consistent Effects on Tuning Ratio Prime (Tr').**

- Comparison of Tuning Ratio prime (Tr') value of 6 "spatially mismatched" VPM neurons before and after cortical stimulation. Cortical stimulation increased Tr' value from 0.83 to 1.63, but not significantly ( $p < 0.09$ ).
- Comparison of the response magnitude of 6 VPM neurons before and after cortical stimulation. Stimulating cortex decreased the response magnitude to the direction that cortex preferred slightly (21 vs. 19 spikes/50 stimuli,  $p < 0.41$ ). However, average response magnitude to other 3 directions decreased significantly (26 vs. 14 spikes/50 stimuli,  $p < 0.01$ ).
- Normalized tuning curves of 6 VPM neurons aligned by the direction prime (the direction cortex preferred). No "re-directing" effect by cortical stimulation was detected.



## Discussion

The most important insight derived from these results is that an increase of cortical feedback from layer VI neurons in barrel columns profoundly influences the directional bias in thalamic relay neurons. These findings add a new dimension to our understanding of the way that cortex adjusts sensory transmission properties through thalamic relay neurons. A testable hypothesis is that these cortical influences are used to optimize feature detection. Our data demonstrate that active cortical feedback from BFC is accurate enough to selectively enhance the response of single VPM neurons in one specific parameter of sensory coding. Selective increases in cortical feedback augments the response magnitude of homologous VPM neurons that are angularly matched with cortex, indicating that cortical feedback regulates the information transfer of whisker stimuli in the direction which cortex prefers. Furthermore, analysis of  $Tr'$  indicates that the modulation of angular tuning by cortical feedback selectively facilitates the response magnitude to the preferred direction of cortical neurons. The redirection effect by cortex is linked to the period of stimulation, indicating that cortex is capable of allocating more thalamic relay neurons to represent incoming information in the direction that cortex dictates, which could result in an increase of the processing power for this feature of whisker engagement. Cortical reallocation of directional preference appears to be restricted to homologous VPM neurons, since focally increasing cortical feedback to the adjacent non-homologous barrel columns has a clearly different (suppressive) influence, and fails to show consistent “re-directing” of VPM tuning:

the corticothalamic correspondence ( $Tr'$ ) increased after the stimulation procedure, but not significantly. Hence both the whisker map and direction preference map in thalamus are actually regulated by cortex simultaneously so that both maps could coordinate in harmony. But the cortical modulation of the direction tuning map appears to operate only on those VPM neurons that are in “matched” barreloids, which indicates that under urethane anesthesia angular tuning is not linked in different barrel columns. The results suggest that computation of angular information of whisker movements may be restricted to the homologous barreloid-barrel circuit, since under our recording conditions there was no regulation from one barrel column to non-homologous barreloids. The weak crosstalk between angular tuning sub-barrel structures in different barrel columns could be due to the limited sample size. However, unlike the highly consistent data from the 3 both “spatially and angularly matched” VPM units, examining 6 “spatially and angularly non-matched” units didn’t show an inter-unit consistency. Responses to surround whiskers are strongly influenced by intracortical connections (Armstrong-James et al., 1991; Fox et al., 2003), thus details of angular information transferred between barrel columns may be suppressed under urethane anesthesia.

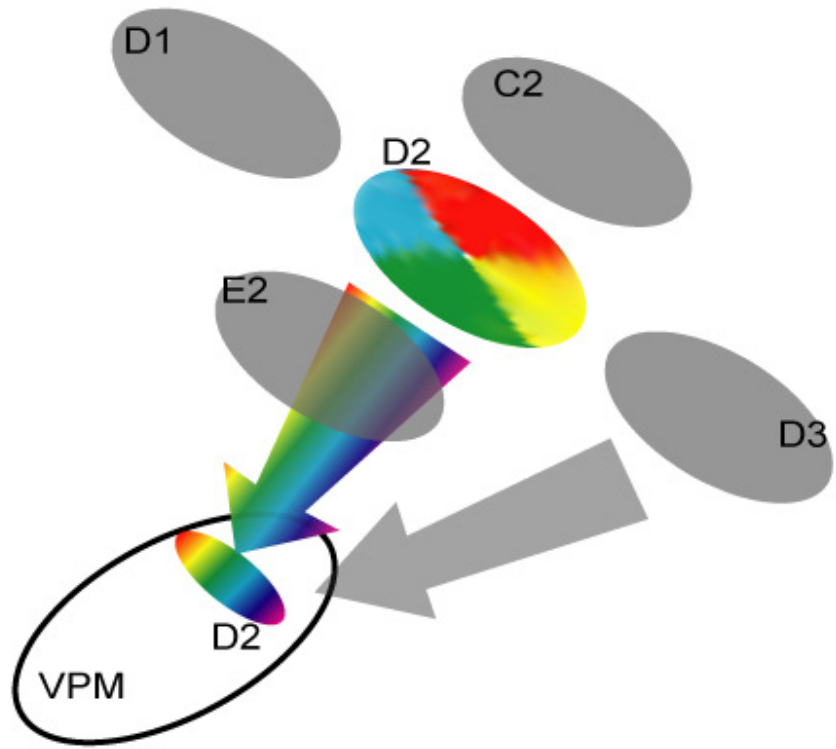
Trains of electrical stimuli in cortex activate a population of neurons within a certain radius from the tip of the stimulating electrode, so feedback neurons with different angular tuning properties (different preferred directions) could be activated simultaneously under our conditions. From our preliminary studies to detect the horizontal spread of activation in layer VIa during 30 mins stimulation,

it is clear that the activating effect on feedback neurons by the electrical stimulation procedure is dependent on the distance from the electrode tip and the decay time. The number of angular tuning sub-barrel structures activated is hard to determine, since the actual size and arrangement of these sub-barrel domains, or “minicolumns”, is still controversial (Bruno et al., 2003; Andermann and Moore, unpublished). From our literature review, we speculate that feedback neurons within more than one angular tuning sub-barrel domain will be activated, which implies that the results we recorded in VPM neurons actually could be a mixture of effects by activating neurons from several angular tuning sub-barrel structures nearby (e.g. as in Fig. 4-3). However, neurons close to the electrode tip would be expected to be most affected and we interpret proximity as the major variable causing the shifts in the angular tuning curves of VPM neurons. Cortical neurons along the vertical axis (i.e. deeper layer V neurons above and layer VIb neurons below the stimulating site) can also have been activated, but we consider that layer V activation can only be very limited, for the following reasons: first, layer V neurons never project directly to VPM, nor send collaterals to the thalamic reticular nuclei (RTN) (Deschenes et al., 1998); second, lesioning corticobulbar projections didn't appear to alter the cortical modulation of receptive field properties of VPM neurons, although a relatively larger activating zone occurs after releasing bicuculline at 1500  $\mu\text{m}$  (Temereanca and Simons, 2004). It is also possible that VPM neurons could have been antidromically activated by the electrical stimulation in cortex, especially when the stimulating electrode was in the homologous barrel columns, although no changes in spontaneous discharge

were detected in VPM neurons when we recorded immediately after the stimulating procedure. In any case, the antidromic activation could NOT explain the obvious difference in results between spatially-and-angularly-matched group and spatially-matched-but-angularly-mismatched group, where VPM neurons would have been equally activated antidromically. We also realize that our experiment design is not optimized for detecting linkages between minicolumns in different barrel columns. Studies using other paradigms such as conditioning-test stimuli in awake animals may be able to address this question. Other studies have shown that neurons in the primary sensory cortices are influenced by higher order cortical areas as well, unfortunately, the interactions between BFC and other cortical areas, such as SII and MI, still remains to be clarified in regard to their effect on VPM and POm nuclei.

Our data demonstrate an exact influence of BFC on VPM neurons that is largely dependent on whether the VPM neurons share the same properties. Cortical feedback modulates receptive field properties of VPM neurons in either homologous barreloids or adjacent barreloids, but modulates both receptive field and angular tuning properties only in homologous VPM neurons. The apparent distinction leads to our model of how VPM neurons are influenced by cortex, as shown in Figure 4-10. We propose that two general channels exist in the corticothalamic feedback

**a**



**b**

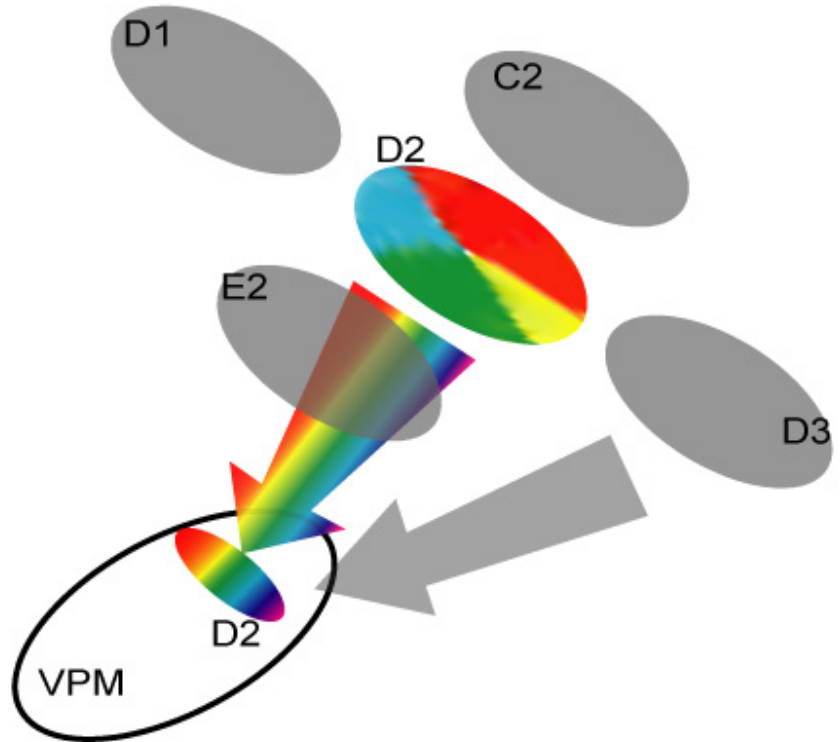


**Figure 4-10. A Model for Cortical Modulation of Tuning Properties of VPM Neurons.**

- a.** In the normal adult rat brain, BFC projects extensively back to VPM. Yet for neurons in one certain barreloid, for example, D2 barreloid, the feedback of the homologous barrel column (D2) is functionally distinct from that of the non-homologous barrel columns (C2/D3/E2/D1). Feedback from the adjacent barrel columns produce a predominantly suppressive influence (gray), while D2 barrel column generally facilitate the response of D2 barreloid cells to D2 whisker stimulations (colorful). The data demonstrate that even the feedback from the homologous barrel columns is not functionally homogeneous. Hence two general channels appear to exist in the corticothalamic feedback system. One channel, which is the specific channel, is from the homologous barrel column to the barreloid. In this channel the cortical feedback is able to facilitate the response to the D2 whisker and regulate the direction preference of D2 whisker movements. The other channel, which is the non-specific channel, consists of the feedback outside the homologous barrel column, probably mainly from the immediately adjacent barrel columns. The non-specific channel doesn't have consistent influence on angular tuning but only produces a suppressive effect. The two channels work seamlessly together in the active brain, which constantly re-allocates neural resources to the most behaviorally repetitious stimulus features.
- b.** When the cortical feedback for a certain stimulus is augmented, for example, the feedback to the whisker movements in upward direction increased (enlarged red sector in D2 barrel), the angular tuning map in the corresponding (D2) barreloid would be shifted using the specific channel in a way that expands the area representing the upward stimulus (shifted spectrum in D2 barreloid). In this way more neural resources could be allocated to process the information of the upward whisker movement. At the same time, feedback from the D2 barrel would also cause a suppressive effect on the surround barreloids through the non-specific channel so the response contrast to D2 whisker movements would be increased. One use of this mechanism would be for specific and non-specific feedback channels to optimize the detection of novel features.

system. One channel consists of the feedback projections from homologous barrel column to one barreloid, where the feedback exerts quite specific and detailed influences on thalamic relay neurons, capable of operating on a certain value of one stimulus parameter (i.e., the direction of whisker movements); another channel is from the feedback outside the homologous barrel column, probably only from the immediately adjacent barrel columns, where the cortical influence is non-specific, producing only a suppressive effect. The two channels work seamlessly together in the active brain, which constantly re-allocates neural resources to the most behaviorally important stimulus features. Previously we showed that suppressing cortical feedback elevated the response threshold of VPM neurons, resulting in a shift to the right in the thalamic cell response curve. Here we demonstrated the opposite effect on the response curves of VPM neurons after enhancing the cortical feedback selectively. Thus, we speculate that cortex may regulate the responsiveness of thalamic relay neurons by modulating their firing threshold. Studies focusing on the metabotropic glutamate receptors and other inputs to VPM will help to understand the exact molecular mechanisms for threshold adjusting.

Recent studies in auditory, somatosensory and visual systems in bats, cats, rats and monkeys have found that neocortex is capable of modulating the transmission mode, synchronization, tuning properties and/or the balance of center/surround of the receptive field of thalamic relay neurons (Sillito and Jones, 2002; Sherman and Guillery, 2002; Suga and Ma, 2003; Suga et al., 2003). The relationship of tuning between thalamic neurons recorded and cortical neuron

manipulated, has gained support from studies in the auditory system where cortex has been shown clearly to move subcortical cell responses toward the best frequency of the cortical locus stimulated (Suga and Ma, 2003). Similarly, in rat whisker system, data from several labs suggested that cortical influence on thalamic relay neurons could take several forms (Diamond et al., 1992b; Krupa et al., 1999; Temereanca and Simons, 2004; Yuan et al., 1985; 1986), especially in shifting the center/surround contrast of RF map in clustered VPM neurons (Temereanca and Simons, 2004). Our results also support the idea that cortical feedback profoundly influences the directional preference of thalamic relay neurons. They also indicate that the tuning curves of thalamic relay neurons are generated from the ascending sensory inputs and refined continually by the cortical feedback. Cortex could attentively optimize the sensory pathway for feature detection. The next steps will focus on the synaptic/molecular mechanisms that permit the adult brain to maintain and revise computational maps at each level along the sensory pathway according to experience.



## CHAPTER V

### **SUMMARY AND PROSPECT: ROLE OF SPIKE-TIMING-DEPENDENT PLASTICITY IN THE ACTIVE MODULATION OF TUNING PROPERTIES OF THALAMIC RELAY NEURONS BY BARREL FIELD CORTEX IN RATS**

Experiments presented in the preceding chapters lead to a deeper view of how thalamic responses are dynamically modulated by the feedback from corresponding cortical areas. Beginning with the interaction between the bilateral integration and corticothalamic feedback, studies in this thesis demonstrated that the ipsilateral corticothalamic feedback pathway is influenced indirectly by contralateral, as well as ipsilateral cortical areas, that project to primary sensory cortex. The influence can act through mechanisms that regulate the response threshold of thalamic relay neurons to test stimuli. And we advanced our understanding of the corticothalamic system further by showing that cortical modulation could operate precisely on one specific parameter: the angular tuning map, in a way caters to the preference of cortex. These effects could result in a magnifying/minifying effect on the tuning maps by temporarily and reversibly increasing or decreasing the sensitivity to certain stimuli or enlarging/shrinking the information representation area in the thalamus.

## **Implications of Response Threshold on Neural Coding Strategies: Information Transmission Fidelity**

It is a general belief that neural information is encoded by spike trains in nervous systems. Thus the central issue of neural information processing is the coding strategies employed by single neurons and populations of neurons. Although a detailed knowledge of specific neural codes is still fragmentary, available data identify two major categories of neural coding methods: rate coding and temporal coding. Rate coding simply states that information is encoded by the number of spikes per stimulus per unit time, while temporal coding emphasizes that the temporal structure, or the timing of neural discharge (inter-spike interval), is important. Obviously when the unit time used in rate coding approaches zero, the rate coding becomes indistinguishable from temporal coding. Both types of coding are both used in the real brain.

Due to the fluctuation of membrane potential caused by local and distant inputs, it is impossible for information to be transferred between neurons, or populations of neurons, without any modifications. In fact, information needs to be filtered and integrated for various purposes, which implies that the spiking pattern (the output) of one neuron does not necessarily replicate that of its strongest inputs. Hence a feasible coding strategy has to simultaneously satisfy both the transmission efficiency and transmission fidelity. In this thesis, we touched on this issue by examining the dynamic transformation of neural inputs to outputs of sensory neurons in rat's vibrissa system at single neuron level, where the question could be simplified to investigating the stimulus-response curve of the neuron.

As shown in Figure 3-2, the response curves are always sigmoidal in shape and the slope near threshold is steep. The response threshold can be defined along the stimulus-response curve, above which the neuron would discharge significantly more than background. Here we showed that the responding features and the possible coding strategies the neurons could use have profound influences on the information transmission and processing in sensory systems.

### **Implications of Response Threshold on Rate Coding: Response Saturation**

In rat's vibrissa system, as the response magnitude was plotted against the stimulus intensity, we noticed that the response magnitude increases as the stimulus intensity increases only when the stimulus intensity is within the dynamic range between the threshold and maximum response (Armstrong-James and Fox, 1987; Gibson and Welker, 1983a; Li and Ebner, 2006, also see Fig. 3-2, 3-3). If the stimulus intensity is well above the dynamic range, i.e., the stimulus is "supramaximal", the responses of the sensory neuron will not increase even though the stimulus continue to increase. In other words, the response will be saturated by high-intensity stimuli. The response saturation eliminates the difference of neural representation between stimuli. Thus for neurons with rate-coding, information can only be encoded and propagated with proper meaning when the stimulus is within the dynamic intermediate range, which is somewhere above, but near the response threshold. For VPM neurons that may use temporal coding, supra-maximal stimuli drive them with constant

latency, which would greatly increase response synchrony in thalamus, and provide powerful inputs to both excitatory and inhibitory circuitries in BFC. However, one should also notice that the abnormally strong drive may result in disturbance in the continual excitatory/inhibitory balance in the cortical network, which may alter the efficiency of neural information processing. On the other hand, the test stimuli should have relevance to natural stimuli encountered by a rat. Previous studies usually employed stimuli that deflected whiskers tremendously (e.g., ramp-and-hold stimuli deflecting whiskers by more than 1mm and air-puff stimuli often move a whisker by 2-4mm). These stimuli produce reliable maximal responses at saturation level but may not facilitate the study of subtle events. Our results support the idea that studies on cortical excitability should select stimulus parameters relevant to the experimental goal, since subtle thalamic and cortical responses could depend on the stimulus configuration used to test the system. If the level of the test stimuli was too high or too low the target neuron could be saturated or under-driven by the whisker stimulation as a result of excitability changing during the experiment.

### **Implications of Response Threshold on Rate Coding: the Preferential Range**

Fig. 3-2 and 3-3 also show that the most dramatic phase of the response curves is around the response threshold. The steep slope of the response curve around the threshold indicates that it is the “sensitive” area of the responsiveness since even the smallest change in the stimulus intensity will introduce considerable change in neuronal firing. Furthermore, from the response curves, it

can also be seen that different stimuli can be greatly distinguished by the response magnitude only when the stimuli are within the intermediate range. Thus for neurons using rate-coding, only information within the intermediate range can be encoded efficiently, hence this range is actually the “preferential range” or “favorite range” of the sensory neuron. The existence of the preferential range determines that the stimulus we selected to detect the mechanisms for neural systems should be within the favorite range of neurons, which are relevant or comparable to the natural stimuli.

### **Implications of Response Threshold for Temporal Coding: Temporal Signature of Responses**

Neural information can be encoded by spike rate (rate coding) or temporal structure of the response (inter-spike interval, or temporal coding). For neurons that encode information with temporal coding, difference between stimuli is encrypted by the temporal structure of responses. Thus the temporal structure of responses acts as the “signature” of different stimuli. Figure 3-3 compares the PSTHs of VPM neurons in response to stimuli at various intensities. It is clear that as the intensity decreases, VPM neurons fire fewer spikes with longer response modal latency, and these spikes are scattered in the PSTH, which could lead to a decrease of firing synchrony between VPM neurons. The loss of firing synchrony in thalamus could result in a response decrease of those cortical neurons that require synchronized inputs from the thalamus. Thus scattered responses may compromise the co-incidence detecting in cortex for whisker stimuli. Furthermore, the scattering of spiking along the time axis in PSTHs

indicates responses to different stimuli may lose their temporal signature, such as when the angular tuning is mismatched between thalamic and cortical neurons.

### **Possible Mechanism for the Active Selection of Incoming Information by Cortex**

In Chapter IV we demonstrated that barrel field cortex could actively modulate the angular tuning curves of thalamic relay neurons in the homologous barreloid towards the direction that cortical neurons are tuned to. Our data also showed that whether the stimuli were within the preferential range might have substantial impact on the information transmission and processing in sensory systems. However, to explain the attentive selection in the functioning brain, mechanisms operating on a much shorter time-scale still need to be defined. One possible candidate is spike-timing-dependent plasticity (STDP) (for review, Abbott and Nelson, 2000; Bi and Poo, 2001; Bi and Rubin, 2005).

Based on Hebb's postulate (Hebb, 1949), modification of synaptic efficacy by correlated neural activity is a possible substrate for adaptive cognitive functions such as learning and memory. Elegant studies have elucidated that the brain adjusts its structure and functions according to experience, and long-term potentiation/depression (LTP/LTD) (Bliss and Lomo, 1973) has been proposed as the driving mechanism for activity-dependent synaptic changes (Bienenstock et al., 1982; Lisman, 1989). However, the timing of the pre- and postsynaptic spikes, as originally outlined in Hebb's postulate, is also important to the induction of synaptic plasticity (Hawkins et al., 1983; Levy and Steward, 1983;

Walters and Byrne, 1983). This feature, captured by the spike-timing-dependent plasticity (STDP) (Markram et al., 1997; Magee and Johnson, 1997), is functionally important in learning and memory (for review, Abbott and Nelson, 2000; Bi and Poo, 2001; Bi and Rubin, 2005). STDP has been studied in cortex (layer II/III, IV and V) (Egger et al., 1999; Feldman et al., 2000) and hippocampus (Markram et al., 1997; Magee and Johnson, 1997) of various species in vivo and in vitro. Since neocortex deals with continuous information flow, more localized and dynamic mechanism(s) underlying the “attentive” selection of the most relevant ongoing information needs to be clarified. The close-in-time interaction between cortex and thalamus suggests that these modulations may depend on STDP, since the reciprocity of CT projections indicates that cortical regulation is precise. CT “feedback” has been shown to actively enhance the contrast of thalamic relay cells (Cudeiro and Sillito 1996; Przybylski et al., 2000; Sillito and Jones 1997; Sillito et al. 1993). Thus it is necessary to specify whether STDP is one possible mechanism for cortex to continuously “re-focus” on the most behaviorally important “hot spot”. Unfortunately, convincing data has not appeared.

Our data showed that in the rat’s vibrissa system BFC regulated both the RF and angular tuning properties of VPM neurons simultaneously. It is our particular interest to examine the synaptic and subcellular mechanisms that underlie the cortical selection of the incoming messages from subcortical levels with corticothalamic feedback. Both in vivo and in vitro approaches will be adopted. In in vitro experiments, stimulations to the layer VI of either the

homologous or nonhomologous barrel columns by current injection or laser scanning photostimulation could be closely coupled with the test stimuli. Calcium/optical Imaging and extra/intracellular recording could be carried out in VPM in vitro. In vivo experiments will also be carried out to test whether small changes in the timing of layer VI stimulations relative to stimulations of the principal whisker will facilitate or depress responses in thalamic relay neurons. The fundamental question, how the cortex could continuously “refocus” to the most behaviorally important “hotspot” within the neuronal representation of the outer world, could be addressed. Furthermore, since the synaptic efficacy in thalamocortical and corticothalamic pathways is under the influence of many modulators, the role of various neurotransmitter systems in the active modulation of STDP in thalamic relay neurons by cortex, could be studied. These are important future questions.



## REFERENCES

- Abbott LF and Nelson SB. Synaptic plasticity: taming the beast. *Nat Neurosci* 3: 1178-1183, 2000.
- Ahissar E. Temporal-Code to Rate-Code Conversion by Neuronal Phase-Locked Loops. *Neural Comput* 10: 597-650, 1998.
- Ahissar E, Sosnik R and Haidarliu S. Transformation from temporal to rate coding in a somatosensory thalamocortical pathway. *Nature* 406: 302-306, 2000.
- Ahissar E and Kleinfeld D. Closed-loop Neuronal Computations: Focus on Vibrissa Somatosensation in Rat. *Cereb Cortex* 13: 53-62, 2003.
- Akers R.M. and Killackey H.P. Organization of corticocortical connections in the parietal cortex of the rat. *J Comp Neurol* 181: 513-517, 1978.
- Aldes LD and Boone TB. Organization of projections from the principal sensory trigeminal nucleus to the hypoglossal nucleus in the rat: an experimental light and electron microscopic study with axonal tracer techniques. *Exp Brain Res* 59: 16-29, 1985.
- Alitto HJ and Usrey WM. Corticothalamic feedback and sensory processing. *Curr Opin Neurobiol* 13: 440-445, 2003.
- Alloway KD, Hoffer ZS and Hoover JE. Quantitative comparisons of corticothalamic topography within the ventrobasal complex and the posterior nucleus of the rodent thalamus. *Brain Research* 968: 54-68, 2003.
- Andersen P, Junge K and Sveen O. Cortico-fugal facilitation of thalamic transmission. *Brain Behav Evol* 6: 170-184, 1972.
- Armstrong-James M and George MJ. Bilateral receptive fields of cells in rat Sm1 cortex. *Exp Brain Res* 70: 155-165, 1988.
- Armstrong-James M, Fox K and Das-Gupta A. Flow of excitation within rat barrel cortex on striking a single vibrissa. *J Neurophysiol* 68: 1345-1358, 1992.
- Armstrong-James M, Welker E and Callahan CA. The contribution of NMDA and non-NMDA receptors to fast and slow transmission of sensory information in the rat SI barrel cortex. *J Neurosci* 13: 2149-2160, 1993.
- Armstrong-James M, Diamond ME and Ebner FF. An innocuous bias in whisker use in adult rats modifies receptive fields of barrel cortex neurons. *J Neurosci* 14: 6978-6991, 1994.

- Armstrong-James M and Millar J. Carbon fibre microelectrodes. *J Neurosci Methods* 1: 279-287, 1979.
- Armstrong-James M, Fox K and Millar J. A method for etching the tips of carbon fibre microelectrodes. *J Neurosci Methods* 2: 431-432, 1980.
- Armstrong-James M and Fox K. Spatiotemporal convergence and divergence in the rat S1 "barrel" cortex. *J Comp Neurol* 263: 265-281, 1987.
- Armstrong-James M, Callahan C and Friedman M. Thalamo-cortical processing of vibrissal information in the rat. I. Intracortical origins of surround but not centre-receptive fields of layer IV neurones in the rat S1 barrel field cortex. *J Comp Neurol* 303: 193-210, 1991.
- Armstrong-James M and Callahan C. Thalamo-cortical processing of vibrissal information in the rat. II. spatiotemporal convergence in the thalamic ventroposterior medial nucleus (VPM) and its relevance to generation of receptive fields of S1 cortical "barrel" neurones. *J Comp Neurol* 303: 211-224, 1991.
- Arvidsson J. Somatotopic organization of vibrissae afferents in the trigeminal sensory nuclei of the rat studied by transganglionic transport of HRP. *J Comp Neurol* 211: 84-92, 1982.
- Bai W-Z, Ishida M and Arimatsu Y. Chemically defined feedback connections from infragranular layers of sensory association cortices in the rat. *Neuroscience* 123: 257-267, 2004.
- Barbaresi P, Spreafico R, Frassoni C and Rustioni A. GABAergic neurons are present in the dorsal column nuclei but not in the ventroposterior complex of rats. *Brain Res* 382: 305-326, 1986.
- Beckstead RM. An autoradiographic examination of corticocortical and subcortical projections of the mediodorsal-projection (prefrontal) cortex in the rat. *J Comp Neurol* 184: 43-62, 1979.
- Belford GR and Killackey HP. Vibrissae representation in subcortical trigeminal centers of the neonatal rat. *J Comp Neurol* 183: 305-321, 1979.
- Bi Gq and Poo Mm. Synaptic modification by correlated activity: Hebb's postulate revisited. *Annual Review of Neuroscience* 24: 139-166, 2001.
- Bi GQ and Rubin J. Timing in synaptic plasticity: from detection to integration. *Trends in Neurosciences* 28: 222-228, 2005.
- Bienenstock EL, Cooper LN and Munro PW. Theory for the development of neuron selectivity: orientation specificity and binocular interaction in visual cortex. *J Neurosci* 2: 32-48, 1982.

Bliss TV and Lomo T. Long-lasting potentiation of synaptic transmission in the dentate area of the anaesthetized rabbit following stimulation of the perforant path. *J Physiol* 232: 331-356, 1973.

Bokor H, Frere SGA, Eyre MD, Slezia A, Ulbert I, Luthi A and Acsady L. Selective GABAergic Control of Higher-Order Thalamic Relays. *Neuron* 45: 929-940, 2005.

Bourassa J., Pinault D. and Deschenes M. Corticothalamic projections from the cortical barrel field to the somatosensory thalamus in rats: a single-fibre study using biocytin as an anterograde tracer. *Eur J Neurosci* 7: 19-30, 1995.

Brecht M, Preilowski B and Merzenich MM. Functional architecture of the mystacial vibrissae. *Behav Brain Res* 84: 81-97, 1997.

Brecht M and Sakmann B. Dynamic representation of whisker deflection by synaptic potentials in spiny stellate and pyramidal cells in the barrels and septa of layer 4 rat somatosensory cortex. *The Journal of Physiology* 543: 49-70, 2002.

Brown A and Waite P. Responses in the rat thalamus to whisker movements produced by motor nerve stimulation. *J Physiol (Lond)* 238: 387-401, 1974.

Bruno RM, Khatri V, Land PW and Simons DJ. Thalamocortical Angular Tuning Domains within Individual Barrels of Rat Somatosensory Cortex. *J Neurosci* 23: 9565-9574, 2003.

Calford MB and Tweedale R. Interhemispheric transfer of plasticity in the cerebral cortex. *Science* 249: 805-7, 1990.

Carvell GE, Simons DJ, Lichtenstein SH and Bryant P. Electromyographic activity of mystacial pad musculature during whisking behavior in the rat. *Somatosens Mot Res* 8: 159-164, 1991.

Carvell G and Simons D. Biometric analyses of vibrissal tactile discrimination in the rat. *J Neurosci* 10: 2638-2648, 1990.

Castro-Alamancos MA. Properties of Primary Sensory (Lemniscal) Synapses in the Ventrobasal Thalamus and the Relay of High-Frequency Sensory Inputs. *J Neurophysiol* 87: 946-953, 2002.

Castro-Alamancos MA. Dynamics of sensory thalamocortical synaptic networks during information processing states. *Prog Neurobiol* 74: 213-247, 2004.

Chapin JK and Lin CS. The somatic sensory cortex of the rat. In: *The Cerebral Cortex of the Rat*, edited by Kolb B and Tees RC. Boston: MIT, 1990, p. 341-358.

Chiaia NL, Rhoades RW, Bennett-Clarke CA, Fish SE and Killackey HP. Thalamic processing of vibrissal information in the rat. I. Afferent input to the medial ventral posterior and posterior nuclei. *J Comp Neurol* 314: 201-216, 1991a.

Chiaia NL, Rhoades RW, Fish SE and Killackey HP. Thalamic processing of vibrissal information in the rat: II. Morphological and functional properties of medial ventral posterior nucleus and posterior nucleus neurons. *J Comp Neurol* 314: 217-236, 1991b.

Chmielowska J, Carvell GE and Simons DJ. Spatial organization of thalamocortical and corticothalamic projection systems in the rat Sml barrel cortex. *J Comp Neurol* 285: 325-338, 1989.

Cipolloni PB and Peters A. The termination of callosal fibers in the auditory cortex of the rat: A combined Golgi-electron microscope and degeneration study. *J Neurocytol* 12: 713-726, 1983.

Clarey JC, Tweedale R and Calford MB. Interhemispheric modulation of somatosensory receptive fields: evidence for plasticity in primary somatosensory cortex. *Cereb Cortex* 6: 196-206, 1996.

Crabtree JW, Collingridge GL and Isaac JTR. A new intrathalamic pathway linking modality-related nuclei in the dorsal thalamus. *Nat Neurosci* 1: 389-394, 1998.

Crabtree JW and Isaac JTR. New Intrathalamic Pathways Allowing Modality-Related and Cross-Modality Switching in the Dorsal Thalamus. *J Neurosci* 22: 8754-8761, 2002.

Crabtree JW. Intrathalamic sensory connections mediated by the thalamic reticular nucleus. *Cell Mol Life Sci* 56: 683-700, 1999.

Crick F and Koch C. Constraints on cortical and thalamic projections: the no-strong-loops hypothesis. *Nature* 391: 245-250, 1998.

Cruikshank SJ, Landisman CE, Mancilla JG and Connors BW. Connexon connexions in the thalamocortical system. In: *Progress in Brain Research Cortical Function: a View from the Thalamus*, edited by Casagrande VA. Elsevier, 2005, p. 41-57.

Cudeiro J and Sillito AM. Spatial frequency tuning of orientation-discontinuity-sensitive corticofugal feedback to the cat lateral geniculate nucleus. *J Physiol (Lond)* 490: 481-492, 1996.

De Biasi S, Frassoni C and Spreafico R. GABA immunoreactivity in the thalamic reticular nucleus of the rat: a light and electron microscopical study. *Brain Res* 399: 143-147, 1986.

DeFeudis FV. Physiological and behavioral studies with muscimol. *Neurochem Res* 5: 1047-1068, 1980a.

DeFeudis FV. Binding studies with muscimol; relation ty synaptic gamma-aminobutyrate receptors. *Neuroscience* 5: 675-688, 1980b.

Deschenes M, Timofeeva E and Lavallee P. The Relay of High-Frequency Sensory Signals in the Whisker-to-Barreloid Pathway. *J Neurosci* 23: 6787, 2003.

Deschenes M, Veinante P and Zhang Z. The organization of corticothalamic projections: reciprocity versus parity. *Brain Research Reviews* 28: 286-308, 1998.

Deschenes M, Timofeeva E, Lavallee P and Dufresne C. The vibrissal system as a model of thalamic operations. In: *Progress in Brain Research*, Elsevier, 2005, p. 31-40.

Desilets-Roy B, Varga C, Lavallee P and Deschenes M. Substrate for Cross-Talk Inhibition between Thalamic Barreloids. *J Neurosci* 22: 218RC, 2002.

Diamond ME, Huang W and Ebner FF. Laminar comparison of somatosensory cortical plasticity. *Science* 265: 1885-1888, 1994.

Diamond M, Armstrong-James M and Ebner F. Somatic sensory responses in the rostral sector of the posterior group (POm) and in the ventral posterior medial nucleus (VPM) of the rat thalamus. *J Comp Neurol* 318: 462-476, 1992a.

Diamond M, Armstrong-James M, Budway M and Ebner F. Somatic sensory responses in the rostral sector of the posterior group (POm) and in the ventral posterior medial nucleus (VPM) of the rat thalamus: dependence on the barrel field cortex. *J Comp Neurol* 319: 66-84, 1992b.

Dorfl J. The musculature of the mystacial vibrissae of the white mouse. *J Anat* 135: 147-154, 1982.

Dorfl J. The innervation of the mystacial region of the white mouse: A topographical study. *J Anat* 142: 173-184, 1985.

Ebara S, Kumamoto K, Matsuura T, Mazurkiewicz JE and Rice FL. Similarities and differences in the innervation of mystacial vibrissal follicle-sinus complexes in the rat and cat: a confocal microscopic study. *J Comp Neurol* 449: 103-119, 2002.

Ebner FF and Myers RE. Corpus Callosum and the Interhemispheric Transmission of Tactual Learning. *J Neurophysiol* 25: 380-391, 1962.

Edeline JM, Hars B, Hennevin E and Cotillon N. Muscimol Diffusion after Intracerebral Microinjections: A Reevaluation Based on Electrophysiological and Autoradiographic Quantifications. *Neurobiol Learn Mem* 78: 100-124, 2002.

- Egger V, Feldmeyer D and Sakmann B. Coincidence detection and changes of synaptic efficacy in spiny stellate neurons in rat barrel cortex. *Nat Neurosci* 2: 1098-1105, 1999.
- Ergenzinger E, Glasier M, Hahm J and Pons T. Cortically induced thalamic plasticity in the primate somatosensory system. *Nat Neurosci* 1: 226-229, 1998.
- Erisir A, Van Horn SC and Sherman SM. Relative numbers of cortical and brainstem inputs to the lateral geniculate nucleus. *PNAS* 94: 1517-1520, 1997.
- Erzurumlu RS and Killackey HP. Efferent connections of the brainstem trigeminal complex with the facial nucleus of the rat. *J Comp Neurol* 188: 75-86, 1979.
- Erzurumlu RS, Bates CA and Killackey HP. Differential organization of thalamic projection cells in the brain stem trigeminal complex of the rat. *Brain Research* 198: 427-433, 1980.
- Fanselow EE and Nicolelis MAL. Behavioral Modulation of Tactile Responses in the Rat Somatosensory System. *J Neurosci* 19: 7603-7616, 1999.
- Feldman DE. Timing-based LTP and LTD at vertical inputs to layer II/III pyramidal cells in rat barrel cortex. *Neuron* 27: 45-56, 2000.
- Feldman SG and Kruger L. An axonal transport study of the ascending projection of medial lemniscal neurons in the rat. *J Comp Neurol* 192: 427-454, 1980.
- Feldmeyer D, Egger V, Lubke J and Sakmann B. Reliable synaptic connections between pairs of excitatory layer 4 neurones within a single 'barrel' of developing rat somatosensory cortex. *J Physiol (Lond)* 521: 169-190, 1999.
- Fitzgerald O. Discharges from the sensory organs of the cat's vibrissae and modification in their activity by ions. *J Physiol* 98: 163-178, 1940.
- Fox K, Wright N, Wallace H and Glazewski S. The Origin of Cortical Surround Receptive Fields Studied in the Barrel Cortex. *J Neurosci* 23: 8380-8391, 2003.
- Friedberg MH, Lee SM and Ebner FF. The contribution of the principal and spinal trigeminal nuclei to the receptive field properties of thalamic VPM neurons in the rat. *Journal of Neurocytology* 33: 75-85, 2004.
- Friedberg MH, Lee SM and Ebner FF. Modulation of Receptive Field Properties of Thalamic Somatosensory Neurons by the Depth of Anesthesia. *J Neurophysiol* 81: 2243-2252, 1999.
- Fuentealba P, Crochet S, Timofeev I, Bazhenov M, Sejnowski TJ and Steriade M. Experimental evidence and modeling studies support a synchronizing role for electrical coupling in the cat thalamic reticular neurons in vivo. *Eur J Neurosci* 20: 111-119, 2004.

- Garraghty PE. Functional reorganization in adult monkey thalamus after peripheral nerve injury. *Neuroreport* 2: 747-750, 1991.
- Gentet LJ and Ulrich D. Electrophysiological characterization of synaptic connections between layer VI cortical cells and neurons of the nucleus reticularis thalami in juvenile rats. *Eur J Neurosci* 19: 625-633, 2004.
- Ghazanfar A, Krupa D and Nicolelis M. Role of cortical feedback in the receptive field structure and nonlinear response properties of somatosensory thalamic neurons. *Exp Brain Res* 141: 88-100, 2001.
- Gibson JM and Welker WI. Quantitative studies of stimulus coding in first-order vibrissa afferents of rats. 1. Receptive field properties and threshold distributions. *Somatosens Mot Res* 1: 51-67, 1983a.
- Gibson JM and Welker WI. Quantitative studies of stimulus coding in first-order vibrissa afferents of rats. 2. Adaptation and coding of stimulus parameters. *Somatosens Mot Res* 1: 95-117, 1983b.
- Gibson JM. A quantitative comparison of stimulus-response relationships of vibrissa-activated neurons in subnuclei oralis and interpolaris of the rat's trigeminal sensory complex: receptive field properties and threshold distributions. *Somatosens Res* 5: 135-155, 1987.
- Glickstein M and Sperry R. Intermanual somesthetic transfer in split-brain Rhesus monkeys. *J Comp Physiol Psychol* 53: 322-327, 1960.
- Gottschaldt KM and Vahle-Hinz C. Merkel cell receptors: structure and transducer function. *Science* 214: 183-186, 1981.
- Gould HJ III and Kaas JH. The distribution of commissural terminations in somatosensory areas I and II of the grey squirrel. *J Comp Neurol* 196: 489-504, 1981.
- Groenewegen HJ and Berendse HW. The specificity of the 'nonspecific' midline and intralaminar thalamic nuclei. *Trends Neurosci* 17: 52-57, 1994.
- Grunberg BS and Krauthamer GM. Vibrissa-responsive neurons of the superior colliculus that project to the intralaminar thalamus of the rat. *Neurosci Lett* 111: 23-27, 1990.
- Guedel AE. Signs of inhalational anesthesia. A fundamental guide. *Inhalational Anesthesia* 10-52, 1920.
- Guic-Robles E, Valdivieso C and Guajardo G. Rats can learn a roughness discrimination using only their vibrissal system. *Behav Brain Res* 31: 285-289, 1989.

- Guillery RW. A quantitative study of synaptic interconnections in the dorsal lateral geniculate nucleus of the cat. *Z Zellforsch Mikrosk Anat* 96: 39-48, 1969.
- Guillery RW. Anatomical evidence concerning the role of the thalamus in corticocortical communication: a brief review. *J Anat* 187: 187-192, 1995.
- Guillery R, Feig S and Lozsadi D. Paying attention to the thalamic reticular nucleus. *Trends in Neurosciences* 21: 28-32, 1998.
- Guillery R and Sherman S. Thalamic Relay Functions and Their Role in Corticocortical Communication: Generalizations from the Visual System. *Neuron* 33: 163-175, 2002.
- Guillery R and Harting J. Structure and connections of the thalamic reticular nucleus: Advancing views over half a century. *J Comp Neurol* 463: 360-371, 2003.
- Haidarliu S and Ahissar E. Size gradients of barreloids in the rat thalamus. *J Comp Neurol* 429: 372-387, 2001.
- Halata Z and Munger BL. Sensory nerve endings in rhesus monkey sinus hairs. *J Comp Neurol* 192: 645-663, 1980.
- Harris RM. Morphology of physiologically identified thalamocortical relay neurons in the rat ventrobasal thalamus. *J Comp Neurol* 251: 491-505, 1986.
- Harris J and Diamond M. Ipsilateral and contralateral transfer of tactile learning. *Neuroreport* 11: 263-266, 2000.
- Hartings JA, Temereanca S and Simons DJ. High Responsiveness and Direction Sensitivity of Neurons in the Rat Thalamic Reticular Nucleus to Vibrissa Deflections. *J Neurophysiol* 83: 2791-2801, 2000.
- Hartings JA, Temereanca S and Simons DJ. Processing of Periodic Whisker Deflections By Neurons in the Ventroposterior Medial and Thalamic Reticular Nuclei. *J Neurophysiol* 90: 3087-3094, 2003.
- Hartmann MJ, Johnson NJ, Towal RB and Assad C. Mechanical Characteristics of Rat Vibrissae: Resonant Frequencies and Damping in Isolated Whiskers and in the Awake Behaving Animal. *J Neurosci* 23: 6510-6519, 2003.
- Hawkins RD, Abrams TW, Carew TJ and Kandel ER. A cellular mechanism of classical conditioning in Aplysia: activity-dependent amplification of presynaptic facilitation. *Science* 219: 400-405, 1983.
- Hayama T and Ogawa H. Regional Differences of Callosal Connections in the Granular Zones of the Primary Somatosensory Cortex in Rats. *Brain Res Bull* 43: 341-347, 1997.



- Hayashi H. Distributions of vibrissae afferent fiber collaterals in the trigeminal nuclei as revealed by intra-axonal injection of horseradish peroxidase. *Brain Res* 183: 442-446, 1980.
- Hazama M, Kimura A, Donishi T, Sakoda T and Tamai Y. Topography of corticothalamic projections from the auditory cortex of the rat. *Neuroscience* 124: 655-667, 2004.
- Hebb D. *The Organization of Behavior*. Wiley, 1949.
- Henderson TA and Jacquin MF. What makes subcortical barrels? In: *Cerebral Cortex Vol 11*, edited by E.G.Jones and I.T.Diamond. New York: Plenum Press, 1995, p. 123-187.
- Hendrickson AE, Hunt SP and Wu JY. Immunocytochemical localization of glutamic acid decarboxylase in monkey striate cortex. *Nature* 292: 605-607, 1981.
- Hess R and Murata K. Effects of glutamate and GABA on specific response properties of neurones in the visual cortex. *Exp Brain Res* 21: 285-297, 1974.
- Hillenbrand U and van Hemmen JL. Adaptation in the corticothalamic loop: computational prospects of tuning the senses. *Philos Trans R Soc Lond B Biol Sci* 357: 1859-1867, 2002.
- Hoggan G and Hoggan FE. Forked nerve endings in hairs. *J Anat* 27: 224-231, 1892.
- Hoogland PV, Welker E and Van der Loos H. Organization of the projections from barrel cortex to thalamus in mice studied with Phaseolus vulgaris-leucoagglutinin and HRP. *Exp Brain Res* 68: 73-87, 1987.
- Houser CR, Vaughn JE, Barber RP and Roberts E. GABA neurons are the major cell type of the nucleus reticularis thalami. *Brain Res* 200: 341-354, 1980.
- Huerta MF, Frankfurter A and Harting JK. Studies of the principal sensory and spinal trigeminal nuclei of the rat: projections to the superior colliculus, inferior olive, and cerebellum. *J Comp Neurol* 220: 147-167, 1983.
- Hupe J, James A, Payne B, Lomber S, Girard P and Bullier J. Cortical feedback improves discrimination between figure and background by V1, V2 and V3 neurons. *Nature* 394: 784-787, 1998.
- Innocenti MG. General Organization of Callosal Connections in the Cerebral Cortex. *Cereb Cortex* 5: 291-353, 1986.
- Ito M. Processing of vibrissa sensory information within the rat neocortex. *J Neurophysiol* 54: 479-490, 1985.

- Ito M. Response properties and topography of vibrissa-sensitive VPM neurons in the rat. *J Neurophysiol* 60: 1181-1197, 1988.
- Ito M and Kato M. Analysis of variance study of the rat cortical layer 4 barrel and layer 5b neurones. *The Journal of Physiology* 539: 511-522, 2002.
- Iwamura Y, Iriki A and Tanaka M. Bilateral hand representation in the postcentral somatosensory cortex. *Nature* 369: 554-556, 1994.
- Iwamura Y. Bilateral receptive field neurons and callosal connections in the somatosensory cortex. *Philos Trans R Soc Lond B Biol Sci* 355: 267-273, 2000.
- Iwamura Y, Taoka M and Iriki A. Bilateral Activity and Callosal Connections in the Somatosensory Cortex. *Neuroscientist* 7: 419-429, 2001.
- Jacquin MF, Woerner D, Szczepanik AM, Riecker V, Mooney RD and Rhoades RW. Structure-function relationships in rat brainstem subnucleus interpolaris. I. Vibrissa primary afferents. *J Comp Neurol* 243: 266-279, 1986a.
- Jacquin MF, Golden J and Panneton WM. Structure and function of barrel 'precursor' cells in trigeminal nucleus principalis. *Dev Brain Res* 43: 309-314, 1988.
- Jacquin MF, Golden J and Rhoades RW. Structure-function relationships in rat brainstem subnucleus interpolaris: III. Local circuit neurons. *J Comp Neurol* 282: 24-44, 1989a.
- Jacquin MF, Barcia M and Rhoades RW. Structure-function relationships in rat brainstem subnucleus interpolaris: IV. Projection neurons. *J Comp Neurol* 282: 45-62, 1989b.
- Jacquin MF and Rhoades RW. Cell structure and response properties in the trigeminal subnucleus oralis. *Somatosens Mot Res* 7: 265-288, 1990.
- Jacquin M, Renehan W, Mooney R and Rhoades R. Structure-function relationships in rat medullary and cervical dorsal horns. I. Trigeminal primary afferents. *J Neurophysiol* 55: 1153-1186, 1986b.
- Jacquin M, Renehan W, Rhoades R and Panneton W. Morphology and topography of identified primary afferents in trigeminal subnuclei principalis and oralis. *J Neurophysiol* 70: 1911-1936, 1993.
- Jensen KF and Killackey HP. Terminal arbors of axons projecting to the somatosensory cortex of the adult rat: I. The normal morphology of specific thalamocortical afferents. *J Neurosci* 7: 3529-3543, 1987.
- Jones EG and Powell TP. Electron microscopy of synaptic glomeruli in the thalamic relay nuclei of the cat. *Proc R Soc Lond B Biol Sci* 172: 153-171, 1969.

- Jones EG. Some aspects of the organization of the thalamic reticular complex. *J Comp Neurol* 162: 285-308, 1975.
- Jones EG, Burton H and Porter R. Commissural and cortico-cortical "columns" in the somatic sensory cortex of primates. *Science* 190: 572-574, 1975.
- Jones EG and Wise SP. Size, laminar and columnar distribution of efferent cells in the sensory-motor cortex of monkeys. *J Comp Neurol* 175: 391-438, 1977.
- Jones EG. Thalamic circuitry and thalamocortical synchrony. *Philos Trans R Soc Lond B Biol Sci* 357: 1659-1673, 2002.
- Kaitz SS and Robertson RT. Thalamic connections with limbic cortex. II. Corticothalamic projections. *J Comp Neurol* 195: 527-545, 1981.
- Kalil R and Chase R. Corticofugal influence on activity of lateral geniculate neurons in the cat. *J Neurophysiol* 33: 459-474, 1970.
- Kida H, Shimegi S and Sato H. Similarity of Direction Tuning Among Responses to Stimulation of Different Whiskers in Neurons of Rat Barrel Cortex. *J Neurophysiol* 94: 2004-2018, 2005.
- Kim U and Ebner FF. Barrels and septa: separate circuits in rat barrels field cortex. *J Comp Neurol* 408: 489-505, 1999.
- Knudsen E, Lac S and Esterly S. Computational Maps in the Brain. *Annual Review of Neuroscience* 10: 41-65, 1987.
- Koch C. The action of the corticofugal pathway on sensory thalamic nuclei: a hypothesis. *Neuroscience* 23: 399-406, 1987.
- Koralek KA, Jensen KF and Killackey HP. Evidence for two complementary patterns of thalamic input to the rat somatosensory cortex. *Brain Res* 463: 346-352, 1988.
- Koralek KA, Olavarria J and Killackey HP. Areal and laminar organization of corticocortical projections in the rat somatosensory cortex. *J Comp Neurol* 299: 133-150, 1990.
- Krogsgaard-Larsen P., Krogsgaard-Larsen P., Arnt J. and Arnt J. GABA receptor agonists: relationship between structure and biological activity *in vivo* and *in vitro*. *Adv Exp Med Biol* 123: 303-321, 1979.
- Krubitzer LA, Sesma MA and Kaas JH. Microelectrode maps, myeloarchitecture, and cortical connections of three somatotopically organized representations of the body surface in the parietal cortex of squirrels. *J Comp Neurol* 250: 403-430, 1986.

- Krubitzer LA, Clarey JC, Tweedale R and Calford MB. Interhemispheric connections of somatosensory cortex in the flying fox. *J Comp Neurol* 402: 538-559, 1998.
- Krupa DJ, Wiest MC, Shuler MG, Laubach M and Nicolelis MAL. Layer-Specific Somatosensory Cortical Activation During Active Tactile Discrimination. *Science* 304: 1989-1992, 2004.
- Krupa D, Ghazanfar A and Nicolelis M. Immediate thalamic sensory plasticity depends on corticothalamic feedback. *Proc Natl Acad Sci U S A* 96: 8200-8205, 1999.
- Krupa D, Matell M, Brisben A, Oliveira L and Nicolelis M. Behavioral Properties of the Trigeminal Somatosensory System in Rats Performing Whisker-Dependent Tactile Discriminations. *J Neurosci* 21: 5752-5763, 2001.
- Kwegyir-Afful EE and Keller A. Response Properties of Whisker-Related Neurons in Rat Second Somatosensory Cortex. *J Neurophysiol* 92: 2083-2092, 2004.
- Lam YW and Sherman SM. Mapping by Laser Photostimulation of Connections Between the Thalamic Reticular and Ventral Posterior Lateral Nuclei in the Rat. *J Neurophysiol* 94: 2472-2483, 2005.
- Land PW and Simons DJ. Metabolic and structural correlates of the vibrissae representation in the thalamus of the adult rat. *Neurosci Lett* 60: 319-324, 1985.
- Land P, Buffer SJ and Yaskosky J. Barreloids in adult rat thalamus: three-dimensional architecture and relationship to somatosensory cortical barrels. *J Comp Neurol* 355: 573-588, 1995.
- Landisman CE, Long MA, Beierlein M, Deans MR, Paul DL and Connors BW. Electrical Synapses in the Thalamic Reticular Nucleus. *J Neurosci* 22: 1002-1009, 2002.
- Lavallee P and Deschenes M. Dendroarchitecture and Lateral Inhibition in Thalamic Barreloids. *J Neurosci* 24: 6098-6105, 2004.
- Lavallee P, Urbain N, Dufresne C, Bokor H, Acsady L and Deschenes M. Feedforward Inhibitory Control of Sensory Information in Higher-Order Thalamic Nuclei. *J Neurosci* 25: 7489-7498, 2005.
- Lee S, Friedberg M and Ebner F. The role of GABA-mediated inhibition in the rat ventral posterior medial thalamus. I. Assessment of receptive field changes following thalamic reticular nucleus lesions. *J Neurophysiol* 71: 1702-1715, 1994.
- Lee SH and Simons DJ. Angular Tuning and Velocity Sensitivity in Different Neuron Classes Within Layer 4 of Rat Barrel Cortex. *J Neurophysiol* 91: 223-229, 2004.

- Leonard C. The prefrontal cortex of the rat. I. Cortical projection of the mediodorsal nucleus. II. Efferent connections. *Brain Res* 12: 321-343, 1969.
- Levy WB and Steward O. Temporal contiguity requirements for long-term associative potentiation/depression in the hippocampus. *neuroscience* 8: 791-797, 1983.
- Li J, Guido W and Bickford ME. Two Distinct Types of Corticothalamic EPSPs and Their Contribution to Short-Term Synaptic Plasticity. *J Neurophysiol* 90: 3429-3440, 2003.
- Li L, Rema V and Ebner FF. Chronic Suppression of Activity in Barrel Field Cortex Downregulates Sensory Responses in Contralateral Barrel Field Cortex. *J Neurophysiol* 94: 3342-3356, 2005.
- Li L and Ebner F. Balancing bilateral sensory activity: callosal processing modulates sensory transmission through the contralateral thalamus by altering the response threshold. *Experimental Brain Research* 1-19, 2006.
- Lichtenstein SH, Carvell GE and Simons DJ. Responses of rat trigeminal ganglion neurons to movements of vibrissae in different directions. *Somatosens Mot Res* 7: 47-65, 1990.
- Lisman J. A Mechanism for the Hebb and the Anti-Hebb Processes Underlying Learning and Memory. *PNAS* 86: 9574-9578, 1989.
- Liu XB, Honda CN and Jones EG. Distribution of four types of synapse on physiologically identified relay neurons in the ventral posterior thalamic nucleus of the cat. *J Comp Neurol* 352: 69-91, 1995.
- Liu XB and Jones EG. Predominance of corticothalamic synaptic inputs to thalamic reticular nucleus neurons in the rat. *J Comp Neurol* 414: 67-79, 1999.
- Lo FS, Lu SM and Sherman SM. Intracellular and extracellular in vivo recording of different response modes for relay cells of the cat's lateral geniculate nucleus. *Exp Brain Res* 1991: 2-317, 1991.
- Lu SM and Lin RC. Thalamic afferents of the rat barrel cortex: a light- and electron-microscopic study using Phaseolus vulgaris leucoagglutinin as an anterograde tracer. *Somatosens Mot Res* 10: 1-16, 1993.
- Lubke J, Egger V, Sakmann B and Feldmeyer D. Columnar Organization of Dendrites and Axons of Single and Synaptically Coupled Excitatory Spiny Neurons in Layer 4 of the Rat Barrel Cortex. *J Neurosci* 20: 5300-5311, 2000.
- Ma PM and Woolsey TA. Cytoarchitectonic correlates of the vibrissae in the medullary trigeminal complex of the mouse. *Brain Res* 306: 374-379, 1984.

Ma P. The barrelettes--architectonic vibrissal representations in the brainstem trigeminal complex of the mouse. I. Normal structural organization. *J Comp Neurol* 309: 161-199, 1991.

Magee JC and Johnston D. A Synaptically Controlled, Associative Signal for Hebbian Plasticity in Hippocampal Neurons. *Science* 275: 209-213, 1997.

Markram H, Lubke J, Frotscher M and Sakmann B. Regulation of Synaptic Efficacy by Coincidence of Postsynaptic APs and EPSPs. *Science* 275: 213-215, 1997.

Martin JH. Autoradiographic estimation of the extent of reversible inactivation produced by microinjection of lidocaine and muscimol in the rat. *Neurosci Lett* 127: 160-164, 1991.

McCormick DA, Connors BW, Lighthall JW and Prince DA. Comparative electrophysiology of pyramidal and sparsely spiny stellate neurons of the neocortex. *J Neurophysiol* 54: 782-806, 1985.

McCormick DA. Neurotransmitter actions in the thalamus and cerebral cortex and their role in neuromodulation of thalamocortical activity. *Prog Neurobiol* 39: 337-388, 1992.

Melaragno HP and Montagna W. The tactile hair follicles in the mouse. *Anat Rec* 115: 129-149, 1953.

Mignard M and Malpeli J. Paths of Information Flow Through Visual Cortex. *Science* 251: 1249-1251, 1991.

Minnery BS and Simons DJ. Response Properties of Whisker-Associated Trigeminothalamic Neurons in Rat Nucleus Principalis. *J Neurophysiol* 89: 40-56, 2003.

Minnery BS, Bruno RM and Simons DJ. Response Transformation and Receptive-Field Synthesis in the Lemniscal Trigeminothalamic Circuit. *J Neurophysiol* 90: 1556-1570, 2003.

Mishima K. Facilitatory and inhibitory processes in the thalamic ventrobasal nucleus of the rat. *Jpn J Physiol* 42: 193-210, 1992.

Mountcastle VB, Talbot WH, Sakata H and Hyvarinen J. Cortical neuronal mechanisms in flutter-vibration studied in unanesthetized monkeys. Neuronal periodicity and frequency discrimination. *J Neurophysiol* 32: 452-484, 1969.

Mountcastle VB. Introduction. Computation in cortical columns. *Cereb Cortex* 13: 2-4, 2003.

- Naik SR, Guidotti A and Costa E. Central GABA receptor agonists: comparison of muscimol and baclofen. *Neuropharmacology* 15: 479-484, 1976.
- Newberry NR and Nicoll RA. Comparison of the action of baclofen with gamma-aminobutyric acid on rat hippocampal pyramidal cells in vitro. *J Physiol* 360: 161-185, 1985.
- Nicolelis MA, Lin RC, Woodward DJ and Chapin JK. Induction of immediate spatiotemporal changes in thalamic networks by peripheral block of ascending cutaneous information. *Nature* 361: 533-536, 1993.
- Nicolelis M, Baccala L, Lin C and Chapin J. Sensorimotor Encoding by Synchronous Neural Ensemble Activity at Multiple Levels of the Somatosensory System. *Science* 268: 1353-1358, 1995.
- Oda S. Ultrastructure and Distribution of Corticothalamic Fiber Terminals From the Posterior Cingulate Cortex and the Presubiculum to the Anteroventral Thalamic Nucleus of the Rat. *Brain Res Bull* 42: 485-491, 1997.
- Oertel WH, Graybiel AM, Mugnaini E, Elde RP, Schmechel DE and Kopin IJ. Coexistence of glutamic acid decarboxylase- and somatostatin-like immunoreactivity in neurons of the feline nucleus reticularis thalami. *J Neurosci* 3: 1322-1332, 1983.
- Ohara PT and Lieberman AR. The thalamic reticular nucleus of the adult rat: experimental anatomical studies. *J Neurocytol* 14: 365-411, 1985.
- Ohara PT and Havton LA. Dendritic architecture of rat somatosensory thalamocortical projection neurons. *J Comp Neurol* 341: 159-171, 1994.
- Ohara PT and Havton LA. Dendritic arbors of neurons from different regions of the rat thalamic reticular nucleus share a similar orientation. *Brain Res* 731: 236-240, 1996.
- Ojima H. Terminal morphology and distribution of corticothalamic fibers originating from layers 5 and 6 of cat primary auditory cortex. *Cereb Cortex* 4: 646-663, 1994.
- Olavarria JF, Van Sluyters RC and Killackey HP. Evidence for the complementary organization of callosal and thalamic connections within rat somatosensory cortex. *Brain Res* 291: 364-368, 1984.
- Olavarria JF and Van Sluyters RC. Comparison of the patterns of callosal connections in lateral parietal cortex of the rat, mouse and hamster. *Anat Embryol (Berl)* 191: 239-242, 1995.
- Paulsen O and Sejnowski TJ. Natural patterns of activity and long-term synaptic plasticity. *Current Opinion in Neurobiology* 10: 172-180, 2000.

- Peschanski M. Trigeminal afferents to the diencephalon in the rat. *Neuroscience* 12: 465-487, 1984.
- Petersen CCH and Sakmann B. The Excitatory Neuronal Network of Rat Layer 4 Barrel Cortex. *J Neurosci* 20: 7579-7586, 2000.
- Pettit MJ and Schwark HD. Receptive field reorganization in dorsal column nuclei during temporary denervation. *Science* 262: 2054-2056, 1993.
- Phelan KD and Falls WM. The spinotrigeminal pathway and its spatial relationship to the origin of trigeminospinal projections in the rat. *Neuroscience* 40: 477-496, 1991.
- Pidoux B and Verley R. Projections on the cortical somatic I barrel subfield from ipsilateral vibrissae in adult rodents. *Electroencephalogr Clin Neurophysiol* 46: 715-726, 1979.
- Pierret T, Lavallee P and Deschenes M. Parallel Streams for the Relay of Vibrissal Information through Thalamic Barreloids. *J Neurosci* 20: 7455-7462, 2000.
- Pinault D, Bourassa J and Deschenes M. The axonal arborization of single thalamic reticular neurons in the somatosensory thalamus of the rat. *Eur J Neurosci* 7: 31-40, 1995.
- Pinault D and Deschenes M. Anatomical evidence for a mechanism of lateral inhibition in the rat thalamus. *Eur J Neurosci* 10: 3462-3469, 1998a.
- Pinault D and Deschenes M. Projection and innervation patterns of individual thalamic reticular axons in the thalamus of the adult rat: A three-dimensional, graphic, and morphometric analysis. *J Comp Neurol* 391: 180-203, 1998b.
- Pinault D. The thalamic reticular nucleus: structure, function and concept. *Brain Research Reviews* 46: 1-31, 2004.
- Polley DB, Rickert JL and Frostig RD. Whisker-based discrimination of object orientation determined with a rapid training paradigm. *Neurobiology of Learning and Memory* 83: 134-142, 2005.
- Przybyszewski AW, Gaska JP, Foote W and Pollen DA. Striate cortex increases contrast gain of macaque LGN neurons. *Vis Neurosci* 17: 485-494, 2000.
- Rauschecker JP. Cortical control of the thalamus: top-down processing and plasticity. *Nat Neurosci* 1: 179-180, 1998.
- Reep R and Winans S. Efferent connections of dorsal and ventral agranular insular cortex in the hamster, *Mesocricetus auratus*. *Neuroscience* 7: 2609-2635, 1982.



Reinecke S., Dinse H.R., Reinke H. and Witte O.W. Induction of bilateral plasticity in sensory cortical maps by small unilateral cortical infarcts in rats. *Eur J Neurosci* 17: 623-627, 2003.

Reiter HO and Stryker MP. Neural plasticity without postsynaptic action potentials: less-active inputs become dominant when kitten visual cortical cells are pharmacologically inhibited. *Proc Natl Acad Sci U S A* 85: 3623-3627, 1988.

Rema V and Ebner FF. Lesions of Mature Barrel Field Cortex Interfere with Sensory Processing and Plasticity in Connected Areas of the Contralateral Hemisphere. *J Neurosci* 23: 10378-10387, 2003.

Rehman WE and Munger BL. Degeneration and regeneration of peripheral nerve in the rat trigeminal system. I. Identification and characterization of the multiple afferent innervation of the mystacial vibrissae. *J Comp Neurol* 246: 129-145, 1986.

Rehman WE, Stansel SS, McCall RD, Rhoades RW and Jacquin MF. An electron microscopic analysis of the morphology and connectivity of individual HRP-labeled slowly adapting vibrissa primary afferents in the adult rat. *Brain Res* 462: 396-400, 1988.

Rehman W, Jacquin M, Mooney R and Rhoades R. Structure-function relationships in rat medullary and cervical dorsal horns. II. Medullary dorsal horn cells. *J Neurophysiol* 55: 1187-1201, 1986.

Rhoades R, Belford G and Killackey H. Receptive-field properties of rat ventral posterior medial neurons before and after selective kainic acid lesions of the trigeminal brain stem complex. *J Neurophysiol* 57: 1577-1600, 1987.

Rice FL, Mance A and Munger BL. A comparative light microscopic analysis of the sensory innervation of the mystacial pad. I. Innervation of vibrissal follicle-sinus complexes. *J Comp Neurol* 252: 154-174, 1986.

Rice FL, Fundin BT, Arvidsson J, Aldskogius H and Johansson O. Comprehensive immunofluorescence and lectin binding analysis of vibrissal follicle sinus complex innervation in the mystacial pad of the rat. *J Comp Neurol* 385: 149-184, 1997.

Rouiller EM and Welker E. A comparative analysis of the morphology of corticothalamic projections in mammals. *Brain Research Bulletin* 53: 727-741, 2000.

Rouiller EM and Durif C. The dual pattern of corticothalamic projection of the primary auditory cortex in macaque monkey. *Neuroscience Letters* 358: 49-52, 2004.

Ryugo D and Weinberger N. Corticofugal modulation of the medial geniculate body. *Exp Neurol* 51: 377-391, 1976.

Sachdev R, Jenkinson E, Zeigler H and Ebner F. Sensorimotor plasticity in the rodent vibrissa system. In: *The Mutable Brain: Dynamic and plastic features of the developing and mature brain.*, edited by Jon H. Kaas. Amsterdam: Harwood Academic Publishers, 2001, p. 123-164.

Saporta S and Kruger L. The organization of thalamocortical relay neurons in the rat ventrobasal complex studied by the retrograde transport of horseradish peroxidase. *J Comp Neurol* 174: 187-208, 1977.

Scheibel ME and Scheibel AB. The organization of the nucleus reticularis thalami: a Golgi study. *Brain Res* 1: 43-62, 1966.

Schnitzler A, Salmelin R, Salenius S, Jousmaki V and Hari R. Tactile information from the human hand reaches the ipsilateral primary somatosensory cortex. *Neurosci Lett* 200: 25-28, 1995.

Semba K and Komisaruk BR. Neural substrates of two different rhythmical vibrissal movements in the rat. *Neuroscience* 12: 761-774, 1984.

Sherman SM and Guillery RW. Functional organization of thalamocortical relays. *J Neurophysiol* 76: 1367-1395, 1996.

Sherman SM. Dual response modes in lateral geniculate neurons: mechanisms and functions. *Vis Neurosci* 13: 205-213, 1996.

Sherman SM. A wake-up call from the thalamus. *Nat Neurosci* 4: 344-346, 2001a.

Sherman SM. Tonic and burst firing: dual modes of thalamocortical relay. *Trends Neurosci* 24: 122-126, 2001b.

Sherman S and Guillery R. The role of the thalamus in the flow of information to the cortex. *Phil Trans R Soc Lond B* 357: 1695-1708, 2002.

Shin HC, Won CK, Jung SC, Oh S, Park S and Sohn JH. Interhemispheric modulation of sensory transmission in the primary somatosensory cortex of rats. *Neurosci Lett* 230: 137-139, 1997.

Shiple M. Response characteristics of single units in the rat's trigeminal nuclei to vibrissa displacements. *J Neurophysiol* 37: 73-90, 1974.

Shosaku A. A comparison of receptive field properties of vibrissa neurons between the rat thalamic reticular and ventro-basal nuclei. *Brain Res* 347: 36-40, 1985.

- Shoykhet M, Doherty D and Simons DJ. Coding of deflection velocity and amplitude by whisker primary afferent neurons: implications for higher level processing. *Somatosens Mot Res* 17: 171-180, 2000.
- Shu Y and McCormick DA. Inhibitory Interactions Between Ferret Thalamic Reticular Neurons. *J Neurophysiol* 87: 2571-2576, 2002.
- Shuler M, Krupa D and Nicolelis M. Bilateral Integration of Whisker Information in the Primary Somatosensory Cortex of Rats. *J Neurosci* 21: 5251-5261, 2001.
- Shuler M, Krupa D and Nicolelis M. Integration of Bilateral Whisker Stimuli in Rats: Role of the Whisker Barrel Cortices. *Cereb Cortex* 12: 86-97, 2002.
- Sillito AM, Cudeiro J and Murphy PC. Orientation sensitive elements in the corticofugal influence on centre-surround interactions in the dorsal lateral geniculate nucleus. *Exp Brain Res* 93: 6-16, 1993.
- Sillito AM and Jones HE. Context-dependent interactions and visual processing in V1. *J Physiol Paris* 90: 205-209, 1997.
- Sillito A, Jones H, Gerstein G and West D. Feature-linked synchronization of thalamic relay cell firing induced by feedback from the visual cortex. *Nature* 369: 479-482, 1994.
- Sillito A and Jones H. Corticothalamic interactions in the transfer of visual information. *Phil Trans R Soc Lond B* 357: 1739-1752, 2002.
- Simons DJ and Carvell GE. Thalamocortical response transformation in the rat vibrissa/barrel system. *J Neurophysiol* 61: 311-330, 1989.
- Simons DJ. Response properties of vibrissa units in rat SI somatosensory neocortex. *J Neurophysiol* 41: 798-820, 1978.
- Simons DJ. Temporal and spatial integration in the rat SI vibrissa cortex. *J Neurophysiol* 54: 615-635, 1985.
- Simons DJ and Carvell GE. Thalamocortical response transformation in the rat vibrissa/barrel system. *J Neurophysiol* 61: 311-330, 1989.
- Smith RL. The ascending fiber projections from the principal sensory trigeminal nucleus in the rat. *J Comp Neurol* 148: 423-445, 1973.
- Spacek J and Lieberman AR. Ultrastructure and three-dimensional organization of synaptic glomeruli in rat somatosensory thalamus. *J Anat* 177: 487-516, 1974.
- Spreafico R, Battaglia G and Frasconi C. The reticular thalamic nucleus (RTN) of the rat: cytoarchitectural, Golgi, immunocytochemical, and horseradish peroxidase study. *J Comp Neurol* 304: 478-490, 1991.

Steindler DA. Trigemino-cerebellar, trigemino-tectal, and trigemino-thalamic projections: a double retrograde axonal tracing study in the mouse. *J Comp Neurol* 237: 155-175, 1985.

Steiner H, Huston JP and Morgan S. Apomorphine reverses direction of asymmetry in facial scanning after 10 days of unilateral vibrissae removal in rat: vibrissotomy-induced denervation supersensitivity? *Behav Brain Res* 22: 283-287, 1986.

Steriade M, McCormick DA and Sejnowski TJ. Thalamocortical oscillations in the sleeping and aroused brain. *Science* 262: 679-685, 1993.

Steriade M, Domich L and Oakson G. Reticularis thalami neurons revisited: activity changes during shifts in states of vigilance. *J Neurosci* 6: 68-81, 1986.

Steriade M and Timofeev I. Neuronal Plasticity in Thalamocortical Networks during Sleep and Waking Oscillations. *Neuron* 37: 563-576, 2003.

Suga N, Xiao Z, Ma X and Ji W. Plasticity and corticofugal modulation for hearing in adult animals. *Neuron* 36: 9-18, 2003.

Suga N and Ma X. Multiparametric corticofugal modulation and plasticity in the auditory system. *Nat Rev Neurosci* 4: 783-794, 2003.

Sugitani M, Yano J, Sugai T and Ooyama H. Somatotopic organization and columnar structure of vibrissae representation in the rat ventrobasal complex. *Exp Brain Res* 81: 346-352, 1990.

Sumitomo I and Iwama K. Neuronal organization of rat thalamus for processing information of vibrissal movements. *Brain Res* 415: 389-392, 1987.

Swadlow HA. Efferent neurons and suspected interneurons in binocular visual cortex of the awake rabbit: receptive fields and binocular properties. *J Neurophysiol* 59: 1162-1187, 1988.

Swadlow HA. Efferent neurons and suspected interneurons in S-1 vibrissa cortex of the awake rabbit: receptive fields and axonal properties. *J Neurophysiol* 62: 288-308, 1989.

Temereanca S and Simons D. Functional Topography of Corticothalamic Feedback Enhances Thalamic Spatial Response Tuning in the Somatosensory Whisker/Barrel System. *Neuron* 41: 639-651, 2004.

Temereanca S and Simons DJ. Local Field Potentials and the Encoding of Whisker Deflections by Population Firing Synchrony in Thalamic Barreloids. *J Neurophysiol* 89: 2137-2145, 2003.

Timofeeva E, Merette C, Emond C, Lavallee P and Deschenes M. A Map of Angular Tuning Preference in Thalamic Barreloids. *J Neurosci* 23: 10717-10723, 2003.

Timofeeva E, Lavallee P, Arsenault D and Deschenes M. Synthesis of Multiwhisker-Receptive Fields in Subcortical Stations of the Vibrissa System. *J Neurophysiol* 91: 1510-1515, 2004.

Timofeeva E, Dufresne C, Sik A, Zhang ZW and Deschenes M. Cholinergic Modulation of Vibrissal Receptive Fields in Trigeminal Nuclei. *J Neurosci* 25: 9135-9143, 2005.

Tsumoto T, Creutzfeldt OD and Legendy CR. Functional organization of the corticofugal system from visual cortex to lateral geniculate nucleus in the cat (with an appendix on geniculo-cortical mono-synaptic connections). *Exp Brain Res* 32: 345-364, 1978.

Usrey W and Fitzpatrick D. Specificity in the axonal connections of layer VI neurons in tree shrew striate cortex: evidence for distinct granular and supragranular systems. *J Neurosci* 16: 1203-1218, 1996.

Van der Loos H. Barreloids in the mouse somatosensory thalamus. *Neurosci Lett* 7: 23-30, 1976.

Varga C, Sik A, Lavallee P and Deschenes M. Dendroarchitecture of Relay Cells in Thalamic Barreloids: A Substrate for Cross-Whisker Modulation. *J Neurosci* 22: 6186-6194, 2002.

Vaughan DW. Thalamic and callosal connections of the rat auditory cortex. *Brain Res* 260: 181-189, 1983.

Veinante P, Lavallee P and Deschenes M. Corticothalamic projections from layer 5 of the vibrissal barrel cortex in the rat. *J Comp Neurol* 424: 197-204, 2000a.

Veinante P, Jacquin MF and Deschenes. Thalamic projections from the whisker-sensitive regions of the spinal trigeminal complex in the rat. *J Comp Neurol* 420: 233-243, 2000b.

Veinante P and Deschenes M. Single- and Multi-Whisker Channels in the Ascending Projections from the Principal Trigeminal Nucleus in the Rat. *J Neurosci* 19: 5085-5095, 1999.

Villa A, Rouiller EM, Simm GM, Zurita P, de Ribaupierre Y and de Ribaupierre F. Corticofugal modulation of the information processing in the auditory thalamus of the cat. *Exp Brain Res* 86: 506-517, 1991.

Vincent SB. The function of the vibrissae in the behavior of the white rat. *Behav Monogr* 1: 1-81, 1912.

- Vincent SB. The tactile hair of the white rat. *J Comp Neurol* 23: 1-34, 1913.
- Waite PM and Cragg BG. The peripheral and central changes resulting from cutting or crushing the afferent nerve supply to the whiskers. *Proc R Soc Lond B Biol Sci* 214: 191-211, 1982.
- Waite PM and Jacquin MF. Dual innervation of the rat vibrissa: responses of trigeminal ganglion cells projecting through deep or superficial nerves. *J Comp Neurol* 322: 233-245, 1992.
- Waite P. Somatotopic organization of vibrissal responses in the ventro-basal complex of the rat thalamus. *J Physiol (Lond)* 228: 527-540, 1973a.
- Waite P. The responses of cells in the rat thalamus to mechanical movements of the whiskers. *J Physiol (Lond)* 228: 541-561, 1973b.
- Wallace H, Glazewski S, Liming K and Fox K. The Role of Cortical Activity in Experience-Dependent Potentiation and Depression of Sensory Responses in Rat Barrel Cortex. *J Neurosci* 21: 3881-3894, 2001.
- Walters ET and Byrne JH. Associative conditioning of single sensory neurons suggests a cellular mechanism for learning. *Science* 219: 405-408, 1983.
- Welker C. Microelectrode delineation of fine grain somatotopic organization of (Sml) cerebral neocortex in albino rat. *Brain Res* 26: 259-275, 1971.
- Welker C and Woolsey TA. Structure of layer IV in the somatosensory neocortex of the rat: description and comparison with the mouse. *J Comp Neurol* 158: 437-453, 1974.
- Welker C. Receptive fields of barrels in the somatosensory neocortex of the rat. *J Comp Neurol* 166: 173-189, 1976.
- Welker WI. Analysis of sniffing of the albino rat. *Behaviour* 22: 223-224, 1964.
- Wiest MC, Bentley N and Nicolelis MAL. Heterogeneous Integration of Bilateral Whisker Signals by Neurons in Primary Somatosensory Cortex of Awake Rats. *J Neurophysiol* 93: 2966-2973, 2005.
- Wilent WB and Contreras D. Synaptic Responses to Whisker Deflections in Rat Barrel Cortex as a Function of Cortical Layer and Stimulus Intensity. *J Neurosci* 24: 3985-3998, 2004.
- Williams MN, Zahm DS and Jacquin MF. Differential foci and synaptic organization of the principal and spinal trigeminal projections to the thalamus in the rat. *Eur J Neurosci* 6: 429-453, 1994.

Wise SP. The laminar organization of certain afferent and efferent fiber systems in the rat somatosensory cortex. *Brain Res* 90: 139-142, 1975.

Wise SP and Jones EG. The organization and postnatal development of the commissural projection of the rat somatic sensory cortex. *J Comp Neurol* 168: 313-343, 1976.

Wise SP and Jones EG. Developmental studies of thalamocortical and commissural connections in the rat somatic sensory cortex. *J Comp Neurol* 178: 187-208, 1978.

Wong-Riley M and Welt C. Histochemical changes in cytochrome oxidase of cortical barrels after vibrissal removal in neonatal and adult mice. *Proc Natl Acad Sci U S A* 77: 2333-2337, 1980.

Woolsey TA, Anderson JR, Wann JR and Stanfield BB. Effects of early vibrissae damage on neurons in the ventrobasal (VB) thalamus of the mouse. *J Comp Neurol* 184: 363-380, 1979.

Woolsey T and Van der Loos H. The structural organization of layer IV in the somatosensory region (SI) of mouse cerebral cortex: the description of a cortical field composed of discrete cytoarchitectonic units. *Brain Res* 17: 205-242, 1970.

Woolston DC, La Londe JR and Gibson JM. Comparison of response properties of cerebellar- and thalamic-projecting intercalated neurons. *J Neurophysiol* 48: 160-173, 1982.

Yan J and Suga N. Corticofugal Modulation of Time-Domain Processing of Biosonar Information in Bats. *Science* 273: 1100-1103, 1996.

Yan W and Suga N. Corticofugal modulation of the midbrain frequency map in the bat auditory system. *Nat Neurosci* 1: 54-58, 1998.

Yoshida A, Sessle BJ, Dostrovsky JO and Chiang CY. Trigeminal and dorsal column nuclei projections to the anterior pretectal nucleus in the rat. *Brain Res* 590: 81-94, 1992.

Yu C, Derdikman D, Haidarliu S and Ahissar E. Parallel thalamic pathways for whisking and touch signals in the rat. *PLoS* in press: 2006.

Yuan B, Morrow T and Casey K. Responsiveness of ventrobasal thalamic neurons after suppression of S1 cortex in the anesthetized rat. *J Neurosci* 5: 2971-2978, 1985.

Yuan B, Morrow T and Casey K. Corticofugal influences of S1 cortex on ventrobasal thalamic neurons in the awake rat. *J Neurosci* 6: 3611-3617, 1986.

Zhang LI, Tao HW, Holt CE, Harris WA and Poo Mm. A critical window for cooperation and competition among developing retinotectal synapses. *Nature* 395: 37-44, 1998.

Zhang Y, Suga N and Yan J. Corticofugal modulation of frequency processing in bat auditory system. *Nature* 387: 900-903, 1997.

Zhang Y and Suga N. Corticofugal Amplification of Subcortical Responses to Single Tone Stimuli in the Mustached Bat. *J Neurophysiol* 78: 3489-3492, 1997.

Zhang Y and Suga N. Modulation of Responses and Frequency Tuning of Thalamic and Collicular Neurons by Cortical Activation in Mustached Bats. *J Neurophysiol* 84: 325-333, 2000.

Zhang ZW and Deschenes M. Intracortical Axonal Projections of Lamina VI Cells of the Primary Somatosensory Cortex in the Rat: A Single-Cell Labeling Study. *J Neurosci* 17: 6365-6379, 1997.

Zucker E and Welker WI. Coding of somatic sensory input by vibrissae neurons in the rat's trigeminal ganglion. *Brain Res* 12: 138-156, 1969.